A DETAILED INVESTIGATION INTO DIAMOND-BEARING XENOLITHS FROM NEWLANDS KIMBERLITE, SOUTH AFRICA

VOLUME I: TEXT

By

ANDREW H MENZIES

University of Cape Town

Thesis submitted in fulfilment of the requirements for the Degree of Doctor of Philosophy

in the Department of Geological Sciences, University of Cape Town

February, 2001

The copyright of this thesis vests in the author. No quotation from it or information derived from it is to be published without full acknowledgement of the source. The thesis is to be used for private study or non-commercial research purposes only.

Published by the University of Cape Town (UCT) in terms of the non-exclusive license granted to UCT by the author.

University of Cape Town

ACKNOWLEDGEMENTS

This thesis has been a long time in the making and had the input of a lot of people, all of whom, to varying degrees, have helped shaped this work, but more importantly, me. Below I have attempted to mention all of you - although I know I will fail. Nevertheless, it cannot express my eternal gratitude for the contribution you have made to my life.

The first and foremost person to thank is my supervisor John Gurney. His guidance, support, direction, and patience for this thesis will always be remembered. Without his never-ending inspiration in this field of research I would not have had the opportunities and experienced everything that I have - including meeting some of the most important people in my life.

I am grateful to Collin Cotterrell and Gem Mining for allowing us access to the Newlands kimberlites, concentrates and diamonds. Their support resulted in the discovery of some amazing specimens.

Throughout this project I was lucky enough to have worked with and learnt from numerous people at many institutions from around the world. Without their support this thesis would not be what it is. Hopefully I can remember most of you, but if your name does not appear here, it is not for lack of gratitude on my behalf, rather my ailing memory as time passes on. Special thanks to Rick Carlson, Steve Shirey, Eric Hauri, Joe Boyd and Chris Haddidiakos from the Carnegie Institution of Washington; the late Dick Rickard and Dane Gerneke at UCT; Judith Milledge and Andy Beard from University College London; Ben Harte, Richard Hinton, and Simon Burgess from University of Edinburgh. Other people that I have had significant discussions with include Herb Helmstaedt, Mark Hutchenson, Dan Frost, Mark Buntzen, Gail Kiviets, Ingrid Chinn, Petrus Le Roux, Andreas Spath, and Kalle Westerlund.

To Paul and Warren – we finish in the same year, we get married in the same year.....what next? To the rest of my friends, all the fun times we have together make it worth all the effort.

A special thanks to the boys and girls at Mineral Services, who have supported me through the long process of putting this thesis into a final product. Your patience and understanding have not gone un-noticed.

Personal thanks to my family back in NZ – mum and dad, Nichole, Nana Hewitt and Nana Menzies – who supported me when I left them behind on my journey into the great unknown of South Africa. And since I have been gone, a special welcome to the family to Patrick and Natalia.

Finally, but definitely not last, to my best friend Gill and our wonderful son Rylan – hopefully now we will have a lot more time and I won't be so stressed in the evenings. Words can't express how I feel.

ABSTRACT

This study involves a detailed investigation of diamond-bearing peridotite and eclogite from Newlands kimberlite, located on the Kaapvaal craton, South Africa.

Eighteen peridotitic garnet macrocrysts (1 to 3 cm in size) containing diamond, and one with graphite, consist predominantly of lilac garnet with diamond (or graphite) ± chromite and altered silicates. The garnets are predominantly high-Cr (> 8 wt%), Ti-depleted, and extremely sub-calcic (< 3 wt%). However, three specimens have high-Cr calcic compositions. The chromites are Cr-rich, Ti-depleted, whilst the solitary olivine is $Fo_{93.4}$. The sub-calcic garnets display a narrow range of trace element signatures, depleted in Zr, Y, Ga, and Ti, whilst Sr and LREE's are enriched. The $[REE]_n$ patterns are all very similar and display a sinusoidal shape. The most calcic diamondiferous garnet analysed at Newlands yields a $[REE]_n$ pattern similar to "fertile" mantle garnets. The major and trace element geochemistry of the sub-calcic garnets is similar to inclusions in diamonds and diamond-bearing peridotites world-wide. Geothermometry yields temperatures ranging from 900 to 1050 °C, equivalent to pressures of 40 to 55 kbar (based on a 37-38 mW/m^2 geotherm determined from Newlands coarse peridotites). This P-T range is within the diamond stability field. Four diamond-bearing peridotitic garnet macrocrysts are Re depleted and yield a range of ages spanning from the Proterozoic (minimum T_{RD} 1.77 Ga) to the mid-Archæan (maximum T_{MA} 3.52 Ga).

Seventeen eclogites (2 to 6 cm in size) containing diamond are dominated by coarse-grained garnet and clinopyroxene, with primary trace phases including sulphides and rutile. Alteration is pervasive and ranges from minor grain boundary effects to massive mineral (primarily clinopyroxene) replacement. The garnets have Na_2O concentrations greater than 0.07 wt%, whilst the clinopyroxenes have K_2O concentrations greater than 0.08 wt%. Both phases are Fe-rich and Ca- and Mg- poor relative to other eclogites from Newlands. The garnets display a very restricted range of trace element compositions and are relatively enriched in Ga, Zn, Mn and Ti, and depleted in Cr and Ni relative to most diamond-free eclogites from Newlands. The garnets have similar $[REE]_n$ patterns that are $[HREE]_n$ enriched. The clinopyroxenes

also display a restricted range of trace element compositions (with one exception), and are relatively enriched in Ga, Zn, Zr, Mn and Ti, and depleted in Ni relative to diamond-free eclogites from Newlands. The clinopyroxenes have similar $[REE]_n$ patterns that are $[LREE]_n$ enriched. Bulk rock major element compositions (calculated assuming a 50:50 garnet-clinopyroxene ratio) are compositionally similar to ancient (Proterozoic or Archæan?) magnesian basalts. A statistical analysis of eclogites at Newlands indicates that those associated with diamonds have a discernible geochemistry. The diamond-bearing eclogites, with one exception, have textures and mineral geochemistry equivalent to Group I (and Group B) eclogites (depending on the classification scheme used). Geothermometry yields temperatures between 920 to 1080 °C, equivalent to pressures between 42 and 58 kbar (based on a 37-38 mW/m^2 geotherm), which lies within the diamond stability field. Re-Os systematics for the diamond-bearing eclogites are indicative of formation ages in the Archæan. These eclogites had $^{187}Os/^{188}Os$ substantially higher than chondritic mantle at circa 3 Ga. The Re-Os systematics, major and trace element mineral chemistry, and stable isotopes (albeit preliminary) of the diamond-bearing eclogites from Newlands are consistent with a protolith that has interacted within surficial environments. This implies the operation of plate tectonics since the early part of the Earths history.

The peridotitic diamonds occur in two primary forms, namely (< 1 mm) single octahedra or octahedral aggregates. The eclogitic diamonds range in size from approximately 100 μm within diamond aggregates to large single crystals up to 2 mm. The dominant morphology is octahedral but there are also significant numbers of cubes and dodecahedrons, and some cubo-octahedrons. Cathodoluminescence indicates that the eclogitic diamonds grew in at least three distinct periods. FTIR spectra indicate that the peridotitic and eclogitic diamonds display different nitrogen concentrations and platelet peak positions. Specifically, the vast majority of harzburgitic diamonds are Type II (or near Type II) whilst all eclogitic diamonds are Type I, with significantly higher N concentrations. Based on these criteria, the majority of diamonds at Newlands are of eclogitic origin. Furthermore, this difference implies that the peridotitic and eclogitic diamonds at Newlands are derived from separate sources. Both sets of diamonds have type IaAB aggregation states ranging from 0 to 20 %, consistent with diamond formation in the Archæan for both

parageneses. Time-averaged temperatures imply that the diamonds formed at higher temperatures than their ambient levels at the time of kimberlite eruption.

The early Proterozoic to mid-Archæan Re-Os ages obtained for both the diamond-bearing garnet macrocryst and diamond-bearing eclogites at Newlands overlap the major crustal building periods of the Kaapvaal craton (de Wit et al., 1992). This implies that cratonic root stabilisation beneath the Kaapvaal craton is potentially coeval with crustal formation (Kramers, 1979; Richardson et al., 1984; Richardson et al., 1990; Richardson and Harris, 1997). The presence of diamond implies that the SCLM may have extended to depths of approximately 200 km by the end of the Archæan. In addition, the apparent lack of any systematic age variation with calculated equilibrium conditions implies that the SCLM and overlying continental crust nuclei have been coupled since formation. Once formed, these assemblages remain coupled and, under favourable circumstances, can survive the destructive forces of plate tectonics.

TABLE OF CONTENTS: VOLUME I

INTRODUCTION

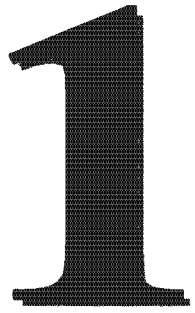

1.1 INTRODUCTION

The study of the upper mantle has reached a relatively mature stage, with current investigations generally focusing on very specific questions or hypotheses. Over the past two decades a wealth of new information has become available - to date there have been seven International Kimberlite Conferences (IKC), with the 7th IKC in 1998 attracting over 600 delegates, several hundred abstracts and more than 100 manuscripts. Nevertheless, the broad topic relating diamonds and their upper mantle host rocks is controversial, and a clear model for diamond genesis does not exist.

Relatively few rocks have been found that directly link diamond to the host rock type. In general, upper mantle studies pertaining to diamond genesis have been based on mineral inclusions encapsulated within diamond, diamonds obtained from run-of-mine production, or diamond-free upper mantle xenoliths. Ergo, current models pertaining to diamond genesis and their relationship with rock types in the upper mantle are based on independent lines of evidence and inferred relationships. Nevertheless, the relatively few studies of diamond-bearing xenoliths are consistent with such models, yet there remain many unanswered questions. Consequently, detailed multi-faceted studies of diamonds and their host xenoliths are potentially an important source of information to constrain and evolve current hypotheses on diamond formation and genesis.

This study will focus on the detailed investigation of the nature and chemical composition of diamond-bearing xenoliths from Newlands kimberlite, located on the Kaapvaal craton, South Africa. The results should help to elucidate and evaluate current models of diamond formation and genesis. Below is a summary of the current evidence and ideas relating diamonds to the upper mantle.

1.2 DIAMONDS AND THEIR MINERAL INCLUSIONS

Diamond is an economically valuable precious mineral and, in addition, is of primary interest in upper mantle studies due to its extraordinary physical and chemical properties and the constraints that these provide. The most common rock type that hosts diamond is kimberlite. However, it is generally believed, based in part on radiogenic dating of mineral inclusions (see section 1.2.3), that diamonds are exotic or xenocrysts and not cognate with the formation of the kimberlite. Accordingly, the kimberlite is just a transportation medium. In addition to kimberlite (and occasionally lamproite), diamonds can often be found in secondary placer deposits (Gurney, 1989), and extremely rarely in other ultrabasic rocks and high-pressure metamorphic assemblages (Sobolev and Shatsky, 1990; Shatsky and Sobolev, 1993; Shatsky et al., 1995). Furthermore, diamonds are known to exist in meteorites and shock-formed impact craters, however such diamonds are predominantly polycrystalline, commonly extremely small, and may have hexagonal symmetry (lonsdaleite) (Gurney, 1989).

Diamond is essentially composed of the element carbon. Sixty-eight elements have been recorded as impurities in diamond, however only nitrogen and boron are known to substitute into the tetrahedral lattice (Sellschop, 1975, 1992). Diamond is naturally stable at mantle pressures and temperatures (greater than ~50 kbar and ~1000 °C). At the Earth's surface diamond is metastable, although the rate of reaction is infinitely slow (Berman and Simon, 1955; Kennedy and Kennedy, 1976; Bundy, 1980). Diamond is by far the hardest known naturally occurring mineral, and is chemically inert, unaffected by the strongest acids (Field, 1992). The low diffusion rates of nitrogen and noble gases through the diamond lattice structure allow diamond to maintain an internal mantle record over extended geological periods (Ozima and Zashu, 1983; Ozima, 1989). Consequently, encapsulated minerals within diamonds can be (in likelihood) protected from diffusive exchange with the surrounding mantle and thus remain unaffected by physical or chemical changes in their local environment. Therefore, inclusions in diamonds can represent "*pristine*" samples of the original minerals formed during the period of diamond crystallisation. In addition, diamond is an excellent conductor and thus any inclusion will yield temperatures that

either represent ambient mantle temperatures (for touching inclusions) or diamond formation temperatures (for separate inclusions – if deemed to be in equilibrium). In contrast, the diamond host rock is an open system that will re-equilibrate in response to local changes in pressure, temperature or chemical conditions.

1.2.1 Diamond source region mineralogy

Diamond inclusion studies from numerous kimberlite locations around the world have yielded a wealth of information, particularly about ancient mantle conditions and the diamond source region beneath cratons around the world. Extensive early studies of mineral inclusions in diamonds (for example, Meyer and Boyd, 1969; Sobolev et al., 1969, 1973; Sobolev, 1977) revealed two dominant mineral associations – the first is mineralogically and chemically broadly akin to *peridotite* (predominantly olivine, accompanied by orthopyroxene, lesser Cr-pyrope garnet and chromite, and by minor diopsidic clinopyroxene), and the other *eclogite* (predominantly pyrope-almandine garnet and omphacitic clinopyroxene). These associations were confirmed by a host of other diamond inclusion studies, for example, see Tsai et al. (1979), Harris and Gurney (1979), Meyer (1987), Harris (1987), Gurney (1989), Harris (1992), and Stachel and Harris (1997a). In addition, other less common diamond parageneses may exist in conjunction with the dominant peridotitic and eclogitic parageneses. A minor *websterite* diamond paragenesis exists, particularly noticeable at Orapa (Gurney et al., 1984). However very few other examples are recorded and it is probable that websteritic diamonds may be related to the eclogitic diamond paragenesis (Gurney, 1989).

Sulphide diamond inclusions are very common and unusually occur well in excess of their modal abundance in either peridotite or eclogite xenoliths (Sharp, 1966; Meyer, 1987; Gurney, 1989; Bulanova et al., 1990). Sulphide diamond inclusions are associated with both the peridotitic and eclogitic diamond parageneses, however, there are geochemical compositional differences between the two (Yefimova et al., 1983; Bulanova et al., 1990, 1996; Pearson et al., 1999). Based on the numerous sulphide inclusions observed, often within a small diamond volume and near the centre, it has been suggested that sulphides could be a seed or catalyst for diamond

growth (Sharp, 1966; Gurney, 1989; Bulanova et al., 1990, 1996; 1998). Also, it was suggested that a *sulphide* diamond paragenesis might exist (Deines and Harris, 1995).

A number of other minerals have also been identified as inclusions in diamonds - some of which are associated with either the peridotitic or eclogitic diamond parageneses (but, in general, only occur rarely), whilst a minor, but significant, percentage are of uncertain paragenesis (for examples see Meyer, 1987, and Harris, 1992). As new studies are undertaken more minerals are identified as diamond inclusions (for example, Stachel et al. (1998a), and Kopolova et al. (1997)). A few rare inclusions in diamonds are of very high-pressure origins, such as ferro-periclase, perovskite, majorite and tetragonal almandine-pyrope, and are believed to be derived from the lower mantle (Moore and Gurney, 1985, 1989; Harte and Harris, 1994; Harris et al., 1997).

Overall, peridotitic inclusions in diamonds are the most common, however, the ratio of peridotitic to eclogitic diamond inclusions varies dramatically from location to location, and even within diamond populations at one location (Meyer, 1987; Gurney, 1989; Harris, 1992). For example, eclogitic inclusions in diamonds are common or dominant (up to 90%) at Orapa (Gurney et al., 1984b), Argyle (Hall and Smith, 1984), Jagersfontein (Gurney, 1989), and Klipspringer (Westerlund, 2000), whilst at Finsch eclogitic diamonds were an order of magnitude more abundant amongst larger diamonds than in smaller varieties (Gurney, 1989; Gurney and Zweistra, 1995). Furthermore, the diamond inclusion ratio does not always mirror the xenolith ratio. For example at Roberts Victor the majority of xenoliths are eclogite - indeed, it is the type locality (Hatton, 1978; Hatton and Gurney, 1987) - yet inclusions in diamonds are predominantly of peridotitic affinity (Gurney et al., 1984a). It should also be noted that the diamond inclusion ratios are generally determined from small diamonds, and it is not known if this distribution is representative of other diamond sub-populations. Indeed, there is some evidence they are not (Gurney, 1989).

Whilst (the majority of) inclusions in diamonds are mineralogically associated with either peridotite or eclogite, they yield distinctive geochemical signatures. Peridotitic (P-type) diamond inclusions are commonly extremely depleted in major element compositions relative to "*fertile*" lherzolite. Olivine and orthopyroxene display high

Mg-numbers and, in addition, garnet is predominantly high-Cr and extremely sub-calcic (Meyer, 1987; Gurney, 1989; Harris, 1987, 1992). Furthermore, these garnets are relatively depleted in Zr, Y and Ga but paradoxically relatively enriched in incompatible elements Sr and light REE's (Richardson et al., 1984; Shimizu and Richardson, 1987; Griffin et al., 1992, 1993; Shimizu and Sobolev, 1995).

Eclogitic (E-type) diamond inclusions predominantly yield garnet compositions that have trace levels of Na_2O (greater than 0.07 wt%) and clinopyroxene compositions with trace levels of K_2O (greater than 0.08 wt%) (Gurney, 1984; McCandless and Gurney, 1989; Gurney et al., 1993; Gurney and Zweistra, 1995). In addition the garnets have elevated levels of TiO_2, whilst the whole rock is low in Cr. Such compositions are similar to those observed in eclogites that display coarse "cumulate textures" (large subhedral to rounded garnets in a matrix of clinopyroxene - termed Group I eclogites) (McCandless and Gurney, 1989). The theoretical whole rock compositions of eclogitic diamond inclusions are often basaltic and yield high temperatures of equilibration (O'Hara and Yoder, 1967; MacGregor and Carter, 1970; Ireland et al., 1994).

1.2.2 Diamond source region P-T

The mineralogy and chemical composition of inclusions in diamonds (both P- and E-types) indicate that the primary environment for diamond formation is within the upper mantle. Multiple high P-T experiments indicate that diamond is naturally stable within the upper mantle at pressures and temperatures greater than ~50 kbar and ~1000 °C (Berman and Simon, 1955; Kennedy and Kennedy, 1976; Bundy, 1980), based on an average cratonic geotherm of 40 mW/m^2 (Pollack and Chapman, 1977). This is supported by the mineralogy and geothermobarometric calculations of inclusions in diamonds. For example, peridotitic diamond inclusions yield pressures and temperatures within the diamond stability field, commonly 50 – 60 kbar and 950 – 1200 °C with rare maxima of ~ 70 kbar and 1400 °C (Meyer, 1987; Gurney, 1989; Griffin et al., 1992; Griffin and Ryan, 1995). Eclogitic diamond inclusions similarly yield temperatures that would be within the diamond stability field on similar

geotherms. However no geobarometer currently exists for eclogitic compositions to confirm their theoretical high-pressure origin.

The confining pressure of fluid and mineral inclusions within diamonds is consistent with formation at these high pressures (Schrauder and Navon, 1993, 1994; Navon, 1991, 1999). Infra-red microspectroscopy of solid submicroscopic inclusions of CO_2 in diamonds reveals spectral shifts corresponding to internal pressures of 70 - 100 kbar at mantle temperatures (Schrauder and Navon, 1993).

Garnets with solid solution of a majoritic component $(MgFe)SiO_3$, that are only stable at very high pressures, are recorded from Monastery, South Africa (Moore and Gurney, 1985), Jagersfontein, South Africa (Deines et al., 1991), Letseng-la-Terai, Lesotho (McDade and Harris, 1999), and Sao Luiz, Brazil (Harte and Harris, 1994). In addition, mineral phases expected in the lower mantle (greater than 300 km), such as (Mg,Fe)-perovskite and tetragonal almandine-pyrope, have recently been observed in diamonds from Sao Luiz (Harte and Harris, 1994; Harris et al., 1997; Hutchinson, 1997). Such mineral inclusions indicate that diamond formation extends to potentially great depths, even from within the lower mantle.

1.2.3 The age of diamond formation

The age of diamond formation is difficult to determine accurately or precisely. Direct determinations on diamonds - incorporating Fourier transform infrared (FTIR) spectroscopy or radiogenic noble gases - are highly imprecise. Indirect determinations based on radiogenic isotope systematics of inclusions in diamonds, although geologically more precise, are constrained by underlying assumptions. Nevertheless, it has been established for some, perhaps most, natural diamonds that a considerable time interval has elapsed between diamond growth and sampling from the upper mantle by the kimberlite (Kramers, 1979; Richardson et al., 1984; Smith et al., 1989; Richardson et al., 1993; Richardson and Harris, 1997; Richardson et al., 1998). In such a scenario, these diamonds are xenocrysts, and not phenocrysts, within the kimberlite. However, whether the diamonds formed in a discrete event, sporadically, or continuously over a substantial period of time, is disputed.

There are only two demonstrated exceptions to the above. The first is the Proterozoic Premier kimberlite where the eclogitic silicate inclusions indicate diamond formation ages close to that of the kimberlite (Richardson, 1986). Nevertheless, other lines of evidence from FTIR studies of Premier diamonds indicate that they are not kimberlite phenocrysts and that they probably formed in the upper mantle (geologically) shortly before kimberlite eruption (Field, 1992). The second is a P-Type sulphide inclusion that yields an age within error of the Koffiefontein kimberlite (Pearson et al., 1998). Furthermore, FTIR on the gem-quality diamond indicates that is has un-aggregated nitrogen, consistent with its young age (Pearson et al., 1998).

To date, peridotitic diamond inclusions have yielded radiogenic ages from the early Proterozoic to the Archæan. The first dating of inclusions in diamonds, based on sulphides from the Kimberley and Finsch kimberlites, yielded model Pb ages in excess of 2 Ga (Kramers, 1979). Later, pooled harzburgitic garnet diamond inclusions from the same two locations yielded model ages of 3.2 ± 0.1 Ga (Richardson et al., 1984). Similar garnets from Udachnaya yield an isochron age of 2.0 ± 0.1 Ga (Richardson and Harris, 1997). Lherzolitic garnet diamond inclusions from Premier kimberlite yielded a model age of 1.93 ± 0.04 Ga (Richardson et al., 1993). Peridotitic sulphides (based on associated olivine inclusions within the same diamond) from Udachnaya yield Re-Os isochron ages of ~ 2 Ga (Pearson et al., 1998b).

In contrast to peridotitic diamond inclusions, the eclogitic diamond inclusions studied so far are younger and span the Proterozoic. Isochron ages, based on Sm-Nd from clinopyroxene and garnet, are 1580 ± 60 for Argyle (Richardson, 1986), 1150 ± 60 for Premier (Richardson, 1986), 1580 ± 60 for Finsch (Richardson et al., 1990), 990 ± 50 for Orapa (Richardson et al., 1990), and 1520 ± 20 for Jwaneng (Richardson et al., 1998). In addition, E-type sulphide diamond inclusions from Udachnaya yielded model ages of 3.1-3.5 ± 0.3 Ga (Pearson et al., 1998, 1999). These ages indicate that the eclogitic diamond paragenesis is not temporally related to the peridotitic diamond paragenesis, even within the same pipe.

A similar, although imprecise, spread of ages is implied from FTIR studies. Diamonds predominantly have highly aggregated nitrogen, commonly equivalent to mantle residence times on the order of a billion year time scale (although this is temperature dependent; for example, Evans, 1992; Taylor et al., 1996). However, a few diamonds have unaggregated nitrogen, that implies considerably shorter geological mantle residence times, even possibly less than a million years (although, again, this is temperature dependent; op. cit.). It should be noted that the vast majority of these latter diamonds are of uncertain paragenesis, frequently fibrous, and often cubes or coats. However, there are a few exceptions. Noticeable a sulphide inclusion from a gem-quality diamond, believed to be of peridotitic affinity, yielded a Re-Os model age within error of the Cretaceous age of the host Koffiefontein kimberlite (Pearson et al., 1998b).

Recent studies have questioned the idea that diamonds with peridotitic inclusions are of ancient origins (Shimizu and Sobolev, 1995; Shimizu et al., 1997; Sobolev et al., 1997; Pearson et al., 1998). A study of single Cr-pyrope garnet diamond inclusions from Udachnaya revealed over an order of magnitude compositional variations for several trace elements (Shimizu and Sobolev, 1995; Shimizu et al., 1997). The variation in Sr (from less than 10 ppm to greater than 700 ppm), combined with implied extreme fluid-crystal partition coefficients, led Shimizu and co-workers to suggest a model of disequilibrium garnet crystallisation that was quenched by diamond encapsulation and the rapid eruption of the Udachnaya kimberlite shortly thereafter. This implied diamond ages contemporaneous with the kimberlite. However, this model is in contradiction to pooled Cr-pyrope garnet diamond inclusions from the same location that yield Sm-Nd model ages of ~2 Ga (Richardson and Harris, 1997). In support of this ancient age, all the diamonds from which the latter garnets were extracted had a nitrogen aggregation status corresponding to mantle resident times well in excess of those required for garnet homogenisation (Richardson and Harris, 1997).

1.2.4 Sources for Diamond formation and growth

Very little is proven about the diamond source carbon species and growth rate of diamonds. The morphology and growth patterns of diamonds suggest growth from a

(metasomatic?) fluid or melt (Sunagawa, 1984, 1989). However, depending on the prevailing redox conditions, the source carbon for the diamonds may be in the form of CO_2, CO, CH_4 or other hydrocarbon species. A range of studies indicate that the oxygen fugacity varies between the FMQ (fayalite + O_2 = magnetite + quartz) and IW (iron wustite) boundaries within the upper mantle (Eggler and Baker, 1982; Daniels and Gurney, 1991; Ballhaus et al., 1991; Bulanova, 1995). Over this oxygen fugacity range, and combined with diamond stability field P-T's, all of the above mentioned carbon species may be in equilibrium with diamond. For example, Haggerty (1986, 1994) emphasised that variable conditions at the lithosphere-asthenosphere boundary allow either the reduction of CO_2 or the oxidation of CH_4 to readily occur when carbon species transgress the asthenosphere-lithosphere boundary.

Diamonds can record very complex growth histories. This is noticeable in variations in CL patterns from zone to zone within a diamond, in nitrogen concentration and aggregation states, and in nitrogen and carbon stable isotopes (for example, Mendelssohn and Milledge, 1995; Bulanova, 1995; Chinn 1995; Fitzsimmons et al., 1998; Hauri et al., 1999). In addition, diamonds from George Creek grew, were resorbed, and then grew again in the presence of CO_2 (Chinn, 1995; Chinn et al., 1995). In addition, coats are common on diamonds, whilst inclusions of diamond within diamond are well known (Gurney, 1989). Sulphide inclusions in a single diamond from Udachnaya have yielded a range in Pb model ages, decreasing from core to rim (Rudnick et al., 1993; Pearson et al., 1998). The above evidence indicates that diamond growth can be episodic, but the period of each diamond growth phase or between each growth episode is uncertain.

There have been a multitude of studies on the carbon isotopic composition of diamonds that have established a clear distinction between peridotitic and some eclogitic diamonds (for example, see Deines, 1980; Galimov, 1991; Kirkley et al., 1991; Boyd et al., 1994; and references therein for a detailed review). Peridotitic diamonds have a $\delta^{13}C$ range of between +1 to -10 ‰, with the vast majority clustering more closely around a mean of - 4.6 ‰. The vast majority of peridotitic diamonds are within 3 ‰ of the mean. In contrast, eclogitic diamonds span a far broader $\delta^{13}C$ range from +3 to - 35 ‰. However, it is noticeable that eclogitic diamonds display a multi-

modal distribution, with a significant proportion overlapping peridotitic diamonds (between –3 to –7 ‰) (op. cit.). Whilst peridotitic diamonds are believed to be derived from primordial mantle carbon – and thus represent its isotopic state – this cannot account for the $\delta^{13}C$ range in eclogitic diamonds. Consequently, various theories have been proposed to account for the large spread of $\delta^{13}C$ in eclogitic diamonds. These include isotopic fractionation (Javoy et al., 1984, 1986; Galimov, 1991), primordial mantle heterogeneities (Deines 1980; Deines et al., 1987), and subducted carbon (Kirkley et al., 1991). The $\delta^{13}C$ range displayed by eclogitic diamonds is strikingly similar to those for carbonate minerals and hydrocarbons and is the basis for the latter theory, which is currently the most popular. Other indirect lines of evidence from inclusions in diamonds also support this theory. The oxygen isotopic composition of eclogitic garnet and clinopyroxene diamond inclusions (Lowry et al., 1993) and diamond-bearing eclogites (Kyser, 1991; Ireland et al., 1994; Mattey et al., 1994; Jacob et al., 1994) deviates significantly from mantle values. Similarly, sulphur and lead isotopic compositions of eclogitic sulphide diamond inclusions are outside the expected mantle range (Eldridge et al., 1991, 1995). Collectively, this provides strong evidence that some material involved in the formation of eclogitic diamonds and their host xenoliths did not originate in mantle, the most likely source are protoliths that have experienced surfical processes, such as recycled oceanic crust and overlying sediments (Kirkley et al., 1991; Boyd et al., 1994). Against this, Cartigny et al. (1999) proposes that the N isotopes do not fit such a model, however, the current understanding of the behaviour of nitrogen in the mantle is poor.

1.3 DIAMOND-BEARING XENOLITHS

The vast majority of information summarised above is based on either diamond mineral inclusions or diamond sub-populations obtained from run-of-mine production. Relatively few specimens exist where diamond is observed in a mantle xenolith. Furthermore, diamond-bearing xenoliths that contain diamonds with silicate inclusions of the same mineralogy as the host xenolith are almost unheard of. Whilst diamond-bearing specimens are rare, it is also a function of the availability and accessibility of obtaining suitable samples from kimberlite locations. This is

primarily controlled by mining operations, and accordingly, leads to a conundrum for researchers, as mining operations dictate the processing of kimberlite (or lamproite) ore to liberate diamonds thereby destroying diamond-bearing xenoliths.

Nevertheless, diamond-bearing xenoliths are occasionally found, and confirm the evidence from inclusions in diamonds, namely the association of diamond with both peridotite and eclogite. However, in contrast to inclusions in diamonds, diamond-bearing eclogites are relatively more common than diamond-bearing peridotites (Gurney, 1989). Furthermore, diamond-bearing xenoliths typically rarely contain sulphides as a trace phase, if at all, even though sulphides are one of the dominant inclusions observed.

A literature survey has revealed that less than thirty diamond-bearing peridotites[1] have been reported from around the world compared to many hundreds of diamond-bearing eclogites. The majority of the peridotites are from the Siberian craton, Russia, and, in particular, the Udachnaya kimberlite (Pokhilenko et al., 1977; Sobolev et al., 1984; Pokhilenko and Sobolev, 1986), with specimens also reported from Mothae in Lesotho (Dawson and Smith, 1975), Schaffer in the USA (McCallum and Eggler, 1976), Finsch in South Africa (Shee et al., 1982; Viljoen et al., 1992), Roberts Victor in South Africa (Viljoen et al., 1994), Aikhal in Russia (Sobolev et al., 1969; Sobolev et al., 1984; Pokhilenko and Sobolev, 1986), Mir in Russia (Sobolev et al., 1984; Pokhilenko and Sobolev, 1986), and Argyle in Australia (O'Neill et al., 1986; Jaques et al., 1990). With the exception of Udachnaya, all the other studies report only a few specimens from each location, and in some cases, only one.

Many of the diamond-bearing peridotites are altered to various extents. For example, those from Aikhal are altered to such a degree that primary mineralogy cannot be determined (Sobolev et al., 1969), whilst those from southern Africa commonly display serpentinisation of olivine and orthopyroxene (Shee et al., 1982; Viljoen et al., 1992). The diamond-bearing peridotites from Argyle (Australia) have experienced retrograde metamorphism in the spinel field that has resulted in partial re-equilibration with the total break down of garnet to heterogeneous aggregates of fine-

[1] The term "peridotite" is not used as per its common definition, but rather to represent any xenolith of peridotitic affintiy.

grained chrome spinel plus metamorphic minerals (O'Neill et al., 1986; Jaques et al., 1990). In contrast, the samples from Udachnaya (Siberia) are fresh but have unusually coarse mineralogy (olivine crystals up to 10 cm in maximum dimension).

The majority of the southern Africa diamond-bearing peridotites have garnet compositions that are lherzolitic and not harzburgitic – for example, four of five samples from Finsch, five of ten from Roberts Victor, and the solitary sample from Mothae (Dawson and Smith, 1975; Shee et al., 1982; Viljoen et al., 1992; Viljoen et al., 1994). Only samples from Udachnaya, Roberts Victor and Aikhal yield high-Cr sub-calcic garnet geochemistry similar to that displayed by the abundant garnet diamond inclusions analysed world-wide (Pokhilenko et al., 1977; Sobolev et al., 1984; Viljoen et al., 1994). Several of these samples also contain high-Cr chromites, similar to chromite diamond inclusions world-wide. Calculated equilibrium conditions for the diamond-bearing peridotites are within the diamond stability field and overlap the P-T range indicated by peridotitic diamond inclusions.

The lack of diamond-bearing harzburgitic peridotites world-wide is remarkable given that harzburgitic inclusions are the dominant diamond paragenesis. For example, at Finsch it is estimated that over 95% of diamonds in the –5 +6 sieve size are of the harzburgitic paragenesis (Gurney et al., 1979), yet only one diamond-bearing harzburgite has been found compared to four diamond-bearing lherzolites (Viljoen et al., 1992). Even then, this solitary diamond-bearing harzburgite is not as sub-calcic as diamond-inclusions analysed from Finsch (Gurney et al., 1979). The reason(s) for this apparent paradox is unknown. Garnets of similar major and trace element geochemistry exist as macrocrysts in kimberlite and therefore the garnet inclusion geochemistry does not represent unique relict compositions. Instead, it is likely that the diamond-bearing peridotites disaggregate. One proposed mechanism involves the break down of carbonate minerals in peridotite xenoliths from decompression during ascent to the surface in the kimberlite (Harte et al., 1980; Harte and Gurney, 1981; Boyd and Gurney, 1982).

Diamond-bearing eclogites have been reported from a variety of locations around the world – the first were recorded from Newlands (Beck 1898, 1899; Bonney, 1899, 1900; Wagner, 1911, 1914). Others locations include Udachnaya, Siberia (Jerde et

al., 1993; Snyder et al., 1993; Ireland et al., 1994; Jacob et al., 1994), Mir, Siberia (Taylor et al., 1996; Snyder et al., 1997), Bellsbank, South Africa (Viljoen, 1995), Star, South Africa (Gurney and Hatton, 1989), Frank Smith, South Africa (Rickwood et al., 1969), Roberts Victor, South Africa (Johnson, 1908; Rickwood et al., 1969), and Orapa, Botswana (Shee and Gurney, 1979; Robinson et al., 1984; Viljoen et al., 1996), to name a few. The geochemistry of eclogitic minerals is often similar that of inclusions in diamonds from the same locality, for example Mir, Siberia (Sobolev, 1977). However, elsewhere there may be large differences, for example Star, South Africa (Gurney and Hatton, 1989). Temperatures of equilibration place the diamond-bearing eclogites within a range consistent with diamond stability on assumed geotherms at pressures greater than 45 kbar. No accurate geobarometer exists for eclogitic mineralogy.

1.4 AIM

Whilst the relationship between peridotite or eclogite and diamond is well established, the origin of the diamond-bearing peridotite or eclogite is disputed and hampered by lack of evidence. This study is unique in that it involves a detailed investigation of two suites of diamond-bearing xenoliths from one location, namely peridotite and eclogite from Newlands kimberlite. It is the first simultaneous study of diamond-bearing peridotite and diamond-bearing eclogite from one source. This may be particularly instructive in elucidating the relationship between peridotitic and eclogitic diamonds, if any. The overall aim of this project is to investigate the age and evolution of the diamonds and associated diamond-bearing upper mantle sampled by the Newlands kimberlite. The results will be compared to the diamond-free upper mantle samples from Newlands, as well as inclusions in diamonds and diamond-bearing xenoliths from around the world.

The study of diamond-bearing upper mantle xenoliths can yield important information relating to the (genetic) relationship between the diamonds and their host xenolith and the geological processes and events that have affected them over time, both pre and post diamond formation. However, such studies are hindered by the lack of suitable samples to analyse as they are extremely rare. Newlands has provided both diamond-

bearing peridotite and eclogite in significant numbers and it is apparent that the Newlands kimberlites contain a wealth of significant geological information in the field of upper mantle studies. The only scientifically documented locality where a similar study has been possible to date is the Udachnaya kimberlite in Siberia (Pokhilenko et al., 1977; Sobolev et al., 1984; Pokhilenko and Sobolev, 1986).

To achieve the aim of this thesis the following were implemented:

- Intensive sampling of the upper mantle component of Newlands kimberlites to assemble representative suites of diamond-bearing peridotite and eclogite.
- At the same time a substantial suite of diamond-free peridotite and eclogite, as well as other upper mantle components, such as websterites, megacrysts and mineral macrocrysts, were collected.
- Diamonds from the -1000 μm fraction were obtained.
- The diamondiferous assemblages were studied in detail by means of:
  - Electron microprobe (EMP) for mineral major element compositions.
  - Proton microprobe (PMP) and Ion microprobe (IMP) for trace element distribution in minerals.
  - Mass spectrometry for Re and Os systematics.
  - FTIR for spectral studies of the diamonds.
- Where relevant the diamond-free xenoliths were also characterised using similar methods so that the relationship between the diamond-bearing xenoliths and the upper mantle as a whole could be thoroughly investigated.

The diamond-bearing samples, which form the core of this study, are small and extremely rare. As a result, care was required in choosing which analytical techniques to use and in which order so as to maximise the potential geochemical information for later interpretation. Detailed descriptions of the various techniques and operating conditions are given in the appropriate chapters and Appendix I.

1.5 THESIS OUTLINE

This thesis is presented in two volumes: Volume I contains the text and references, whilst Volume II contains the appropriate Figures, Tables, Plates and accompanying

Appendices. In addition, Volume I has been divided into five parts. Part I is an introduction section and summarises current knowledge and theories regarding the origin of diamonds. It also provides a background to the Newlands kimberlites and the xenoliths to be analysed in this thesis. Parts II and III focus on diamond-bearing peridotite and diamond-bearing eclogite xenoliths from Newlands, respectively. In addition, several inclusions in diamonds derived from the diamond-bearing peridotites, as well as a sub-set of both diamond-free peridotite and eclogite from Newlands have been studied for comparison. Detailed results for major and trace element concentrations, geothermobarometry determinations, and Re-Os radiogenic isotopes will be presented. Part IV concentrates on the diamonds from the xenoliths and compares them to Newlands run-of-mine diamonds. This section includes diamond descriptions, cathodoluminescence, and FTIR determinations. Part V consolidates the previous sections with a review of current hypotheses of the formation of the various components of the upper mantle and a detailed discussion of the Newlands specimens in relation to these hypotheses.

NEWLANDS KIMBERLITE AND ITS UPPER MANTLE XENOLITH SUITE

2

2.1 NEWLANDS KIMBERLITE

2.1.1 The Newlands kimberlite pipe and dyke complex

The Newlands kimberlite occurrences are part of a larger cluster of Group II kimberlites located approximately 60 km north west of Kimberley, South Africa, in the Barkly West district (Gurney et al., 1991). Newlands is sited on portion 1 of farm 172, 20 km to the NW of Barkly West near the Harts river. Figure 2.1 highlights the position of the Newlands kimberlites relative to the other known kimberlites in the area. The Newlands kimberlites, as well as other kimberlites in the Barkly West district (e.g. Frank Smith, Bellsbank, Bobbejan) and the foremost topographical features, are aligned along major structural features in a NE-SW direction. Newlands intrudes thin flat lying to gently undulating Dwyka shales and mudstones that dip at low angles to the west. These shales and mudstones lie conformably on Dwyka tillite that in turn lies unconformably on the Precambrian Ventersdorp lava. Dolerite sills up to 3 m thick intrude the area, frequently outcropping, and are covered by a thin layer of immature soil with numerous calcrete horizons. A detailed stratigraphy of the area, taken from a 260 m borehole on the Newlands property, is presented in van Coller (1995). The narrow elongate lenticular kimberlite dykes, which are generally less than 1 m in width, are locally referred to as *fissures*, whilst the associated small pipe-like kimberlite pipes, which commonly do not persist to any great depth, are locally called *blows*. Henceforth, in this study the Newlands kimberlite cluster, which consists of both dykes and pipes, will be referred to as just "*Newlands*".

The various kimberlite pipes and dykes are all very micaceous and of Group II affinity (Smith et al., 1985a; van Coller, 1995). A Rb-Sr isochron of kimberlite whole rock and phlogopite macrocrysts yields an age of 114.1 ± 1.6 Ma (Smith et al.,

1985b). This age is similar to other Group II kimberlites in the Barkly West district (~ 110 Ma to 120 Ma: Smith et al., 1985b). In contrast, nearby Group I kimberlites are younger (~ 80 Ma to ~ 95 Ma) (Smith et al., 1985b). Newlands consists of a series of en-echelon kimberlite dykes trending N30°E, on which there are at least 5 kimberlite pipes to the surface. These small diatremes have previously been numbered 1 through 5, respectively, with pipes 1 and 2 located on the northern dyke and pipes 3, 4, and 5 on the southern dyke (Figure 2.2, Plate 2.1). The pipes vary in size from ~30 m to ~90 m diameter at surface - pipe 2 has the largest areal extent (at approximately 0.15 hectares). Mining of pipe 2 to over 120 m below surface reveals that it increases in size with depth, having an ~70° dip contact with country rock (van Coller, 1995). The kimberlite dykes are visible leading into and away from both pipe 1 and pipe 2 (Plates 2.2 and 2.3). In general, these dykes are ~ 1 – 2 m at the pipe circumference but pinch and swell along strike. Structural relationships reveal that external kimberlite dykes pre-date, whilst internal dykes post-date the kimberlite pipes (this study; van Coller, 1995).

Smith (1983) suggested a possible relationship between Newlands and Frank Smith kimberlites based on their similar phlogopite Rb-Sr isochron age and their geographical proximity (~ 10 km apart) parallel to the trend of the dykes. However, van Coller (1995) rejected this based on a petrographic and geochemical study of the various Newlands kimberlite pipes and dykes which he concluded were more akin to the Bellsbank kimberlite dykes.

2.1.2 Historical Background

Newlands kimberlite was discovered in the late nineteenth century but has only been sporadically prospected or mined ever since. In 1879 George Paton applied for rights to prospect for diamonds at Newlands and mining commenced in 1881. By 1889 over 2000 carats had been mined, with an average yield of 14 carats per 100 loads[2] (Matter, 1972). Many 3 to 6 carat diamonds were found, however, the larger stones - up to 15 carats - were generally of poor quality (op. cit.). After funds were raised in London a plant was erected in 1896 and a shaft sunk to a depth of 140 m in the belief

[2] one load is approximately three quarters of a tonne

that fresh kimberlite (or "blue ground") would yield higher grades (Gräichen, 1903). Mining continued until 1903 when the company went into voluntary liquidation. During this period several studies were made of both the Newlands kimberlites and its various xenoliths. Three historically important studies are those of Bonney (1899, 1900), Beck (1898, 1899), and Gräichen (1903) that describe the discovery of the first diamond-bearing eclogite in the world and record the association between pyrope and diamond. Gräichen (1903) also reported on the small but abundant high quality diamonds. For the next few decades attempts were repeatedly made to revive Newlands without success. The owners of the farm (the Du Plessis') on which Newlands is situated prospected from 1956 to 1959. Over this period they mined both pipe 2 and pipe 3, with an average grade of 9-10 carats per hundred tons. The largest diamond recovered was of poor quality and weighed 23 carats. In 1976 pipe 1 was sampled and yielded a grade of 25 carats per 100 loads (Daniels, 1980). Activity again ceased until 1994 when Gem Mining set-up a prospecting plant for processing both the kimberlite and the old tailings of pipe 2 and for assessing material from the other associated pipes. Prospecting continued until the beginning of 1997 after which time activity has ceased on Newlands.

2.1.3 Previous Studies of Newlands kimberlite and its xenoliths

Upon the opening of the first mining period in Newlands' history several geologists visited the site to investigate the various kimberlite pipes and dykes. What they found astounded them when compared to other observations of the various kimberlite bodies known in the Kimberley area at the time. A vast range of heavy minerals and other xenoliths were recorded - of particular importance were the various descriptions of "*concretions in the kimberlite that contain diamonds*" (Gräichen, 1903). These include the first reported occurrence of diamondiferous eclogite in the world (Bonney, 1899), and some of the first diamond-bearing pyrope garnets (Beck, 1898, 1899). This lead Beck (1898) to write:

"The future openings (of Newlands mine) may be of great importance to geology especially as the remarkable connection between garnet and diamonds will be shown up clearly."

This statement of Beck is a century old but it is only recently that some form of understanding of this relationship has come to light. Early studies by Beck (1898, 1899), Bonney (1899, 1900) and Gräichen (1903) all noted the geological significance of the xenoliths found in Newlands kimberlite and "*the appearance of diamonds in firm connection with pyrope*" (Beck, 1898). They also realised the importance of the discoveries upon the question of diamond genesis, where they had divergent views. Bonney (1899) suggested that the diamond-bearing eclogites were "*water-worn boulders*" derived from the Dwyka Conglomerate. Meanwhile Beck (1898) regarded the "*garnet pyroxene*" aggregates as early segregations from the kimberlite magma. Although the suggestion of Bonney (1899) for the source of the eclogite is clearly wrong, the overall concept that the eclogites are accidental inclusions in the kimberlite is valid.

The various kimberlite pipes and dykes were petrographically and geochemically studied in detail by van Coller (1995). A variety of selected upper mantle xenoliths were analysed in several other studies, generally as part of larger investigations. Daniels (1980) investigated a selected few of the unusual mantle xenoliths found at Newlands, including a detailed geochemical study of a peridotite displaying unique banding. Green garnet macrocrysts were described by Lawless (1977), whilst Griffin and Ryan (1995) analysed a variety of garnet macrocrysts for major and trace elements, in particular, to apply their empirical Ni thermometer. Smith et al. (1989) analysed a solitary diamond-bearing eclogite from Newlands for major element compositions and Sr and Nd isotopic systematics as part of their larger detailed study of southern African diamond-bearing eclogites and eclogitic diamond inclusions.

2.1.4 Kimberlite description and petrography

2.1.4.1 Kimberlite dykes

Regional fracture patterns trend NE-SW and govern the kimberlite dykes orientations. The Newlands dykes are thin, vertical, sub-parallel sheets concentrated in narrow zones. The dykes pinch and swell along strike, often bifurcating, reaching a maximum width of just over a metre and narrowing down to stringers only centimetres wide. The dykes are visible in the pit walls of pipe 2 (Plate 2.2) and pipe

1 (Plate 2.3), and can be traced for 10's of metres both on surface and under-ground. The dyke running to the north of pipe 2 extends for between 10 and 20 metres at surface before thinning and bifurcating into stringers on the centimetre scale; in contrast, the same dyke (?) underground (at the 60 m level) extends for ~ 50 metres before thinning.

Structural relationships indicate that the dykes both pre- and post- date the pipes. Precursor dykes are truncated by the kimberlite pipes and also can be recognised as inclusions within those kimberlite pipes. Contemporaneous dykes are linear offshoots of the kimberlite pipe into the wall rock, whilst later dykes occur internally within the kimberlite pipes but do not penetrate into the surrounding wall rock (this study; van Coller, 1995). Most of the kimberlite dykes in the area are good aquifers and thus have undergone intense weathering and secondary carbonatisation. Even so, two types of "fresh" kimberlite dyke material were recognised by van Coller (1995); both have a hypabyssal macrocrystic texture with a high proportion of olivine grains and an opaque rich, fine-grained matrix.

2.1.4.2 Kimberlite pipes

Five kimberlite pipes have been identified at surface and outcrop on two sub-parallel dykes (Figure 2.2). The kimberlite pipes can also be elongate in the direction of the trend of the dykes. Multiple kimberlite phases have been identified at each of the various pipes. Pipe 2, where prospecting has allowed observations to a depth of 120 m, has at least three phases that are distinguishable on a macro-scale, primarily based on the variety and amount of mantle, crustal and country xenoliths. Plate 2.4 displays a sharp contact between two phases - one phase volumetrically contains well in excess of 50 % of country rock and basement xenoliths whereas the other phase contains < 5 %. Van Coller (1995) identified ten petrographically distinct kimberlite phases at Newlands from the five pipes - all group II micaceous hypabyssal kimberlites based on the classification scheme of Clement and Skinner (1979) and Skinner and Clement (1979). The kimberlites have a mica rich groundmass with numerous well-rounded olivine macrocrysts and contain abundant mantle minerals, particularly garnet. The various pipes show a wide range in the amount and variety of xenoliths, even within the one pipe (Plate 2.4 through 2.7). The different phases could not, however, be

separated on the basis of their groundmass phlogopite or spinel geochemistry (van Coller, 1995).

2.1.5 Newlands Diamonds

Newlands is well known for the quality of the diamonds it produces, however, they are generally small with very few recorded large diamonds. Original reports from the turn of the century described the diamonds as chiefly "*octahedrons, very sharp in form*" (Beck, 1899) that averaged between 0.1 and 0.2 cts (Gräichen, 1903). Only pipe 2 has ever been mined for an extended period of time, although pipe 1 has been prospected repeatedly. Pipe 2 is the only kimberlite pipe potentially economic with grades varying between 17 to 60 cpht[3] (this study, Table 2.1 and 2.2; van Heerden and Gurney, 1994).

The first noticeable feature from Table 2.2 is the lack of "larger" diamonds, that is, diamonds that weigh greater than 1 carat. This is consistent with a detailed diamond assessment study performed by van Heerden and Gurney (1994) where only 6 diamonds greater than 1 carat (the largest less than 3 carats) were reported from a far greater tonnage of processed ore than the data presented in Table 2.2. Furthermore, historical diamond reports note the lack of large diamonds (Gräichen, 1903; Matter, 1972). Noticeably, the smaller sieve size makes up over half the production except in the case where 3 diamonds of larger than 1 ct were found. This is similar to the findings of van Heerden and Gurney (1994) even though there was a much higher grade of 50 cpht. Accordingly, Newlands has been regarded as a "*small*" stone (<1 ct) mine.

The second noticeable feature is the grade of just under 20 cpht. This is markedly lower than the average 50 cpht recently reported in the study of van Heerden and Gurney (1994), but marginally higher than the historical yielded of between 8 to 15 cpht (C. Cotterrell, pers. com.; Matter, 1972). A likely explanation for the variety of grade observed within pipe 2 is the complex spatial relationships of the different kimberlite phases (at least three) and the resulting varying dilution factors of xenoliths. As

[3] cpht = carats per hundred tonnes

mentioned earlier, xenoliths may volumetrically contribute over 50 % of the kimberlite (Plate 2.4 through 2.7).

2.2 NEWLANDS XENOLITHS INVESTIGATED IN THIS STUDY

Samples were collected at regular intervals by the author and John Gurney during prospecting of Newlands by Gem Mining between 1994 and 1997. The majority of the specimens were collected from the coarse concentrate[4] by sorting through all the oversize (1-10 cm) and selecting the lower crust and upper mantle xenoliths. Samples were also collected from kimberlite ore stock piles and from old floor dumps. Several thousand specimens were studied under a binocular microscope and classified into mantle rock types. All the diamond-bearing samples and a selection of other upper mantle xenoliths were chosen for further petrographic and analytical work. The full list of diamond-bearing xenoliths selected for further study is given in Tables 3.1 and 8.1, respectively, along with their mineral assemblages. The vast majority of mantle xenoliths were derived from pipe 2, however, some specimens were also collected from pipe 3 and from old mine dump floors.

The primary emphasis of this thesis is on the diamond-bearing peridotitic garnet macrocrysts and diamond-bearing eclogites. For clarity the Newlands xenoliths will be termed ***"diamond-bearing"*** and ***"diamond-free"*** throughout this thesis. This classification is based purely on the observed presence or absence of diamonds in each xenolith and cannot be equated with a genetic classification, particularly given the small size of many of the samples. Indeed, it is highly probable that some xenoliths were in co-existence with diamond but the sample entrained within the kimberlite and brought to the surface did not contain diamond.

The mineralogical variety of xenoliths observed at Newlands is extensive (Table 2.3). Newlands has yielded peridotites ranging from dunites and harzburgites to lherzolites, with and without garnet and chromite. In addition, Newlands is one of the few locations where eclogite is common. The eclogites display a range of mineralogies, including rutile, sulphide, kyanite and corundum bearing varieties. Furthermore,

[4] Coarse concentrate is material that has been through the mine primary crusher.

websterites and wehrlites are also present, although relative to peridotite and eclogite they are rare. As with Roberts Victor, garnet websterites (orthopyroxene-bearing eclogites?) are quite common, with the orthopyroxene at Newlands preserved as opposed to the ubiquitous alteration at Roberts Victor (Hatton, 1978). Phlogopite-bearing (metasomatised?) peridotites also are common. Megacrysts of garnet, pyroxenes and olivine are common, as are the rarer green (high chromium, high calcium) garnets. However, one of the more notable occurrences at Newlands, and the main topic of this thesis, are the presence of diamond-bearing peridotitic garnet macrocrysts and diamond-bearing eclogites.

PERIDOTITIC XENOLITHS: SAMPLE DESCRIPTION AND PETROGRAPHY

3

3.1 INTRODUCTION

Newlands peridotitic xenoliths were primarily collected from the coarse concentrate, which is predominantly less than 5 cm in maximum dimension. In addition, samples were collected from kimberlite ore stockpiles and from old dumps, some of which were much larger (up to 40 cm in maximum dimension). The vast majority of xenoliths were derived from pipe 2, whilst a minor proportion were collected from pipe 3 and others from old mine dumps of untraceable origin (although pipe 2 is the most likely source). The samples obtained from the coarse concentrate are irregularly shaped with "fresh" breakage surfaces, due to processing in the primary crusher, rather than the rounded nature of many larger xenoliths collected from the old dumps or kimberlite ore stockpiles, and recognised at other locations (for example, the large rounded eclogites from Roberts Victor (Hatton, 1978)).

Newlands contains a plethora of upper mantle xenoliths, many of which are peridotites and macrocrysts of peridotitic affinity. Several of the peridotitic garnet macrocrysts contain diamonds. According to IUGS classifications, a peridotite must contain greater than 50% olivine, however, the garnet macrocrysts are included in this section as the mineral compositions are of peridotitic affinity (see Chapter 4).

The coarse peridotite xenoliths selected for further study were based on their suitability for defining conditions of equilibration. Hence the freshest specimens that contained both garnet and orthopyroxene (and thus allow the widest range of geothermobarometers for P-T calculations) were preferred. In addition, consideration was given to harzburgites that had the distinctive garnet colour potentially associated with high-Cr sub-calcic garnet compositions. Such coloured garnets are believed to be associated with peridotitic diamonds and could be compared with the diamond-

bearing garnet macrocrysts. The terminology used to describe peridotite xenolith and xenocryst textures is based primarily on the classification of Harte (1977). Peridotite textures are sub-divided into "*coarse*", "*porphyroclastic*", "*mosaic-porphyroclastic*", and "*granuloblastic*" on the basis of grain size, grain boundaries and the number of porphyroclasts. Each of these textures can further be subdivided using more descriptive textural terms such as equant, tabular, disrupted, fluidal or laminated. For definition of these terms and examples the reader is referred to Harte (1977) and references therein.

Metasomatism is widely recognised to have affected mantle xenoliths and is extensively documented and reviewed in the literature, in particular for southern African peridotites (Harte et al., 1975; Gurney et al., 1975; Harte, 1977, 1983; Dawson, 1984; Waters, 1986; Harte, 1987; Harte et al., Erlank et al., 1987; Winterburn, 1987; Winterburn and Harte, 1987; Menzies and Hawkesworth, 1987; Harte and Hawkesworth; 1989; Menzies, 1990; Winterburn et al., 1990; Burgess, 1997; Burgess and Harte, 1999; Griffin et al., 1999). Metasomatism has two important styles: "*modal*" metasomatism that leads to the introduction of new minerals, and "*cryptic*" metasomatism where the chemical composition of the mineral(s) has changed (Harte, 1977, 1983; Dawson, 1984). In addition, metasomatism may be broadly classified into primary (or early) and secondary (or late stage), where the former refers to interaction with fluids or melts in the mantle domain and prior to entrainment in the kimberlite, whilst the latter refers to interaction with the kimberlite just prior to entrainment or on route to the surface (op. cit.). Primary metasomatism may result in the introduction of coarse-grained minerals that may be in textural equilibrium but are commonly enriched in certain elements not previously abundant in the rock (Harte, 1983). Often these metasomatic minerals are difficult to distinguish texturally from the primary minerals. In contrast, secondary metasomatism is commonly very obvious, with fine-grained serpentine, phlogopite, amphibole and spinel occurring in between the primary minerals or within cracks in the primary minerals. In addition, there may be very-fine grained alteration products, such as kelyphite, which appear around the rims of the various primary mineral phases, in particular garnet. These features are believed to be the result of decompression reactions with kimberlite-derived fluids on route to the surface (Spetsius, 1995; Spetsius and Griffin, 1998).

3.2 DIAMOND-BEARING PERIDOTITIC GARNET MACROCRYSTS

Eighteen peridotitic garnet macrocrysts were observed to contain diamond and one with graphite. Two spectacular samples contain over ten diamonds visible on a freshly broken surface (Plates 3.1 to 3.3), whilst another specimen contains a diamond with both garnet and chromite inclusions (Plates 3.4 to 3.6). Table 3.1 summarises the various phases observed in each specimen, whilst Plates 3.1 to 3.18 display the various diamond-bearing garnet macrocrysts in hand specimen. They range from 1 to 3 cm in their longest dimension and weigh between 1 and 8 grams. A variable percentage (from 0 up to 60 %) is covered by a dull thick (up to several hundred microns) kelyphite coat (Plates 3.11 and 3.12). The garnet and other mineral phases are exposed on fresh breakage surfaces that are most likely the result of crushing in the recovery plant. The kelyphite coats sometimes have indentations often containing the remnants of altered silicates. Rarely diamond or other mineral phases (mostly altered silicates) are exposed through the kelyphite. Plates 3.11 and 3.12 show examples of a diamond protruding through the kelyphite coat of sample AHM E4 and AHM E7, respectively.

The mineralogy of the diamond-bearing peridotitic garnet macrocrysts consists predominantly of "*lilac*" garnet with diamond (or graphite) ± chromite and altered silicates. No primary clinopyroxene was observed in any of the specimens. Altered silicates were observed in many samples, with the majority presumed to be olivine on the basis of shape and alteration product. Only one specimen (AHM 58) contained a fresh olivine core, whilst another specimen (AHM D8) contains a large (nearly 5 mm) sulphide spherule. Primary chromite occurs in over half the samples (11 of the 18 diamond-bearing xenoliths), but only as a minor phase. Its exact modal abundance is difficult to determine due to the small size of the xenocrysts. The chromites are commonly 1 – 2 mm subhedral to euhedral octahedral crystals (for example Plates 3.3 and 3.7). There appears to be a spatial association between the altered silicates (olivine?), chromite (when present), and diamond (Plates 3.3, 3.7, 3.8, 3.9, 3.18). For example, the diamonds in sample AHM 164 are all exposed within a large chromite, itself contained within a larger altered silicate (Plates 3.7, 3.8, and 3.9), whilst in sample

AHM D1 two individual chromites were in contact with two octahedral diamonds (Plates 3.1 and 3.3). The close association of diamond and chromite is also highlighted in sample AHM D2 where they occur together as well as chromite occurring as inclusions within the diamond (Plates 3.5 and 3.6). In addition, two samples (AHM D1 and AHM D5) contain what may be primary phlogopite; however it is not possible to distinguish in hand specimen from severely altered orthopyroxene (see Plate 3.1).

All of the garnet macrocrysts appear to be single garnet crystals, with all other mineral phases present as inclusions (except fracture filling material). In addition, altered silicates and several diamonds were observed within or outside the kelyphite (Plates 3.11 and 3.12). Garnet accounts for between 60% to 90% of the modal mineralogy, with altered silicates comprising the majority of the other mineral phases. In the (relatively) larger (2 – 3 cm) samples the altered silicates comprise between 5 to 15 % whereas for the (relatively) smaller (1 – 2 cm) samples they may comprise up to 30 %. Diamond and chromite (when present) comprise on the order of 1%, although no accurate determinations were made. This carbon content or grade is several orders of magnitude greater than observed in the Newlands kimberlite, or indeed, any diamondiferous kimberlite.

The garnets have varying quantities of sub-parallel cracks or fractures that are all in-filled with secondary mineralisation (Plate 3.4, 3.17, 3.20, 3.21, and 3.22). Both phlogopite and spinels are commonly observed (Plate 3.21 and 3.22) and occasionally calcite. This mineralisation, along with garnet kelyphitisation, is in likelihood due to interaction with the kimberlite en route to the surface. The fracturing ranges in width from fifty to several hundred microns. Whilst none of the samples contained primary clinopyroxene, one specimen (AHM D10) contained secondary clinopyroxene within the garnet fractures. The garnets often contained inclusions of altered silicates, commonly spanning between 300 μm up to 2 mm, with one sample ~ 5 mm (Plate 3.13). The kelyphite rind on the garnet macrocrysts often display various zones (recognisable by their colours under polarised light) that are of different bulk compositions. Detailed descriptions of the diamonds in the peridotitic garnet macrocrysts (and others from Newlands) are given in Part IV of this thesis.

3.2.1 Inclusions in diamonds

Inclusions were observed in several diamonds extracted from the garnet macrocrysts. The majority were small dark clouds, presumably sulphides or graphite, scattered intermittently throughout the diamond. Silicate inclusions were definitively observed in four diamonds, two from AHM D2 and two from AHM D4. The two diamonds from sample AHM D2 contained multiple dark red brown-black inclusions, two of which were confirmed as chromite. Furthermore, one of the chromites (~200 μm) was touching a small (~20 μm) garnet inclusion (Plate 3.6; see also Plate 4.1 and 4.2). These diamonds displayed no evidence of cracks that may have allowed fluids to interact with the inclusions. The two diamonds from AHM D4 contained garnet inclusions; however, the nature of the diamonds (aggregates with serrate lamellae) meant that the inclusions were only observed in the broken diamond fragments. They are thought to be inclusions due to their location within the fragmented diamond and the octahedral morphology of the garnet. The presence of brown material in association with the garnet inclusions and fractures within the diamond suggest that the inclusions were exposed to mantle fluids. However, it is uncertain whether these relate to the kimberlite or proto-kimberlite fluids or ancient fluids trapped with the inclusion at the time of diamond formation.

3.3 Diamond-free Peridotitic Garnet Macrocrysts

Several hundred diamond-free peridotitic garnet macrocrysts were inspected under a binocular microscope. The absence of diamond from these specimens does not preclude their relationship to the peridotitic diamond paragenesis; it is a classification purely derived from physical observation and carries no genetic connotations. These garnet macrocrysts are similar to the diamond-bearing garnet macrocrysts described above, but display a greater range of characteristics. For example, a significant portion contain primary clinopyroxene, whilst others yield fresh olivine and orthopyroxene. Further, the garnet macrocrysts display a wide variety of garnet colours from light mauve to deep lilac. However, the size of the garnet macrocryst, the kelyphitic rind, and highly fractured nature of the garnet all affect the garnet colour in hand specimen, and it is only small "pristine" chips of the garnet that reveal

true colour. Consequently no relationships between colour and garnet composition were examined, although such relationships do exist elsewhere (Gurney and Switzer, 1973; Klump, 1995; Gurney et al., 1995).

3.4 COARSE PERIDOTITES

The range of xenoliths at Newlands is diverse and includes both chromite and garnet bearing lherzolites and harzburgites (see Chapter 2). In addition, both websterites and pyroxenites are present. (Although by definition these two rock types are not peridotites, as per IUGS definitions, they are included in this section for brevity). In essence, all these xenoliths display similar textures and differences can be regarded as variations rather than distinct textural groups. Approximately 50 peridotites were sectioned, and selected samples were analysed for major elements, trace elements and Re-Os isotopes.

The majority of peridotites were obtained from the coarse concentrate and commonly range up to 5 cm in maximum dimension. Several samples collected from old floors or kimberlite ore stockpiles were up to 40 cm in maximum dimension. Both garnet lherzolites and garnet harzburgites are common whilst chromite peridotites are rare, even more so in association with garnet. The small xenoliths were commonly very fresh - rarely was olivine or orthopyroxene altered. In the larger peridotites (> 10 cm) olivine and orthopyroxene were commonly totally serpentinised within 3 cm of the outer surface. Olivine was also generally partially serpentinised throughout the remainder of the xenolith. The modal mineralogy of the lherzolites and harzburgites vary dramatically, in likelihood due to their coarse grained mineralogy combined with their small size. For example, olivine and orthopyroxene are the dominant mineralogy whilst garnet and clinopyroxene commonly modally comprise less than 5%. However, in some rare cases clinopyroxene and garnet together may comprise more than 50% of the xenolith which is thus not true lherzolite or harzburgite. No detailed point counting was undertaken, as the majority of samples were too small and often the grain size too large to accurately represent the source mantle rocks from which they were derived. This is supported by the geochemistry of some of the garnets from mineralogical harzburgites that are calcium saturated (see Chapter 4),

indicating that the garnet in likelihood crystallised in equilibrium with clinopyroxene, even though in many cases (c.f. the garnet macrocrysts) no clinopyroxene was present in the xenolith.

All of the peridotites can be texturally classified as *coarse* (Harte, 1977) or *granular* (Boyd and Nixon, 1972; 1975) (Plates 3.23 through 3.46). Furthermore, the specimens described petrographically displayed equant mineral phases with very few samples exhibiting tabular or vaguely orientated crystallisation. In no cases (either in hand specimen or petrographically) were porphyroclastic, mosaic-porphyroclastic, or granuloblastic textured peridotites observed. These features are customarily associated with high-temperature peridotite suites (for example Boyd, 1973, 1974; Boullier and Nicolas, 1973, 1975; Harte et al., 1975, Harte, 1975) that are found in Group I kimberlites but not in Group II kimberlites such as Newlands.

Grain sizes are variable between specimens and even within a specimen (Plate 3.25 through 3.46). Olivine and orthopyroxene commonly are equant and range from 1 mm to over 10 mm (for example Plates 3.27 to 29). In sample AHM 721 orthopyroxene reaches a maximum size of 25 mm. Garnets and clinopyroxene display the most variability and within any one specimen garnet may range from 500 μm to over 5 mm (Plate 3.25, 3.29, and 3.30). However, no garnets were observed of the scale equivalent to the garnet macrocrysts, even in the large xenoliths collected from the dumps that were up to 40 cm in maximum diameter. Occasionally mineral phases were observed as small inclusions (~100 μm) within other phases.

The mineral phases display a range of grain boundaries from classical triple junctions (for example, Plates 3.25, 3.26, and 3.34) to smoothly curving (for example, Plates 3.23, 3.24, and 3.32). An orthopyroxene from sample AHM C3 displays triple junctions with olivine and garnet on one side and has smooth curved mineral boundaries on the other (Plate 3.33 and 3.34). The mineral phases are frequently highly fractured and cracked, customarily in-filled with secondary mineralisation. Furthermore, in nearly all the specimens, the mineral grain boundaries are separated by in-filling phlogopite and spinels, probably derived from interaction with kimberlitic fluids (for example, Plates 3.35, 3.41, and 3.42). This fluid infiltration and

mineralisation is often pervasive throughout the samples and in localised areas, normally around and through olivine, and can be modally dominant with larger secondary phlogopites and spinels. The garnets display variable amounts of kelyphitisation (Plate 3.25, 3.26, 3.29 and 3.30), however, it is rarely as extensive as observed at other locations, for example Udachnaya (Spetsius, 1995; Spetsius and Griffin, 1998).

Olivine and orthopyroxene occasionally display undulose extinction, evidence of strain and small-scale deformation (Plates 3.35 and 3.36), whilst orthopyroxene infrequently contains exsolution (Plates 3.37 to 3.44). The exsolution is prevalently in the form of lamellae with long blades in the core that decrease in size near the rim (Plates 3.38, 3.43, and 3.44) and, rarely, in the form of blebs. The exsolving phase is probably a Ca-rich clinopyroxene. Furthermore, sample AHM 752 displays elongate garnet and clinopyroxene minerals that appear to be interstitial to the much larger orthopyroxene grains (Plates 3.39, 3.40, 3.45 and 3.46). In Plates 3.45 and 3.46 the garnet has an unusual shape that wraps around several grains of both olivine and orthopyroxene.

3.5 DISCUSSION

The diamond-bearing garnet macrocrysts from Newlands are different to other diamond-bearing peridotites from around the world in two major respects. Firstly, the diamond-bearing garnet macrocrysts from Newlands are not true peridotites, that is, olivine is not the dominant mineral. At most, altered silicates (olivine and orthopyroxene ?) may modally constitute 30 % of the Newlands garnet macrocrysts, but more commonly only 5 to 15 %, whilst garnet comprises between 60 to 90 %. (Although these modal percentages are highly unlikely to be representative of the rock that the xenolith is derived from in the upper mantle). In contrast, diamond-bearing peridotites from elsewhere are dominantly olivine, with the samples from Udachnaya modally comprising of over 95% olivine whilst garnet is only a minor phase, commonly modally less than 5 % (Sobolev et al., 1984).

Secondly, the diamond-bearing garnet macrocrysts from Newlands are single garnet crystals, commonly greater than 1 cm, some as large as 3 cm. Furthermore, these are minimum dimensions of the true crystal size as all of the macrocrysts are broken; it is estimated that some of the garnet crystals may be at least 5 cm in maximum dimension. In contrast, diamond-bearing peridotites from elsewhere commonly have relatively smaller garnet crystals. For example, at Udachnaya garnets range in size from 0.2 to 5.0 mm (Sobolev et al., 1984), whilst at Finsch they range from 1 to 12 mm but are most commonly around 3 mm (Shee et al., 1982; Viljoen et al., 1992).

The diamond-bearing garnet macrocrysts from Newlands are similar to other diamond-bearing peridotites in some respects. Firstly, olivine and orthopyroxene is almost ubiquitously altered. For example, in all seven diamond-bearing peridotites from Aikhal the olivine has been serpentinised (Sobolev et al., 1969; Sobolev, 1977; Sobolev et al., 1984), whilst the outer 3 centimetres of the large diamond-bearing peridotites from Finsch are also serpentinised (Shee et al., 1982; Viljoen et al., 1992). The only exceptions are the diamond-bearing peridotites from Udachnaya where serpentinisation has only occurred along fractures within the olivine megacrysts (Sobolev et al., 1984). Secondly, the samples from Newlands are similar in dimensions to many of the samples, for example Aikhal, but smaller than the few large diamond-bearing peridotites. For example, four diamond-bearing peridotites from Finsch have a maximum dimension greater than 19 cm (Shee et al., 1982; Viljoen et al., 1992) whilst two from Udachnaya range up to 14 cm in maximum dimension (Sobolev et al., 1984). Although the Newlands samples are from the coarse concentrate, which has a maximum dimension of 10 cm, nevertheless the diamond-bearing garnet macrocrysts are between 1 and 3 cm. Thirdly, the Newlands garnets all have a partial outer rind of kelyphite. Fourthly, chromite is present in over half of the diamond-bearing garnets from Newlands and common amongst diamond-bearing peridotites from Udachnaya (Sobolev et al., 1984) and Aikhal (Sobolev et al., 1984). Furthermore, the chromites are commonly on the order of 1 mm flat-faceted octahedral crystals.

Sobolev et al (1984) divided diamond-bearing peridotites (known at the time) into two categories according to the their texture and structure: namely Type I (equigranular with some signs of deformation) and Type II (large megacrysts). Nearly all of the

samples from Udachnaya are classified as Type II and dominated by fragments of megacryst olivine grains that range in size from at least 2.1 cm up to 14.3 cm and comprise over 95 % of the specimen (Sobolev et al., 1984). Under such a classification scheme, all the Newlands samples would also classify as Type II, however, they would be distinctive in that garnet is the dominant megacryst and not olivine.

PERIDOTITIC XENOLITHS: MAJOR ELEMENT MINERAL GEOCHEMISTRY

4

4.1 INTRODUCTION: GARNET GEOCHEMISTRY - LITERATURE TERMINOLOGY

The minerals associated with diamonds, in general world-wide, have well defined compositional ranges – noticeably, diamond inclusion garnet pyropes are high in MgO and Cr_2O_3 and low in CaO (for example, see Gurney and Switzer, 1973; Sobolev, 1977; Harris and Gurney, 1979; Tsai et al., 1979; Gurney, 1984; Meyer, 1987; Harris, 1992; Stachel et al., 1998). There is a variety of terminology used in the modern literature for distinguishing different parageneses of chrome pyropes, and in particular, those associated with diamonds. Detailed studies of garnets from a variety of kimberlite locations has shown that all diamondiferous pipes contain high-Cr low-Ca garnets, similar to diamond inclusions (Gurney et al., 1978; Gurney, 1984). Such garnets can be distinguished in Cr_2O_3 – CaO space using the "*G10/G9 line*" or the "*85 % line*" or the "*lherzolite line*". Note, however, that none of these terms are exact - the true significance of this line is in diamond exploration where all known diamondiferous kimberlites yield garnets that plot in the low calcium field defined by this line (Gurney et al., 1993).

Nevertheless, garnets that plot in the low calcium field (left of the line) are termed G10 or harzburgitic garnets, whilst those that are calcium saturated (right of the line) are termed G9 or lherzolitic garnets, respectively. It should be noted that both the G10/G9 and harzburgite/lherzolite terminology, based on this boundary in Cr_2O_3 – CaO space, are neither geochemically nor mineralogically correct. The original statistical classification of Dawson and Stephens (1975) incorporates all the major and minor elements of garnet compositions from a variety of geological settings and derived 11 garnet groups, of which G9 (Group 9) and G10 (Group 10) are associated with lherzolitic and harzburgitic garnets, respectively. However, the compositions of lherzolitic garnets, which are associated with calcium saturated rocks that contain

clinopyroxene, is a function of pressure, temperature and the whole rock bulk chemistry (Sobolev, 1977; Gurney, 1984; Boyd et al., 1993; Gurney et al., 1993; Gurney and Zweistra, 1995). Furthermore, some of the lherzolitic garnets are also known to be diamond indicators (Richardson et al., 1993). The majority of G10 garnets are from harzburgites (and plot in the low calcium field), but some are derived from lherzolites that have equilibrated at very high (> 50 kbar) pressures, whist the boundary line derived by Gurney (1984) approximates 45 kbar only (Gurney et al., 1993).

Consequently, no current terminology based on garnet compositions is 100 % accurate in relation to garnet paragenesis. That is, garnets that plot in the G9 field may actually be harzburgitic, or alternatively, garnets that plot in the G10 field may actually be lherzolitic garnets. In particular, both cases are possible if they plot close to the boundary line of Gurney (1984). Nevertheless, this line has proved to be a useful discriminator for diamond potential on a world-wide basis (Gurney et al., 1993; Gurney and Zweistra, 1995).

In this thesis (unless defined petrogenetically) the terminology of G10 or harzburgitic garnet pertains to a garnet that plots to the left of the boundary line of Gurney (1984) and is regarded as sub-calcic, whereas a G9 or lherzolitic garnet plots to the right and is assumed to be saturated in calcium.

4.2 METHODOLOGY

4.2.1 Analytical Techniques and Operating Conditions

Mineral analyses for major and minor elements were made using electron microprobes (EMP) housed at three different locations – namely, the University of Cape Town (UCT), Carnegie Institute of Washington (CIW), and the University College London (UCL). In addition, major and minor element maps were made using a proton microprobe (PMP) housed at the national accelerator centre (NAC), Cape Town, as well as the CIW EMP. Explicit details of the set-up and analytical

conditions of each EMP and the PMP are given in Appendix I, whilst all analyses are presented in Appendix II.

4.2.2 Sample description

In excess of 200 garnet macrocrysts were analysed in this study for major element compositions. The garnet macrocrysts contain a variety of other silicate mineral phases, including chromite, olivine and orthopyroxene (commonly altered) and clinopyroxene. Whole rock compositions have not been determined using either a recognised analytical technique (i.e. XRF) or by combining EMP analyses based on the modal mineralogy as both procedures would produce data lacking in accuracy and precision. In particular, the peridotitic diamond-bearing garnet macrocrysts are up to 80 % garnet, and thus are not modally representative of the rock source they were derived from in the mantle. Therefore, analyses for major and minor elements are on individual mineral phases only.

The diamonds from AHM D4 were broken and their inclusions extracted and mounted similar to methods described in Chinn (1995). These included one garnet from each of the diamonds, which were 100 and 120 μm in maximum dimension, respectively. Both garnets displayed octahedral morphology, initiated by the diamond host. In contrast, the diamond from AHM D2 was polished until two inclusions were exposed and then analysed in situ (see Plate 3.6b, Chapter 3). A backscatter image indicated that one of the inclusions was actually comprised of a ~100 μm chromite in contact with a ~20 μm garnet (Plate 4.1 and 4.2). These diamond inclusions were all analysed using EDS on the EMP housed at UCL, while the garnet macrocrysts from which they were derived were analysed using WDS on the EMP housed at UCT.

4.3 PERIDOTITIC GARNET GEOCHEMISTRY

4.3.1 Diamond-bearing Peridotitic Garnet Macrocrysts

Representative garnet compositions from the diamond-bearing garnet macrocrysts are given in Table 4.1. They are mineralogically chrome pyropes, exhibiting high Cr_2O_3

concentrations (greater than 8 wt%) and a diverse range of compositions. They display a range of CaO concentrations, with the majority highly sub-calcic (CaO content less than 3 wt%) (Figure 4.1). However, 5 of the 18 diamond-bearing garnet macrocrysts trend towards and extend well into the high-Cr G9 field. Two of these samples are mildly sub-calcic G10 garnets, whilst the other three are calcic G9 garnets - two of which (AHM E7 and AHM E4) yield the highest Cr_2O_3 and CaO concentrations (12.2 and 7.8 wt%, and 12.5 and 9.2 wt%, respectively) of any peridotitic garnet analysed at Newlands. The solitary graphite-bearing sample has a lherzolitic composition, however, the Cr content is significantly lower than the diamond-bearing lherzolitic garnet macrocrysts. Figure 4.1 presents the garnet Cr_2O_3 – CaO variations in diamond-bearing garnet macrocrysts from Newlands compared to (a) diamond-free garnet macrocrysts, (b) diamond-bearing peridotites from around the world, and (c) inclusions in diamonds from around the world.

The diamond-bearing G10 garnets yield high Cr#'s[5] and Mg#'s[6] (Figure 4.2) and plot in the magnesian-rich sector of the ternary Ca-Mg-Fe diagram (Figure 4.3). In contrast, the diamond-bearing G9 garnets yield decidedly lower Mg#'s and plot (relatively) towards the calcium-rich sector of the ternary Ca-Mg-Fe diagram (Figure 4.3). The high Mg#'s of between 80 to 83 for the highly sub-calcic garnets lowers dramatically to between 74 and 77 for the mildly sub-calcic garnets and then to less than 70 for the three calcic garnets (Figure 4.2). Indeed, the most calcic G9 diamond-bearing garnet macrocryst (AHM E4) records the lowest Mg# (58) of all Newlands garnet macrocrysts.

Titanium is at or below EMP detection limits (~ 0.04 wt% TiO_2) for the highly sub-calcic garnets, whereas it is measurable for the five garnets that extend towards G9 compositions (with a maximum TiO_2 concentration of 0.5 wt%) (Figure 4.4). Manganese concentrations are relatively constant (MnO ranging between 0.28 and 0.35 wt%), with the exception of sample AHM E4 (0.42 wt%) (Figure 4.5). However, this higher MnO concentration may arise from a Cr interference peak (sample AHM E4 has the highest Cr content of any peridotitic garnet at Newlands). The Mn content of garnet is a function of equilibration temperature and this may explain the lack of

[5] Cr# = 100 * Cr / (Cr + Al)
[6] Mg# = 100 * Mg / (Mg + Fe + Ca + Mn)

Mn variation (with one exception) (Shimizu and Allegre, 1978; Brey et al., 1990; Delany et al., 1979; Smith et al., 1991; Grütter et al., 1999).

Multiple core - rim analyses indicate that, in general, the garnets are well homogenised. Detailed point traverses of three diamond-bearing garnet macrocrysts (samples AHM D1, A and AHM D10) yield major and minor element compositions that are predominantly within 2 standard deviations (Figure 4.6 through 4.8). Where there are some subtle compositional changes, there are no systematic variations, i.e. small elemental increases between core and rim for one sample can be reversed for another. Moreover, the subtle changes are commonly at the garnet edge bordered by kelyphite and extend between 50 to 100 μm into the garnet. The occasional individual point spikes observed in some of the analyses can be linked to the many sub-parallel fractures that occur in the garnet macrocrysts (see Chapter 3).

Detailed PIXE elemental maps using a PMP (primarily for trace elements, see Chapter 5) show that Cr and Fe both decrease over short distances towards and within sub-parallel linear features that correspond to fractures within the garnet. The maximum extent of any diffusion effect is on the order of 50 to 100 μm into the garnet before Cr and Fe return to their normal levels (Figure 4.9 a and b). This zonation may be due to a large PMP beam size (commonly ~ 10 μm) and thus large excitation volume (at least 30 μm diameter) that will excite atoms within the garnet but also within any mineral adjacent to the garnet edge or underneath the garnet (if the contact between the garnet and adjacent mineral is not perpendicular to the beam). If this is true then the measurement will be of two overlapping mineral phases resulting in the appearance of an elemental concentration gradient.

4.3.2 Inclusions in diamonds

Representative compositions of the garnet diamond inclusions and the host garnet macrocrysts are given in Table 4.2. The two garnet inclusions from two diamonds from sample AHM D4 yield similar compositions to the host xenolith. There are some subtle elemental differences, for example Cr_2O_3, however, this is likely to be a function of different analytical techniques and different major element reduction

techniques - the host xenolith being analysed by WDS at UCT and the inclusion by EDS at UCL (see Appendix I). The secondary mineralisation around the garnet, indicating that the inclusion has probably re-equilibrated with the surrounding mantle environment may explain the lack of difference in composition.

In contrast, the garnet inclusion from sample AHM D2 (in contact with a chromite inclusion, see section 4.4.2) clearly has a different composition to the host xenolith (Table 4.2). The inclusion is more sub-calcic (CaO average of 1.1 wt% compared to 1.8 wt% for the xenolith garnet) and lower in Cr_2O_3 (average of 8.9 wt% compared to 9.7 wt%) (Figure 4.10). All other elemental concentrations are different resulting in a lower Mg# and Cr# ratio for the garnet diamond inclusion (Figure 4.11). However, both are highly depleted with titanium commonly below EMP detection limits.

4.3.3 Diamond-free Peridotitic Garnet Macrocrysts

All the garnet macrocrysts are mineralogically chrome pyropes and display an extensive range of Cr_2O_3 – CaO compositions, with Cr_2O_3 concentrations extending from minimum of ~ 1.5 wt% to a maximum of ~ 10 wt%. Noticeably, a high proportion of the garnets are classified as G10's, many of which are mildly to highly sub-calcic (Figure 4.12a). There is a noticeable compositional gap that separates the high-Cr and low-Cr G10 garnets (Figure 4.12a). There appear to be three distinct, but overlapping, compositional groups or trends in garnet Cr_2O_3 - CaO space (Figure 4.12b). The G10 garnets can be divided into high-Cr and low-Cr groups, with the preponderance associated with the high-Cr group. The former group is defined by higher Cr_2O_3 contents (> 7.5 wt%) and a distinct relationship of marginally increasing Cr_2O_3 with increasing CaO that extends into the G9 field. The latter group has lower Cr_2O_3 concentrations (< 6 wt%) and displays a range of CaO that may also extend into the G9 field. This group is the least populous, and is overlapped by the third group, the calcic G9 garnets, which plot parallel to the G10/G9 boundary. Due to the potential overlapping nature of the three groups their limits cannot be determined based on the garnets Cr_2O_3 - CaO compositions alone. Significantly, the high-Cr garnets overlap the Cr_2O_3 - CaO geochemical characteristics of the diamond-bearing garnet macrocrysts described in the previous section (see section 4.3.1).

There is a clear separation of the garnet macrocrysts into two major groups if the dominant octahedral cations (Cr#) are plotted against the dominant tetrahedral cations (Mg#) (Figure 4.2a). The first grouping is equivalent to the high-Cr garnets whilst the second is a combination of the low-Cr G10 and G9 garnets. It is apparent that the low-Cr G9 garnets extend to lower Mg#'s, whilst the low-Cr G10 garnets extend to high Mg#'s (Figure 4.2a). This plot highlights two important features not discernible from their Cr_2O_3 – CaO compositions. First, all the high-Cr G9 garnets are definitively related to the high-Cr G10 garnets and do not fall on a continuation of the "lherzolitic trend". Secondly, some of the low-Cr G10 garnets are associated with the calcic G9 garnets on the "lherzolitic trend" and vice versa, that is, it is not possible to separate these garnet groups on major element composition alone.

The ternary Ca-Mg-Fe diagram displays the highly depleted, magnesian-rich nature of the "harzburgitic" G10 garnets relative to the "lherzolitic" G9 garnets (Figure 4.3). Moreover, the G10 garnets trend along a constant Fe ratio[7] of ~ 12.5 to more calcium-rich compositions. In contrast, the G9 garnets have lower magnesium concentrations and extend into a more Fe and Ca rich composition that is always greater than an Fe ratio of 12.5.

The minor elements of Ti and Mn display small but noticeable variations (Figure 4.4 and 4.5). The high-Cr garnets display a trend of increasing TiO_2 as the garnets approach the lherzolitic trend; for example, the extremely sub-calcic G10 garnets are predominantly below detection limits whilst the G9 garnets are between 0.10 and 0.32 wt%. The low-Cr G10 and G9 garnets also commonly yield detectable TiO_2 up to a maximum of ~ 0.5 wt%. Only a handful of garnets yield TiO_2 greater than 0.4 wt%, often used as an indicator of metasomatic activity in the mantle (Harte and Gurney, 1975; Gurney et al., 1975; Harte, 1983; Matthews et al., 1992). The high-Cr garnets yield a narrow range of MnO concentrations (the majority between 0.25 and 0.4 wt%) whilst the low-Cr G10 and G9 garnets display a slightly broader range extending up to a maximum of 0.65 wt%.

[7] Fe ratio = 100 * Fe / (Fe+Ca+Mg)

The garnet macrocrysts that contain primary clinopyroxene plot on the lherzolitic trend (Figure 4.13a). Noticeably, with one exception, they do not extend to high-Cr values (> 8 Cr_2O_3 wt%). Furthermore, the majority plot within the G9 field, however two fall on the edge of the G10 field. This illustrates that the G10/G9 boundary is not absolute for separating G10 harzburgitic garnets from G9 lherzolitic garnets, as discussed earlier in this chapter.

The garnet macrocrysts that contain primary chromite are predominantly high-Cr highly sub-calcic G10 garnets, whilst only one high-Cr G9 garnet and 5 low-Cr G10 and G9 garnets contain chromite (Figure 4.13b).

An additional 19 diamond-free garnet macrocrysts were analysed from blow 3. These garnets display a similar geochemical pattern to the blow 2 garnets discussed above, in particular, a number are high-Cr sub-calcic G10 garnets (Figure 4.13c).

As with the diamond-bearing garnet macrocrysts, multiple core - rim analyses indicate that the garnets are well homogenised. Detailed traverses of four garnet macrocrysts (samples AHM 40, AHM 70, AHM 72, and AHM 76) yield major and minor element compositions that are generally within 2 standard deviations (Figures 4.14 through 4.17). Even though there are some subtle compositional changes, there are no systematic variations, i.e., small increases from core to rim for one sample are reversed for another. Samples AHM 70 and AHM 72 indicate subtle changes between the garnet edge (with kelyphite) and between 50 to 100 μm into the garnet, however, the variations are small, and not considered important to this study.

4.3.4 Coarse Peridotites

Relatively fewer coarse peridotites were analysed compared to the garnet macrocrysts yet the coarse peridotites display a similar range of Cr_2O_3 - CaO compositions. Several of the coarse peridotites are mineralogically harzburgites and have high-Cr, highly sub-calcic garnets that overlap the diamond-bearing garnet macrocrysts (Figure 4.18a).

The coarse peridotites that contain clinopyroxene overlap the diamond-free garnet macrocrysts that contain clinopyroxene and plot sub-parallel to the lherzolitic trend (Figure 4.12c). Furthermore, all have $Cr_2O_3 < 6$ wt%. Two samples (AHM 716 and AHM 717) yield very low-Cr garnets (< 2 wt% Cr_2O_3) and thus this commonly applied cut-off to separate peridotitic garnets from eclogitic garnets does not work well at Newlands. Samples AHM C2 and AHM 730 are mineralogically harzburgites yet have garnet compositions that are lherzolitic - thus they are likely to have equilibrated with clinopyroxene.

In general, the garnets from the peridotite xenoliths display only slight elemental variations, none of which are systematic. However, there are two exceptions (Table 4.3). Sample AHM C3 is an unusual garnet (~ 1000 μm in maximum dimension) with two areas of distinctly different compositions (Figure 4.19). The bulk of the garnet is dominated by a high-Cr highly sub-calcic, low Ti garnet (Cr_2O_3: 7.56 wt%; CaO: 2.27 wt%; TiO_2: n.d.) similar to the bulk of the diamond-bearing macrocrysts. In contrast, a small section of the garnet is relatively enriched in Cr, Ca and Ti (Cr_2O_3: 9.65 wt%; CaO: 4.29 wt%; TiO_2: 0.66 wt%). The variations in Cr, Ca, Mg and Al are clearly highlighted in elemental maps (Figure 4.19). The sample petrography indicates that the more calcic part of the garnet may be in response to metasomatism that has surrounded and infiltrated the garnet resulting in the formation of phlogopite, spinel and other secondary minerals (see Chapter 3). Other major elemental variations also occur and are highlighted in Table 4.3.

Sample AHM 730 defines similar compositional changes except that the variation occurs in a thin (~50 μm) garnet rind. In this case, the starting (or core) composition is lherzolitic whilst the edge is even more calcic (Table 4.3). Nevertheless, the directions of compositional changes are the same as those described above, and, in some cases, far more extreme. The only exception is FeO, which increases rather than decreases slightly.

4.4 CHROMITE GEOCHEMISTRY

4.4.1 Diamond-bearing Peridotitic Garnet Macrocrysts

Primary chromite is present in 11 of the 18 diamond-bearing garnet macrocrysts. Representative chromite compositions are given in Table 4.4. All the chromites display a relatively restricted compositional range with high Cr_2O_3 concentrations (62 to 65 wt%) and MgO values between 13 and 15 wt% (Figure 4.20). The chromites are highly depleted, with the majority having Cr#'s greater than 75 and titanium below 0.2 wt%. The chromites contain a range of silica concentrations from below detection limits up to 0.6 wt%.

The samples display a wide range in stoichiometrically calculated FFM[8] ratios, with the majority between 16 and 48, but one sample up to 62. Several chromites also contain significant amounts of silica, all of which also have high FFM ratios. Stoichiometrically calculated ferric iron[9]. is relatively low but ranges up to a maximum ratio of 37. However the accuracy of these values are questionable given that three samples have impossible negative values. Manganese concentrations are generally low (< 0.35 wt% MnO), with two samples extending up to 0.8 wt%.

Detailed point traverses and multiple core – rim analyses indicate small heterogeneities, such as increases in Cr (sample AHM 164) and Ti (sample AHM D3) or decreases in Fe (sample AHM 164). This is similar to variations observed in chromites from peridotites from Argyle (Jaques et al., 1990). However, such small variations may be due to edge effects during the analysis of very small chromites.

4.4.2 Inclusions in diamonds

Representative compositions of the chromite diamond inclusions and the host garnet macrocryst (AHM D2) are given in Table 4.4. Notably, the chromites (one of which is in contact with the garnet inclusion described earlier in section 4.3.2) both display intra- and inter- elemental variations relative to each other and the xenolith chromites.

[8] FFM = 100 * Fe^{2+} / (Fe^{2+} + Mg)
[9] ferric iron = 100 * Fe^{3+} / (Fe^{3+} + Fe^{2+})

Individually, the chromites display a remarkable internal variability, with the four major chromite oxides (Cr_2O_3, Al_2O_3, FeO and MgO) varying by over 1 wt% (Table 4.4). Even so, there are still significant compositional differences between the two inclusions and the xenolith chromites, as highlighted in the Cr_2O_3 – MgO plot (Figure 4.20c). The xenolith chromite has a Cr_2O_3 concentration (xenolith: average 64.6 wt%) that plots in between the two inclusions (A: average 66.47 wt%, B: average 61.64 wt%). However, the other dominant octahedral cation (aluminium) decreases from xenolith to inclusions such that both the inclusions have a higher Cr#. Similarly, the xenolith chromite has an FeO concentration that plots in between the two inclusions, but the other dominant tetrahedral cation (magnesium) decreases from xenolith to inclusions such that both the inclusions have a lower MMF ratio. The chromite inclusions and xenolith chromites are both depleted in TiO_2, whilst the inclusions have appreciably higher silica (between 0.4 and 1.5 wt% SiO_2) and manganese (between 1 to 2 wt% MnO) concentrations (Table 4.4). These levels are some of the highest concentrations observed in the world to date. It has been suggested that high MnO concentrations (0.6 to 0.9 wt%) in diamond inclusion chromites were due to the overlap of Cr Kα and the Mn Kα peaks (Stachel and Harris, 1997a). However, a detailed WDS scan shows that the Mn Kα and Cr Kα peaks are resolvable (Figure 4.21) and that the magnitude of the Mn Kα peak is equivalent to values between 1 and 2 wt% MnO (Andy Beard, pers. com., 1997).

4.4.3 Diamond-free Peridotitic Garnet Macrocrysts

Primary chromite is present in a small but significant percentage of garnet macrocrysts. Thirty-one garnet macrocrysts were analysed for chromite, 26 associated with a high-Cr G10 garnets, 3 associated with low-Cr G10 garnets, and 2 associated with low-Cr G9 garnets. The chromites display a large range of compositions with many yielding high-Cr concentrations (Cr_2O_3 > 60 wt%) (Figure 4.20), all of which are associated with the high-Cr sub-calcic garnets (4.12d). Magnesium and titanium concentrations are diverse (MgO: 7 to 17 wt%; TiO_2: below detection limits to in excess of 2 wt%). Both the Cr# and MMF ratio also display a wide range of values. Several chromites contain significant amounts of silica but not as high as the chromite inclusions.

4.4.4 Coarse Peridotites

Very few peridotite xenoliths were observed to contain chromite, and of those selected for further investigation only two had primary chromite (AHM 731 and AHM C4). Their compositions overlap some of the chromites from diamond free garnet macrocrysts. However, they are low in Cr_2O_3 (53.5 to 55 wt%) and Al_2O_3 (9.9 to 12.7 wt%) and high in TiO_2 (1.2 to 1.9 wt%) relative to chromites from diamond-bearing garnet macrocrysts.

4.5 OLIVINE GEOCHEMISTRY

4.5.1 Diamond-bearing Peridotitic Garnet Macrocrysts

Olivine is commonly pervasively altered in the majority of diamond-bearing garnet macrocrysts. However, one sample (AHM 58) contained a fresh olivine core within an altered silicate. A representative composition is given in Table 4.2. This olivine has a high forsterite content of 93.3 mol% (Figure 4.22). NiO and MnO concentrations are 0.35 (Figure 4.23) and 0.13 wt%, respectively, whilst both chromium and calcium contents are below detection limits. Elemental PIXE maps for Fe, Ni and Mn of the olivine grain display no zonation.

4.5.2 Diamond-free Peridotitic Garnet Macrocrysts

Olivine is commonly pervasively altered in the majority of garnet macrocrysts and hence the limited number of samples analysed. In total, only six olivines were analysed: one associated with a high-Cr G10 garnets, one with a low-Cr G10 garnet, and 4 with low-Cr G9 garnets. The forsterite content covers a relatively narrow compositional range of between 92 to 94 mol% (Figure 4.22). Nevertheless, the two olivines associated with G10 garnets have a forsterite content greater than 93 mol% whereas those associated with G9 garnets have forsterite contents less than 93 mol% (Figure 4.23). Nickel contents range from 0.27 to 0.47 wt% and display no systematic variation with forsterite content. Too few specimens are associated with

orthopyroxene and no accurate modal determinations exist to confirm the relationship between the Ni content of olivine and modal orthopyroxene, as observed by Boyd and Canil (1997). Manganese, Cr and Ca concentrations are commonly below detection limits.

4.5.3 Coarse Peridotites

All the lherzolites and harzburgites selected for analysis contain fresh olivine. In total, fourteen olivines were analysed: four associated with high-Cr G10 garnets, one associated with low-Cr G10 garnets, and nine from low-Cr G9 garnets. The forsterite content covers a (relatively) large compositional range between 88 to 94 mol% (Figure 4.22). The lower values (89 - 91 mol%) are associated with the lherzolite paragenesis whereas the higher values (92 - 94 mol%) are associated with the harzburgite paragenesis. Nickel concentrations range from 0.28 to 0.64 wt%, with a mode at 0.35 wt% (Figure 4.23). The value of 0.64 wt% is extremely high compared to other recorded values in this study and from around the world (Griffin et al., 1989; O'Reilly et al., 1995). The manganese concentrations range from below detection limits to 0.10 wt% with no significant difference between those associated with lherzolitic and harzburgitic garnets. The chromium contents are also commonly below detection limits with only two harzburgitic samples yielding measurable concentrations up to 0.04 wt%. Similarly, the calcium contents are also predominantly below detection limits with five lherzolite olivines scattering up to values of 0.04 wt%, consistent with equilibration with clinopyroxene (Köhler and Brey, 1990).

4.6 ORTHOPYROXENE GEOCHEMISTRY

4.6.1 Diamond-bearing Peridotitic Garnet Macrocrysts

No fresh orthopyroxene was observed in any of the diamond-bearing garnet macrocrysts.

4.6.2 Diamond-free Peridotitic Garnet Macrocrysts

Orthopyroxene, like olivine, is commonly altered and, thus, very few samples were analysed. Only 5 garnet macrocrysts yielded fresh orthopyroxene, one associated with a high-Cr G10 garnet, none associated with low-Cr G10 garnets, and four associated with low-Cr G9 garnets. The orthopyroxenes are mineralogically enstatites and display a restricted range of Mg#'s between 93.3 to 94.6 mol%, with the highest value associated with the solitary high-Cr G10 garnet (Figure 4.24). The four orthopyroxenes associated with low-Cr calcic garnets have a CaO concentration range (0.21 and 0.27 wt%) that is consistent with crystallising in equilibrium with clinopyroxene. These four "lherzolitic" orthopyroxenes yield lower Cr_2O_3 concentrations (0.25 to 0.33 wt%) than the solitary "harzburgitic" orthopyroxene (up to 0.42 wt%). Aluminium is relatively constant (between 0.49 and 0.57 wt% Al_2O_3) - such low concentrations are consistent with their derivation at high pressures within the diamond stability field (see geothermobarometry discussion in Chapter 6). Other minor elements range from below detection limits to very low values and show no systematic variation between the harzburgitic and lherzolitic orthopyroxenes (MnO < 0.13 wt%; NaO between 0.05 and 0.11 wt%, K_2O and TiO_2 below detection limits).

4.6.3 Coarse Peridotites

All the lherzolites and harzburgites selected for analysis contained fresh orthopyroxene. Sixteen orthopyroxenes were analysed, including four associated with high-Cr G10 garnets, one associated with low-Cr G10 garnet, ten associated with G9 garnets, and one from a garnet free peridotite. The orthopyroxenes are mineralogically enstatites and display a wide range of Mg-numbers from 89.8 to 94.3 mol%. Noticeably, all the harzburgitic orthopyroxenes yield Mg-numbers greater than 93.5, whereas the lherzolitic orthopyroxenes scatter to lower values (Figure 4.24). The majority of orthopyroxenes have low Al_2O_3 concentrations, varying between 0.30 to 0.60 wt%. The generally low Al concentrations imply derivation from a relatively deep (high-pressure) environment that extends well into the diamond stability field (see Chapter 6). The CaO concentrations vary from 0.19 to 0.36 wt%, MnO from 0.05 to 0.13 wt%, NaO from 0.03 to 0.07 wt%, Cr_2O_3 from 0.11 to 0.39 wt%, TiO_2 from below detection limits up to very high concentrations of 0.09 wt%,

whilst K_2O is below detection limits. The orthopyroxenes associated with harzburgites are generally lowest in Mn, Ca, Na, Ti and highest in Cr relative to the lherzolite orthopyroxenes. However, there is some overlap and the distinction is not clear-cut.

Two orthopyroxenes, however, record very different compositions to those described above. Orthopyroxenes from samples AHM E2 and AHM C1 yield markedly higher concentrations of Al_2O_3 (1.4 wt% and 2.6 wt%), CaO (0.49 wt% and 0.73 wt%), and Cr_2O_3 (0.63 and 0.80 wt%), respectively. Sample AHM E2 is the only sample with no observed garnet and thus its high Al content is consistent with a low-pressure origin, potentially outside the garnet stability field. Furthermore, this may explain its variation in other elements such as Ca and Cr. In contrast, sample AHM C1 occurs in association with a high-Cr mildly sub-calcic G10 garnet. This is further discussed in Chapter 6.

4.7 CLINOPYROXENE GEOCHEMISTRY

4.7.1 Diamond-bearing Peridotitic Garnet Macrocrysts

No primary clinopyroxene was observed in any of the diamond-bearing garnet macrocrysts.

4.7.2 Diamond-free Peridotitic Garnet Macrocrysts

Clinopyroxene was present in numerous garnet macrocrysts, of which 22 were analysed. All the clinopyroxenes were associated with low-Cr G9 or low-Cr marginally sub-calcic G10 garnets. They are mineralogically chromian augites or chromian diopsides and display a range of compositions. The Mg#'s cluster predominantly between 93 and 95 mol% but scatter down to 88.9 mol% (Figure 4.25), whilst the Ca#'s[10] cluster predominantly between 45 and 47 mol% but scatter down to 42 mol% (Figure 4.26). Clinopyroxenes that have a Ca# greater than 45 mol% are augites whilst those below are diopsides (Morimoto, 1988; Deer, Howie and

[10] Ca# = Ca / (Ca+Mg+Fe+Mn)

Zussman, 1992). All the clinopyroxenes have Cr_2O_3 (1.4 to 4.3 wt%) and Al_2O_3 (1.9 to 4.0 wt%) compositions that plot in the field associated with garnet lherzolites (Figure 4.27). Other elements also display some variation: TiO_2 ranging from below detection limits up to 0.33 wt%, but clustering below 0.10 wt%, NaO from 1.66 to 4.17 wt% but clustering around 2.5 to 3 wt%, and potassium predominantly below EMP detection limits with only four samples recording detectable, but very low, concentrations.

4.7.3 Coarse Peridotites

Nine lherzolites were selected for analysis, all of which are associated with low-Cr G9 garnet compositions. The clinopyroxenes display a wide range of compositions with Mg-numbers ranging between 90 and 96 mol% and the Ca-numbers between 43 and 48 mol%. In contrast to clinopyroxenes associated with garnet macrocrysts, those from coarse peridotites do not yield a distinct Mg# or Ca# mode (Figure 4.25 and 4.26). All the clinopyroxenes have Cr_2O_3 (0.95 to 2.2 wt%) and Al_2O_3 (1.6 to 4.2 wt%) compositions associated with garnet lherzolites (Figure 4.25). Minor elements are variable with TiO_2 ranging from below detection limits up to 0.45 wt% and NaO from 1.1 to 2.8 wt%. Potassium is below detection limits. These clinopyroxenes yield some subtle differences to the garnet macrocrysts. Although both display a wide range of compositions that overlap, the coarse peridotites generally have lower Cr concentrations and Mg#, but this may relate to the small data set.

4.8 General Discussion

The geochemistry of the garnets, chromites, and solitary olivine associated with the diamond-bearing peridotitic garnet macrocrysts from Newlands are similar to those observed in diamond-bearing peridotites and inclusions in diamonds world-wide. For example, the high-Cr, low-Ti, sub-calcic garnet geochemistry is similar to diamond-bearing peridotites from Udachnaya in Russia (Pokhilenko et al., 1977; Sobolev et al., 1984; Pokhilenko and Sobolev, 1986), Mothae in Lesotho (Dawson and Smith, 1975), Schaffer in the USA (McCallum and Eggler, 1976), Finsch in South Africa (Shee et al., 1982; Viljoen et al., 1992), Roberts Victor in South Africa (Viljoen et al., 1994),

Aikhal in Russia (Sobolev et al., 1969; Sobolev et al., 1984; Pokhilenko and Sobolev, 1986), Mir in Russia (Sobolev et al., 1984; Pokhilenko and Sobolev, 1986) (Figure 4.1). Similarly, the high-Cr, low-Ti chromite geochemistry (Figure 4.20) and the highly depleted nature of the solitary olivine are similar to their respective mineral counterparts from these diamond-bearing peridotites (when present). Furthermore, the diamond-bearing garnet macrocrysts from Newlands, as with diamond-bearing peridotites from other locations, in particular Finsch and Udachnaya, do not extend into the most extreme sub-calcic region (<1.5 wt% CaO) displayed by world-wide inclusions in diamonds (Figure 4.1c).

Nevertheless, there are some notable exceptions at Newlands to geochemical parameters described above. Firstly, three of the diamond-bearing garnet macrocrysts have garnet compositions that are calcium saturated and plot in the G9 field. Significantly, these garnets have higher Cr and Ca concentrations than the few diamond-bearing lherzolites and, with one exception, lherzolitic diamond inclusions world-wide (KRG database[11]), respectively. A small group of the world-wide diamond-bearing peridotites and a minor percentage of garnet diamond inclusions have low-Cr calcic garnets that plot in the G9 field on the lherzolitic trend. There are no equivalent garnet compositions amongst the diamond-bearing garnet macrocrysts at Newlands described in this study. The relationship between harzburgitic and lherzolitic diamonds is uncertain - indeed, it is unproven whether they represent distinct diamond parageneses. Nevertheless, at Newlands, there is evidence to suggest that the high-Ca, high-Cr diamond-bearing garnet macrocrysts are geochemically related to the harzburgitic diamond-bearing garnet macrocrysts even though they fall on an extension to the lherzolite trend.

Secondly, the olivine has a higher magnesium and lower Ni concentration than olivines from diamond-bearing peridotites around the world. In contrast, it overlaps the mode of the world-wide inclusions in diamonds (Figure 4.22). Thirdly, the chromites from the diamond-bearing garnet macrocrysts at Newlands are similar in MgO concentrations to the few specimens from the Kaapvaal craton (12.5 to 14 wt%)

[11] The KRG (Kimberlite Research Group) is based at the University of Cape Town and has put together an extensive "diamond database". For more information contact Eva Anckar (Eva@geology.uct.ac.za).

which are significantly higher than chromites from beneath the Siberian craton (11 to 12 wt%). Furthermore, the Newlands and Kaapvaal chromites (from diamond-bearing garnet macrocrysts or peridotites) have lower Cr# and higher MMF ratios than those from beneath the Siberian craton.

4.8.1 Diamond-bearing garnet macrocrysts and other garnet macrocrysts

4.8.1.1 Garnet compositions

The garnet compositions from the diamond-bearing garnet macrocrysts are predominantly high-Cr, extremely sub-calcic G10's, but trend into the high-Cr, Ca saturated field. A similar range of garnet compositions was observed for a multitude of diamond-free garnet macrocrysts, which completely overlap the diamond-bearing garnet macrocrysts but, importantly, define a larger data set - in particular there are a greater number of high-Cr mildly sub-calcic (G10) and high-Cr calcic (G9) garnets. Together they form a continuum in Cr_2O_3 - CaO compositions from extremely sub-calcic to highly calcic compositions (Figure 4.1). The relationship between the high-Cr garnets from diamond-bearing and diamond-free garnet macrocrysts is also highlighted in a Ca-Mg-Fe ternary diagram. Notably, all the high-Cr garnets extend along a constant Fe ratio of ~ 12.5. Furthermore, there is also a similar trend of increasing Ti with Ca. Based on major element mineral chemistry, it is likely that high-Cr garnets from the diamond-bearing and diamond-free garnet macrocrysts experienced the same evolution in the mantle beneath Newlands. Furthermore, the lack of diamonds in these garnet macrocrysts is likely to be a function of sample size rather than genesis. The only possible exception is diamond-bearing sample AHM E4. This sample has the highest Cr_2O_3 - CaO composition of any garnet at Newlands and it is uncertain whether this sample is at the limits of the high-Cr garnet trend or, alternatively, an anomaly. Whilst its geochemical composition lies on an extension of the high-Cr garnets in geochemical plots, there is a compositional gap.

The significance of this trend is uncertain. However, it should be noted that the compositional differences between the garnet diamond inclusion and the host xenolith garnet composition (sample AHM D2) are sub-parallel to the above Cr-Ca trend. In addition, two peridotites (samples AHM C3 and AHM 730) have zoned garnets where

the differences are also parallel to this trend, moving from lower Ca and Cr to higher Ca and Cr compositions.

There appears to be a minor compositional gap between the high-Cr (> 8 wt%; incorporating all the diamond-bearing samples) and the low-Cr (< 8 wt%) garnets at Newlands. The lherzolitic trend (G9 garnets) is known to extend to high-Cr concentrations at numerous locations world-wide - empirical evidence suggests that lherzolitic garnets can incorporate up to 16 to 18 wt% Cr_2O_3 (Sobolev et al., 1973; Sobolev, 1977; Gurney, 1984; Rickard et al., 1989; Grütter et al., 1999). However, at Newlands the garnet macrocrysts and coarse peridotites in equilibrium with clinopyroxene (with one exception) all have Cr_2O_3 concentrations less than 8 wt%. Thus the compositional gap separating these two groups may stem from the presence or absence of clinopyroxene, respectively. The Ca-saturation of garnets in the presence of clinopyroxene depends not only the Cr content of garnet, but also the pressure, temperature and other minor elements such as Na (Sobolev, 1977; Gurney, 1984; Boyd et al., 1993; Gurney et al., 1993; Gurney and Zweistra, 1995; Stachel and Harris, 1997; Griffin et al., 1999). Such high-Cr G9 garnets have been related to harzburgite peridotites (both diamond-bearing and diamond-free - defined mineralogically) from Finsch (Shee et al., 1982; Skinner, 1989; Viljoen et al., 1994). Therefore, it is probable that the high-Cr calcic garnet macrocrysts at Newlands did not equilibrate with clinopyroxene and are harzburgitic in paragenesis. This suggests that the high-Cr, Ca saturated garnets may be a continuation of the high-Cr G10 group and not the lower-Cr G9's, that is, not an extension of the lherzolite trend. Significantly, at Newlands, all the diamond-bearing garnet macrocrysts fall into the high-Cr group. Similarly, all the diamond-bearing harzburgites from around the world have garnet compositions that overlap these garnets from Newlands (see Figure 4.1b). However, this compositional gap is not noticeable in the diamond inclusion garnet compositions from around the world, and the sample set at Newlands is relatively small. Thus it is difficult to assess the significance of this compositional gap in relation to diamond formation.

The physical relationship between harzburgite and lherzolite in the SCLM mantle is uncertain. Evidence suggests that lherzolite is by far the dominant rock type (Boyd, 1973; Nixon and Boyd, 1973; Harte, 1977; Nixon, 1987; Boyd, 1989; Harte and

Hawkesworth, 1989; Boyd et al., 1997). Consequently subsolidus metamorphic re-equilibration will drive the harzburgite towards lherzolite compositions. Specifically, subsolidus metamorphic re-equilibration will increase Ca in the harzburgitic garnet. Therefore, the Cr-Ca compositional trend displayed by diamond-bearing and high-Cr garnets can be explained by the volumetrically smaller harzburgite re-equilibrating with the volumetrically dominant lherzolite.

4.8.1.2 Chromite compositions

Chromites from diamond-bearing garnet macrocrysts at Newlands are high-Cr (Cr_2O_3: > 60 wt%), Ti-depleted (TiO_2: below detection limits) with MgO concentrations between 13 to 15 wt%. Such compositions are similar to chromite diamond inclusion compositions and diamond-bearing peridotites world-wide. In addition, many of the chromites from diamond-free garnet macrocrysts have similar compositions at Newlands. Noticeably all of these chromites are associated with high-Cr sub-calcic garnets that overlap garnet compositions from diamond-bearing garnet macrocrysts. The high Cr_2O_3 contents of the chromites from the inclusions in diamonds, diamond bearing garnet macrocrysts and several other diamond-free garnet macrocrysts is in accordance with equilibration with olivine, orthopyroxene and garnet but not clinopyroxene (Webb and Wood, 1986).

Whilst garnet compositions from diamond-bearing peridotites from the Kaapvaal and Siberian cratons are similar there is a noticeable difference between the composition of chromites associated with diamond-bearing peridotites. Noticeably, the chromites from diamond-bearing garnet macrocrysts (and also high-Cr diamond-free garnet macrocrysts) at Newlands are similar in MgO concentrations (13 to 15 wt%) to the two diamond-bearing peridotites from Roberts Victor (both locations on the Kaapvaal craton), but are significantly higher in MgO than chromites from diamond-bearing peridotites from Udachnaya and Aikhal (both on the Siberian craton: MgO concentrations - 11 to 12 wt%). The reasons for this are uncertain.

4.8.2 Changing mantle physiochemical conditions since diamond formation

The optimal stability of garnet is obtained when the largest 3+ (Cr) and 2+ (Ca) major constituent ions are proportionally added or removed from the lattice structure (Novak and Gibbs, 1971). Consequently, there is an implicit coupling of chromium and calcium and they should respond similarly in garnet to changes in the chemical and physical environments (Novak and Gibbs, 1971).

The geochemical differences between the garnet and chromite diamond inclusions and their host xenolith (sample AHM D2) can be used as a gauge of changes in mantle physiochemical conditions over geologic time since diamond formation. The silicate diamond inclusions (should) represent pristine mantle conditions at the time of diamond formation whereas the host xenolith (should) reflect the sum of all processes affecting its local mantle environment. In addition, as time progresses and physical conditions change the host xenolith and touching chromite and garnet inclusions will re-equilibrate while the solitary chromite inclusion cannot. Furthermore, if there is any subsequent mantle metasomatic activity, as indicated by petrography (Chapter 3) and prevalent at nearby kimberlites (Harte, 1977; Dawson, 1980; Burgess et al., 1998; Griffin et al., 1999), only the host xenolith will be modified whilst the inclusions in diamonds are protected from any interaction and chemical adjustment. Consequently, geochemical differences between the solitary chromite inclusion and touching chromite and garnet inclusion will result from P-T changes while geochemical differences between the touching chromite and garnet inclusion and the host xenolith will include the effects of metamorphic or metasomatic activity. To determine these changes in physical and chemical conditions assumes that the inclusions and host xenoliths started with the same composition or followed observed changes in chromites within single diamonds from core to rim (Bulanova and Pavlova, 1991; Bulanova, 1995) that coincide with the trend of chromite crystallisation deduced from ultrabasic mantle xenoliths (Haggerty, 1979). Whilst it is not possible to deduce an accurate sequence of events based solely on geochemical parameters – as several possibilities could account for the observed differences – several key observations imply certain changes in the local environment.

Sample AHM D2 is the first documented xenolith that contains garnet and chromite of peridotite affinity both as inclusions in diamonds and as a primary phase of the xenolith hosting the diamond. Notably the host xenolith has a garnet composition that is more calcic than the diamond inclusion garnet (CaO: 1.8 vs 1.1 wt%). The source of the variation in the garnet and chromite diamond inclusions from sample AHM D2 is unknown. A similar compositional difference is implied at Udachnaya and Finsch where the garnet compositions of diamond-bearing peridotites or concentrates do not extend to the lowest CaO contents of garnet diamond inclusions from these locations (Sobolev et al. 1969, 1973; Gurney et al., 1979; Shee et al., 1982, Gurney, 1985).

The high silica concentration in the chromite diamond inclusions is potentially related to high pressures (Woodland and O'Neill, 1993) and temperatures (A. Doroshev and G. Brey, unpub. data, from Stachel and Harris, 1997) at diamond formation. The silica content of the chromite inclusions (average: 1.38 wt% and 0.63 wt%, respectively) is significantly higher than the host xenolith (average: below EMP detection limits) implying a substantial decrease in pressure and/or temperature since diamond formation.

The intra- and inter- geochemical variation between the two inclusion chromites implies changes in local chemical equilibria during diamond growth. Even though the scale of elemental variations are large, they are similar in magnitude to multiple chromite inclusions in a single diamond from Udachnaya (Bulanova, 1995). This variation were interpreted as evolution trends of progressive chromite crystallisation (Bulanova, 1995). An alternative explanation is that the chromite and garnet inclusions re-equilibrated in response to P-T changes since diamond formation, whilst the solitary chromite inclusion could not. Assuming the two chromite inclusions had similar starting compositions then the lower chromite Cr# may represent a decrease in pressure since diamond formation based on garnet - chromite Cr-isopleths (Figure 3: Brey et al., 1991).

PERIDOTITIC XENOLITHS: TRACE ELEMENT MINERAL GEOCHEMISTRY

5

5.1 INTRODUCTION

Trace elements are theoretically useful in defining geochemical reservoirs for the origin of geochemical melts – for example, see Harte (1983), Menzies and Hawkesworth (1987), and Harte et al. (1993). In particular, it may be possible to distinguish groups of xenoliths with a similar genesis and chemical evolution in the mantle. The normalisation of trace elements to chondritic values (in particular, for REE's) yields patterns that depict factors such as the degree of fertility or depletion and equilibrium with other mineral phases or fluid or melt percolating through the rock. Trace elements will be discussed in terms of either absolute abundance or normalised to C1-chondrite using the values of McDonough and Sun (1995).

The concentration of any trace element that is incorporated into a mineral phase is subject to numerous factors, however, ionic charge and radius are the dominant controls. The variation of ions substituting into a mineral phase based on differing charge and size was defined by Goldschimdt (1937), as summarised by Henderson (1982):

- Ions of similar radii and the same charge will enter into a crystal in amounts proportional to their concentration in a liquid.
- An ion of smaller radius but with the same charge as another will be preferentially incorporated into a growing crystal.
- An ion of the same radius but with a higher charge than another will be preferentially incorporated into a growing crystal.

5.2 METHODOLOGY

Garnets were analysed for specific Large Ion Lithophile Elements (LILE), Rare Earth elements (REE) and High Field Strength Elements (HFSE) using the two well-established analytical techniques of PIXE and SIMS. PIXE was performed using the proton microprobe (PMP) housed at the National Accelerator Centre (NAC), South Africa, whilst SIMS was performed using the Cameca IMS 4f ion microprobe (IMP) housed at the University of Edinburgh, Scotland, and the Cameca IMS 6f ion microprobe housed at Carnegie Institute of Washington, USA.

5.2.1 Analytical Techniques and Operating Conditions

The analytical set-up conditions of both the PMP and two IMP's are described briefly below as well as Appendix I.

5.2.1.1 Proton Microprobe (PMP)

Analyses were made using a proton microprobe (PMP) at the National Accelerator Centre (NAC), Cape Town. The NAC PMP facility has been described in detail by Prozesky et al (1995). A 3 MeV proton beam from a van de Graff accelerator was used to analysis grain mounts and polished sections. X-rays were detected using, originally, a PGT 30mm^2 and, latter, a LINK 80mm^2 Si(Li) detector. Optimal Al filter thickness was 120 μm and the beam was focused too less than 10 μm spot size. Due to the depth of penetration of the proton beam polished thin sections were prepared to approximately 70 μm thickness as a standard procedure.

The major elements of Cr, Fe and Mn were determined using both the PMP and EMP - comparisons yield a very good one-to-one correlation over a large Cr compositional range (Figure 5.1) given the relatively large PMP major element error (2σ: ~0.5 wt%). In practice, other studies reporting PMP data normalise their data to their EMP Fe concentrations (for example see Griffin et al., 1989; Griffin et al., 1992). However, given a Fe 1σ error of approximately 0.3 wt% using PMP and the good agreement with EMP data (Figure 5.1), that correction process was *not* applied in this study.

5.2.1.2 Ion Microprobe (IMP)

Analyses were made at the University of Edinburgh using the Cameca IMS 4f ion microprobe (IMP). The ion microprobe facility housed at Grant College, Edinburgh was described in detail by Hinton (1996) and Harte and Kirkley (1996). Elements analysed in garnet include selected REE's as well as Ti, Sr, Y, Zr, Nb and Ba. Beam currents of 5-10 nA and beam sizes of 10-20 μm were used. The international glass NBS-610 as well as an in-house garnet were used as standards and analysed at repeated intervals throughout the runs. The reference element for garnet analyses was Si, which was pre-determined by electron microprobe. One diamond-bearing garnet macrocryst was analysed for comparison at the Department of Terrestrial Magnetism, Carnegie Institute of Washington, using a Cameca IMS 6f.

5.2.2 Sample Description

The PMP is ideal for analysing transition and HFSE elements such as Ni, Mn, Zr and Y. PMP analyses were determined on 67 Cr-pyrope garnet macrocrysts from Newlands. An additional 57 samples were combined from a larger Ni thermometry study of southern African kimberlites to enlarge the data set (Menzies and Baumgartner, 1998; unpublished data). Rare Earth Elements (REE's) were also determined in 28 of these using the ion microprobe (IMP). These included 16 of the diamond-bearing garnet macrocrysts, 10 diamond-free garnet macrocrysts and 4 coarse peridotites. Note that three of these samples (including two diamond-bearing specimens) analysed by IMP were not analysed by PMP. Figure 5.2 displays the Cr_2O_3 – CaO composition of the garnets for which trace elements were determined.

Garnets were predominantly analysed as chips in a polished probe mount and consequently there is no spatial resolution for the majority of samples. Nevertheless, multiple analyses (normally three) were performed on all samples to test for homogeneity. Several specimens were analysed as polished sections, and thus spatial resolution was possible. In such a case, multiple analyses were made on each garnet, two for the core and two for the rim composition of the garnet. In addition, a detailed

study was made on diamond-bearing garnet macrocryst sample AHM D1, where twelve PMP and eleven IMP analyses were made.

5.2.2 Comparison of IMP and PMP

Both PMP and IMP analytical techniques were very precise and yielded good agreement where common elements were determined. The IMP is calibrated against known standards whereas the PMP is a theoretically based absolute technique and does not require standardisation. The two techniques are suitable for analysing different suites of elements and thus can be considered complementary. Only the elements Zr and Y in peridotitic garnets, Sr in clinopyroxene, and Cr in eclogitic garnets are of suitable concentration and nature that they can be determined by both PMP and IMP.

Figure 5.3 shows the comparison between Zr and Y for 25 garnets analysed by both techniques. In general, there is a very good agreement and the analyses are predominantly within error of the one-to-one line. However, there are some very aberrant results. The reasons for this are unknown but may relate to real heterogeneity in the sample as both techniques analysed the same grain but not necessarily the exact same spot. Alternatively, the variation may relate to the presence of micro-inclusions in the garnets, particularly as the garnets are highly fractured (see Chapter 3) and both techniques have a large beam size and thus excitation volume (>30 μm). This is particularly so for Sr, which is extremely low in garnets but relatively elevated in kimberlitic magmas. Diamond-bearing garnet macrocryst was analysed numerous times by both techniques. The precision for both IMP and PMP (based on the variation of the analyses, accounting for the possible effects of minor heterogeneity) was within the counting statistics errors for each analyses.

5.3 RESULTS

5.3.1 Diamond-bearing Peridotitic Garnet Macrocrysts

Representative garnet compositions from the diamond-bearing garnet macrocrysts are given in Table 5.1. The garnets from the highly sub-calcic harzburgitic (G10) diamond-bearing garnet macrocrysts display a narrow range of trace element signatures. Compared to "fertile" lherzolitic garnets they are relatively depleted in Zr, Y, Ga, and Ti (Figures 5.4 through 5.6). In contrast, Sr - whilst commonly only of the order of 1 to 10 ppm - is relatively enriched (Figure 5.7). The maximum Sr concentration recorded is 38 ppm in sample AHM D4. The $[REE]_n$[12] patterns are all very similar and display the unusual sinusoidal pattern first observed by Shimizu and Richardson (1987). In detail, there is an increase of LREE's from $[La]_n$ (at ~ chondritic levels) through to a peak at either $[Pr]_n$ or $[Nd]_n$ (at ~ 10X chondritic levels) followed by a decline in MREE's resulting in an inflexion point or trough varying between $[Ho]_n$ and $[Tm]_n$ (at ~ chondritic levels). The greatest variability in the $[REE]_n$ pattern is commonly accentuated in the $[HREE]_n$, which either continue to decline or level out from the $[MREE]_n$ (as in samples AHM D2, AHM D3, AHM 58 and AHM D1), or alternatively, increase from the $[MREE]_n$ (as in samples AHM D4, AHM D6 or AHM D7). The former is the most common. Furthermore, in nearly all cases the $[HREE]_n$ decrease to equivalent or below $[La]_n$.

In general, the two mildly sub-calcic garnets (AHM D10 and A) and the three calcic garnets (AHM E7, E and AHM E4) overlap or are enriched in Zr, Y, Ga, and Ti, whilst depleted in Sr (Figure 5.3 to 5.7) relative to the highly sub-calcic garnets from diamond-bearing samples described above. Of these five garnets only three were analysed for REE's. Sample A (which is a mildly sub-calcic G10 garnet) has a similar $[LREE]_n$ enriched sinusoidal pattern to the highly sub-calcic garnets described above (Figure 5.8). Sample AHM E7 (which is a calcic G9 garnet) also has a similar $[LREE]_n$ enriched sinusoidal pattern, however, the $[HREE]_n$ are relatively enriched compared to $[La]_n$. In contrast, sample AHM E4 (which is the most Cr-rich calcic garnet analysed at Newlands) yields a pattern of increasing $[LREE]_n$ through to

[12] $[REE]_n$ = normalised REE value

$[MREE]_n$ that plateaus for $[HREE]_n$ (Figure 5.8 and 5.9) – similar to fertile lherzolitic mantle garnets analysed in other studies (for example Nixon, 1987; Shimizu and Richardson, 1987; Hoal et al., 1994; Stachel et al., 1998).

Even though all the diamond-bearing garnets (with the exception of AHM E4) yield similar $[REE]_n$ patterns, there are subtle differences. Firstly, they can be divided into two groups on the basis of the magnitude of LREE enrichment, namely those with $[Pr]_n$ and $[Nd]_n$ above or below 10X chondrite, respectively (Figure 5.10). However, this visible compositional gap does not appear to be linked to any major or trace element concentration. Secondly, all the sub-calcic garnets have a LREE peak at $[Pr]_n$ or $[Nd]_n$ and display a prominent $[Gd]_n$ enrichment with HREE either remaining flat or increasing slightly (Figure 5.8). In contrast, the calcic sample (AHM E7) has a LREE enrichment peak at $[Sm]_n$ and a smoothly decreasing MREE pattern with no $[Gd]_n$ enrichment. However, it should be noted that these $[Gd]_n$ enrichemnts may be an artefact of the ion-probe oxide correction procedure.

The garnets are homogeneous. Transition metals and HFSE's (Ni, Zn, Zr, Ti and Y) are commonly within error of each other - for example, the Zr concentration in garnet from AHM D1 was between 8-10 ppm for 11 IMP analyses and 7 to 11 ppm for 12 PMP analyses. Similar homogeneity within the garnets is also displayed by samples AHM D9 and A, where ten or more PMP analyses were made (Table 5.3). For the most part, the LREE's and MREE's are within error, whilst HREE's display some heterogeneity. For example, specimens AHM D1, AHM D4, AHM D5, AHM D7, and AHM 4 all have $[LREE]_n$ (with the exception of $[La]_n$) and $[MREE]_n$ values within error, yet the $[HREE]_n$ display a large relative variation (Figure 5.8). It is probable that this is due to the low absolute concentrations of HREE's that are close to analytical detection limits and thus result in larger relative errors.

5.3.1.1 Trace element maps

As with the major element maps discussed in Chapter 4, the trace element maps of garnets from peridotitic diamond-bearing garnet macrocrysts are homogeneous (Figure 5.12). The majority of trace elements mapped by PMP (for example Sr, Zn, Ga, Y; see Figure 5.12) are below dynamic mapping detection limits indicating that

the relative depletion of the garnet is homogeneous throughout. Significantly, none of the specimens display "*order of magnitude*" variation in Sr, such as those reported for several Siberian inclusions in diamonds (Shimizu and Sobolev, 1995; Shimizu et al., 1997). In addition, the elemental maps for Rb, Sr and Ge indicate sub-parallel linear enrichment areas. These areas of enrichment correspond to the various fractures prevalent throughout the garnets (see Chapter 3) and are likely to be related to melt infiltrated mineralisation or metasomatism (Figure 5.12).

5.3.2 Diamond-free Peridotitic Garnet Macrocrysts

Garnets from diamond-free peridotitic garnet macrocrysts analysed for trace elements display a comprehensive range of major element compositions, and similarly the trace element signatures are diverse, noticeably greater than the garnets from diamond-bearing garnet macrocrysts. Representative garnet compositions from the diamond-free garnet macrocrysts are given in Table 5.2.

The high-Cr sub-calcic garnets (samples AHM 9, AHM 60, AHM 72, AHM 87, AHM 110, AHM E8, and B) display characteristics that overlap the diamond-bearing samples: viz. depletion in Zr, Y, Ga, and Ti (Figure 5.4 through 5.7). However, only sample AHM 87 has a sinusoidal $[REE]_n$ pattern that overlaps garnets from the diamond-bearing samples (Figure 5.13). Samples AHM 110, AHM 72, AHM E8 and B all have a similar $[LREE]_n$ sinusoidal pattern, outside that defined by the diamond-bearing samples, whilst samples AHM 9 and AHM 60 (both high-Cr extremely sub-calcic garnets) yield $[REE]_n$ patterns that are relatively flat and distinctly different to the diamond-bearing samples.

The low-Cr calcic garnets are relatively enriched in Ga, Y, Zr and Ti (Figure 5.4 through 5.7) and depleted in Sr. Only four samples were analysed for REE's and the resultant $[REE]_n$ patterns are diverse. Sample D (which is graphite-bearing) and sample C have a $[LREE]_n$ sinusoidal pattern similar to the garnets from the diamond-bearing samples. However, the MREE's are enriched for sample D whilst both the MREE's and HREE's are enriched for sample C (Figure 5.13). Sample AHM E9 displays a lherzolitic mantle garnet signature (that is, an increase from light to heavy

REE's) whilst sample AHM 74 has an irregular $[LREE]_n$ pattern – most likely due to extremely low LREE concentrations that approach analytical detection limits.

The low-Cr sub-calcic garnets display a mixture of trace element signatures. This was the smallest data-set analysed, however the most sub-calcic garnets are depleted in Y, Zr, Ti and Ga - similar to the high-Cr garnets – while the more calcic garnets are relatively enriched in these elements. No samples from this group were analysed for REE's.

5.3.3 Coarse Peridotites

Four garnets were analysed from coarse peridotites – all of which were later analysed for Re-Os systematics (see Chapter 7). Whilst mineralogically all four are harzburgites, sample AHM 730 has a garnet composition more synonymous with the lherzolitic paragenesis. The other three samples (AHM C3, AHM C4, and AHM 731) have high-Cr, highly sub-calcic garnets that are associated with the diamond-bearing garnet macrocrysts (see Chapter 4). These garnets are similarly depleted in Zr, Y, Ga, and Ti (Figure 5.4 through 5.7) as well as displaying sinusoidal $[REE]_n$ patterns (Figure 5.14). However, the HREE's are relatively depleted compared to the garnets from the diamond-bearing samples. In contrast, the solitary calcic garnet is enriched in Zr, Y, Ga, and Ti as well as displaying a $[REE]_n$ pattern more commonly observed for lherzolitic mantle garnets.

As mentioned in Chapter 4, sample AHM C3 contains a garnet that has a very sub-calcic domain together with a more calcic (but not calcium saturated) region (see Figure 4.19). Interestingly, the most sub-calcic domain of the garnet is relatively depleted in Zr, Y and Ga (Figure 5.15), and has a $[LREE]_n$ enriched sinusoidal pattern, as per garnets from diamond-bearing specimens of similar major element composition. In contrast, the more calcic region of the garnet, although still of G10 composition, is relatively enriched in Zr, Y and Ga, and has a $[REE]_n$ pattern more distinctive of lherzolitic mantle garnets (Figure 5.14).

5.4 DISCUSSION

5.4.1 Trace elements

The trace element signatures displayed by the garnets from diamond-bearing garnet macrocrysts at Newlands (viz. relatively depleted in Ti, Zr, Y and Ga, enriched in Sr, and a sinusoidal $[LREE]_n$ enriched pattern) are similar to those for garnet diamond inclusions from around the world, although the published data-set is relatively limited. For example, garnet diamond inclusions from the Kaapvaal craton (Shimizu and Richardson, 1987; Griffin et al., 1992; Shimizu et al., 1989), the Siberian craton (Shimizu and Sobolev, 1995; Shimizu et al., 1997) and the Ghanaian shield (Stachel et al., 1998) all have similar depleted signatures. In addition, the few garnets from diamond-bearing garnet peridotites around the world that have been analysed for trace elements also display similar signatures (Stachel et al., 1998).

The Sr concentrations in the sub-calcic garnets from the diamond-bearing garnet macrocrysts at Newlands are close to the detection limits of single point analyses and well below dynamic mapping limits using the proton microprobe. Point analyses reveal that Sr is on the order of 1 to 10 ppm, but often below detection limits. In addition, dynamic mapping of the diamond-bearing garnet macrocrysts displays Sr enrichment (in addition to Rb and Ge) along lineaments that are related to cracks and phlogopite mineralisation within the garnet. Whilst the Sr concentrations in the garnets are relatively enriched compared to garnets in "fertile" lherzolitic mantle, they do not display any Sr heterogeneity over several orders of magnitude, as observed in garnet diamond inclusions from Udachnaya (Shimizu and Sobolev, 1995; Shimizu et al., 1997). Thus Sr heterogeneity and implied Sr partitioning coefficients cannot be invoked for the Newlands diamond-bearing garnet macrocrysts, as for the garnet diamond inclusions from Udachnaya (Shimizu and Sobolev, 1995; Shimizu et al., 1997), to imply a young age of peridotitic diamond formation close to kimberlite eruption.

High-Cr sub-calcic garnets from diamond-free garnet macrocrysts or peridotites at Newlands and around the world (for example Nixon et al., 1987; Shimizu and Richardson, 1987; Hoal et al., 1994; Stachel et al., 1998) also yield similar trace

element signatures. However, at Newlands, only one diamond-free garnet (AHM 87) yields a garnet $[REE]_n$ pattern entirely within the range displayed by garnets from the diamond-bearing samples. Some garnets, including those with high-Cr extremely sub-calcic compositions, yield similar $[LREE]_n$ enriched sinusoidal patterns yet there are subtle but distinct differences.

5.4.1.1 The behaviour of REE's

REE's display a relatively predictable behaviour: as their atomic number increases the REE trivalent cation steadily decreases in size, and therefore REE substitution in to peridotite mineral phases is chiefly controlled by their changing ionic radius (Goldschmidt, 1937; as summarised by Henderson, 1982). Substitutions of the smaller HREE's are preferential over the LREE's for the dominant peridotite mineral phases of olivine, orthopyroxene, and garnet. The sole exception is clinopyroxene, where LREE's are more compatible. However, the relative amount incorporated into each phase is largely controlled by the lattice into which it is substituting – for peridotitic minerals, REE's substitute most readily into garnet, then clinopyroxene, orthopyroxene, and finally olivine, although olivine and orthopyroxene essentially incorporate zero REE's. The relative compatibility of REE in the various phases can be quantified by their relative partitioning with a melt co-efficient. A variety of experimental and empirical studies have shown that REE are extremely incompatible in olivine and orthopyroxene (mineral-melt partition coefficients on the order of 0.0001 to 0.01). They are mildly incompatible for clinopyroxene (with the partition coefficients approaching 0.5 for HREE's) and range from highly incompatible LREE (with partition coefficients on the order of 0.01), through increasingly compatible MREE's, to compatible HREE's (for example D_{Er} is ~2.5 and D_{Lu} is ~20) for garnet. Therefore, garnet represents the only phase that will preferentially take up REE's from a melt in a harzburgite, whilst both garnet and clinopyroxene will in a lherzolite.

This nature of REE's explains the pattern observed in lherzolitic garnets. They are LREE depleted (as this is preferentially taken up in the clinopyroxene), increasing through the MREE's to plateau for the HREE at levels orders of magnitude greater than chondrite. Such patterns are observed in several samples from Newlands – all of which lie on the lherzolitic trend and are assumed to be in equilibrium with

clinopyroxene (for example sample AHM E9: see Figure 5.13). Unusual REE patterns in garnets, such as the sinusoidal LREE enriched pattern of garnet associated with diamonds, are more difficult to explain and imply multi-staged processes (Shimizu and Richardson, 1987; Stachel et al., 1998).

Sample AHM E4 is the only diamond-bearing garnet macrocryst that has a garnet with a $[REE]_n$ pattern similar to "fertile" lherzolite mantle garnets and not the $[LREE]_n$ enriched sinusoidal pattern described above for all the other diamond-bearing specimens. However, this is not entirely unexpected given its distinctive major element composition – it has the highest Cr and Ca concentrations of any garnet from Newlands analysed in this study (see Chapter 4). Furthermore, there is a distinct major element compositional gap with the other peridotitic garnets making it unclear what the relationship is between this specimen and the other diamond-bearing garnet macrocrysts – that is, whether it is a geochemical end-member of a single series, or representing a separate diamond-forming process in its own right at Newlands.

5.4.2 Mantle metasomatism

Two major types of metasomatism are commonly recognised as occurring within the mantle, namely "modal" and "cryptic" metasomatism (Harte, 1977, 1983; Dawson, 1984). Modal metasomatism of the diamond-bearing garnet macrocrysts appears to be minor at Newlands. The Sr, Rb and Ge enrichment revealed in the elemental maps is clearly associated with secondary phlogopite and spinel prevalent within fractures in the garnet. These minerals are likely to have crystallised from a kimberlitic (or an earlier precursor) fluid and are unlikely to be related to any form of ancient metasomatism. However, it is not possible to determine if any fine-scale modal metasomatism occurred – for example, like the garnet metasomatism and crystallisation from infiltrating melt at Matsoku (Matthews et al., 1992) - as no high-resolution extremely detailed studies were undertaken.

There is, however, evidence to suggest that two major types of ancient cryptic metasomatism occurred. The highly depleted nature and sinusoidal LREE enriched garnets from the diamond-bearing garnet macrocrysts, as well as many of the diamond-free garnet macrocrysts, combined with their high-Cr concentration, are

believed to preclude their formation in chemical equilibrium with any known silicate or carbonate magma (Shimizu and Richardson, 1987; Stachel and Harris, 1997). In contrast, Burgess (1987) and Burgess and Harte (1998) suggest that the sinusoidal REE patterns of garnets may arise as a result of extensive garnet fractionation from basic-ultrabasic melt, because of the extreme variation in garnet/melt distribution coeffiecents across the REE. In either case, these trace element signatures are the result of an ancient metasomatic event that was depleted in LILE's such as Ti and Zr and enriched in LREE. The timing of this metasomatic event is difficult to determine, however all age evidence suggests that the processes forming these garnets occurred in the Archaean (for example, Richardson, 1984). Shimizu and Richardson (1987) advocate that the metasomatic event affected the garnet in the residual harzburgite prior to diamond formation.

It is apparent that, for many of the high-Cr sub-calcic garnets, Zr, Y, Ga, and Ti all increase as Ca increases, whilst the opposite is true for Sr. However, this is not a direct relationship – that is, some of the calcic G9 garnets are as depleted in Zr, Y, Ga, and Ti as some of the G10 garnets. It is uncertain whether the REE's were affected during this enrichment event, although the two calcic diamond-bearing macrocrysts analysed display elevated $[HREE]_n$. Sample AHM E7 has $[HREE]_n$ greater than $[La]_n$ whilst sample AHM E4, the most calcic garnet, has a REE pattern that is HREE enriched and similar to "fertile" mantle garnets. No diamond-free garnet macrocrysts with similar major element compositions were analysed and thus it is unknown whether the trace element signature of AHM E4 is an original fingerprint or affected by metasomatism. Nevertheless, it appears that after diamond formation (as the diamond inclusion is the most depleted garnet analysed (see Chapter 4)) Ca and some HFSE's and LILE's were re-introduced into some of the high-Cr sub-calcic garnets.

Thus, the high number of diamonds with inclusions of such compositions imply that diamond crystallisation primarily occurred before metasomatism could go to completion, that is, the garnets returned to a fertile lherzolitic composition. Secondly, this would imply that the redox and geochemical environment of the harzburgite was suitable for diamond crystallisation. Recently, however, it has been shown that the unusual sinusoidal LREE enriched patterns observed in these garnets may be caused by a single stage crystallisation from a highly evolved metasomatic melt (Burgess,

1997; Burgess and Harte, 1999). However, it is unlikely that such a melt can account for the high-Cr concentration observed in these garnets (Canil and Wei, 1992).

Similar major and trace element observations were made for garnet diamond inclusions from Udachnaya and Premier (Richardson and Harris, 1997). These garnet inclusions yielded ages around 2 Ga indicating a minimum age for the ancient metasomatism to have occurred. This is supported by the homogeneity of the diamond-bearing samples, which suggests that it did not occur around the time of kimberlite emplacement, thus precluding the kimberlite (or precursor) melt itself.

PERIDOTITIC XENOLITHS: GEOTHERMOBAROMETRY

6

6.1 INTRODUCTION – THE USE OF GEOTHERMOBAROMETRY

The early work of Boyd and co-workers (e.g. Boyd and England, 1960, Davies and Boyd, 1966; Boyd, 1973; Boyd and Nixon, 1973; Boyd, 1974; Boyd et al., 1976) introduced the usefulness of geothermobarometry in constraining the physical and chemical properties of upper mantle xenoliths and metasomatic processes that may have occurred therein. Over the last two decades numerous pressure-temperature (P-T) experiments, empirical observations and thermodynamic considerations have generated a plethora of both geothermometers and geobarometers applicable to xenoliths derived from the upper mantle. Detailed assessments and reviews of widely used geothermobarometers have been periodically written to incorporate new calibrations and the reader is referred to discussions in the following papers: Carswell and Gibb (1980, 1987), Finnerty and Boyd (1984, 1987), Nickel and Green (1985), Finnerty (1989), and Brey and Köhler (1990) and references therein.

The results of these detailed investigations yield varying interpretations as to which geothermobarometers provide the best precision and/or accuracy, particularly over the large compositional and P-T ranges observed in the upper mantle. The assessment of any geothermobarometer is extremely difficult as there are very few invariant reactions that may be used as absolute references for xenoliths derived from the upper mantle (Finnerty and Boyd, 1987). In general, each geothermobarometer is experimentally, empirically or theoretically calibrated for ideal and simple systems over a limited P-T and compositional range of the upper mantle. Consequently any geothermobarometer may be erroneous when applied to natural xenoliths and thus uncertainty exists when extrapolating to the entire upper mantle environment. Therefore, the geologic interpretation of geothermobarometry results must be cautious

and P-T's are commonly determined for suites of rocks using several geothermobarometer combinations that are in agreement.

All geothermobarometers are based on the premise that changing physical conditions affect the chemical compositions of the minerals comprising the host rock (Wood and Fraser, 1977). A range of mass balance chemical reactions can be written that represent such changes and are commonly a function of both pressure and temperature - very rarely are either totally independent of the other (op. cit.). Therefore, an iterative combination of both a geothermometer and geobarometer is required to constrain a xenolith in P-T space. Accordingly, the accuracy of the P-T calculation is limited to the derivation and calibration of both. Different geothermobarometer combinations are known to yield P-T's that may vary by hundreds of degrees and tens of kilobars for a single xenolith (Finnerty and Boyd, 1984). Such fluctuations are clearly inadequate in attempting to determine absolute positions, however, in general, various combinations of geothermobarometers will maintain the relative positions of upper mantle xenoliths or xenolith suites.

In addition, the presence of certain minerals within some upper mantle xenoliths provides independent constraints on P-T conditions. For example kyanite, coesite, diamond and graphite are commonly used to infer minimum or maximum pressures or temperatures of residence within the upper mantle, although these minerals are normally rare in upper mantle xenoliths.

6.2 Review of Geothermobarometers

The mineral phases most commonly used in geothermobarometry of upper mantle xenoliths include olivine, orthopyroxene, clinopyroxene, garnet and spinel. For meaningful geothermobarometer results the relevant pair of mineral phases must coexist and be in chemical equilibrium. Ideally, for optimal comparison of a variety of geothermobarometers, a xenolith should contain four or five mineral phases. In practice, however, many xenoliths display alteration (e.g. olivine to serpentine) or a mineral phase is absent due to the small sample size or paragenesis (for example harzburgites lack clinopyroxene whilst eclogites may lack olivine or orthopyroxene).

The systems considered of primary interest in upper mantle geothermobarometry are:

- Fe-Mg exchange (between garnet and clinopyroxene, garnet and olivine, and garnet and orthopyroxene) thermometry,
- Pyroxene solvus thermometry,
- Al-in-orthopyroxene (coexisting with pyrope) barometry, and
- Trace element thermometry.

Newlands kimberlite contains a wide range of upper mantle xenoliths and xenocrysts to which a wealth of geothermobarometers can be applied. However, no single geothermobarometer combination can yield P-T's for all the various xenoliths and xenocrysts. Therefore, the P-T results must be carefully integrated to yield useful overall information and infer the local mantle stratigraphy beneath Newlands – in particular, to incorporate eclogite xenoliths (see Chapter 11). In addition, there is no unanimous agreement in the literature as to the "best" or "most appropriate" geothermobarometers that should be applied to the variety of natural xenoliths. The study of Brey and Köhler (1990) recommended pyroxene solvus thermometers combined with current Al-in-orthopyroxene calibrations, in particular their own temperature and pressure calibrations. In addition, several other geothermometers were found to reproduce the experimental results of Brey et al. (1990) just as satisfactorily; these include the thermometers of O'Neill and Wood (1979), Brey and Köhler (1990: Ca-in-orthopyroxene), and Krogh (1988), and the barometer of Nickel and Green (1985). Special note was made of the Fe-Mg thermometers (which comprise the majority of calibrated geothermobarometric systems) as no allowance is (normally) made for Fe^{3+}. Therefore calculations may be erroneous. Consequently, with the exception of O'Neill and Wood (1979) and Krogh (1988), Fe-Mg thermometers were not recommended in the above studies, even though the experimental runs of Brey et al. (1990) supposedly contained no ferric iron and thus the effect of ferric iron on Fe-Mg thermometers could not adequately be assessed.

If the mineral species have little or no ferric iron, as some do, or alternatively [Fe^{3+}(Mineral X)/ Fe^{3+}(Mineral Y) = 1], then the ferric iron effect is negated and the thermometer may still be appropriate. Whilst studies show that orthopyroxene,

clinopyroxene, garnet and spinel can contain various amounts of ferric iron (for example, Luth et al., 1993; Canil and O'Neill, 1996) a recent study has revealed that for any one xenolith the mineral phases often contain similar concentrations (Sobolev et al., 1999). Moreover, in general, there is not a lot of Fe^{3+} in peridotitic mantle, in particular where diamond was the stable form of carbon. This may explain why the Fe-Mg thermometers of O'Neill and Wood (1979) and Krogh (1998) yield satisfactory results for the experimental runs (Brey and Köhler, 1990).

Pearson et al. (1994) analysed 5 diamond-bearing peridotites and 5 graphite-bearing peridotites to assess the various geothermometers. They concluded that both the geothermobarometry combinations of Brey and Köhler (1990) with MacGregor (1974) and Finnerty and Boyd (1987) with MacGregor (1974) place the xenoliths within the correct diamond-graphite stability field. Therefore, whilst theoretical arguments may count against thermometers such as Finnerty and Boyd (1987) and barometers such as MacGregor (1974), they often yield geologically satisfactory results.

The Ni thermometer calibrations are of benefit to mantle geothermobarometry as they are independent of pressure (Canil, 1994; Ryan et al., 1996) and can be determined from the chemical composition of single peridotitic garnets that are typically abundant in kimberlite concentrates. Such thermometers are particularly useful in this study, as the garnet macrocrysts - including the diamond-bearing specimens - are primarily comprised of garnet and, in some cases, minor chromite. For these xenocrysts, multiphase geothermometers are not applicable. Trace element analysis of garnet and chromite macrocrysts derived from kimberlite concentrates over the past decade has led to the development of two (conflicting) "Ni-in-garnet" geothermometers and a "Zn-in-chromite" geothermometer (although of poor precision). However, no current geobarometer can be applied to single garnet or chromite grains whilst other geothermobarometers are able to constrain both pressure and temperature in multiphase xenoliths.

Therefore, from the above discussion, a range of geothermobarometers will be considered in this study. The various geothermometers and geobarometers, their derivations, and the combinations used are listed in Table 6.1, 6.2 and 6.3,

respectively. Henceforth, the geothermobarometers will be referred to using an abbreviation of their author(s) and year of publication, as per Table 6.1 and 6.2.

6.3 METHODOLOGY

The geothermobarometry results will be discussed in two sections, namely trace element geothermobarometry on both diamond-bearing and diamond-free peridotitic garnet macrocrysts, and multiphase geothermobarometry on peridotite xenoliths and xenocrysts. Multiphase xenolith pressure and temperature (P-T) calculations were primarily determined using a geothermobarometry program developed by, and obtained from D. Smith[13].

Ni concentrations were determined on 67 Cr-pyrope garnet macrocrysts using the PMP (note that the IMP is not suitable for determining Ni see Chapter 5). A further 57 concentrate garnets from Newlands were analysed in another study as part of a larger investigation of southern African kimberlitic garnets (Menzies and Baumgartner, 1998; unpublished data) and are incorporated to enlarge the data set. It should be noted, however, that these additional garnets are predominantly lherzolitic garnets with Cr_2O_3 and CaO concentrations of 4.5 to 7 wt% and 4 to 5.5 wt %, respectively, and are equivalent to the high-Cr calcic G9 garnets. The Cr_2O_3-CaO compositions of all these garnets are displayed in Figure 5.1.

The coarse peridotites analysed from Newlands can be classified into five groups consisting of 8 garnet harzburgites, 1 harzburgite, 8 garnet lherzolites, 6 lherzolitic garnet macrocrysts and 1 garnet websterite (see Table 6.4). All the xenoliths contained fresh mineral phases. Where possible core and rim analyses were determined on at least two grains for each mineral phase and averages used for geothermobarometry calculations (analyses presented in Appendix II). Two samples had pronounced garnet heterogeneity (see Chapter 4): AHM C3 contains a garnet with two distinct areas of differing composition (one section is substantially enriched in Ca and minor amounts of Cr), whereas the garnet in AHM 730 has a 50 to 100 μm (reaction?) rim of different composition to the main body of garnet. Thus

geothermobarometers were calculated for both core and rim compositions. Several of the coarse peridotites and garnet macrocrysts containing olivine, orthopyroxene, and spinel have had their garnets analysed for Ni and chromites for Zn to compare trace element thermometers with multiphase thermometers.

6.4 TRACE ELEMENT GEOTHERMOBAROMETRY

6.4.1 Diamond-bearing Garnet Macrocryst Geothermobarometry

The Ni concentrations for the diamond-bearing garnet macrocrysts are present in Table 5.1b along with T_{Ni}Ryan96 and T_{Ni}Canil94. The error of the PMP is approximately 3-4 ppm for Ni at 1 sigma and this similar to the precision of the instrument based on multiple analyses of the same grain. Such errors are equivalent to variations in both T_{Ni} thermometers of ~ 30 °C, which is less than the calibration errors of ~ 50 °C for each T_{Ni} thermometers. The two T_{Ni} thermometers yield similar results for the diamond-bearing garnet macrocrysts, with T_{Ni}Ryan96 extending to slightly lower temperatures. The temperatures range between 900 to 1100 °C with the majority between 950 to 1050 °C (Figure 6.1). In either case, all the diamond-bearing garnet macrocrysts fall within the diamond stability field based on a 37-38 mW/m^2 geotherm (as indicated by multiphase xenolith geothermobarometry – see section 6.5). Furthermore, there is no noticeable difference between the temperatures of the 14 diamond-bearing G10 garnet macrocrysts and two diamond-bearing G9 garnets.

The solitary graphite-bearing garnet macrocryst (Sample D) has a Ni concentration lower than all the diamond-bearing garnet macrocrysts. The T_{Ni}Ryan96 temperature of 890 °C implies a diamond-graphite boundary at approximately 900 °C, which corresponds to a geotherm of 37 to 38 mW/m^2 and is consistent with multiphase xenolith geothermobarometry (see section 6.5). In contrast, T_{Ni}Canil94 yields a temperature of 980 °C, consistent with a diamond-graphite boundary at close to 1000 °C. This implies a higher geotherm (~ 40 mW/m^2) that is inconsistent with multiphase xenolith geothermobarometry.

[13] The program is available from Doug Smiths' personal web site at the University of Texas: www.utexas.edu.

Multiple trace element analyses on individual samples indicate that there is no intra-grain zonation (see Chapter 5) and Ni was no exception. In all cases Ni concentrations (and thus temperatures) were within analytical error. For example, a 1000 μm traverse of diamond-bearing garnet macrocryst AHM D1 yields Ni concentrations ranging from 34 to 39 ppm, which corresponds to temperatures of 917 to 958 °C using T_{Ni}Ryan96 or 995 to 1019 °C using T_{Ni}Canil94. Similarly, a 1000 μm traverse of diamond-bearing garnet macrocryst AHM D9 (performed on two separate runs) has Ni concentrations ranging from 40 to 49, which corresponds to temperatures of 963 to 1025 °C using T_{Ni}Ryan96 or 1024 to 1058 °C using T_{Ni}Canil94.

Assuming that the garnets lie on a steady state continental geotherm of 37-38 mW/m^2, then a temperature range of 900 to 1100 °C corresponds to pressures of between 40 and 60 kbar.

6.4.2 Diamond-free Garnet Macrocryst Geothermobarometry

The two T_{Ni} thermometers yield differing results for the diamond-free garnet macrocrysts: T_{Ni}Ryan96 temperatures range between 750 to 1100 °C whilst T_{Ni}Canil94 ranges between 900 to 1100 °C (Figures 6.1). This divergence is a function of the systematic difference between the two thermometers, where T_{Ni}Ryan96 consistently yields lower temperatures than T_{Ni}Canil94 for Ni concentrations below 60 ppm, as is the case for the vast majority of garnets analysed from Newlands. Nevertheless, there is a noticeable difference between the G10 and G9 garnets, independent of the Ni geothermometer. Considering T_{Ni}Ryan96 only, the high-Cr G10 garnets record temperatures predominantly falling between 900 and 1000 °C, all within the diamond stability field. The five G10 samples that yield temperatures less than 900 °C, and fall with the graphite stability field, are all relatively low-Cr G10's that are only mildly sub-calcic (Figure 6.2). In contrast, the G9 garnets yield temperatures that range down to 750 °C, noticeably lower and well into the graphite stability field. These differences, although less apparent, are still noticeable using T_{Ni}Canil94, although they occur at slightly elevated temperatures.

Noticeably, regardless of Ni thermometer, there are no high temperature garnets (> 1200 °C). This is consistent with the absence of sheared peridotites (see Chapter 3) and lack of high-Ti and high-Zr garnets (see Chapter 4 and 5) at Newlands. The temperature range displayed by the diamond-free G10 garnets is similar to that displayed by the diamond-bearing samples, all yielding temperatures that can be expected to lie within the diamond-stability field (greater than 900 °C, Figure 6.2).

6.4.3 Newlands Garnet Geotherm

The garnet geotherm is difficult to demarcate (Figure 6.3). In addition, there is a (systematic) difference depending on which T_{Ni} calibration is used. The systematic difference between the empirical and experimental temperature calibrations yields garnet P-T plots, with T_{Ni}Canil94 compressing the temperature range and yielding a higher "garnet geotherm" and indicating the failure of the method to generate a convincing envelope of P-T points (Menzies and Baumgartner, 1998).

The T_{Ni}Ryan96-P_{Cr} plot can be interpreted in two ways: firstly, a 35 mW/m^2 geotherm, which ignores four diamond-free garnet macrocryst points as anomalous, or, secondly, a 33 mW/m^2 geotherm which encompasses all the garnets, but is constrained by only four samples. Either option, however, is lower than the robust xenolith geotherm (defined in section 6.5). It is also lower than the garnet geotherm for Newlands obtained by Griffin and Ryan (1995).

These low geotherms would correspond to very low P-T's for entry into the diamond stability field - a geotherm of 33 mW/m^2 would correspond to the diamond stability field starting at ~ 690 °C and a 35 mW/m^2 geotherm at ~ 785 °C. Such geotherms place the graphite-bearing garnet macrocryst well into the diamond stability field and thus creates a paradox. Accordingly, it is suggested that the low garnet geotherms indicated by T_{Ni}Ryan96-P_{Cr} are wrong. In contrast, T_{Ni}Canil94-P_{Cr} displays less scatter and defines a more refined garnet geotherm envelope of ~ 37 mW/m^2. Even so, a similar paradox still exists, with the graphite-bearing garnet macrocrysts T_{Ni}Canil94 falling well within the diamond stability field. It should be noted that

although in both cases the graphite-bearing garnet macrocryst is ~ 100 °C into the diamond stability field, it is plausible to have metastable graphite within the diamond stability field for extended periods of time (Kennedy and Kennedy, 1976). Nevertheless, it is apparent that P_{Cr} does not yield consistent results with either of the nickel thermometers or the xenolith geothermometers at Newlands.

6.4.4 Chromite geothermometry of Garnet Macrocrysts

The data set is relatively small with only thirteen chromites from seven diamond-bearing G10 garnet macrocrysts as well as eleven chromites from eleven diamond-free garnet macrocrysts analysed for comparison. Chromites from diamond-bearing garnet macrocrysts yield T_{Zn}Ryan96 ranging between 1000 to 1200 °C, with a mode at 1100 to 1150 °C (Figure 6.4). Chromites from diamond-free garnet macrocrysts also have a mode at 1100 to 1150 °C, but extend down to temperatures of 850 °C (Figure 6.4). The majority of these T_{Zn} temperatures are well in excess of their garnet counterparts, indeed any of the garnets from Newlands (which yield a maximum temperature at ~ 1100 °C).

Griffin and Ryan (1995) use the Cr_2O_3- T_{Zn}Ryan96 plot to estimate geotherms based on isopleths determined from Brey et al. (1991). Whilst the data from Newlands is sparse, the maximum envelope in a plot of Cr_2O_3- T_{Zn}Ryan96 (Figure not shown) is consistent with a geotherm between 30 and 40 mW/m^2 (based on Figure 15 from Griffin and Ryan, 1996). However, it is not possible to refine the chromite geotherm estimate further.

6.5 Multiphase Geothermobarometry

The multiphase xenoliths (including lherzolites, harzburgites, peridotitic garnet macrocrysts, and a websterite) yield pressures and temperatures (P-T's) spanning a large portion of the upper mantle. Temperatures range between 750 to 1200 °C and pressures from between 30 to 65 kbar, equivalent to depths of approximately 100 to 200 km. No high temperature xenoliths (commonly defined as greater than 1200 °C) were observed, which is consistent with petrographic and geochemical observations.

The range of temperatures and pressures for each of the peridotite xenolith suites are displayed in Figures 6.5 and 6.6, respectively.

Various geothermobarometer combinations applied to garnet lherzolites and lherzolitic garnet macrocrysts yield a uniform P-T range of between 750 to 950 °C and 30 to 50 kbar (Figures 6.5a and 6.6a). In contrast, geothermobarometer combinations applied to harzburgites yield a range of P-T values significantly higher (best estimate: 950 to 1150 °C and 40 to 65 kbar) than lherzolites and lherzolitic garnet macrocrysts, but not as consistent (Figures 6.5b and 6.6b). The solitary websterite yields the lowest P-T's (Figures 6.5c and 6.6c). Noticeably, harzburgites record the highest P-T's and fall within the diamond stability field, whilst the lherzolites and lherzolitic garnet macrocrysts have lower P-T's and straddle the diamond-graphite boundary. The solitary websterite has one of the lowest P-T's and falls within the graphite stability field.

In some cases the absolute P-T for any individual xenolith or xenolith suite may vary between geothermobarometer combination, however their relative positions remain consistent. For example, the lherzolitic garnet macrocrysts plot in the restricted range of 780 to 820 °C using TAi94 whereas they yield a range of 880 to 950 °C using TONW79. Furthermore, both the thermometers and barometers are sensitive to their respective pairing. For example, the lherzolite suite yields a PBKN90 range from ~ 45 to 55 kbar when combined with either THar84 or TONW79, but ~ 60 to 75 kbar with TGan96. Similarly, considering an individual sample (AHM 731) yields TONW79 of 1085 °C when combined with PMac74 but 1202 °C when combined with PBKN90.

The range of individual P-T positions and resultant geotherms are shown in Figures 6.7 a-l, with the results summarised in Table 6.2. Strikingly, the various geothermobarometer combinations consistently yield similar geotherms. The majority of the combinations yield a geotherm of between 37 to 38 mW/m^2, however some combinations display scatter. This scatter may be due to dis-equilibrium mineral assemblages – as evidenced by geochemical evidence in several of the harzburgitic xenoliths, for example AHM C3, AHM 730, or AHM C1 (see Chapters 4

and 5). Alternatively, it may relate to extrapolation of the geothermobarometers to outside their calibrated range. Furthermore, the Al-in-orthopyroxene barometer is very temperature dependent and requires accurate analyses of minor constituents in orthopyroxene and often EDS EMP analyses (used for some xenoliths in this study) for Na in orthopyroxene are incorrect (Smith, pers. com., 1998). Similarly, the TONW79 thermometer is very sensitive to the olivine forsterite content – for example, a change of 0.5fo is equivalent to a change of 180 °C - and thus accurate olivine analyses are required.

A striking feature of any combination incorporating PBKN90 is that the lherzolitic garnet macrocrysts always yield higher pressures for equivalent temperatures relative to the garnet lherzolites. The eight garnet lherzolites have a garnet Cr_2O_3 composition of between 1.6 and 3.9 wt% (the majority around 1.7 wt%) whereas the garnet macrocrysts have a significantly higher garnet Cr_2O_3 concentration of between 4.6 and 5.7 wt%. The starting experimental materials used to calibrate PBKN90 include a synthetic mix "Baro" (garnet Cr_2O_3: 2.25 wt%) and sheared garnet lherzolite J4 from Jagersfontein (garnet Cr_2O_3: 2.04 wt%), both of which are similar to the Cr_2O_3 concentrations of the lherzolite xenoliths garnet, but significantly less than the lherzolitic garnet macrocrysts. Thus it appears that PBKN90 requires a Cr-correction factor to account for higher Cr concentrations in garnet. Under this assumption, empirical evidence at Newlands implies the high-Cr lherzolitic garnet macrocrysts pressure is overestimated by 3 to 5 kbar using PBKN90.

6.6 Discussion

6.6.1 The Cr concentration of Garnet

Experimental and empirical evidence show that the Cr content of chromite and pyrope garnet is strongly dependent on pressure, temperature and the Cr distribution coefficient between garnet and chromite (Brey et al., 1991; Daniels and Gurney, 1991). The seven diamond-bearing garnet macrocrysts with associated chromite have garnet CCA (22 to 27) and chromite CCA (84.5 to 85.5) that corresponds to temperatures of 1150 to 1250 °C and pressures of 42 to 46 kbar (based on the

isopleths of Brey et al. (1991)). However, this P-T range is in the graphite stability field at Newlands (based on a 37 to 38 mW/m^2 geotherm), and thus creates a paradox. Therefore the P-T relationship between the CCA of garnet and chromite are inaccurate, however, as noted by Brey et al. (1991), Fe and Ca are likely to affect the Cr content and appropriate corrections are required.

6.6.2 The effect of ferric iron on geothermobarometry

Stoichiometric Fe^{3+} calculations for peridotitic garnets are generally zero or extremely low (Fe^{3+}/Fe^{Total} less than 0.10). In contrast, clinopyroxene from diamond-free garnet macrocrysts have Fe^{3+}/Fe^{Total} ratios of up to 0.80. However, such high ratios are in contrast to mössbauer determinations on peridotitic clinopyroxenes that yield maximum Fe^{3+}/Fe^{Total} values of 0.40 (Canil and O'Neill, 1996; see detailed discussion in section 11.4.1) and therefore the stoichiometric calculated ratios of some peridotitic clinopyroxenes in this study are unlikely to be correct. This may be due to the low iron content in clinopyroxenes magnifying errors in the site allocation calculations, in particular, the silica and sodium contents are important in ferric iron determinations (Giaramita and Day, 1990). Consequently, calculated temperatures correcting for the presence of Fe^{3+} calculated from stoichiometry in peridotitic samples from Newlands are potentially unreasonable and unlikely to be more robust than assuming all Fe as ferrous. Furthermore, Sobolev et al. (1999) recently analysed a suite of xenoliths from the Siberian craton using Mössbauer and observed that when ferric iron was present it was generally at equivalent levels in both garnet and clinopyroxene. Thus the ferric iron effect on temperature is small and consequently no allowance for ferric iron has been made.

6.6.3 Comparison of T_{Ni}, T_{Zn} and xenolith geothermometers

In this study very few samples can be compared using the T_{Ni}, T_{Zn} and multiphase xenolith geothermometers. In addition, the multiphase xenolith geothermometers are all pressure dependent (to some extent), and thus reliant on the geobarometer with which they are combined, whereas the current T_{Ni} and T_{Zn} calibrations are independent of pressure. Nevertheless, a limited comparison is possible.

In most cases the Ni thermometers fall within the general spread displayed by the various multiphase xenolith geothermobarometers (Figure 6.8). However, on an individual level differences do occur, but the variations are no greater than occur between the numerous multiphase xenolith thermometers observed in this study and noted in numerous other geothermobarometric reviews (for example, Carswell and Gibb (1980, 1987), Finnerty and Boyd (1984, 1987), Nickel and Green (1985), Finnerty (1989), and Brey and Köhler (1990)). Comparisons between T_{Ni}Ryan96 and the other thermometers are commonly within 10 % of the mean. For example, comparing T_{Ni}Ryan96 vs TONW79 (for both pressure combinations of PMac74 and PBKN90) plots sub-parallel to the one-to-one line (Figure 6.8), with TONW79 commonly 50 to 100 °C greater for temperatures above 900 °C. Such a relationship is not unexpected given that TONW79 was one of the four geothermobarometers used to calibrate the empirical Ni thermometer. In contrast, T_{Ni}Canil94 does not yield good results. For example comparison of T_{Ni}Canil94 vs TONW79 (for both pressure combinations of PMac74 and PBKN90) diverge rapidly from a one-to-one line.

Comparison of either Ni thermometer with TBKN90 or TKr88 yields poor agreement, however, the data-set is small. The study of Mofokeng (1999) on a variety of xenoliths from Jagersfontein and Matsoku showed that TBKN90 displayed substantial differences with T_{Ni}Ryan96 at low temperatures. The same pattern is displayed at Newlands, albeit for a small data-set. Possible explanations for this differnce include: the difference in closure temperature between two-pyroxene solvus and the Ni concentration in garnet; the T_{Ni}Ryan96 calibration is based on extrapolation beyond the calibrated range of TONW79; and the imprecise temperature calculation based on the steep slope of pyroxene solvus at low-T.

Diamond-bearing sample AHM 58 yields an overall range of 100 °C, all within the diamond stability, using various geothermometers, for example T_{Ni}Ryan96 of 966 °C, T_{Ni}Canil94 of 1025 °C and TONW79 1069 °C (at 50 kbar). Combined with the results above, it is impossible to determine the "best" geothermometers as they are all within the diamond stability field and within 10 % of each other. Currently, upper mantle geothermobarometry is incapable of providing P-T's more accurate or precise than this.

The trace element thermometers of T_{Zn}Ryan96 and T_{Ni}Ryan96 yield inconsistent results. This is unexpected since T_{Zn}Ryan96 was calibrated against T_{Ni}Ryan96 (Ryan et al., 1996). The chromite thermometer T_{Zn}Ryan96 is often higher by between 100 and 200 °C and sometimes more (Figure not shown). These calculated temperatures are also at the upper extremities compared to other calculations for any xenolith from Newlands and are therefore likely to be wrong. The discrepancy between T_{Zn}Ryan96 and T_{Ni}Ryan96 is significant and indicates that the zinc thermometer calibration against T_{Ni}Ryan96 is not accurate. Even though T_{Zn}Ryan96 is calibrated against T_{Ni}Ryan96, the variation in upper mantle temperatures for any given Zn-in-chromite concentration renders T_{Zn}Ryan96 inappropriate for individual samples or small sample sets. For example, the same Zn concentration in chromite is obtained for samples associated with garnets ranging in T_{Ni}Ryan96 from 1150 to 950 °C (see Figure 14: Griffin and Ryan, 1995).

6.6.4 The upper mantle beneath Newlands

Newlands has a particularly high percentage of garnets sampled from within the diamond stability field. Of the 124 garnets analysed (this study combined with van Heerden et al., unpub. data)), 74 % are derived from within the diamond stability field (assuming a 37 - 38 mW/m^2 geotherm). Furthermore, the vast majority of harzburgitic G10 garnets are within the diamond stability field. The temperature overlap of the various garnet groups may have important implications for the mantle stratigraphy. Whilst thermometers are not extremely accurate or capable of defining small scale changes of mantle stratigraphy, the overlap of G9 and G10 garnets implies small-scale intermixing of lherzolite and harzburgite rather than large discrete units of either composition. This overlap has been observed at other locations on the Kaapvaal and Siberian cratons (for example, Griffin and Ryan, 1995; and references therein).

The various geothermobarometer combinations yield P-T distributions for lherzolites that predominantly lie between 37 and 38 mW/m^2 geotherms. These "low" geotherms are supported by numerous other lines of evidence, as discussed in the previous sections. Such geotherms are similar to other Group II kimberlites in southern Africa,

for example Finsch and Roberts Victor (Skinner, 1989; Clement and Reid, 1989; Griffin and Ryan, 1995; Herman Grütter, pers. com., 1999). Moreover, it is distinctly different from what is regarded as a "*normal*" cratonic geotherm of ~ 40 mW/m^2 (Pollock and Chapman, 1977) and displayed by many (Group I) kimberlites in southern Africa, for example Northern Lesotho kimberlites (Nixon and Boyd, 1973; Boyd and Nixon, 1975; Finnerty and Boyd, 1987), Koffiefontein (Bell, 1981), Monastery (Boyd, 1975), Jagersfontein (Harte, 1987; Finnerty and Boyd, 1987; Mofokeng, 1999), Matsoku (Mofokeng, 1999), and Kimberly (Boyd and Nixon, 1978).

PERIDOTITIC XENOLITHS: RE-OS SYSTEMATICS

7

7.1 INTRODUCTION

Previous radiogenic isotopic studies of mantle peridotites and peridotitic diamond inclusions have concentrated on the use of incompatible element isotopic systems such as Rb-Sr, Sm-Nd and U-Th-Pb. These systems can be, and usually are, reset by mantle metasomatic events. In contrast, Re and Os are strongly fractionated from one another during the production of a mafic protolith by partial melting of mantle peridotite. Compared to the Rb-Sr or Sm-Nd systems, the degree of Re and Os fractionation can be several of orders of magnitude greater because Re is moderately incompatible during melting whereas Os can be strongly compatible. The large change in Re/Os that occurs during melting causes the Os isotopic composition of the melt to rapidly diverge from that of its mantle source, subsequent to melting. Because of this large shift in the parent-daughter ratio, later chemical modification of the rock by metamorphism, metasomatism, or partial melting, potentially will result in less obfuscation of the initial protolith formation age than would occur in any other available isotopic system. Therefore, Re-Os systematics can potentially "*see through*" these events and record the original depletion event, thus making it the ideal system to constrain the formation age of cratonic peridotite xenoliths (Chesley et al., 1998; Carlson et al., 1999).

7.2 SAMPLE DESCRIPTION

Six diamond-bearing peridotitic garnet macrocrysts, three diamond-free peridotitic garnet macrocrysts and six peridotite xenoliths were analysed for whole rock Re-Os isotope systematics (Table 7.1). In addition, one diamond-bearing garnet macrocryst (AHM D2) and two diamond-free garnet macrocrysts (AHM 87 and AHM C9) also contained significant primary chromite, which was analysed as a mineral separate.

The peridotite xenoliths are comprised primarily of unaltered coarse-grained olivine and orthopyroxene with minor amounts of garnet. None of the samples contained primary clinopyroxene, however, due to the coarse grain and small sample size, modal concentrations have large undefined uncertainties. Garnets from Newlands peridotite xenoliths display a wide range in Cr_2O_3 and CaO compositions. The diamond-bearing garnet macrocrysts analysed for Re-Os all have Cr_2O_3 concentrations greater than 7.5 wt %, the majority of which were highly sub-calcic (Figure 7.1). None of the diamond-bearing calcic G9 garnets were analysed for Re-Os. Note that two of the diamond-free garnet macrocrysts (AHM 87 and AHM 110) and four of the low-T coarse peridotite xenoliths (AHM 731, AHM C1, AHM C3 and AHM C4) have similar garnet compositions to those from the diamond-bearing garnet macrocrysts.

7.3 SAMPLE PREPERATION AND ANALYTICAL PROCEDURE

All analyses were determined on whole rock samples with the exception of three chromite separates. Each sample was broken into small fragments and then powdered. Between 1 and 3 grams of each sample was spiked with ^{190}Os and ^{185}Re, digested in 4 ml concentrated HCl and 2 ml concentrated HNO_3, and sealed in a Pyrex Carius tube for digestion following the method of Shirey and Walker (1995). This digestion technique dissolves "*platinum-group element minerals, metals, and sulphides and evidently sufficiently reacts with silicates to release most or all Re and Os contained in a silicate matrix*" (Shirey and Walker, 1995). Therefore, it is believed that all the Re and Os from the garnet macrocryts and periodotites (this chapter) and eclogites (Chapter 13) was extracted even though residues were observed in the carius tube after digestion for 24 hours at ~ 220 °C. Os was separated from Re by a two stage distillation. The Os cut was further purified by micro-distillation. The sample remaining after distillation was then passed through two sets of pre-cleaned AG1-X8 ion exchange columns. The average Re blank, Os blank and Os yield are <12 pg, <2 pg and 50 to 80 %, respectively. The 2 pg Os blank is inconsequential to sample sizes used in this study, however a Re blank of 12 pg was subtracted from all analyses shown in Table 7.1. All rhenium and osmium isotope analyses were performed at the Department of Terrestrial Magnetism (DTM), Carnegie Institution of

Washington. The samples were run by negative thermal ionisation mass spectrometry (NTIMS) generally following the procedures outlined in Creaser et al. (1991). Detailed descriptions of the analytical procedures and operating conditions are given in Appendix I as well Shirey (1997) and Pearson et al. (1995b).

7.4 Re-Os Concentration Systematics

A summary of whole rock rhenium and osmium concentrations and isotopic compositions for the three groups of Newlands peridotitic xenoliths are shown in Table 7.1. Also included are three chromite separates analysed from three of the samples.

7.4.1 Rhenium

Re concentrations for Newlands peridotitic xenoliths vary considerably (Figure 7.2), but are significantly lower than that expected for fertile mantle (0.26 ppb: Morgan, 1986). The maximum Re concentration of 0.1164 ppb is less than half that estimated for fertile mantle. Whilst the garnet macrocrysts have Re concentrations that extend to lower and higher levels than the low-T coarse peridotite xenoliths, the overall range is small and extremely low when compared to other Kaapvaal peridotite xenoliths. For example, the majority of samples are significantly lower than the average determined for a variety of Kaapvaal peridotite suites (0.084 ppb: Carlson et al., 1999). This is consistent with the extremely depleted nature of the Newlands peridotitic xenoliths, with some of the diamond-bearing garnet macrocrysts having Re concentrations less than 10 ppt.

Re partitions into melts with a distribution coefficient similar to Al (Reisberg and Lorand, 1995), and, therefore, in any depletion event all the Re would be expected to partition into the melt. Kaapvaal peridotite xenoliths, however, consistently show low, but varying Re concentrations that display little correlation with Al_2O_3 (Walker et al., 1989; Pearson et al., 1995a; Carlson et al., 1999, this study). This suggests that Re concentrations in Kaapvaal peridotite xenoliths are not controlled by partial melting alone (Carlson et al., 1999). Instead, melt and/or kimberlite metasomatism is

likely to affect the peridotite Re concentrations, particularly given the several orders of magnitude difference in Re concentrations between most melts and depleted peridotite. Therefore it is resonable to assume that the samples with the lowest Re concentration will be the least affected by any Re-enrichment metasomatic event. Samples AHM D2 and AHM 110 have the lowest Re concentrations of 6.5 and 7.9 ppt, respectively. These levels are similar to Re concentrations of 3 to 6 ppt observed in "apparently unmetasomatised" peridotite xenoliths from San Carlos (Morgan et al., 1991), Namibia (Pearson et al., 1995a) and the Kaapvaal (Pearson et al., 1995a), and thus might represent approximate Re levels of unmetasomatised peridotite xenoliths after large-scale melt extraction.

The highest Re concentrations of a Newlands peridotite are 117 and 112 ppt for samples AHM D4 and AHM D10, respectively. Whilst these higher Re contents might reflect metasomatic addition of Re, they are still low compared to estimates of the Re content of fertile mantle (Figure 7.2). Furthermore, the slightly higher Re contents are consistent with the Os isotopic composition of these two samples, which yield Re-Os model ages of 2.1 and 3.3 Ga, respectively. In contrast, many peridotite xenoliths affected by Re addition give Re-Os model ages older than the age of the Earth, a clear sign of recent Re addition. Nevertheless, sample AHM D10 displays evidence of metasomatism; the garnet has the highest Ca content of all the diamond-bearing G10 garnet macrocrysts (Figure 7.1) and there is secondary mineralisation of clinopyroxene and spinel along cracks in the garnet.

7.4.2 Osmium

Newlands peridotite xenoliths display considerable scatter in Os concentrations (Figure 7.3), with approximately half having concentrations higher than fertile mantle (3.4 ppb: Morgan, 1986). This is consistent with Os behaving as a compatible element during melting. The overall range is similar to that for peridotite xenoliths from across the Kaapvaal (Carlson et al., 1999). Such high Os concentrations are difficult to explain in terms of simple melting, and, instead, may relate to the introduction of ultra-trace Os-rich phases. Os in mantle peridotite is known to be concentrated into trace PGE-rich phases (Hart and Ravizza, 1995), and one possibility is sulphides, such as those associated with diamond formation which are known to

have relatively high Os concentrations (Pearson et al., 1998, 1999). Two samples (AHM 58 and AHM 110) have Os concentrations two orders of magnitude lower and $^{187}Re/^{188}Os$ ratios over an order of magnitude greater than all other Newlands or Kaapvaal peridotite xenoliths analysed. Sample AHM 110 also has one of the lowest Re concentrations and, thus, the high $^{187}Re/^{188}Os$ ratio is not the result of Re introduction. Instead, Os appears to have been removed from the xenolith or was absent to begin with. Alteration of the garnet macrocrysts could result in the weathering of sulphides, however, these two specimens do not display any evidence of alteration that is different to any of the other garnet macrocrysts. Indeed, sample AHM 58 is the only diamond-bearing garnet macrocryst from which a fresh core of an altered olivine has been found. If Os is incorporated in ultra-trace phases in the residua after melting then they are likely to be unevenly distributed. Therefore the low Os concentrations in these two samples may be due to the lack of an ultra-trace Os carrying phase within the specimen. This is possible given the small sample size and nearly monomineralic nature of the Newlands garnet macrocrysts and therefore they may not incorporate a representative amount of an ultra-trace Os carrying phase. In contrast, sample AHM D8 appears to have undergone recent Os addition, possibly incorporated within introduced sulphides, similar to peridotite xenoliths from Tanzania (Chesley et al., 1999).

Sample AHM C9 has an Os concentration of 18.4 ppb, higher than any Newlands or Kaapvaal peridotite. However, AHM C9 has a high modal percentage of chromite and a single chromite grain extracted from the sample has an Os concentration of 222 ppb (Table 7.1). This may explain the high whole rock concentration. In contrast, a group of chromites from AHM D2 have an Os concentration of 3.8 ppb (Table 7.1) implying that the Os is incorporated within micro-inclusions and not the chromite lattice.

7.5 Re-Os Isotope Systematics

7.5.1 Diamond-bearing Peridotitic Garnet Macrocrysts

Both diamond-bearing and diamond-free garnet macrocrysts display similar rhenium-osmium isotope systematics. The majority of the samples have Os isotopic compositions that are extremely unradiogenic, with measured $^{187}Os/^{188}Os$ ratios below 0.11620 down to 0.10574 (Table 7.1, Figure 7.4). This is the most unradiogenic Os signature measured to date for a peridotitic xenolith. The unradiogenic Os is consistent with the depleted nature of these peridotitic xenoliths and indicates that the Re-depletion characterising these samples occurred long before entrainment in the host kimberlite.

Four of the specimens (AHM D8, AHM 58, AHM 110 and a chromite separate from AHM 89) have $^{187}Os/^{188}Os$ ratios greater than present day bulk earth. Two of these samples (AHM 58 and AHM 110) also have Os concentrations lower by almost two orders of magnitude compared to the other Newlands peridotite xenoliths. The potential causes of these low Os concentrations have been discussed in section 7.4.2. Such low Os contents cause the two samples to be extremely susceptible to modification of their Os isotopic composition by addition of Os from the host kimberlite. Though the Os isotopic composition of the Newlands kimberlite has not been determined, other kimberlites have Os isotopic compositions approaching that measured for samples AHM 58 and AHM 110 (Walker et al., 1989; Carlson et al., 1999). This suggests the possibility that the Os isotopic compositions of these two samples are recording interaction with the host kimberlite. Sample AHM D8, with a relatively high $^{187}Re/^{188}Os$, has a "normal" Os concentration, but also contains sulphides that are visible in hand specimen. This is similar to peridotite xenoliths from Tanzania (Chesley et al., 1999) and implies that this sample may have interacted with the host kimberlite or with similar magmas in the mantle beneath Newlands. A similar possibility exists for the chromite separate from sample AHM 89, which may contain micro-inclusions of introduced sulphides.

7.5.2 Low-T coarse peridotite xenoliths

The coarse-grained peridotite xenoliths display extremely consistent rhenium-osmium isotope systematics. Rhenium contents are low, with the samples falling in the range of 31 to 75 ppt (Figure 7.2). This is slightly narrower than the garnet macrocryst range, however, samples AHM C1 and AHM C2 have not been analysed for Re. Osmium whole rock contents vary from 2.9 to 8.8 ppb (Figure 7.3). As with the garnet macrocrysts there is no apparent relationship to garnet Mg# (Figure 7.5), Al/Cr ratio or other indicators of the degree of melt depletion. All the specimens have very consistent Os isotopic compositions that are extremely unradiogenic ($^{187}Os/^{188}Os$ ratios 0.1086 to 0.1112) and have $^{187}Re/^{188}Os$ ratios less than 0.121.

7.6 Discussion

7.6.1 Time Of Depletion

If the Newlands peridotite xenoliths were derived from a common source in a single stage event then the specimens should define a Re-Os isochron. As seen clearly in Figure 7.6, the Newlands peridotite xenoliths, or their various subgroupings (including a two-point "*isochron*" comprised of the whole rock and the chromite separate analyses for sample AHM 87), do not define an isochron. In most cases it is not surprising given that some of the samples may contain a significant introduced Re component. This potential problem was addressed by Walker et al. (1989) who assumed that all Re was removed in the initial depletion event and, therefore, any Re in the sample is kimberlitic or metasomatic in origin. Although this is a broad assumption, it is not unrealistic, particularly since the depletion event should partition all the Re into the melt and leave Os behind in the residua (Walker et al., 1989). Thus, the Re-depletion model age (T_{RD}) assumes a time-averaged $^{187}Re/^{188}Os$ in the sample of zero. At the other extreme, if all the measured Re was left in the residua after the original depletion event then a traditional Re-Os isotope model age (T_{MA}) can be determined. Assuming that the peridotite was derived from a "bulk-mantle"

reservoir[14] then T_{RD} is a minimum age whilst T_{MA} is a maximum age. This method and formulae used are described in detail by Walker et al. (1989) and Carlson et al. (1998). The analytical error in the calculated age is the same as those of the measured isotopic ratio and for this study are commonly significantly less than 0.1 Ga.

The $^{187}Re/^{188}Os$ ratios for both the garnet macrocrysts and low-T coarse peridotite xenoliths are very low (commonly less than 0.05) and, consequently, the growth in ^{187}Os from radiogenic decay is minor. Accordingly, the difference between T_{RD} and T_{MA} is small, generally less than 400 Ma, and the time period of peridotite formation is restricted. Three samples, all garnet macrocrysts (AHM 58, AHM D8 and AHM 110), have negative model ages due to disturbed Re-Os systematics (see earlier) and are excluded from the following age discussions.

First order observations reveal that the peridotite xenoliths were formed between the mid Archæan and early Proterozoic (Figure 7.7 a and b). Neither T_{RD} nor T_{MA} display any discernible variation with P-T conditions (plot not shown). The mode of both T_{RD} and T_{MA} is between 2.5 to 3.0 Ga and is identical to other Re-Os model ages of peridotite xenoliths from the Kaapvaal craton (Figure 7.7 c and d). The three peridotite groups display no significant differences in average ages; mean T_{RD} and T_{MA} are 2.7 and 3.0 Ga for diamond-bearing garnet macrocrysts, 2.4 and 2.9 Ga for diamond-free garnet macrocrysts, and 2.6 and 3.0 Ga for low-T coarse peridotite xenoliths. However, these average ages assume that the xenoliths in each group are cogenetic, which may not be the case. Indeed, if the ages are assessed independently then subtle differences do appear. Interpretation is, however, more subjective due to the limited number of samples.

The diamond-bearing garnet macrocrysts display a wide range in ages, minimum T_{RD} 1.7 Ga, maximum T_{MA} 3.5 Ga. The spread in the ages of the four "undisturbed" diamond-bearing garnet macrocrysts implies three distinct periods of formation (Figure 7.8). Two samples give mean T_{RD}-T_{MA} ages of 3.1 and 3.4 Ga, another sample 2.8 and 2.9 Ga, whilst the last sample yields 1.8 and 2.1 Ga. The mid

[14] Assumed values for "bulk-mantle" reservoir are $^{187}Re/^{188}Os = 0.4243$ and $^{187}Os/^{188}Os = 0.1287$. Note that calculated ages will vary depending on the values used as a reference for "bulk-mantle" resrvoir, for example if carbonaceous chondrites as used then calculated ages may change by ± 200 Ma.

Archæan T_{RD}-T_{MA} period overlaps harzburgitic garnet diamond inclusion model age of 3.3 ± 0.2 Ga (Richardson et al., 1984); the late Archæan T_{RD}-T_{MA} period coincides with a major period of depletion beneath Newlands (this study) and Kimberley Group (Carlson et al., 1999) kimberlites; whilst the Proterozoic T_{RD}-T_{MA} period overlaps the major emplacement at ~2.05 Ga of the Bushveld Igneous Complex (approximately 450 km to the NE) and lherzolitic garnet diamond inclusion model age of 1.93 ± 0.04 Ga (Richardson et al., 1993).

These discrete periods of formation are not as clear if the diamond-free garnet macrocrysts are considered. Sample AHM 87 has a relatively high $^{187}Re/^{188}Os$ ratio that leads to a large difference between T_{RD}-T_{MA} model ages (2.2 to 2.9 Ga). This overlaps the late Archæan period of diamond-bearing garnet macrocryst formation. However, the large difference between T_{RD}-T_{MA} ages leads to far greater uncertainty and, therefore, AHM 87 may have formed at a separate time to the diamond-bearing garnet macrocrysts. Sample AHM C9 garnet major element composition is different to the diamond-bearing garnet macrocrysts and thus it is unlikely to be cogenetic. Even so, its age also corresponds to the middle period of diamond-bearing macrocryst formation.

In contrast to the variability displayed by the garnet macrocrysts, the low-T coarse peridotite xenoliths have a relatively narrow range in ages (T_{RD}: 2.4 to 2.8 Ga). Of this group, the solitary lherzolitic sample (AHM 730), based on garnet composition, reveals no significant age difference. The most appropriate formation age for the low-T xenoliths is approximately 2.7 to 2.8 Ga (Figure 7.8). This corresponds with ages for peridotite xenoliths from the Kimberley group (Carlson et al., 1999), 60 km to the SE, and implies a significant depletion event at this time beneath this area of the Kaapvaal craton. This age is also coincident with the collision of the Kaapvaal and Zimbabwe cratons (de Wit et al., 1992).

ECLOGITE XENOLITHS: SAMPLE DESCRIPTION AND PETROGRAPHY

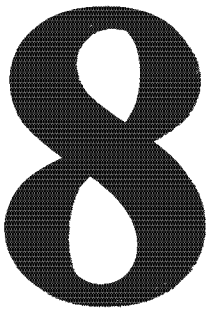

8.1 INTRODUCTION

Newlands eclogites were primarily collected from the coarse concentrate, which ranges in size from 1 - 10 cm in the longest dimension. In addition, samples were collected from kimberlite ore stock-piles and from old floor dumps, some of which were much larger. The eclogites obtained from the coarse concentrate are irregular in shape with fresh breakage surfaces rather than the rounded nature observed for many larger peridotite xenoliths collected in the old dumps at Newlands or eclogites from locations such as Roberts Victor (Hatton, 1986; Hatton and Gurney, 1987). The eclogites represent parts of larger xenoliths broken by the processing plant crushers.

The eclogites display a variety of appearances in hand specimen; for example both the garnet and clinopyroxene colours and the extent of alteration (of clinopyroxene) vary dramatically. The eclogites were subdivided into five distinct groups (termed groups *NewA* through *NewE*) on the basis of megascopic texture (in particular grain size and mineral colour), mineralogy, and degree of alteration. Their size is commonly within the range 4 to 6 cm in length and 2 to 4 cm in width and depth, and of irregular shape. The diamond-bearing eclogites are termed Group *NewE*, whilst eclogite Group *NewD* is essentially equivalent to Group *NewE* eclogites except that they do not contain diamond.

8.2 DIAMOND-BEARING ECLOGITE (GROUP NEWE)

Seventeen diamond-bearing eclogites have been examined. These eclogites vary from 2 to 6 cm in their longest dimension and are modally dominated by the bi-minerallic assemblage of garnet and clinopyroxene. The eclogites are coarse grained with modal proportions of garnet to clinopyroxene ranging from 60:40 to 30:70. These estimates

are imprecise due to the small sample size (5 to 30 grams) and large grain size (up to 1 cm). These eclogites may not accurately represent the source rock from which they were derived, particularly in a 2-D slide, and consequently no detailed point counting was undertaken. All have similar garnet and clinopyroxene grain sizes and colours and show variable degrees of fracture development. Trace primary phases observed include diamond, sulphide aggregates and rutile. Table 8.1 summarises the various phases observed in each specimen, whilst Plates 8.1 through 8.18 display some of the diamond-bearing eclogites in hand specimen. Neither kyanite nor corundum were observed in these specimens, but they have been noted in other diamond-bearing eclogites from Newlands and in diamond-free eclogites (for example, see Bonney, 1900; Rickwood et al., 1969; Rickwood and Mathias, 1970; this study).

In thin section the garnet and clinopyroxene make up over 90 % of the modal constituents (Plates 8.19 to 8.30). The xenoliths display no evidence of banding, are generally massive and contain garnet set in matrix of, or occasionally, poikilitically enclosed by clinopyroxene. This texture is similar to that of Group I eclogites studied by MacGregor and Carter (1970) and MacGregor and Manton (1986). Alteration (due to metasomatism or kimberlite invasion) is pervasive and ranges from minor grain boundary intrusions to massive mineral (primarily clinopyroxene) replacement (Plate 8.19 to 8.23).

Garnets are orange to pale orange, subequant and appear relatively free from alteration. They display a range of grain sizes, frequently from 2 to 5 mm but ranging to over 20 mm. In addition they also (rarely) occur as small poikilitic inclusions (less than 500 μm) within clinopyroxene. The garnets are generally rounded or have irregular outlines that are embayed by the clinopyroxene. Smaller garnets may occur at triple junctions of clinopyroxene grains. Unusually, very few of the garnets have a noticeable kelyphitic rim, and when it is present it is extremely thin.

The clinopyroxenes are transparent and show a wide range of shades from dark to pale green. They range in size from 2 mm up to 20 mm and regularly occur as smaller inclusions poikilitically enclosed by garnet, more commonly than vice versa (Plate 8.26 through 8.28). For example, a clinopyroxene and sulphide, each

approximately 50 μm in diameter, are enclosed by garnet from sample AHM K6 (Plate 8.28). They also display various stages of alteration. The alteration is pervasive but in any one section may affect between 30 and 80 % of the clinopyroxene. The alteration can be divided into two types: the first is turbid in transmitted light, very fine-grained and opaque (Plates 8.19 through 8.20) whereas the second is patchy, not as fine-grained and surrounds the large relic islands of clinopyroxene (Plates 8.33 and 8.34). The latter alteration type is more common. Moreover, it is possible that the former alteration type may represent the extensive end product of the latter alteration type. In hand specimen the alteration appears as a lighter shade of green or creamy white.

The eclogites also display a high degree of pervasive metasomatism with the introduction of secondary minerals such as phlogopite, amphibole, calcite and possibly some opaque oxides (Plates 8.23, 8.24, 8.25 and 8.29). No exsolution features were observed in either garnet or clinopyroxene. Phlogopite grains are commonly very small (100 to 500 μm) and in contact with garnet or altered clinopyroxene while calcite primarily is located between the phlogopite grains separating the primary phases.

Sulphide aggregates have been observed in the majority of petrographic polished sections of the diamond bearing eclogites. They predominantly occur as ovoid or elongate blebs up to 500 μm in diameter located interstitial to, or enclosed by garnet and clinopyroxene (Plates 8.25, 8.27 and 8.28). The sulphide phases of pyrrhotite, pentlandite and chalcopyrite have been identified: pyrrhotite is the dominant phase with minor, but significant amounts of both pentlandite and chalcopyrite. Each sulphide aggregate has similar modal phase proportions and also displays a distinctive spatial distribution: pyrrhotite in the centre with orientated exsolved lenses of pentlandite, and peripheral rims of chalcopyrite (shown clearly by trace element mapping, see Chapter 11).

Each of the eclogites contained several diamonds protruding from the surface. The exact number of diamonds contained in each xenolith is not possible to determine due to several of the diamonds splintering into multiple fragments upon breaking of the

xenolith. The recent development of tomography, a new technique that creates a 3-D image of a xenolith (Schulze et al., 1996; Keller et al., 1999), would help determine the number of diamonds and whether or not any spatial relationship existed with other mineral phases or structural properties of the xenolith. The diamonds were located within both the garnet and clinopyroxene or along grain boundaries. Some of the diamonds occur in fractures in the eclogite (Plate 8.10), however the number of diamonds that fall into this category is unknown. Diamond modally comprises on the order of 1%, although no accurate determinations were made. This carbon content or grade is several orders of magnitude greater than observed in the Newlands kimberlite, or indeed, any diamondiferous kimberlite. Detailed descriptions of the eclogitic diamonds (as well as others) are given in Part IV.

8.3 DIAMOND-FREE ECLOGITES

8.3.1 Group NewA Eclogites

These eclogites are generally smaller than the other groups, with a maximum dimension of 4 cm, and are irregularly shaped. They appear to be remarkably fresh with broken surfaces on all sides. Modal proportions of garnet to clinopyroxene are approximately 50:50, however this is subjective due to the small sample size. The eclogites have a granular texture with equant euhedral interlocking garnet and clinopyroxene grains, commonly around 2-6 mm in size (Plate 8.35, 8.36). The grain size of garnets and clinopyroxenes within individual xenoliths does not appear to vary a great deal. The garnets range in colour from deep orange to dark red-brown whilst the clinopyroxenes range from pale to dark green. Even though the clinopyroxene displays a variety of shades of green it is not related to alteration. In fact, metasomatism and alteration appears to be minimal in this group (Plate 8.35, 8.36).

8.3.2 Group NewB Eclogites

These eclogites are large compared to the other groups and range up to 8 cm in the longest dimension. Clinopyroxene appears to have a higher modal abundance than garnet. However, the large grain size precludes any accurate determination of modal

proportions. The garnets are commonly euhedral, light orange in colour and range up to 2 cm in size. The clinopyroxenes are dark green and display a variety of grain sizes. Furthermore, the clinopyroxene shows the affects of alteration, with minor amounts of light green to white friable mineralisation.

8.3.3 Group NewC Eclogites

These eclogites are commonly 3 to 6 cm in maximum dimensions. Clinopyroxene appears to have a higher modal abundance than garnet, however, the large grain size preclude any accurate determination of modal proportions. The garnets are a pale orange and range up to 1 cm in size. The clinopyroxenes are light apple green, and yield a range in sizes. In addition, they display various stages of alteration. The majority of these eclogites also contain trace amounts of rutile.

8.3.4 Group NewD Eclogites

This group is similar to diamond-bearing eclogites (see above), except that there are no diamonds exposed on the surface of the xenolith. Otherwise, in hand specimen they are texturally equivalent.

8.3.5 Other Eclogites from Newlands

A variety of eclogites have been reported in other studies from Newlands. Undoubtedly many of those eclogites fall outside the five groups described above. These include both kyanite and corundum bearing eclogites noted in this study and those of Rickwood et al. (1969) and Rickwood and Mathais (1970). Such a detailed examination of all these xenoliths is outside the scope of this study.

8.4 Discussion

The macroscopic descriptions and petrography of the diamond-bearing eclogites from Newlands is similar to that displayed by the majority of diamond-bearing eclogites from around the world, for example Bellsbank (Viljoen, 1995) and Udachnaya (Jerde

et al., 1993; Beard et al., 1996; Taylor et al., 1997). In general diamond-bearing eclogites display a range of primary modal mineralogy, may contain minor amounts of oxides and sulphides, have diamonds of various sizes and morphologies, and have variable alteration of clinopyroxene. However, not all eclogites from around the world fall into this broad description. For example, the diamond-bearing eclogites from Mir contain "*predominantly sharp-edged octahedra*" ... "*and are very different compared to diamonds from Udachnaya eclogites and from South African eclogites, where diamonds of variable morphology ... occur*" (Beard et al., 1996).

ECLOGITIC XENOLITHS: MAJOR ELEMENT MINERAL CHEMISTRY

9

9.1 INTRODUCTION: ECLOGITE GEOCHEMISTRY - LITERATURE TERMINOLOGY

Over the years eclogites have been broadly grouped, and subsequently referred to, based on their petrography, mineral chemistry and isotopic composition. MacGregor and Carter (1970) originally proposed a two group classification: all coarse "*cumulate*" textured eclogites were classified as Group I and finer grained "*interlocking*" textured eclogites were classified as Group II. Later, McCandless and Gurney (1989) studied the mineral chemistry of Roberts Victor eclogites that could be visually classified as either Group I or Group II, as well as diamond-bearing eclogites from a variety of locations. The results of their study indicated that the Na concentration in garnet and K concentration in clinopyroxene was significantly enriched in Group I eclogites relative to Group II eclogites and they proposed that levels of 0.09 wt% Na_2O_{Gar} and 0.08 wt% K_2O_{Cpx} be used to distinguish the groups. The Na_2O_{Gar} concentration was latter lowered to 0.07 wt% (Gurney et al., 1993; Gurney and Zweistra, 1995). Moreover, they observed that diamond-bearing eclogites and eclogitic diamond inclusions all yield compositions belonging to Group I eclogites.

An alternative classification scheme has also developed whereby eclogites are classified into three groups. Shervais et al. (1988) combined mineral chemistry and stable and radiogenic isotopes to the original mineralogical classification of Coleman et al. (1965) where eclogites were grouped as A, B or C. Later studies by Taylor and Neal (1989), Neal et al. (1990), Jerde et al. (1993) and Snyder et al. (1997) all refined the various group classifications. In general, Group A eclogites are characterised by high whole rock Mg#'s, low jadeite and Cr-rich clinopyroxenes and Mg- and Cr- rich garnets. In contrast Group B have moderate jadeite contents in clinopyroxenes and Fe-rich garnets, whilst Group C eclogites are characterised by high jadeite contents in

clinopyroxene and Ca- rich garnets. Jerde et al. (1993), however, cautioned against schemes based on eclogites from just the Kaapvaal craton as it may not be applicable to eclogites derived from elsewhere, for example, Siberia, where the protolith may be different.

9.2 METHODOLOGY

9.2.1 Analytical Techniques and Operating Conditions

Analytical details are the same as for the peridotitic xenoliths described in Part II, Chapter 4. Explicit details of the set-up and analytical conditions of each EMP and the PMP are given in Appendix I, whilst analyses are presented in Appendix II.

9.2.2 Sample Description

In total, 17 diamond-bearing eclogites were analysed in detail, whilst approximately 50 diamond-free eclogites were analysed for comparative purposes. Mineral chemistry was determined on both polished sections and probe mounts of seventeen diamond-bearing eclogites and numerous probe mounts of diamond-free eclogites. Hand specimen descriptions and petrography have identified five eclogite populations and a representative sample set from each population was analysed for major elements to determine if they displayed distinctive mineral chemistry.

The majority of specimens analysed in this study are of a relatively small size (commonly less than 6 cm: see Chapter 8). Consequently, no whole rock compositions have been analytically determined as the modal mineralogy is subjective and possibly meaningless. For example, the probe slide of diamond bearing eclogite AHM K17 consists of ~ 25% garnet, whereas the probe slide of diamond-bearing eclogite AHM K6 consists of ~ 80% garnet - neither of which is likely to be the case for the larger xenolith or rock source it was derived from in the mantle. Analyses for both major (and trace elements, see Chapter 11) are therefore on individual mineral phases only.

9.3 ECLOGITIC GARNET GEOCHEMISTRY

9.3.1 Diamond-bearing Eclogites (Group NewE)

The garnets from the diamond-bearing eclogites display a relatively restricted range of compositions (Table 9.1). The garnets have a very narrow range of Mg#'s: 13 of 15 eclogites have a Mg# between 49.2 and 51.6 whilst the other two samples have slighter higher Mg#'s of 54.1 (AHM K16) and 55.0 (AHM K8), respectively. These Mg#'s are relatively low compared to the bulk of other garnets in diamond-free eclogites from Newlands. Such Mg#'s correspond to their relative Fe-rich (FeO: 18 to 21.5 wt%) and Ca- and Mg- poor nature (CaO: 4 to 7.5 wt%; MgO: 11.5 to 13 wt%) (Figure 9.1 a and b and 9.2). In addition, the garnets are Cr-poor (Cr_2O_3: < 0.14 wt%) and Ti- and Mn- rich (TiO_2: 0.23 to 0.29 wt%; MnO: 0.29 to 0.52 wt%) relative to other diamond-free eclogites from Newlands. Moreover, the garnets display the high Na_2O concentrations (0.08 to 0.14 wt%) associated with Group I eclogites (Figure 9.1c), whilst TiO_2 concentrations are not as high as those associated with megacrysts.

Multiple core - rim analyses, detailed point traverse and elemental scans indicate that the garnets are homogeneous. Even though there are some subtle compositional changes, there are no systematic variations. Detailed point traverses of two diamond-bearing garnet macrocrysts (samples AHM K2 and AHM K14) yield major and minor element compositions that are within 2 standard deviations (Figure 9.3 a and b). The occasional individual point spikes observed in some of the analyses can be linked to fractures that occur within the garnet.

It is noticeable that majority of the garnets from the diamond-bearing eclogites have extremely similar compositions – in fact, only four garnets (AHM K8, AHM K13, AHM K15 and AHM K16) display any appreciable variation. Even so, the overall garnet compositional range is small relative to that displayed by the other diamond-free eclogites from Newlands.

9.3.2 Diamond-free Eclogites (Groups NewA through NewD)

The garnets from the diamond-free eclogites display a wide range of compositions. The Mg#'s range from 50.0 to 81.8 with the vast majority significantly higher than the diamond-bearing samples. This corresponds to their relatively Mg-rich and Fe-poor nature (Figure 9.1). Moreover, they display a range of Na_2O concentrations, with all but six samples having less than 0.07 wt%, and thus classifying as Group II eclogites.

Noticeably, five of the six samples from Group NewD, display geochemistry that overlaps (or is similar to) the diamond-bearing eclogites (Figure 9.1). These five samples were identified in Chapter 8 as displaying similar macroscopic features to the diamond-bearing samples except for the absence of diamond.

9.4 ECLOGITIC CLINOPYROXENE GEOCHEMISTRY

9.4.1 Diamond-bearing Eclogites (Group NewE)

The clinopyroxenes from the diamond-bearing eclogites also display a relatively restricted range of compositions (with one notable exception) (Table 9.2). The clinopyroxenes display low Mg#'s: 13 of 15 eclogites have Mg#'s ranging from 74.0 to 77.6, whilst the other two samples have Mg#'s of 81.8 (AHM K16) and 89.0 (AHM K6), respectively. Such Mg#'s numbers correspond to their relative Fe-rich (FeO: 3.3 to 6.9 wt%) and Ca- and Mg- poor (CaO: 13 to 16 wt%; MgO: 10 to 11.5 wt%) nature. Furthermore, the clinopyroxenes are Na-, Ti-, and Mn- rich (Na_2O: 4 - 6 wt%; TiO_2: 0.16 to 0.44 wt%; MnO: n.d. to 0.12 wt%) and Cr-poor (Cr_2O_3: 0.05 to 0.13 wt%) relative to various other diamond-free eclogitic suites from Newlands (Figure 9.4, 9.5, 9.6, 9.7). Moreover, the clinopyroxenes display the high K_2O concentrations (0.12 – 0.18 wt%) associated with Group I eclogites (Figure 9.4).

Multiple core - rim analyses and elemental scans indicate that the clinopyroxenes are homogeneous (Figure 9.3). The clinopyroxenes display various stages and amounts of alteration. In such cases the altered clinopyroxene is commonly enriched in Al and Mg and depleted in Na (Figure 9.3).

It is noticeable that majority of the clinopyroxenes from the diamond-bearing eclogites have extremely similar compositions – in fact, only four clinopyroxenes, as with the garnets (AHM K8, AHM K13, AHM K15 and AHM K16) display any appreciable variation. As with the garnets, the overall clinopyroxene compositional range - with the exception of AHM K8 (see discussion below) - is small relative to that displayed by the other diamond-free eclogites from Newlands.

The clinopyroxene from sample AHM K8 is the exception to the above compositional descriptions (Table 9.2). Indeed, its composition is more akin to many of the other diamond-free eclogites from Newlands. In general, it is Mg- and Ca- rich (MgO: 15 wt% and CaO: 21.2 wt%) and Na-poor (Na_2O: 2 wt%). Furthermore, its has a K_2O concentration of 0.04 wt%, thus classifying as a Group II or Group A eclogite (depending on classification scheme). This is in contrast to all the other diamond-bearing eclogites from Newlands, which are Group I or Group B.

9.4.2 Diamond-free Eclogites (Group New A through NewD)

The clinopyroxenes from the diamond-free eclogites display a range of compositions, with the vast majority significantly different from the diamond-bearing samples. In particular, the diamond-free clinopyroxenes have high Mg#'s ranging from 71.4 to 93.8, corresponding to their relatively Mg- and Ca- rich and Na-poor nature (Figure 9.4). Furthermore, only five samples have K_2O concentrations greater than 0.08 wt% (Figure 9.4) and therefore the vast majority classify as Group II eclogites.

As with the garnets, some clinopyroxenes from samples from Group NewD have compositions that are similar to the diamond-bearing eclogites (Figure 9.4). For example, they have high K_2O concentrations (> 0.08 wt%) and low Mg#'s of ~ 74. In contrast, the next lowest Mg# from all the other diamond-free eclogites is ~ 87.

9.5 DISCUSSION

The major element chemistry of both garnet and clinopyroxene from diamond-bearing eclogites at Newlands (with the exception of sample AHM K8) classify as Group I eclogites as defined by McCandless and Gurney (1989) or Group B eclogites as defined by Shervais et al. (1988) and Taylor and Neal (1989) (Figure 9.6). The diamond-bearing eclogite compositions from Newlands plot within the field observed for eclogitic diamond inclusions and diamond-bearing eclogites from around the world (for example Udachnaya (Jerde et al., 1993; Snyder et al., 1993; Ireland et al., 1994; Jacob et al., 1994), Mir (Snyder et al., 1997, Taylor et al., 1996), Bellsbank (Viljoen, 1995), and Orapa (Reid et al., 1976; Shee, 1978; Shee and Gurney, 1979; Robinson et al., 1984; Viljoen et al., 1996)). However, it should be noted that eclogitic diamond inclusions and diamond-bearing eclogites define an extremely diverse compositional range and the diamond-bearing eclogites from Newlands plot at the Fe-rich, Mg-depleted limits. For example, a study of 16 diamond-bearing eclogites from the Mir kimberlite yielded three distinct eclogitic groups with garnet CaO concentrations ranging from 2.65 to 13.64 wt% (Sobolev, 1983; Beard et al., 1996). In contrast, the diamond-bearing eclogites from Newlands have a garnet CaO concentration range of only 4.5 to 8 wt%, with the vast majority around ~5 wt%.

The bulk rock concentration of major elements (Table 9.2) in the Newlands diamond-bearing eclogites is typical, although extremely restricted, of other upper mantle eclogites, in particular the field of carbonaceous eclogites (for example, Dawson, 1980; McCandless and Gurney, 1997). The bulk rock compositions (calculated assuming a 50:50 garnet-clinopyroxene ratio) are compositionally similar to MORB, both ancient and recent (Dawson, 1980; McCandless and Gurney, 1997). Furthermore, they display distinct differences to continental carbonaceous shales, which are often promoted as the protolith in the subduction hypothesis (McCandless and Gurney, 1997). To account for these differences (as well as stable isotope evidence) McCandless and Gurney (1997) propose that the subducted material contains seafloor-ridge hydrothermal vent biosphere.

The diamond-bearing eclogites appear to be Fe-, Ti-, Mn-, K- and Na- rich, and Cr-, Mg- and Ca- poor relative to other diamond-free eclogites from Newlands. They also

display a lack of zonation, both within a grain and between grains within specimens. This is similar to findings for comprehensive eclogite studies from around the world, e.g. Yakutian eclogites (Snyder et al., 1997; Taylor et al. 1997), Koidu eclogites (Hills and Haggerty, 1989; Fung and Haggerty, 1995), Jagersfontein eclogites (Pyle and Haggerty, 1997), Roberts Victor eclogites (Hatton, 1978; Gurney and Hatton, 1986) and Orapa (Reid et al., 1976; Shee and Gurney, 1979; Robinson et al., 1984; Viljoen et al., 1996).

The Group I eclogites of Newlands have both high garnet Na and clinopyroxene K concentrations (Figure 9.6), similar to eclogitic diamond inclusions and diamond-bearing eclogites from around the world (see above references). Such compositions are believed to be indicative of high-pressure origins (Erlank and Kushiro, 1970; Reid et al., 1976; Moore et al., 1989; McCandless and Gurney, 1989). Thus, the Newlands diamond-bearing samples (and a few of the diamond-free samples) are likely to be derived from a deeper origin than the diamond-free samples that have low concentrations of Na-in-garnet and K-in-clinopyroxene.

Several diamond-free eclogites have garnet and clinopyroxene compositions that are similar to those from diamond-bearing specimens. These samples are from Group NewD – a group of eclogites identified in Chapter 8 as macroscopically similar to diamond-bearing samples. Noticeably, there is a Mg# compositional gap between Group NewE and NewD eclogites and the other eclogites at Newlands.

The vast majority of diamond-free eclogites are classified as Group II based on their Na-in-garnet and K-in-clinopyroxene concentrations. A Na-in-garnet concentration of > 0.07 wt% is often used to infer a potential association with diamonds. However, the recent study of Grütter and Quadling (1999) concluded that "*the sodium content of eclogitic garnet cannot be used in isolation to uniquely identify a diamond association*". In addition, they state that the sodium concentration is determined by, amongst other things, the bulk-rock composition, in particular the sodium and magnesium concentrations of co-existing clinopyroxene, in addition to pressure and temperature influences.

There is one notable exception at Newlands to the above compositional descriptions of diamond-bearing eclogites. Sample AHM K8 has a clinopyroxene composition that is equivalent to Group II eclogites as defined by McCandless and Gurney (1989) or Group A eclogites as defined by Taylor and Neal (1989). However, in contrast to the clinopyroxene, the garnet from this sample clearly classifies as either a Group I or Group B eclogite albeit at the compositional range of the other garnets at Newlands. The clinopyroxene composition is highly unusual for diamond-bearing specimens reported from around the world - no diamond-bearing eclogite from Yakutia has a composition that is similar to the Group A eclogites (Snyder et al., 1997). However, one diamond-graphite sample is known that classifies as a Group II eclogite – namely, HRV247 from Roberts Victor (Hatton, 1978; Hatton and Gurney, 1979). One possible explanation for the low K-in-clinopyroxene concentration was put forward by McCandless and Collins (1989). They observed that the K-in-clinopyroxene concentration in TP121 (a diamond-graphite eclogite from Sloan 2) varied with respect to the crystallographic orientation, suggesting selective K migration out of the clinopyroxene lattice, possibly during partial melting from metasomatism and/or decompression.

Diamond-bearing eclogites from Newlands have been analysed in other studies, namely Sobolev and Kuznetsova (1966), Rickwood and Mathias (1970), Smith et al (1989), and O'Reilly and Griffin (1995). The garnet and clinopyroxene compositions plot within the limits of the larger data-set analysed here. Specifically, none of the samples has a clinopyroxene composition similar to AHM K8.

ECLOGITIC XENOLITHS: TRACE ELEMENT MINERAL CHEMISTRY

10

10.1 INTRODUCTION

Even though garnet and clinopyroxene are the only modally significant phases, these eclogites may not accurately represent the source rock from which they were derived due to their small sample size. Consequently no detailed point counting was undertaken. Nevertheless, Ireland et al. (1994) showed that the modal variations of garnet and clinopyroxene did not significantly alter whole rock trace element determinations and consequently whole rock compositions have been determined assuming a 50:50 ratio of garnet and clinopyroxene.

REE are believed to behave in a predictable manor. Based on the current mineral-melt distribution coefficients (see discussion in Chapter 5) clinopyroxene will be relatively enriched in LREE's over garnet and vice versa for HREE. Furthermore, the compatibility of REE's into each of these mineral phases is such that the chondrite normalised patterns will be greater than 1 for LREE's in clinopyroxene and HREE's in garnet.

10.2 METHODOLOGY

10.2.1 Analytical Techniques and Operating Conditions

Garnets and clinopyroxenes were analysed for certain Large Ion Lithophile Elements (LILE), Rare Earth elements (REE) and High Field Strength Elements (HFSE) using the two well-established analytical techniques of PIXE and SIMS. PIXE was performed using the proton microprobe (PMP) housed at the National Accelerator Centre (NAC), South Africa, whereas SIMS was performed using the Cameca IMS 4f

ion microprobe (IMP) housed at the University of Edinburgh, Scotland, and the Cameca INS 6f ion microprobe housed at Carnegie Institute of Washington, USA.

The analytical set-up conditions of both the PMP and IMP housed at Grant College, Edinburgh are described in Chapter 5. Analyses of eclogitic garnet and clinopyroxene were made using the Cameca INS 6f ion microprobe housed at Carnegie Institute of Washington, USA. The IMP housed at Carnegie is described in detail by Hauri et al. (1996). Elements analysed in garnet and clinopyroxene include selected REE's as well as Li, Be, Sc, Ti, Cr, Rb, Sr, Y, Zr, Nb, Ba, and Hf analyses. Beam currents of 5-10 nA and beam sizes of 10-20 μm were used. The international glass 30-2 as well as an in-house garnet were used as standards and analysed at repeated intervals throughout the runs. The reference element for both clinopyroxene and garnet analyses was Si. The SiO_2 concentration was pre-determined by electron microprobe. The quoted uncertainties in the data tables are counting statistics only and therefore represent lower limits.

The precision and accuracy of both techniques are very good. Details are presented in Chapter 5.

10.2.2 Sample Description

Garnets and clinopyroxenes were predominantly analysed as chips in a polished probe mount and consequently there is no spatial resolution for the majority of samples. However, these included a chip from AHM K2 for which the garnet and clinopyroxene are touching. Nevertheless, multiple analyses (normally three) were performed on all samples to test for homogeneity. Several specimens were analysed as polished sections, however, where spatial resolution was maintained. In general, multiple analyses were made on each garnet and clinopyroxene, two for the core and two for the rim composition of the garnet. Further analyses were made where evidence of compositional variation was found in any garnet. Representative garnet and clinopyroxene analyses from both diamond-bearing and diamond-free eclogites for both PMP and IMP techniques are given in Tables 10.1 through 10.4.

Trace elements will be discussed in terms of either absolute abundances or normalised to C1-chondrite using the values of McDonough and Sun (1995).

10.3 Eclogitic Garnet Trace Element Geochemistry

10.3.1 Diamond-bearing Eclogites (Group NewE)

The garnets display a very restricted range of trace element compositions (Table 10.1). They are relatively enriched in Ga (11 to 14 ppm), Zn (70 to 100 ppm), Mn (2800 to 3500 ppm) and Ti (1450 to 1650 ppm), and depleted in Cr (< 900 ppm) and Ni (25 to 40 ppm) relative to diamond-free eclogites from Newlands (Table 10.1, Figure 10.1 to 10.8). Both Zr and Y yield concentrations overlapping diamond-free eclogites. The garnets also display an extremely consistent REE trace element geochemistry that appears to be significantly different to the other diamond-free samples from Newlands (although only three diamond-free samples were analysed for REE's). As expected the garnets are $[HREE]_n$ enriched. In detail, they are $[LREE]_n$ depleted ($[La]_n < 0.5$ X chondrite), increasing through the $[MREE]_n$ and reaching a plateau for the $[HREE]_n$ between 10 – 20 X chondrite (Figure 10.9). The other noticeable feature of the garnet $[REE]_n$ pattern is a plateau in the $[MREE]_n$ between $[Eu]_n$ and $[Gd]_n$. Consequently, at Newlands, the garnets from the diamond-bearing eclogites are easily distinguished from the diamond-free eclogites on the basis of trace element composition.

As with the major element concentrations, the trace element concentrations of garnets from diamond-bearing eclogites are relatively consistent. This is somewhat unusual relative to the range displayed by the diamond-free eclogites from Newlands and diamond-bearing eclogites from around the world. For example, Y has a range of 19 to 26 ppm, Zr 10 to 14 and Ga 10 to 13 ppm. Furthermore, there is very little variation between the 10 eclogites analysed for REE's - all $[REE]_n$ are within a factor of three, with many less than a factor of two.

The only sample that displays any significant variation is AHM K8. This sample is noticeably enriched in Ni and Zr, and depleted in Cr, Mn, and Zn relative to the other

diamond-bearing eclogites. In most cases the difference is less than a factor of two, however, it is conspicuously either the highest or lowest concentration for the garnets from diamond-bearing samples. The only element that is significantly different is Cr, for which the garnet from AHM K8 has a concentration of ~ 300 ppm, whilst all other diamond-bearing samples have concentrations of ~ 700 to 800 ppm. This is the lowest garnet Cr concentration of any eclogite analysed from Newlands. However, whilst AHM K8 displays differences for transition and HFS elements, its REE pattern is within the range displayed by other diamond-bearing samples.

10.3.2 Diamond-free eclogites (Group NewA through NewD)

Garnets from diamond-free eclogites display a diverse range of trace elements. It is evident that they are significantly different from the diamond-bearing samples. In general, the garnets from diamond-free eclogites are relatively depleted in Ga, Zn, and Ti, and enriched in Ni and Cr (Figure 10.1 through 10.8). Furthermore, the absolute range for any element is general significantly larger than the restricted range displayed by the diamond-bearing eclogites.

Only three garnets from diamond-free eclogites were analysed for REE's – one from each of Group NewA, NewB, and NewC. All diamond-free samples are $[HREE]_n$ enriched, as per the garnets from diamond-bearing eclogites. However, the chondritic levels at which this occurs are different (Figure 10.9). Sample AHM 400 (from Group NewA) has a $[REE]_n$ pattern very similar to the garnets from diamond-bearing eclogites - the only subtle differences are marginally higher $[La]_n$ and $[MREE]_n$ and marginally lower $[Yb]_n$. Noticeably the $[REE]_n$ pattern does display the $[MREE]_n$ plateau between $[Eu]_n$ and $[Gd]_n$ observed in all the garnets from diamond-bearing specimens. Sample AHM 410 (Group NewB) has a similar depleted $[LREE]_n$ signature as the diamond-bearing samples, but is relatively depleted in $[MREE]_n$ and $[HREE]_n$. Furthermore, AHM 410 has a trough at $[Gd]_n$. Sample AHM 415 (Group NewC) is depleted in all $[REE]_n$ (with the exception of $[La]_n$) relative to the diamond-bearing samples.

No garnets from Group NewD eclogites were analysed for trace elements.

10.4 ECLOGITIC CLINOPYROXENE TRACE ELEMENT GEOCHEMISTRY

10.4.1 Diamond-bearing Eclogites (Group NewE)

The clinopyroxenes, as with the garnets, display a very restricted range of trace element compositions (with one exception – sample AHM K8). They are relatively enriched in Ga, Zn, Zr, Mn and Ti, and depleted in Ni relative to diamond-free eclogites from Newlands (Figure 10.1 to 10.8). Consequently, the clinopyroxenes from the diamond-bearing eclogites are easily distinguished from the diamond-free eclogites on the basis of trace element composition. Specifically, Ga is between 17 and 21 ppm, Zn 68 to 92 ppm, Ti 2200 to 2500 ppm, and Ni 160 to 250 ppm. The clinopyroxenes display a very restricted $[REE]_n$ pattern. As expected, it is $[LREE]_n$ enriched (Figure 10.9). In detail, the clinopyroxenes are enriched in $[LREE]_n$ ($[La]_n$ ~ 10-20 X chondrite) and decrease smoothly through $[MREE]_n$ and $[HREE]_n$ to approximately chondritic levels.

Diamond-bearing sample AHM K8 is the solitary exception to the above compositional descriptions. In contrast to other clinopyroxenes from diamond-bearing eclogites, its trace element composition is more akin to diamond-free eclogites. Specifically, it is relatively enriched in Ni and depleted in Ga, Zr, Zn, Mn and Ti (Figures 10.1 through 10.8). Most notably, however, it has a $[REE]_n$ pattern different to the diamond-bearing samples – it is enriched in $[La]_n$ and depleted in $[HREE]_n$ (Figure 10.9).

10.4.2 Diamond-free eclogites (Group NewA through NewD)

Clinopyroxenes from diamond-free eclogites display a diverse range of trace element signatures – the majority of which are significantly different from diamond-bearing eclogites. The clinopyroxenes from Group NewD are similar to the diamond-bearing eclogites. Excluding this group, the other clinopyroxenes are, in general, relatively depleted in Ga, Zr, Zn, Mn and Ti, and enriched in Ni and Cr (Figures 10.1 to 10.8). Furthermore, the absolute range for any element is general significantly larger than the restricted range displayed by the diamond-bearing eclogites.

Only three clinopyroxenes from diamond-free eclogites were analysed for REE's – one from each of Group NewA, NewB, and NewC (Figure 10.9). Two of the samples display a decrease of $[LREE]_n$ to $[HREE]_n$. However, the chondritic levels at which this occurs are different to clinopyroxenes from the diamond-bearing eclogites. Sample AHM 400 (from Group NewA) has a very similar pattern to the diamond-bearing samples except that $[La]_n$ is higher whilst the $[HREE]_n$ are marginally lower. Sample AHM 410 (from Group NewB) is enriched in $[LREE]_n$ and $[MREE]_n$ and depleted in $[HREE]_n$ relative to diamond-bearing eclogites. Sample AHM 415 has an unusually jagged pattern and is relatively depleted in all $[REE]_n$. Such a pattern is in likelihood due to the low level of REE's that are close to analytical detection limits.

10.5 TRACE ELEMENT MAPS

Trace element maps of the diamond-bearing eclogites show that both garnet and clinopyroxene are homogeneous (figures not shown). Furthermore, they highlight the infiltration of melt (kimberlitic?) into the eclogite resulting in mineralisation along the garnet and clinopyroxene grain boundaries. This is observed as increases in Rb, Sr and Ga along grain boundaries.

10.6 DISCUSSION

The diamond-bearing eclogites from Newlands display trace element signatures (including HFSE's, LILE's and REE's) that are within ranges defined by inclusions in diamonds and diamond-bearing eclogites from around the world. However, the range displayed is relatively restricted and generally falls at either the minimum or maximum concentrations observed around the world. For example, at Newlands Ni in garnet ranges from 25 to 40 ppm, whilst in diamond-bearing eclogites from Yakutia it ranges from 27 to 140 ppm (Spetsius and Griffin, 1997). Similarly, at Newlands Zn ranges from 70 to 100 ppm, whilst at Yakutia it ranges from 29 to 92 ppm (op. cit.). Furthermore, the REE's do not display the variation observed in diamond-bearing eclogites in the Yakutian kimberlite field (Snyder et al., 1997 and references therein). Their REE patterns are, however, similar to the '*typical*' clinopyroxenes and garnets

identified by Snyder et al. (1997), except for the slightly higher LREE, evidenced by the higher $[La/Nd]_n$ ratio (clinopyroxene: 1.2 to 1.3; garnet: 0.10 to 0.15).

10.6.1 Distribution coefficients

The diamond-bearing eclogites display a very consistent set of partition coefficients. Harte and Kirkley (1996) observed that garnet-clinopyroxene partition coefficient (D_i: where i=element) decreases with increasing garnet Ca# or D_{Ca}. The garnets from Newlands display a very restricted range of Ca concentrations and Ca#'s cluster around 22 with only three samples having slightly higher Ca#'s of 27 (AHM K13 and AHM K15) and 32 (AHM K16). The partition coefficients of the Newlands samples (with one exception) lie within the observed range for eclogites used in the study of Harte and Kirkley (1996). This included only eclogites determined to be in equilibrium from Roberts Victor (Harte and Kirkley, 1996) as well as data from a variety of other studies of eclogites from elsewhere on the Kaapvaal craton as well as the Siberian craton.

10.6.2 Sample AHM K8

Sample AHM K8 has partition coefficients that lie outside the observed range of these data sets, which is not surprising given the different major and trace element compositions. These differences in trace elements observed for the clinopyroxene from diamond-bearing sample AHM K8 are consistent with the major element composition. Furthermore, both the trace and major element compositions are similar to those observed for Group NewA eclogites. Paradoxically, however, the garnet from sample AHM K8 is similar to other diamond-bearing eclogites and distinctly different from Group NewA trace and major element compositions.

10.6.3 Mantle metasomatism

The clinopyroxenes from diamond-free eclogites and sample AHM K8 plot along a Sr/Nd mantle array (~20, O'Nions, 1987). In contrast, the diamond-bearing eclogites plot along an array several orders of magnitude higher. This high Sr/Nd array is also observed for diamond-bearing eclogites (Snyder et al., 1997) and eclogitic diamond

inclusions (Sobolev et al., 1996) from Yakutia. They interpret this enrichment event as ancient metasomatism from a carbonatite magma or fluid that pre-dates diamond formation.

ECLOGITIC XENOLITHS: GEOTHERMOBAROMETRY

11

11.1 INTRODUCTION

Of the five major mineral phases commonly used in upper mantle geothermobarometry (for example see Chapter 6), eclogites (predominantly) only contain garnet and clinopyroxene. Therefore, only thermometers based on the Fe-Mg exchange between garnet and clinopyroxene can currently yield calculated temperatures of equilibration; whilst there is no currently available barometer that can be applied to yield calculated pressures of equilibration. The four thermometer calibrations of Ellis and Green (1979), Krogh (1988), Ai (1994), and Berman et al. (1995) were used in this study. An introduction to geothermobarometry and derivation of the aforementioned thermometers is presented in Chapter 6. Henceforth, the thermobarometers will be referred to using an abbreviation of their author(s) and year of publication, as per Table 6.1 and 6.2.

11.2 METHODOLOGY

Temperature calculations (T) were primarily determined using a geothermobarometric program developed by Doug Smith[15]. Where possible core and rim analyses were determined on at least two grains for each mineral phase and averages used for geothermobarometry calculations. This allowed for a simplistic check of both intra- and inter- grain homogeneity. Where a systematic core - rim difference was observed then both core and rim averages were used for T calculations and compared. Ferric iron contents were stoichiometrically estimated for each mineral phase, the geothermobarometry program re-run, and the results compared.

[15] The program is available from Doug Smiths' personal web site at the University of Texas: www.utexas.edu or email: doug@maestro.geo.utexas.edu.

At present there is no reliable geobarometer that can be applied to mantle eclogites. Therefore a reasonable geologic pressure must be assumed as all of the Fe-Mg garnet-clinopyroxene thermometers are (to varying degrees) pressure sensitive. There are 5 eclogitic groups identified at Newlands (NewA through NewE, as per Chapter 8), one of which is diamond-bearing (Group NewE). The presence of diamond constrains equilibration P-T's at Newlands to above 900 °C and 42 kbar (based on the Newlands xenolith geotherm - see Chapter 6), and therefore a pressure of 50 kbar has been deemed an appropriate starting value for comparison.

11.3 Diamond-Bearing Eclogite Geothermobarometry Results

Based on an assumed pressure of 50 kbar, the diamond-bearing eclogites yield temperatures primarily within the diamond-stability field (with one exception – sample AHM K8, see discussion below). Nevertheless, absolute temperature differences do exist between the various geothermometers. Both TEG79 and TAi94 yield similar temperature ranges of 1000 to 1150 °C, whilst all but two samples record temperatures of 950 to 1000 °C using TKr88, and TBer95 displays no mode and wide range of temperatures of 800 to 1000 °C (Figure 11.1). TBer95 is the only thermometer that places some of the diamond-bearing eclogites outside the diamond stability field (based on the Newlands peridotite derived 37 – 38 mW/m^2 geotherm – see Chapter 6).

Diamond-bearing sample AHM K8 records a substantially lower temperature than all the other diamond-bearing eclogites, with temperatures ranging between 650 to 800 °C (Figures 11.1e to 11.4e). These temperatures all fall within the graphite stability field, even accounting for the low geotherm at Newlands, indicating that the garnet and clinopyroxene may not be in equilibrium. This is not surprising given the significant differences in major and trace element compositions to the other diamond-bearing eclogites. Furthermore, FTIR on the diamonds from this xenolith does not support storage at such low temperatures (see Chapter 16).

11.3.1 Other Eclogite Groups

There is considerable overlap in the temperature ranges between the various eclogite groups. Nevertheless, there are some broad consistencies of relative positions between the various geothermometers, even allowing for the accuracy of the temperatures (Figures 11.5 a-e). Four of the five eclogite groups display distinct temperature modes and narrow temperature ranges (Figures 11.1 a-e to 11.4 a-e). Based on an assumed pressure of 50 kbar, Group NewA eclogites record the lowest temperatures, which are always below 1000 °C. Group NewB records only slightly higher temperatures, whilst Group NewD and Group NewE eclogites overlap completely and record relatively high temperatures (up to 1200 °C). Group NewC eclogites span the largest range of temperatures and overlap all the other groups. The assumed pressure of 50 kbar may be high for some of the eclogites, particularly given the low (relative) geotherm at Newlands. Consequently, the temperature differences between the various eclogitic groups, will in reality, be greater. Nevertheless, it does represent a relative position in the mantle stratigraphy for each of the groups, all be it compressed. Using this method of calculating temperatures, the eclogites range from as low as 700 °C to potentially as high 1200 °C, completely overlapping the diamond-bearing eclogites and peridotites from Newlands. Furthermore, it places many of the eclogites within the diamond stability field.

11.3.2 Pressure Considerations

The temperatures reported above are all calculated at an assumed pressure of 50 kbars. Whilst this is a geologically reasonable estimate for the diamond-bearing eclogites, it may be erroneous for the other eclogites. Any difference in temperatures between eclogitic groups is a minimum, as the pressure effect will result in an even greater temperature distribution. However, a change of 10 kbar results in a concomitant change in temperature of less than 50 °C for TEG79, TKr88 and TBer95 and thus these thermometers may be regarded as relatively pressure insensitive. In contrast, TAi94 changes on the order of 100 °C.

Assuming the eclogites lie on a geotherm (which they may not), then the geotherms intersection with the geothermometers calculated P-T curve for each eclogite might indicate those eclogites ambient P-T conditions prior to kimberlite eruption. Such an assumption is reasonable for Newlands as the diamond-bearing eclogites are Archæan (based on whole rock Re-Os isotope systematics – see Chapter 13), there is no evidence of thermal disturbance, and the calculated temperatures are well in excess of blocking temperatures and thus re-equilibration will be geologically quick. This method was adopted by Toft et al. (1989) and Pyle and Haggerty (1997), who used an assumed Archæan geotherm of 40 mW/m^2, rather than a locally derived geotherm. In this case a geotherm of 37 to 38 mW/m^2 has been calculated for Newlands (see Chapter 6) and is the optimal value to use.

Applying this methodology to the diamond-bearing eclogites at Newlands yields very different results for the various geothermometers (Figures 11.6 a-d). Note that sample AHM K8 intersects the geotherm within the graphite stability field and is exclude from further general discussion here. Only TEG79 and TKr88 define P-T fields entirely within the diamond stability field, but at distinctly different regions - TEG79 defines a P-T region of 1020 to 1080 °C and 50 to 58 kbar whereas TKr88 is from 920 to 1000 °C and 42 to 50 kbar. In contrast, TBer95 defines a region that straddles the diamond-graphite boundary whereas TAi94 does not intersect the geotherm. This implies that the calibrations of TBer95 and TAi94 are not accurate for these eclogite compositions and P-T ranges, and therefore only TEG79 and TKr88 are considered for the other eclogite groups.

Considering TEG79 first yields definitive P-T differences between the various eclogitic groups (Figures 11.6). Group NewA defines a relatively narrow range within the diamond stability field of 950 to 1020 °C and 45 to 52 kbar (Figures 11.7). Group NewB yields a slightly higher and broader P-T range of 1000 to 1120 °C and 48 to 60 kbar (Figures 11.8), whereas group NewD yields a P-T range of 1060 to 1100 °C and 53 to 60 kbar (Figures 11.10). In contrast, Group NewC is extremely variable and temperatures range from 980 up to 1220 °C and 46 to 72 kbar for the 5 eclogites (Figures 11.9). Group NewC, however, displays the most variable mineral chemistry (see Chapter 9) and may actually represent more than one eclogitic group. Similar

results are obtained using TKr88; for example Group New A defines a similar narrow P-T range to TEG79 of 930 to 980 °C and 43 to 50 kbar. Noticeably, all the eclogites yield P-T's within the diamond stability field using this method.

11.4 DISCUSSION

11.4.1 The effect of Fe^{3+} on temperature calculations

All the thermometers considered above are based on Fe^{2+}-Mg. However, EMP measures total iron concentrations - as in this study – and thus any Fe^{3+} is included with Fe^{2+}. The effect of Fe^{3+} on temperature is dependent on the relative proportions in garnet and clinopyroxene. If Fe^{3+}/Fe^{Total} in garnet is greater than in clinopyroxene then temperature will increase or vice versa. Luth et al. (1990) demonstrate that the presence of ~ 12% of Fe as Fe^{3+} in garnets may increase temperatures based on garnet-clinopyroxene Fe-Mg exchange by over 200 °C. To avoid such possible uncertainties Fe^{3+} should be determined accurately using a suitable technique such as Mössbauer (for example, see McCammon, 1999).

In this study no direct measurements were made to determine Fe^{3+} and stoichiometry is used to determine the Fe^{3+} contents of the various mineral phases. However, studies show that this is generally inaccurate for both garnets and clinopyroxenes due to site allocation problems (Luth et al., 1990; Giaramita and Day, 1990, Canil and O'Neill, 1996). Any errors will be magnified in the relatively low iron mineral phases, such as some lherzolite and eclogite clinopyroxenes. Mössbauer analyses have found Fe^{3+}/Fe^{Total} ranging from 7 to 41 % for peridotitic clinopyroxene and from 2 to 12 % in peridotitic garnets (Luth et al., 1990; Luth and Canil, 1993; Canil and O'Neill, 1996). Thus the maximum relative Fe^{3+} content difference is 40 % in favour of clinopyroxene, which would result in lower temperatures on the order of 200 °C in Newlands samples, or 5 % in favour of garnet which would result in higher temperatures of approximately 50 °C. This highlights the possible errors associated with stoichiometrically determined Fe^{3+} and is displayed in Figure 11.11 where approximately half of the samples have a relative Fe^{3+} difference greater than 40 % in favour of clinopyroxene. Therefore, the temperature effect of Fe^{3+} is difficult to

assess without direct measurement, as clearly stoichiometry determinations are inaccurate in many cases.

The various eclogite groups display different ranges of the relative differences of stoichiometric Fe^{3+} between garnet and clinopyroxene, predominantly in favour of clinopyroxene. This is in likely-hood due to the lower Fe content in the clinopyroxene (Total FeO: 3.3 to 6.9 wt%) relative to their associated garnets (Total FeO: 18.8 to 21.3 wt%) and the corresponding errors due to site allocation problems (Luth et al., 1990; Giaramita and Day, 1990; Canil and O'Neill, 1996). Nearly all the Group NewE (diamond-bearing) and Group NewD eclogites display a relative Fe^{3+} difference from 10 % in favour of garnet to 20 % in favour of clinopyroxene (Figure 11.11), whilst Group NewA and Group NewB range from 20 to 60 % in favour of clinopyroxene. In contrast Group NewC displays no distinct grouping and spans the entire range of relative Fe^{3+} changes. Although the relationship is not linear it can be approximately quantified as each 20 % change in relative Fe^{3+} yields a change in temperature of 100 °C for Fe-Mg clinopyroxene-garnet geothermometers (Figure 11.11 a-c).

The temperatures for the various eclogite groups will be lower as calculated Fe^{3+} is (predominantly) greater in clinopyroxene than garnet. For example, the diamond-bearing eclogites minimum TEG79 temperature (at assumed pressure of 50 kbar) will change from 1020 °C to approximately 880 °C, TKr88 from 950 to 850 °C, TAi94 from 1000 to 900 °C and TBer95 from 800 to 700 °C. Even so, the modes of each of TEG79, TAi94 and TKr88 are still within the diamond stability field beneath Newlands. TBer95 was not calculated. The extreme case is two Group NewC eclogites (samples AHM 415 and AHM 417) that yield temperatures between 1100 and 1150 °C assuming total Fe as Fe^{2+}, but when recalculated to incorporate stoichiometric Fe^{3+} the temperatures fall to below 600 °C, a change of over 500 °C. Accounting for Fe^{3+} also results in a lot more scatter in the temperature distribution: TEG79, TKr88 and TAi94 all yield two samples with temperatures below 750 °C (AHM K13 and AHM K8) and one above 1200 °C (AHM K14). The temperature change for Groups NewA and NewB is even greater (up to 300 °C) and yield temperatures well below 600 °C. Therefore, it cannot be assumed that the

temperatures discussed above – at assumed pressures or lying on a geotherm – are accurate, and, at least in some cases are likely to be erroneous. Furthermore, the temperature corrections for stoichiometric Fe^{3+} are consistent with major element compositions. For example, the Group I eclogites (including the diamond-bearing eclogites of Newlands), which have high garnet Na and clinopyroxene K concentrations, indicative of high pressures (Erlank and Kushiro, 1970; Reid et al., 1976; Moore et al., 1989; McCandless and Gurney, 1989) remain in the diamond-stability field after adjusting the various geothermometers for stoichiometric Fe^{3+}. In contrast, Group NewA and NewB, which have low garnet Na and clinopyroxene K concentrations, yield significantly lower P-T's that are in the graphite stability field.

11.4.2 Mantle Stratigraphy considerations beneath Newlands

Given the potential error on determining mantle temperatures (50 – 100 °C), it is possible that all the various groups of eclogites are derived from the same eclogitic unit within the mantle and that the geochemical variation represents different stratigraphic positions within that unit. Such variations within eclogitic units have been proposed for eclogites from the Siberian craton (Jacob et al., 1994; Beard et al., 1996). Alternatively, the P-T range displayed by the various eclogitic groups may be real and thus represent different eclogitic units intermixed with the various peridotitic units, which is how eclogite is usually observed at surface.

The diamond-bearing eclogites yield temperatures in the diamond-stability field that overlap the temperature mode of peridotitic garnets. This implies that mantle geothermobarometry is unable to distinguish various geologic stratigraphic units if they exist or else there is intermixing of eclogite and peridotite within the mantle at depth.

ECLOGITIC XENOLITHS: STATISTICAL ANALYSIS OF GARNET AND CLINOPYROXENE

12

12.1 INTRODUCTION: STATISTICAL PROCEDURES

The major and trace element compositions of garnets and clinopyroxenes from Newlands eclogite xenoliths were statistically analysed using both Principal Component Analysis (PCA) and Discriminant Function Analysis (DFA). These statistical procedures were used to assess whether the diamond-bearing eclogites have a distinctive range of garnet and clinopyroxene compositions relative to the other diamond-free eclogites. A detailed discussion on the statistical procedures employed is beyond the scope of this study but a short summary is presented below.

All statistical procedures were performed using the software package *Statistica*; the reader is referred to the Statistica Manuals (and references therein), as well as Stevens (1986), Harman (1967) and Lawley and Maxwell (1971) for detailed discussions of the application of PCA and DFA. Both these statistical procedures have been used several times in the study of upper mantle geological samples - for example, kimberlite rocks (Ferguson et al., 1975; Danchin et al., 1975; Smith et al., 1985) and garnets from a variety of environments (Dawson and Stephens, 1975).

In summary, PCA analyses the data set as a whole, first detecting any structure in the relationship between the selected variables (and thus reducing the number of relevant variables) and then maximising the variance between all the individual samples. Samples that are potentially related to each other, based on the selected variables, will group together away from other specimens. In contrast, DFA requires that samples be pre-assigned to various groups based on independent criteria (in this study, mineralogy, petrography and hand specimen appearance). Similar to PCA, DFA first detects any structure between the selected variables using Stepwise Discriminant Analysis (SDA). It then calculates the best possible combination of non-correlated

variables that most effectively maximises the variance between the pre-assigned groups. This is achieved by maximising the ratio of between group to within group variance. The resultant derivation can then be used to classify unknown samples into one of the pre-assigned groups (or none of them, as the case may be). Variables are entered into (or removed from) the statistical analysis in a stepwise manner until the best group separation is achieved, that is, when additional variables added to the classification no longer improve the group separation.

Any number of variables (in this case mineral compositions) may be used in these statistical procedures, in this case the major and trace element concentrations of minerals in the various xenoliths. PCA is commonly applied first, as it assumes no natural groupings within the data set. If PCA yielded groups of data that can be identified with other non-geochemical features, such as petrography or hand specimen appearance, then this may be used as a grouping variable and DFA applied. DFA obtains the best possible categorisation of these groupings based on the variables specified.

12.2 METHODOLOGY

For statistical analysis, 15 diamond-bearing xenoliths and 24 diamond-free eclogites (from the other four eclogitic groups) were analysed for major elements; of these only 11 and 20 were analysed for trace elements, respectively. The eclogites have been divided into 5 groups on the basis of mineralogy and hand specimen observations; that is Groups NewA, NewB, NewC, NewD and NewE, as per the classifications in Chapter 8. Note that Group NewE is diamond-bearing, whilst Group NewD is similar to Group NewE in all respects except for the absence of diamond. All groups were weighted as equal for statistical analysis and a F-to-enter value of 3 was used. The trace elements considered for statistical analysis were Ti, Cr, Mn, Ni, Zn, Ga, Sr, Y and Zr. Note that trace elements were not obtained for garnets from Group NewD and accordingly are not incorporated in the relevant statistical analyses. The mineral geochemistry was statistically analysed using the following groupings:

- Clinopyroxene major element composition
- Clinopyroxene major and trace element composition

- Garnet major element composition
- Garnet major and trace element composition
- Clinopyroxene and garnet major element composition
- Clinopyroxene and garnet major and trace element composition

The reasons for the various combinations are twofold. Firstly, to determine if the classifications are different for garnet and clinopyroxene compositions. Secondly, to ascertain if there is a difference in the classifications when trace elements are considered. This is significant as a combination of major and trace elements requires two analytical techniques and often, as is the case in this study, the number of analyses of trace elements is less than for major elements.

12.3 RESULTS

12.3.1 Principle Component Analysis

The eigenvalues and percentage of variance explained for each statistical analysis are displayed in Table 12.1, whilst the factor coefficient scores for each element are listed in Table 12.2. The PCA factor scores for the various statistical analyses are plotted in Figure 12.1 (superimposed are the various eclogite groups). These factor scores explain between 77 % and 89 % of the relevant sample variation. It is noticeable that PCA displays a wide spread of factor scores that appear to form some natural groupings. Moreover, these natural groupings correspond to the predefined eclogite groups (Figure 12.1). The only major exceptions are Groups NewD and NewE, which overlap completely. However, this is expected, and confirms that Group NewD eclogites are geochemically similar to Group NewE (diamond-bearing) eclogites. Noticeably, the 6 eclogite samples from Group NewB display complete separation from the other groupings, whilst the 8 eclogite samples from Group NewA and the 6 eclogite samples from Group NewC display some overlap.

There is, however, one diamond-bearing sample (AHM K8) that appears to have mineral compositions distinctive to other diamond bearing eclogites from Newlands. Moreover, it is only the clinopyroxene composition, and not the garnet composition,

that differs from the other diamond-bearing eclogites (Figure 12.1). In particular, when only clinopyroxene major elements or major and trace elements are considered, PCA associates AHM K8 with Group NewA and NewC clinopyroxenes. In contrast, its garnet composition for both major elements only or major and trace elements is associated with the other diamond-bearing eclogites (Group NewE).

12.3.2 Discriminant Function Analysis

The resultant six statistical discriminant function analyses are shown in Table 12.3, Table 12.4, Table 12.5 and Table 12.6. Table 12.3 lists the importance of the various elements to each of the classifications, presented in their order of entry; Table 12.4 shows the classification matrix for various DFA models; Table 12.5 shows the classification functions for the various DFA models; and Table 12.6 shows the canonical scores (standarised) for the various DFA models.

When clinopyroxene is considered independently and major elements are considered solely there are four dominant elements in the classification, namely (in order of entry) FeO, MgO, CaO, and TiO_2 (Table 12.3). This statistical analysis achieves 100% correct classification of Group NewA, NewB, and NewC, whilst some samples from Group NewD are classified as Group NewE and vice versa (Table 12.5). Noticeably, one diamond-bearing sample from Group NewE (AHM K8) is classified as Group NewA. This is also clearly observed when the canonical variable scores are plotted (Figure 12.2a). When trace elements are considered the number of elements in the classification increases to six and include (in order of entry) MgO, CaO, Sr, TiO_2, MnO, and Zn. This statistical analysis also achieves similar classification efficiency and "*mis-classifications*" as for major elements above (Figure 12.2b and Table 12.4). Interestingly, FeO is the first element entered into the classification (as for when major elements are considered by themselves), however the incorporation of trace elements effectively explains the variation displayed by FeO and it is later therefore removed from the classification.

When garnet is considered independently and major elements are considered solely there are six dominant elements in the classification, namely (in order of entry) FeO, CaO, TiO_2, Na_2O, MnO, and MgO (Table 12.3). Significantly, FeO is by far the most

significant element in the classification. This statistical analysis again achieves 100% correct classification of Group NewA, NewB, and NewC, whilst some samples from Group NewD are classified as Group NewE and vice versa (Table 12.4). Noticeably, and in contrast to statistical analyses incorporating clinopyroxene, sample AHM K8 is associated with other diamond-bearing eclogites (Group NewE) and not Group NewA eclogites. This is also clearly observed when the canonical variables scores are plotted (Figure 12.2c). When trace elements are considered then the number of elements in the classification increases to nine, namely (in order of entry) FeO, CaO, Y, Zn, TiO_2, Na_2O, Zr, Ni, and SiO_2. As with before, FeO is the dominant element in the classification. Moreover, the statistical analysis achieves 100% correct classification of all the eclogitic groups, although there is no Group NewD as no garnet trace elements were made on this group (Table 12.4 and Figure 12.2d).

When the major elements from both garnet and clinopyroxene are considered solely there are six dominant elements in the classification, namely (in order of entry) FeO(Gar), CaO(Gar), MgO(Cpx), TiO_2(Gar), Na_2O(Gar), TiO_2(Cpx). This statistical analysis again achieves 100% correct classification of Group NewA, NewB, and NewC, whilst some samples from Group NewD are classified as Group NewE and vice versa (Table 12.4). Noticeably, and in contrast to statistical analyses incorporating clinopyroxene, sample AHM K8 is associated with other diamond-bearing eclogites (Group NewE) and not Group NewA eclogites. This implies that the garnet composition is dominant in defining the various eclogitic groups. This is also clearly observed when the canonical variables scores are plotted (Figure 12.2e). When trace elements are considered the number of elements in the classification increases to 11, namely FeO(Gar), CaO(Gar), Y(Gar), CaO(Cpx), Zn(Gar), MgO(Cpx), Na_2O(Gar), Cr_2O_3(Gar), Al_2O_3(Cpx), Ga(Gar), and TiO_2(Gar). As with before, FeO is the dominant element in the classification. Moreover, the statistical analysis achieves 100% correct classification of all the eclogitic groups, although there is no Group NewD as no garnet trace elements were made on this group (Table 12.4 and Figure 12.2f).

12.4 Discussion

The results of DFA statistical analysis are similar to those observed using PCA. In all six of the classifications used in this study, DFA achieved excellent separation of the eclogitic groups. This is clearly observed in Table 12.4 where, in all the different statistical analyses, the vast majority of samples are correctly classified. Furthermore, plotting the canonical variable scores for the various samples displays excellent group separation (Figure 12.2). However, the classification is not 100%, and this is addressed below.

The first significant feature is that Group NewD eclogites overlap the diamond-bearing Group NewE eclogites in all the classification schemes (Figure 12.2 and Table 12.4). (Note that no trace element analyses were made on garnets from Group NewD and accordingly there are no Group NewD samples plotted under two of the relevant analytical schemes). The overlap is so complete that several samples from each group are "mis-classified" according to the posterior classification (Table 12.4). Nevertheless, this overlap is expected given that Group NewD eclogites are the same as Group NewE eclogites in all respects except for the absence of diamond. These results confirm their geochemical similarity and imply that they are genetically related to the diamond-bearing eclogites. Furthermore, the absence of diamond is likely to be a function of their small sample size.

The second noticeable feature is that the diamond-bearing samples (Group NewE) and Group NewD plot separate from the other eclogitic groups. This indicates that the eclogites associated with diamond genesis are geochemically distinct from other eclogites at Newlands.

The third noticeable feature is the association of sample AHM K8, a diamond-bearing eclogite, with Group NewA eclogites, based solely on the major and trace element mineral chemistry of clinopyroxene. In contrast, when the garnet composition is considered, sample AHM K8 corresponds to other diamond-bearing eclogites (Group NewE) and Group NewD. Also, when both mineral compositions are considered statistically then the garnet composition dominates the classification and sample AHM K8 is again classified as Group NewE.

All of the classification schemes display a clear distinction for both garnet and clinopyroxene (with one exception) major and trace element compositions for those associated with diamonds and the various other groups at Newlands. Consequently, it is potentially possible to accurately identify (at Newlands) what proportion of concentrate garnets and clinopyroxenes are associated with diamond-bearing eclogite. Diamond exploration companies often use the Na-in-garnet concentration as an indicator of eclogitic diamond potential. However, the recent study of Grütter and Quadling (1999) concluded that "*the sodium content of eclogitic garnet cannot be used in isolation to uniquely identify a diamond association*". Furthermore, they stated that the Na-in-garnet concentration is determined by, amongst other things, the bulk-rock composition, in particular the Na and Mg concentrations of co-existing clinopyroxene, in addition to pressure and temperature influences. Further work, incorporating the compositions of documented eclogites from around the world, would expand and refine the classification scheme identified above for Newlands, and potentially aid in diamond exploration.

ECLOGITIC XENOLITHS: RE-OS SYSTEMATICS

13

13.1 INTRODUCTION

The Re-Os isotopic system was discussed in detail in Chapter 7. Suffice to say that the highly variable Re/Os ratio resulting from mantle melting and the enriched Re concentrations observed in eclogites are conducive to the determination of precise isochrons (assuming a closed system).

13.2 SAMPLE DESCRIPTION AND ANALYTICAL PROCEDURE

Fourteen diamond-bearing eclogites and three diamond-free eclogites were analysed for Re and Os concentrations and isotopic ratios. Sample preparation and analysis is identical to that described in Chapter 7 and in Appendix I.

13.3 RE AND OS CONCENTRATION SYSTEMATICS

13.3.1 Rhenium

Re concentrations of Newlands eclogites vary by nearly two orders of magnitude (Table 13.1). The fourteen diamond-bearing eclogites range from 0.03 to 1.34 ppb, with the majority having concentrations greater than 0.2 ppb (Figure 13.1). The solitary diamond-free eclogite (AHM C5) measured for Re has one of the lowest concentrations at 46 ppt. Four replicate analyses were made on the diamond-bearing samples (Table 13.1). Three of the replicate analyses are within 0.01 ppb, whilst the fourth (sample AHM K8) has the highest and most variable Re concentration (1.18 and 1.34 ppb). The overall Re concentration ranges are remarkably similar to eclogites from Roberts Victor, South Africa (Shirey et al., 1998), but extend to

significantly lower concentrations than diamond-bearing eclogites from Udachnaya, Siberia (Pearson et al., 1995).

13.3.2 Osmium

Osmium concentrations of Newlands eclogites are relatively constant compared to Re, varying by only a factor of 2 (Table 13.1). Diamond-bearing eclogites range from 0.26 to 0.59 ppb, whereas the three diamond-free eclogites record the lowest and highest Os concentrations respectively (Figure 13.2). Replicate analyses of four diamond bearing eclogites display considerable scatter. This is expected as Os is thought to reside in trace PGE-rich phases, such as base-metal sulphides (Hart and Ravizza, 1995; Ruiz et al., 1999) and therefore the powder used for whole rock analyses may not adequately sample the heterogeneous distribution of these trace Os-rich phases.

The Re and Os concentration spread of eclogites for both Newlands and Roberts Victor are strikingly similar, but significantly different to Udachnaya (Figure 13.3 a and b). The Newlands diamond-bearing eclogites (and Roberts Victor eclogites) overlap a variety of compositional fields, including mid-ocean ridge basalts, Archæan basalts (Walker et al., 1989; Martin, 1991; Hauri and Hart, 1996), komatiites (Walker et al., 1988, 1989; Shirey, 1997), and continental flood basalt picrites (Shirey, 1997). In contrast, the Udachnaya field overlaps the low Os concentrations observed in both mid-oceanic and ocean island basalts.

13.4 Re-Os Isotope Systematics

The diamond-bearing eclogites have $^{187}Os/^{188}Os$ ratios (age corrected to the time of eruption) ranging from 0.1579 to 1.4877. The three diamond-free eclogites also display similar, but variable $^{187}Os/^{188}Os$ ratios; AHM C5 is the lowest, AHM C6 is in the middle, and AHM C7 is one of the highest, relative to the Newlands diamond-bearing eclogites (Table 13.1). These ratios are strongly radiogenic and considerably higher than any estimate of the present day Os isotopic composition of the mantle.

Expressed as γ_{Os}[16] (see Table 13.1 for calculation parameters) the Newlands eclogites extend to ranges well in excess of recent oceanic basalts and are similar to the present-day isotopic range of Archæan basalts (Komatiites) (Figure 13.4). The majority of Newlands diamond-bearing eclogites have lower γ_{Os} than their diamond-bearing counter-parts from Udachnaya.

The $^{187}Re/^{188}Os$ ratios are high, with diamond-bearing eclogites ranging from 0.54 to 26.21 (Table 13.1). Even though this range is nearly two orders of magnitude it is significantly lower in absolute range when compared to the diamond bearing eclogites from Udachnaya (Pearson et al., 1995). Only one diamond-free eclogite from Newlands (AHM C5) has been measured for Re and it has the lowest $^{187}Re/^{188}Os$ ratio (0.353) of any eclogite from Newlands.

The highly radiogenic Os signature in the diamond bearing eclogites (γ_{Os} = 23 to 1056) is consistent with their high $^{187}Re/^{188}Os$ ratios and requires long-term isolation from the convecting mantle, assuming an igneous derivation from chondritic mantle. Such high $^{187}Os/^{188}Os$ ratios allow precise model ages to be determined due to the high angle that the osmium evolution curve intersects the "Bulk Earth" reservoir. Osmium isotope evolution trajectories for the diamond-bearing samples display a general convergence between 2.5 and 3.5 Ga (Figure 13.5) and record model ages, assuming single-stage extraction from a chondritic mantle, varying from 3.1 to 18.5 Ga (see Table 13.1 for calculation parameters). The solitary diamond-free sample yields a negative model age indicative of a recent decrease in the Re/Os ratio. This range in model ages could be explained by the eclogitic protolith (MORB) being disturbed by seawater Os and thus yielding erroneously old model ages (i.e. greater than the age of the Earth, Ruiz et al. (1999). On a Re-Os isochron diagram, the samples scatter about a best fit line corresponding to an age of 3 Ga, but this line is strongly controlled by the replicate analyses of sample AHM K8 that have the highest Re/Os of this sample set (Figure 13.6). The two replicates of AHM K8 have sufficient spread in Re/Os and $^{187}Os/^{188}Os$ to define a chord with slope equivalent to an isochron of 3.0 Ga age with an initial $^{187}Os/^{188}Os$ of 0.153. If sample AHM K8

[16] γ_{Os} is the difference (in ‰) in $^{187}Os/^{188}Os$ between the sample and the bulk-mantle at the kimberlite eruption age.

and the diamond-free samples are excluded, a best fit line to the remaining fourteen points (including 1 replicate analysis) corresponds to an age of 3.6 ± 0.6 Ga with an initial $^{187}Os/^{188}Os$ of 0.193 (Figure 13.6).

It should be noted that sample AHM K8, which yields a different clinopyroxene major and trace element composition to other diamond-bearing eclogites, displays Re concentrations and Re-Os isotopic characteristics at the extremes for the Newlands diamond-bearing eclogitic suite, i.e. the highest $^{187}Re/^{188}Os$ and $^{187}Os/^{188}Os$ ratios.

13.5 Discussion

The relatively small range in Os concentrations is consistent with the geochemical similarity of the eclogites. This is in comparison to modern basalt suites where variations in Os content are often significantly larger than in Re content. Two diamond-bearing specimens, and one diamond-free sample, display unusually low Re concentrations, approximately an order of magnitude lower than other Newlands eclogites. The two low-Re diamond-bearing samples yield calculated Re-Os model ages older than Earth indicating either that their Os isotopic compositions were recently increased or that the two samples lost Re recently, perhaps by surficial weathering. Assuming that the old model ages are a result of recent Re-loss, and further assuming a 3 Ga age and chondritic initial Os isotopic composition for these samples, a Re increase of between a factor of 1.4 (AHM C5) and 2.5 (AHM K13) would be necessary in order to explain their Os isotopic compositions. These increases in Re would still leave these samples with unusually low Re contents relative to other Newlands eclogites (below 0.1 ppb). Alternatively, if these samples originally had Re contents similar to the low end of the Re concentration range of the remainder of the samples (circa 0.3 ppb) their relatively unradiogenic Os would result in relatively young Re-Os model ages of between 430 (AHM K15) and 680 Ma (AHM K13). In either case, the relatively low measured $^{187}Os/^{188}Os$ of these samples shows that not all mantle eclogites, assuming a MORB protolith, have radiogenic Os that is disturbed as a result of incorporation of seawater Os prior to subduction (Ruiz et al., 1999). Excluding these three samples, the remainder of the data scatter about a best-fit line of 2.6 Ga (initial $^{187}Os/^{188}Os$ = 0.336) on a Re-Os isochron diagram.

Excluding the compositionally distinct sample AHM K8, which also has the highest Re/Os of all the eclogites, the best fit line to the remainder of the data increases in slope to correspond to an age of 3.1 Ga with initial $^{187}Os/^{188}Os$ of 0.278. This age is similar to that indicated by the two-point chord connecting the replicates of sample AHM K8, though the initial $^{187}Os/^{188}Os$ for AHM K8 at this age is substantially lower.

The fact that the samples show considerable scatter limits the chronological resolution that can be extracted from the data. This scatter could reflect either variations in the initial Os isotopic compositions of the protoliths of these samples, or induced changes in Re/Os, for example incorporation of seawater Os (Ruiz et al., 1999). In spite of the observed scatter, essentially all data groupings provide slopes indicative of formation ages in the Archæan and indicate that the eclogites had $^{187}Os/^{188}Os$ substantially higher than that of a chondritic mantle at circa 3 Ga.

The mid-Archæan age of the Newlands eclogites overlaps the age of the diamond-bearing eclogites from Udachnaya (2.90 ± 0.38 Ga: Pearson et al., 1995). However, the Udachnaya isochron is controlled by the two samples with $^{187}Re/^{188}Os$ ratios greater than 200, which is significantly higher than the other four Udachnaya samples and any sample from this study. The four diamond-bearing eclogites from Udachnaya that have a similar range of $^{187}Re/^{188}Os$ ratios as the samples in this study plot within the scatter about the isochron shown by the Newlands eclogites (Figure 13.7). The overlap in Re-Os ages suggest a similarity in origins between the Newlands and Udachnaya diamond-bearing eclogites, however, the samples from Udachnaya have significantly different Re and Os concentrations (Figure 13.3) and display a diverse major and trace element mineral chemistry (for example Taylor et al., 1997), whereas the Newlands samples are relatively consistent.

The Newlands diamond-bearing eclogites Re and Os concentrations are similar to those from Roberts Victor (Shirey et al., 1998) but are significantly different from Udachnaya (Pearson et al., 1998). This opens up the possibility of different origins for the diamond-bearing eclogite protoliths beneath the Kaapvaal and Siberian cratons. The majority of the samples from Newlands overlap the komatiite field in

Re-Os concentration space but also extend into the fields for primitive ocean island basalt (OIB) and continental flood basalt (CFB) picrites. In contrast, the samples from Udachnaya primarily plot in the evolved mid-ocean ridge basalt field. If the Newlands eclogitic protolith was formed in an Archæan ocean floor environment and accreted to the SCLM then it is likely that it represents ancient (komatiitic?) ocean ridge products or primitive portions of oceanic plateaus or islands.

NEWLANDS DIAMONDS: PHYSICAL CHARACTERISTICS

14

14.1 INTRODUCTION

Diamonds exhibit a vast range of physical characteristics that have been attributed to conditions at the time of diamond crystallisation and growth (primary features) and subsequent residence in the mantle and transportation in the kimberlite (secondary features) (for example, Robinson, 1979; Sunagawa, 1984; Robinson et al., 1989). Accordingly, both primary and secondary features of diamonds provide clues to their origin, subsequent storage history in the mantle, and transportation within the kimberlite. Studies of these features have lead to broad-scale inter-cratonic comparisons - for example the presence of extremely large diamonds from the Kaapvaal craton or the relatively high abundance of colourless octahedra from the Siberian craton (Gurney, 1989). Furthermore, studies of individual locations have noted differences within a craton, or even within a cluster of kimberlites (Gurney, 1989).

The cube (rapid growth in unstable conditions from highly supersaturated solution) and octahedron (slow growth in stable conditions from low supersaturated solution) are the primary growth forms of diamond (Sunagawa, 1984). However, as well as growing as single crystals, diamonds may grow as macles (twins) or aggregates (crystals united in random fashion), coated diamonds, and polycrystalline aggregates (Sungawa, 1984). The most common form of diamond observed in Southern Africa is the tetrahexahedroid or rounded dodecahedron. However, the percentage of tetrahexahedroids varies drastically between kimberlites (Robinson et al., 1989). The tetrahexahedroid is the result of resorption of the primary growth forms of diamond (Robinson, 1979; Sungawa, 1984). Detailed studies of large diamond data sets has classified the resorption into six categories based on the volume of diamond (as a percentage) that is resorbed (Robinson, 1979; Robinson et al., 1989, Otter et al.,

1991). Furthermore, it is possible to have diamonds with two morphologies – commonly a combination of a primary growth form and resorption. Such diamonds are termed hemimorphic or pseudo-hemimorphic and the combination of morphologies is believed to be the result of part of the diamond having been exposed to the kimberlite magma – and thus resorbed – whilst the other half of the diamond is protected within its host xenolith.

The preservation of diamond requires the rapid accent of the kimberlite magma to minimise dissolution (i.e. minimum exposure time of the diamonds to the magma). Other factors determining diamond preservation are the initial size of the diamond, the depth (during ascent) at which the diamonds are liberated from the primary host rocks into the kimberlite as, and the volatile composition and concentration of th ekimberlite magma (Robinson, 1979).

14.2 DIAMOND SAMPLE FROM NEWLANDS

Physical characteristics have been documented for the diamonds extracted from the Newlands peridotitic garnet macrocrysts and eclogites. The diamonds were extracted from the xenoliths by crushing and therefore it is possible that some diamonds may have broken or splintered, thus leading to a bias in the overall diamond description percentages. In addition, not all the diamonds were extracted from all the xenoliths (for example garnet macrocryst AHM D1 and eclogite AHM K2 were not crushed). Furthermore, the total diamond data set is statistically small and therefore the data has been treated as semi-quantitative only.

In addition to the diamonds from xenoliths, subsets of diamonds were selected for Fourier transform infra-red (FTIR) micro-spectroscopy from run-of-mine production. However, due to the nature of FTIR (see Chapter 16) only certain diamonds are suitable, that is, small diamonds that an infra-red beam can pass through. Furthermore, all the diamonds selected for FTIR from the run-of mine production were obtained from the fine fraction (<2000 μm). In contrast, there has been no size limitation to the diamonds observed in the peridotites and eclogites, although the majority are less than 1000 μm, but several range up to ~ 2000 μm.

14.3 PHYSICAL CHARACTERISTICS OF NEWLANDS DIAMONDS

Detailed descriptions of the diamonds extracted from xenoliths are presented in Appendix III. In addition, thousands of diamonds have been inspected from Newlands, including a run-of-mine macro-diamond sample.

14.3.1 Diamonds from peridotitic xenoliths

The diamonds recovered from the Newlands peridotitic xenoliths (Plates 14.1 through 14.12) were generally very small and occur in two primary forms, namely (< 1 mm) single octahedra (Plates 3.2, 3.3, 3.5, 3.6, 3.12) or octahedra aggregates (Plates 3.2, 3.9, 3.13, 3.17, 3.18) (Table 14.1). All the xenoliths contain multiple diamonds or diamond aggregates. For example, AHM D1 contains (at least, on the surface) 5 single colourless octahedra and one diamond aggregate. The diamonds are commonly less that 1000 μm in diameter but may range up to 2000 μm.

The single octahedra are predominantly colourless and euhedral, with sharp edges and they show little or no resorption (class 6 of Robinson et al. (1989)). Some of the octahedra display finely stepped planar surfaces and these triangular plates are often imbricated on one or more of the growth faces. In addition, there are occasionally both positive (growth) and negative (resorption) trigons and hexagons on the primary faces. Birefringence indicates that some of the small octahedrons display minor strain, although no linear array of trigons, demonstrating plastic deformation, were observed on the octahedral diamond surfaces. Some of the octahedra are elongate or flat, with one diamond displaying perfect octahedral growth surfaces and stepped planar surfaces but with the x-axis over 5 times the length of the y-axis.

Several diamonds contain very small black inclusions, sometimes needle-like, believed to be either sulphides or graphite. Three diamonds contain multiple black or deep red-brown inclusions, one extracted from AHM D2 and two from AHM D4. The three diamonds are sharp-edged colourless octahedra displaying no resorption. The diamond from AHM D2 is a euhedral crystal and the inclusions are easily visible with

no visible internal cracks or fractures (see Plates 3.6 a and b, 14.1). It contained over thirty inclusions and after polishing revealed inclusions of garnet and chromite in contact with each other. In contrast, the two diamonds from AHM D4 display irregular growth and have stepped trigonal growth plates making it difficult to observe internal features, such as if there were any cracks or fractures. These inclusions were only observed after the diamonds broke. They are believed to be inclusions due to the imposed diamond morphology on the garnet.

The octahedral aggregates are also generally colourless, although a few are frosted. The aggregates range in size from extremely small (<500 μm) up to several millimetres in size. As with the single octahedra, they appear to show very little or no resorption. Some of the larger octahedra within the aggregates have both stepped planar surfaces and triangular plates. In addition, some of the diamonds have grey clouds of inclusions.

It is notable that, although the data set is small, no dodecahedra or cubes were observed (Table 14.1). Furthermore, there were only a few grey diamonds and no brown, yellow, pink or other known rarer diamond colours amongst the peridotitic garnet macrocrysts. Furthermore, none of the diamonds display hemimorphic or pseudohemimorphic morphologies indicating that the diamonds exposed on the surface of the peridotitic xenoliths were not in contact with the kimberlite magma for any extended periods of time, if at all. Therefore, the peridotitic garnet macrocrysts were in likelihood broken in the processing plant after being mined. The diamonds yielded relatively similar proportions of whole crystals, chipped crystals, broken crystals, and fragments. The high proportion of broken crystals and fragments is most likely due to the method of diamond extraction from the xenolith, and not representative of the crystal state of the peridotitic diamonds.

There was no noticeable physical difference between the diamonds extracted from the high calcium or low calcium garnet macrocrysts.

14.3.2 Diamonds from eclogitic xenoliths

The diamonds recovered from the Newlands eclogite xenoliths (Plates 14.13 through 14.24) display a considerably wider range of characteristics than the diamonds from the peridotitic garnet macrocrysts (Table 14.1). The diamonds range in size from approximately 100 μm within diamond aggregates to large single crystals up to 2 mm - the majority, however, are micro-diamonds less than 1 mm. The dominant morphology is octahedral but there are also significant numbers of cubes and dodecahedrons, and some cubo-octahedrons (Table 14.1). Noticeably, there are very few diamond aggregates, significantly less than in the peridotitic garnet macrocrysts.

The octahedra are predominantly colourless and often display stepped planar growth surfaces. In contrast, other morphologies are chiefly grey or brown. The cubes also display a milky appearance (due to their fibrous nature) and accordingly have a very poor clarity. The different types of morphologies are displayed in various Plates described in Chapter 8 (for example Plates 8.2 and 8.7 each display a single octahedron whilst Plates 8.1, 8.5 and 8.11 each display a single cube). No silicate inclusions were observed in any of the eclogitic diamonds from the xenoliths, however many did contain inclusions of what appear to be graphite or sulphides as small grains or clouds.

The most dominant diamond crystal state was fragments (of unknown original morphology), however whole, chipped and broken diamonds were observed. The significance of these observations is uncertain. The high number of fragments and broken diamonds is probably a result of the method of diamond extraction from the xenolith and not representative of the true crystal state of the eclogitic diamonds. Another possibility is that the diamonds were fragmented due to the differential expansion any diamond inclusions and the host diamond.

Several xenoliths contain diamonds of different morphologies and colours. For example, sample AHM K7 contains two diamonds, one a colourless octahedron whilst the other is a milky grey cube. In another example, sample AHM K3 contains a colourless octahedron, a grey cubo-octahedron, a colourless cubo-octahedron, and a

colourless dodecahedron. It is uncertain whether these diamonds grew in the same event or at different times. Although the mineral chemistry of AHM K8 is significantly different from the other diamond-bearing eclogites (see Chapters 9 and 10), the diamonds are not visually distinctive.

14.3.3 Run-of-mine production

14.3.3.1 Micro-diamonds

The small diamonds described are from the run-of-mine production (< 1000 μm fraction) and not just the diamonds specifically selected for FTIR. The small diamonds cover a vast range of diamond morphologies, colours and clarity. Both octahedra and dodecahedra are abundant whilst other morphologies, such as aggregates, cubes and macles are present, but not as common. Aggregates are not as abundant as suggested by the number observed in the peridotitic xenoliths. This is most likely a result of diamond aggregates breaking apart once extracted from the host xenolith and thus represented as either fragments or very small individual crystals.

The most predominant diamond colours were colourless and grey, whilst brown diamonds are also common. Other diamond colours, such as yellow or pink, were observed but are uncommon whilst blue and green diamonds were extremely rare and have a very low colour intensity. The small diamonds display a vast range of crystal states from whole diamonds through to chipped or broken diamonds and diamond fragments. There were abundant diamond fragments, however, the majority of diamonds were either whole or chipped. Diamond fragments are usually not suitable for FTIR studies and were not selected for detailed examination.

The octahedra often display very little resorption. Small octahedral "*glassies*" form a significant proportion of the diamond population at Newlands and were noted in older records of Newlands diamond production. For example, Beck (1899) described Newlands diamonds as chiefly "*octahedrons, very sharp in form*", whilst Gräichen (1903) noted the lack of larger diamonds with the colourless octahedra averaging

between 0.1 and 0.2 cts. The numerous small colourless octahedral glassies are also observed in other kimberlites in the Barkly West area (where Newlands is located) – for example, at the Frank Smith kimberlite (located approximately 10 km to the NE of Newlands, see Figure 1.1) and also in the nearby Group II kimberlite dykes (Gurney and Menzies, 1998).

14.3.3.2 Macro-diamonds

The macro-diamonds described here are a summary of observations made during this study of the run-of-mine production over a one week period as well as reports compiled by van Heerden and Gurney (1994) and personal observations of C. Cotterrell. No detailed diamond descriptions are provided.

The dominant morphology was octahedral, generally with minor or no obvious resorption. Dodecahedra were less abundant whilst macles, cubes and cubo-octahedra are present but uncommon. The diamonds are predominantly colourless or grey, with browns contributing a noticeable proportion. Very few pink or yellow diamonds were observed, and no blue or green diamonds noted. The majority of the diamonds were broken or fragments.

The octahedra often display stepped planar surfaces growth features on the diamond faces and rarely contained observable inclusions. Only four diamonds in a run-of-mine production parcel of 145 carats were greater than one carat (Table 2.2). Furthermore, none of them were of gem quality - the largest diamond was a 3.0 ct broken fractured brown octahedra.

14.4 DISCUSSION

14.4.1 Peridotitic diamonds

Comparison of the diamonds from Newlands (peridotitic) garnet macrocrysts with diamonds from peridotitic xenoliths from around the world (for example, Udachnaya, Siberia (Sobolev et al., 1984), Schaffer, Wyoming (McCallum and Eggler, 1976),

Finsch, Kaapvaal (Shee et al., 1982; Viljoen et al., 1992)) reveals many similar features. These features include the small (predominantly less than 2 mm) sharp-edged colourless octahedra that often display stepped trigonal growth plates. In addition, there are also notable numbers of macles and aggregates of octahedra.

Exceptions to the above descriptions are the diamonds from peridotite xenoliths from Argyle (Jaques et al., 1990), and a few diamonds from a xenolith from Finsch (Shee et al., 1982). These were also predominantly sharp-edged octahedra like other peridotite xenolith diamonds but, in contrast, are mostly brown. In addition, the Argyle diamonds are heavily frosted. The brown colour may be a result of plastic deformation rather than impurities incorporated at growth (Shee et al., 1982).

The silicate inclusions observed in diamonds AHM D2 and AHM D4 are believed to represent pristine samples of early mantle. However, this assumes that the diamond did not crack or fracture at a later time and thus allow exchange between the surrounding environment and the inclusion. Cracks to and from inclusions can often be assessed via careful examination under a binocular microscope, however, Taylor et al. (1995) showed that this is not ideal due to the possible subsequent annealing of fractured diamond. They recommended that diamonds should be examined using cathodoluminescence. Even so, this still is not 100% effective, as CL is only two-dimensional whereas the crack may emanate in any direction.

The peridotitic diamonds are generally small single crystals – often spatially fairly close to other diamond. Occasionally two octahedral crystals are joined, whilst aggregates are also octahedral. This would be consistent with growth under medium supersaturation conditions (where single octahedral crystals grew from a low supersaturated solution and octahedral aggregates grew from a slightly more saturated solution (Sunagawa, 1984)).

14.4.2 Eclogitic Diamonds

In contrast to the scarce number of diamond-bearing peridotitic xenoliths world-wide, there are numerous studies reporting diamond-bearing eclogites. Furthermore, and again in contrast to peridotitic diamonds, eclogitic diamonds are known to cover a

vast range of diamond morphologies, colour, and clarity. For example, cubes have been reported in eclogites from several studies (this study; Robinson, 1979; Sobolev et al., 1991 (from Beard et al., 1996); Jerde et al., 1993) whilst they have never been reported from diamond-bearing peridotite xenoliths. Examples include the Udachnaya (Sobolev et al., 1991; Jerde et al., 1993), Mir (Beard et al., 1996), Koidu (Hills and Haggerty, 1989), and a variety of southern African locations (Rickwood et al., 1969; Rickwood and Mathias, 1970; Robinson, 1979). However, whilst eclogites appear to display a vast range in diamond characteristics, there are exceptions. For example, a study of diamonds from eclogites from the Mir kimberlite, Siberia yield a preponderance of "*sharp-edged octahedral crystals with very minor resorptional features*" (Bartoshinsky, 1960, Bartoshinsky et al., 1973 – cited in Beard et al., 1996). In addition to sharp-edged colourless octahedra, which predominate in diamonds from peridotites at Newlands, in run-of-mine production there are also numerous cubes, cubo-octahedra and dodecahedra that occur in a variety of colours, most commonly grey and brown. The diamonds extracted from eclogites at Newlands are similar both to the run-of-mine production and to the rest of the world, displaying a diverse range of morphologies, colours and clarity. Whilst Newlands eclogites have some sharp-edged octahedra, they are not dominant.

14.4.3 Differences in diamond populations at Newlands

The differences in appearance between eclogitic and peridotitic diamonds (at Newlands and elsewhere) outlined above indicate that some (if not all) the eclogitic diamonds are in likelihood derived from a different source and/or event than the peridotitic diamonds. For example, cubic diamonds, found associated with eclogite xenoliths only, grow rapidly from solutions that are highly supersaturated where a continuous growth mechanism applies (Sunagawa, 1984).

Furthermore, the differences indicate that the diamonds may have experienced different conditions in the mantle. For example, several eclogitic diamonds at Newlands are brown (as well as numerous run-of-mine diamonds); in contrast, none of the peridotitic diamonds are brown. Studies have suggested that deformation laminae and brown diamonds may be the result of graphitisation along deformation glide planes as a consequence of plastic deformation (Urusovskaya and Orlov, 1964;

Harris, 1992). Consequently, it is possible that the eclogitic diamonds have experienced some type of stress or strain not experienced by the peridotitic diamonds. However, plastic deformation is very temperature dependant and such a premise would imply that at least some eclogitic diamonds resided within the mantle at temperatures greater than 1100 °C for a period of time.

The relationship between these xenolithic diamonds and run-of-mine production is uncertain. The range of diamond morphologies and colours observed in the run-of-mine production imply that the majority of diamonds are derived from eclogitic xenoliths, although a significant proportion are likely to be derived from peridotitic xenoliths. It is not possible, however, to assign a specific ratio, particularly as a prominent diamond group - sharp-edged colourless octahedra - are present in both eclogitic and peridotitic xenoliths and abundant in the run-of-mine production.

NEWLANDS DIAMONDS: CATHODOLUMINESCENCE

15

15.1 INTRODUCTION

The internal structure of diamonds can provide useful information about growth and resorption histories as well as any deformation that may have occurred. These features are easily recognised using cathodoluminescence. Cathodoluminescence (CL) is a surface phenomenon and, therefore, it is most useful for inspecting cut and polished surfaces of diamonds. Whole or broken diamonds can also be inspected, but interpretation can be difficult because the CL will relate to the diamond surface and yield no information on internal growth zones (if they exist).

CL is the electromagnetic radiation emitted by the majority of minerals, including diamond, under electron-beam bombardment due to the excitement of electrons followed by their relaxation (Davies, 1979; Walker, 1979). Several studies indicate that there is a semi-quantitative relationship between CL spectra and point defects (N and H) or intrinsic defects (vacancies or interstitials) (Hanley et al., 1977; Zezin, 1990). However, many of the CL peaks in the spectra are unidentified and luminescence intensity cannot at present be directly related to the concentration of any specific diamond property (Davies, 1979).

A detailed discussion of the origin of CL is beyond the scope of this thesis, and the reader is referred to Davies (1979) and Bulanova (1995) for more information and examples. Several detailed studies have made use of this technique, for example, Zezin, (1990), Otter et al. (1991), Bulanova (1995), Chinn (1995), Trautman et al. (1997), Bulanova et al. (1998), and Davies et al. (1999). It is known that different types of point defects yield different colours and intensities. For example, the various shades of blue CL radiation (which is the most common) are believed to be due to the major impurity nitrogen (Davies et al., 1999), whilst non-luminescence (dark) areas of

CL have been correlated with areas deficient in nitrogen (Taylor et al., 1995). The dark CL areas often observed around silicate mineral inclusions in diamond is believed to the result of aluminium in the inclusions which getters (draws) nitrogen (Collins and Lightowlers, 1979). Thus, CL can be used to identify heterogeneities and different zones within diamonds.

15.2 Samples and Methodology

Ten diamonds from eclogites, two from peridotitic garnet macrocrysts, and 3 from run-of-mine production were cut and polished. In general, diamonds in peridotitic garnet macrocrysts were noticeably smaller than those from eclogite. Only two peridotitic diamond were selected for polishing because of the difficulties experienced with preparing such small stones. The diamonds could not be cut along specific orientations due to their small size and the polishing method. Furthermore, only one octahedral diamond was selected. In addition, diamonds with broken surfaces were inspected to aid with the interpretation of FTIR spectra (Chapter 16).

The polished diamonds were analysed using the SEM housed in the Electron Microscope Unit at the University of Cape Town. Other diamonds were analysed using the Technosyn and Nuclide Luminoscope cathodoluminescence attachments for optical microscopes housed at the Crystallography and Mineral Physics Unit at University College, London. Samples were cleaned by ultrasonic agitation in hydrochloric acid and the dichloromethane and then mounted with water-soluble carbon dag on copper plates (at UCL) or carbon tape (at UCT). Detailed analytical conditions are presented in Appendix I.

15.3 Results

The broken diamonds analysed at UCL displayed variable cathodoluminescence colours. The dominant colour was blue. This was consistent with the presence of nitrogen in the majority of samples from Newlands (see Chapter 16). In addition, both light green and bright yellow colours were observed as well as diamonds with very low CL intensity. However, the CL of the broken diamonds did not reveal any

internal complex growth history - most likely due to the nature of the samples, that is, broken surfaces rather than polished. Therefore, several diamond plates were cut and analysed in more detail. All of these plates, in contrast to the broken diamonds, displayed detailed internal growth and resorption histories.

15.3.1 Diamonds from Eclogitic Xenoliths

All ten eclogitic diamonds display similar internal structures and growth patterns. In most cases the diamonds were not polished through the centre, and therefore it is not possible to determine if there was a nucleation seed for these diamonds. As there was no control as to how they were sectioned due to their small size the observed growth features on the polished surfaces are of differing size and proportions. CL images of the diamonds are displayed in Plates 15.1 through 15.17.

CL indicates that the eclogitic diamonds have at least three growth periods. The first recognisable growth event is octahedral and represented by a bright light grey triangle in the images. The triangle shape is indicative of polishing sub-parallel to a growth face. In the majority of samples this first growth stage displays no resorption whatsoever. For example diamond A from AHM K1 (Plate 15.9 and 15.10) and diamond A from AHM K6 (Plate 15.15) both display sharp triangular zones (bright light grey) of growth in the centre of the image. In contrast, some of the diamonds display no sign of this first growth stage. For example diamond A from AHM K12 (Plate 15.1 and 15.2) or diamond D from AHM K14 (Plate 15.5 and 15.6). However, the first diamond growth stage comprises only a minor volume of the diamond in its final form observed in this study (see Plates 15.3, 15.4, 15.9 and 15.10). Therefore, it is likely that some of the diamond cores are not apparent in the CL images due to the geometry of the polishing process.

The second major period of growth (in which there may have been several minor periods of growth) is terminated by irregular sharp-edged growth faces (that are generally represented by a thin brighter zone relative to the medium grey CL colour of the bulk of the second growth period). The bright zone is probably the result of stepped triangular plates growing on the diamond surface at that time. This is clearly

observed in diamond A from AHM K12 (Plate 15.1 and 15.2), diamond C from AHM K14 (Plate 15.3 and 15.4), and diamond D from AHM K14 (Plate 15.5 and 15.6).

The third major period of growth determines the present day diamond morphologies, all of which are primary growth phases.

Several other features indicative of significant events during growth are apparent in addition to these three episodic periods of growth. Firstly, irregular resorbtion of the first diamond growth stage is observed in only one diamond (diamond C from AHM K14 - Plate 15.3 and 15.4). This is not observed in the other diamonds and possibly represents some local phenomenon and may explain the absence of the core for some diamonds, in particular as a large percentage was resorbed. Secondly, a small growth rim, apparent on three diamonds, immediately after the second major period of growth displays rounded surfaces. This may be the result of growth followed by resorption followed by growth again. It is uncertain whether this is a continuous process or episodic. It is also difficult to establish the percentage of diamonds that were affected. Examples include diamond A from AHM K12 (Plate 15.1 and 15.2), and diamond C from AHM K14 (Plate 15.3 and 15.4). Finally, diamond A from AHM K17 (Plate 15.7, 15.8) displays some irregular growth during part of the second stage of diamond growth. However, it is uncertain whether this is a function of growth and resorption or redistribution of trace elements within the diamond, such as nitrogen, causing a change in CL colours and patterns.

15.3.2 Diamonds from Peridotitic Xenoliths

The two peridotitic diamonds (diamond B from harburgitic AHM D2 and diamond A from lherzolitic AHM E4) were polished – the former broke during polishing, and only the bottom side of the diamond in the image corresponds to the original final growth surface (Plate 15.20). Both diamonds display a complex octahedral growth with no definitive CL boundaries and thus it appears the diamond formed in a single stage growth event (Plate 15.18, 15.19, and 15.20). No diamond seed could be observed as the diamond was not polished to the centre. The final morphology is octahedral with no resorption.

Diamond B from AHM D2 is an important specimen as it contains both a garnet and chromite inclusion. It is noticeable that there is a crack emanating away from the inclusion in two directions. The crack towards the centre clearly does not reach the diamond surface. It is not certain whether the other crack continued to the diamond surface as the diamond is broken. However, initial inspection of the diamond before polishing, under a binocular microscope, did not reveal any cracks or fractures that reached the surface. Nevertheless, it is uncertain whether this is a crack that originated whilst the diamond was resident in the mantle, during ascent in the kimberlite, or during polishing. The presence of small reflective minerals (presumably sulphides) along parts of the crack/fracture eliminate the latter possibility. The infiltrated fluids could originate from the kimberlite or proto-kimberlite magma, from an earlier metasomatic event, or fluids trapped during diamond formation and incorporation of the inclusion depending on the timing of the crack - assuming that the crack is entirely internal, then the latter is likely. This crack would be a result of the diamond moving to lower pressures, the inclusions expanding more than the diamond causing the confining pressures to increase until the differential in pressure causes the diamond to crack.

15.4 DISCUSSION

The sectioning and polishing of the selected diamonds occurred after the completion of the FTIR study. Therefore, it is uncertain whether the different zones observed in the eclogitic diamonds correspond with variations in nitrogen concentration and/or aggregation state. It is believed that CL colour variations are linked to changes in point defects (Davies, 1979) of which nitrogen is the most common. Furthermore, detailed studies of different CL zones in diamonds from Udachnaya and other Yakutian kimberlites (Bulanova, 1995; Trautman et al., 1997), George Creek (Chinn et al., 1998), and Australia (Trautman et al., 1997) have shown that nitrogen concentrations can vary by three orders of magnitude within a diamond, even over as little as ~10-20 μm. Therefore, it appears likely that each episodic growth period may differ in nitrogen concentration and aggregation states.

The eclogitic diamonds indicate that there are multiple episodic events occurring during the diamonds growth. However, there is no basis for determining the time period between each event, indeed the different CL zones may reflect a continuing cycle of growth and resorption and not any lengthy difference in time. Detailed FTIR of these different growth zones may help elucidate this, however, their old age (see Chapter 16) and the imprecise nature of FTIR makes this unlikely. Nevertheless, it is clear that the diamond growth of these eclogitic diamonds is likely to be episodic, as indicated by this and a multitude of other diamond CL studies (for example, Bulanova, 1995; Chinn, 1995; Westerlund, 2000).

NEWLANDS DIAMONDS: FOURIER TRANSFORM INFRA-RED (FTIR) SPECTROSCOPY

16

16.1 INTRODUCTION: REVIEW OF FTIR

Element bonds absorb electromagnetic radiation which result in a distinctive mineral fingerprint. Extremely small quantities (sub parts per million, depending on the type of bond) can influence a mineral's spectrum, thus allowing lattice impurities or defects to be detected. This is particularly useful in the study of diamond, resulting in various diamond classifications, the identification of diamond sub-populations, and geological constraints relating to their genesis.

The presence of nitrogen in the diamond lattice and the associated IR absorption features have been reviewed by many authors. The introduction below is intended to summarise the current knowledge of FTIR; for more detailed information on this subject the reader is referred to Bibby (1982), Clark et al. (1992), Evans (1992), Field (1992) and the references therein.

16.1.1 Diamond optical absorption spectra

It has long been known that diamonds exhibit various optical absorption characteristics (or lack thereof) in both the ultraviolet (UV) and infrared (IR) spectrums. Robertson et al. (1934) noted that some diamonds did not display certain absorption patterns in their UV or IR spectra, from which they proposed the classification of Type I "imperfect" and Type II "perfect" diamonds. Later studies revealed that all diamonds display intrinsic lattice absorption's in part of the mid-infrared region (wavelengths of 4000-1500 cm^{-1}) due to three- and two- phonon transitions (Collins and Fan, 1954; Sutherland et al., 1954; and Lax and Burnstein, 1955). Many diamonds also yield one-phonon absorption, although centrosymmetric crystals, such as diamond, should not display any (Lax and Burnstein, 1955). This

can be explained by the presence of impurities, which create defects that destroy centro-symmetry (op. cit.) and result in the various IR spectra observed in the one-phonon region (Figure 16.1).

Diamond has a variety of absorption patterns in the mid infra-red spectrum (4000 to 650 cm^{-1}) due to the presence (or absence) of impurities or lattice defects. The characteristic spectrum of diamond occurs in the two-phonon region while the one- and three- phonon regions are known to vary due to the presence of nitrogen and hydrogen, respectively (Figure 16.1). Previous research has shown that the one-phonon absorption bands in diamond vary substantially in both structure and magnitude from sample to sample. These absorption patterns have been related to the presence of nitrogen in the lattice. Klyuev et al. (1973) and Evans (1976) suggested that nitrogen is incorporated into the diamond lattice as single substitutional atoms ('S') atoms during natural diamond growth. Elevated temperatures in the mantle subsequently lead to a nitrogen aggregation sequence dependent on mantle residence time of diamonds (Evans, 1976). Exposed to high temperatures and pressures the nitrogen atoms migrate and form aggregates or clusters - firstly "*A defects*", which are nitrogen pairs (Davies, 1976), then "*B defects*", thought to be 4 nitrogen atoms sited tetrahedrally around a vacancy (Loubser and van Wyk, 1981). In association with the onset of B defects is the concomitant formation of platelets.

A very small proportion of nitrogen atoms aggregate to form N3 defects, which display paramagnetic spin, suggesting that they consist of three nitrogen atoms around a vacancy (Loubser and Wright, 1973). The N3 defect shows no absorption in the one-phonon region of the IR spectrum, but does show distinctive absorption in the UV spectrum (Davies and Summersgill, 1973). However, it is estimated that N3 defects in natural diamonds only comprise between 0.1-1% of the total N substitutional concentration (Woods, 1986). The rate of N aggregation determined from high temperature-high pressure (HT/HP) experiments is such that under mantle conditions a majority of diamonds will only partially aggregate, even after several billion years.

A study of several natural diamonds found the 1282 cm^{-1} one-phonon peak to be proportional to their nitrogen content (Kaiser and Bond, 1959). Density measurements and lattice constant determinations were consistent with the presence

of nitrogen atoms, which occupied substitutional sites in the diamond lattice (Kaiser and Bond, 1959). Since this finding intensive research into the IR one-phonon region has further subdivided diamonds into the following currently recognised groups (on the basis of the presence of nitrogen and its aggregation state): Types Ib, IaA, IaB, IIa and IIb and various intermediate mixtures, e.g. Type IaAB. Type I diamonds contain nitrogen and are divided into Type Ib (single substitutional nitrogen), Type IaA (nitrogen aggregates - probably pairs), Type IaB (nitrogen aggregates - probably fours); however, more commonly as mixtures Type IaAB. Type II diamonds contain no FTIR detectable nitrogen and are divided into Type IIa (contain boron) and Type IIb (contain no boron).

Numerous studies of natural diamonds have revealed that the majority contains nitrogen in a form detectable by IR spectroscopy (H.J. Milledge, pers. com; Field, 1992). Type Ia diamonds comprise the majority of natural diamonds, Type II diamonds are rare, whilst Type Ib diamonds are extremely scarce (H.J. Milledge, unpub. data; Evans, 1992). In contrast, synthetic diamonds are always Type Ib or, if higher temperatures are used, a mixture of Type Ib-IaA (Kanda et al., 1990).

16.1.2 Nitrogen Concentration and Aggregation state

Quantitative information about nitrogen content and aggregation state of a diamond can be obtained using the relationships determined by Woods et al. (1990a, 1990b). Evans and Qi (1982) first decomposed IR spectra into its A and B components, which were later modified by Clark and Davey (1984) and Woods (1986) who resolved four other components termed C-F. The E and F spectral components are of unknown structure and origin and comprise relatively minor amounts; consequently they are not considered further. The three components of significance for quantitatively determining nitrogen contents are the A and B defects and platelets corresponding to the A, B and D spectra respectively (Figure 16.1). The extent of nitrogen aggregation is dependent on the initial nitrogen concentration and the temperature history of the diamond while it was resident in the mantle. The derived equations are discussed and presented in Appendix I.

16.1.3 Time-Temperature Calculations

Current knowledge on the behaviour of nitrogen in the diamond lattice can constrain average mantle residence temperature but is not precise enough to allow accurate age calculations (compared to radiogenic studies). Even so, it is capable of defining diamond populations and constraining their geologic history through time-temperature "windows". An improved understanding of nitrogen kinetics is required before quantitative calculations of time are as precise as other techniques. In contrast, temperature calculations are more precise than any geothermobarometer applicable to upper mantle minerals. It should be recognised that nitrogen concentration values are controversial and dependent on a range of assumptions (as outlined in Appendix I). The errors are uncertain, and concentrations should not be treated as absolutes. However, they are relative and independent of the accuracy of the constants, and therefore can be used to assess differences between the Newlands diamonds and semi-quantitatively with other locations.

Nitrogen aggregation is based both on time and temperature, however, temperature is far less sensitive than time. Consequently it can be used in either of two ways:

(i) to calculate diamond ages using pre-determined mantle residence time-averaged temperatures, normally obtained from inclusions in diamonds. (However, it has been observed that FTIR and geothermobarometry can yield substantially different temperatures, for example, touching inclusions from George Creek diamonds yield a temperature mode of 1125 - 1150 °C whilst nitrogen aggregation temperatures yield a mode of 1200 - 1225 °C (Chinn, 1995)), or

(ii) to calculate diamond equilibration time averaged temperatures using pre-determined ages, normally by assuming the diamond is of the same paragenesis to those which have already been dated (not necessarily from the same kimberlite pipe).

It is essential that the constrained variable is fixed as reliably as possible. Commonly, in the past, proxy values have been used.

Temperature can be determined on either xenolith minerals or inclusions in diamonds, however, care is required in interpreting geothermometry results. Rarely are they accurate to better than 50 °C and the temperature recorded is either:

(i) the ambient mantle temperature prior to entrapment in the kimberlite (recorded by minerals in the xenolith or touching inclusions), or

(ii) the temperature of diamond formation (if the inclusions are separate from each other and within the same diamond growth zone).

The temperature used in FTIR calculations is a time-average temperature over the entire history of the specific growth zone or diamond, depending on the position of the IR transmission. Even if the diamond is old, the proxy temperature represents a starting point for which to obtain a geological age (rather than a quantitative age) or, possibly, thermal history information.

The majority of studies to date use the latter procedure (see for example Evans and Harris (1989), Taylor et al. (1990), Chinn (1995), Taylor et al (1995a,b)). However, only a few instances have been reported where FTIR analyses were made on diamonds where independent ages have been determined either on the xenoliths from which they where extracted, for example, eclogitic xenoliths from Roberts Victor (Taylor et al., 1995c) or from silicate or sulphide inclusions from within the diamond(s), for example Richardson and Harris (1997), Pearson et al. (1998) and Pearson et al. (1999).

16.2 SAMPLES

The diamonds analysed in this study can be classified into three groups; namely diamonds from peridotitic (P-type) or eclogitic (E-type) xenoliths, and run-of-mine production of unknown (U-type) paragenesis. Diamonds of peridotitic genesis can be further subdivided into harzburgitic (H-type) or lherzolitic (L-type) on the basis of garnet geochemistry (see chapter 4). Hereafter these diamonds will be respectively referred to as P- (subdivided into H- or L-), E- and U- type diamonds.

All the FTIR spectra of diamonds in this study were made on either whole or broken diamonds. As the infra-red beam traverses the diamond it may travel through several

growth zones of widely differing nitrogen concentrations and aggregation states. An indication of the possibility of different zones within a diamond is the variation shown from multiple FTIR spectra taken from various orientations and positions in this study and others (Bulanova, 1995; Mendelssohn and Milledge, 1995; Chinn, 1995).

Spectra were obtained for 42 diamonds from 15 harzburgitic garnet macrocrysts (H-type), 5 from 4 lherzolitic garnet macrocrysts (L-type), 55 from 18 eclogites (E-type), and approximately 200 run-of-mine diamonds of unknown paragenesis (U-type). The diamonds extracted from xenoliths have a wide range of characteristics, in particular their size, which ranges from whole crystals of up to 2 mm to fragments as small as 150 μm. In contrast, run-of-mine diamonds were meticulously hand-picked from concentrate fines between 600 - 1000 μm for diamonds, from which FTIR samples were selected to cover the range of morphology, colour and resorption categories.

In most cases multiple spectra were taken for each xenolith diamond to assess variability. In contrast, only a single spectrum was obtained for each of the run-of-mine diamonds, generally with the IR transmission through the centre of the diamond. However, it is impossible to determine the exact path due to the beam refracting on the diamond surface, particularly as it is not a plate. It is important to note that many diamonds contained no or very low FTIR detectable nitrogen. In such cases, these Type II or near Type II diamonds contain no spectral information except for the lack of nitrogen concentration.

16.3 METHODOLOGY

The use of fourier transform infra-red (FTIR) microspectroscopy is twofold. Firstly, to define diamond populations based on their spectra and to correlate this with the different diamond parageneses; in particular, to attempt to define the peridotitic and eclogitic diamonds. And secondly, to provide time-temperature information which will constrain the diamond's origin, which can then be compared to independently determined results from radiogenic and geothermometry studies. Each individual diamond is assigned an average concentration to avoid any bias from the different number of spectra obtained for each specimen. In some cases, however, this may not

be appropriate (see discussion later) and therefore the range is that of all individual analyses. The diamondiferous xenoliths of this study provide the first comprehensive suite from a single location on which independent analyses can provide a comparison between geothermobarometry, FTIR spectra, and radiogenic isotope results from a single xenolith specimen.

FTIR time-temperature constraints based on nitrogen kinetics require that one of the two variables are fixed. For this study independent information is available to reliably bound the values for both time and temperature: Re-Os radiogenic isotopes on the diamond-bearing xenoliths constrain the age (Chapter 8 and 13) while geothermobarometry constrains the ambient temperature (Chapter 6 and 11). Therefore, ages can be fixed to obtain accurate time-averaged mantle residence temperatures, or alternatively, the ambient temperatures can be used as a proxy for the time-averaged mantle residence temperatures to obtain formation ages of the diamond. There are, however, inherent problems if, as is very likely, temperature and possibly pressure have varied with time. Furthermore, the diamond may not have a homogeneous nitrogen concentration and aggregation state. Nevertheless, FTIR can yield relevant geological constraints.

Nitrogen aggregation is a function of temperature (and possibly pressure), nitrogen concentration and mantle residence time; as such it is convenient to plot graphs of nitrogen concentration versus %N as B aggregation state, with overlying isotherms or isochrons (depending on which variable is fixed). This graphically highlights possible geological time-temperature constraints as well as identifying any diamond sub-populations.

16.4 FTIR Results

Examples of spectra obtained for Newlands diamonds are shown in Figure 16.2, whilst spectra and numeric processing results for each diamond are shown in Appendix III.

16.4.1 Nitrogen Content

The diamonds from Newlands have FTIR nitrogen concentrations ranging from undetectable up to a maximum of 3600 at. ppm (Figures 16.3 and 16.5). A noticeable percentage of diamonds contain very little or no nitrogen (termed Type II or near Type II diamonds) - all of which are either H-type or of unknown paragenesis. In contrast, every E- and L- type diamond contains substantial nitrogen. Therefore, any specimen from Newlands that is a Type II or near Type II diamond should invariably be of harzburgitic genesis.

Of the 102 diamonds analysed from xenoliths only one from each of H- and E- type overlap (diamond A of harzburgite A, and diamond C of eclogite AHM K12, respectively). This is a statistically very small number, but it does show that the diamond parageneses cannot be entirely separated on the basis of nitrogen concentration alone. Three spectra from this H-type diamond have nitrogen concentrations that are all extreme outliers (Figure 16.3). On the other side, the E-type diamond is within the acceptable range from the median, but, nevertheless, is the only E-type diamond with nitrogen concentrations lower than 600 at. ppm. These two diamonds are intriguing, particularly the H-type diamond, which has a nitrogen concentration a factor of two greater than any other H-type diamond. There is no apparent geological reason to exclude either diamond from the data set, yet they are statistically different from other diamonds of their type. The diamonds do not display any distinctive morphologic features, and the xenoliths from which they are derived are geochemically and petrographically similar to the others of the same diamond paragenesis. If, however, these two diamonds are removed then there is a clear distinction between E- and H- type diamonds: the maximum nitrogen concentration of harzburgitic diamonds is 595 at. ppm whilst the minimum for eclogitic diamonds is greater than 600 at. ppm.

It is particularly noteworthy that the 4 L-group diamonds have nitrogen concentrations spanning this boundary, namely 500 to 900 at. ppm. (Figure 16.3). As a result, diamonds with concentrations in this range cannot be accurately classified. The run-of-mine diamonds show the complete range of concentrations, with the majority overlapping the eclogitic range. Of the approximately 200 diamonds of

unknown paragenesis over two-thirds fall into the eclogitic nitrogen concentration field.

The variation of nitrogen concentration within a single diamond can be up to several hundred at. ppm, whilst the range for a single xenolith can span that of the entire diamond type. As examples, harzburgite AHM D2 contains 3 diamonds: diamond A has a calculated range from 295 to 595 at. ppm, diamond B, 41 to 113 at. ppm, and diamond C, 52 to 352 at. ppm; whilst eclogite AHM K12 also has three diamonds: diamond A has a range of 658 to 980 at. ppm., diamond B, 730 to 1500 at. ppm., and diamond C, 314 to 435 at. ppm. (Note that diamond C is a twin, with distinctive concentrations for each). The largest absolute range shown by a single diamond is 1800 to 3600 at. ppm (sample AHM K14 diamond A), whilst that for diamonds from a single xenolith is 900 to 3600 at. ppm (sample AHM K14).

Multiple spectra of whole diamond crystals from xenolith diamonds commonly yield a N concentration range of less than 100 at. ppm. It is therefore difficult to assess if this represents true variation given the errors involved in establishing %B and μP from IR spectra. Some diamonds, such as those described above, display larger N concentration variations, indicative of nitrogen heterogeneity within the diamond. Nevertheless, it is assumed that a single spectra for each run-of-mine diamond (which were generally whole crystals) is precise, and that any imprecision is not statistically significant as the data-set is large.

16.4.2 Nitrogen Aggregation

The diamonds from all three parageneses that contain detectable levels of nitrogen, without exception, have low aggregation IaAB spectra - from almost pure Type IaA to levels of up to 20% B aggregates. Spectra of the diamonds, indicative of the nitrogen aggregation state at Newlands, are shown in Figure 16.2 whilst the spectra for every diamond are shown in Appendix III. The majority yield less than 12% aggregation, easily observable in the spectra as the 1214 cm^{-1} peak exceeds 1174 cm^{-1} peak. This is unlike many other studies that generally show a spread in the aggregation state, for example George Creek (Chinn, 1995), Mir (Taylor et al., 1995a), Udachnaya

(Richardson and Harris, 1997), Copeton (Meyer et al., 1997), Point Lake (Taylor et al., 1995b) or Chinese (Meyer et al., 1994) diamonds. Individual diamonds from Newlands display ranges of up to 5-6% (absolute) variation in aggregation state. These variations, however, are not large, particularly when compared with maximum estimated errors of 2-3% (absolute). There is no discernible difference between the range of aggregation states of the various diamond groups. L-type diamonds potentially yield the highest aggregation state, however, the sample set is only of 4 specimens and consequently such a conclusion is not firmly established.

16.4.3 Platelet Development

Small platelet peaks are visible in a majority of the spectra that have IR detectable nitrogen. However, a noticeable proportion (~20 %) of both H- and E- type and run-of-mine diamonds display no evidence of platelet formation even though they have equivalent nitrogen concentrations and aggregation states compared to those that do (Figure 16.4). Diamonds from other localities occasionally display similar characteristics, for example Sloan or Chinese diamonds (Meyer et al., 1994; Milledge, pers. com., 1997). The platelet peak position for all diamonds occur at high wave-numbers, ranging from 1361-1378 cm^{-1}. Platelet peak position has been related to platelet size, the smallest platelets corresponding to the highest wave-numbers (Hanley et al., 1977; Clackson et al., 1989). A few spectra have very weak peaks in excess of 1380 cm^{-1}, clustering around 1384 cm^{-1} and forming a distinctive grouping (Figure 16.4). This may not be an extension to smaller platelets but more likely, instead, correspond with a very strong B-N absorption peak.

There is a noticeable difference in the platelet peak position for the H- and E- type diamonds (Figures 16.4, 16.5). Other studies indicate that platelet peak position is related to nitrogen concentration (Chinn, 1995; Chinn et al., 1995; Meyer et al., 1997) and this relationship is also observed for Newlands diamonds, albeit with some scatter (Figure 16.4). Thus, the difference in platelet peak position for H- and E- type diamonds is a function of nitrogen concentration. Whilst it is possible to numerically define the linear relationship between platelet peak position and nitrogen concentration it will only apply at Newlands as the minimum platelet peak position observed is 1361 cm^{-1}, which is likely to be different at other locations.

H-type diamonds have a platelet peak inter-quartile range of 1363 to 1367 cm^{-1}, whereas it is noticeable that E-type diamonds have significantly higher values of 1371 to 1374 cm^{-1}. L-type diamonds fall in between, with values of 1369 to 1373 cm^{-1}. As for nitrogen concentrations, the same two diamonds are statistical outliers with respect to platelet peak position: diamond A of harzburgite A is the only H-type diamond above 1369 cm^{-1} - up to 1374 cm^{-1} - whilst diamond C of eclogite AHM K12 is the only E-type diamond with values below 1368 cm^{-1} - down to 1364 cm^{-1}. If these two specimens are removed then a clear boundary exists between H- and E- group diamonds at 1369 cm^{-1} (Figure 16.4). A significant proportion of H- and E- type diamonds do not display any signs of platelet growth and thus, their paragenesis cannot be distinguished on this basis. It is unknown whether the specimens that have no observed platelet peak never developed one or if the peak was degraded, as HP/HT experiments indicate is possible (Cooper, 1990; Evans et al., 1995). Certain specimens, for example AHM K7, contain some diamonds with platelet peaks and others without. Therefore, it seems unlikely that the platelet peak was degraded as all diamonds from AHM K7 have similar nitrogen concentrations and aggregation states and thus any local thermal perturbation would have affected all the diamonds within the xenolith.

16.4.4 Hydrogen content

A noticeable proportion of the diamonds from H-, L-, and E- groups show the presence of a weak hydrogen peak at 3107 cm^{-1} (Woods and Collins, 1983). In only a few specimens is the hydrogen content sufficient that the subsidiary peak at 1405 cm^{-1} is noticeable. Specimens with the strongest hydrogen peak are of cubic morphology, a relationship noted in diamonds from Kazakhstan (Taylor et al., 1995). The cubic diamonds are E-type or of unknown paragenesis at Newlands. Two visual relationships seem apparent:

(i) diamonds with no IR detectable nitrogen have no IR detectable hydrogen; and

(ii) diamonds with no platelet peak have no IR detectable hydrogen.

There are also two positive relationships, neither of which are very strong, between μ3107 and μ1365, and nitrogen concentration.

16.4.5 Deformation

Absorption at 2443 cm^{-1} (above the intrinsic lattice absorption) is believed to be the result of 'extreme' deformation of diamonds (Chinn, 1995). No such spectral peaks were observed in the diamonds from Newlands, however, it is still plausible that lesser degrees of deformation have occurred. Only a few diamonds show any indication of deformation; both diamond A from harzburgite A and diamond A from harzburgite AHM D2 display birefringence patterns indicative of strain. They also contain the highest concentrations of nitrogen for any of the H-type diamonds. It has been suggested that Type II or near Type II diamonds are normally always deformed and this is related to the absence of platelets which may accommodate some of the strain inflicted on a diamond (Harris et al., 1970; Evans, 1992). However, this does not appear to be true for Newlands.

16.4.6 Diamond Formation Time-Temperature Constraints

Re-Os isotope studies of diamondiferous xenoliths from Newlands yield Archæan model and isochron ages: diamond-bearing (P-type) garnet macrocrysts yield model ages ranging from 2.0 to 3.2 Ga, whilst diamond-bearing eclogites (E-type) yield an isochron age of 3.56 ± 0.6 Ga. Due to the old age of the xenoliths, the temperature constraints are relatively robust. In contrast, small fluctuations in temperatures can cause significant changes in age estimates. The accuracy of current geothermometers applied to mantle rocks is normally 30 to 50 °C, and thus, nitrogen aggregation ages are only diagnostic on a geologic time scale. Geothermometry on xenolith minerals has constrained ambient temperatures to between 900 and 1100 °C for both diamond-bearing peridotitic garnet macrocrysts and eclogites. These are ambient temperatures and are used as proxies for the time-averaged mantle residence temperature required to calculate nitrogen aggregation ages. Therefore, any age is only meaningful if it can be assumed that the ambient mantle storage temperature did not rise or fall significantly to alter the nitrogen aggregation rate throughout the diamonds residence

in the mantle. If the diamond formation temperature and thus time-averaged temperature is significantly greater than the ambient xenolith temperature, as has been postulated (for example Griffin et al., 1992; Bulanova, 1995; Chinn et al., 1995), then the determined age is a maximum. The effect of N zonation within diamonds (which is documented for some diamonds in this study as well as at other locations (Bulanova, 1995; Trautman et al., 1997; Chinn et al., 1998)) is not considered.

16.4.6.1 Harzburgitic diamonds: FTIR time averaged temperatures

Applying the harzburgitic and lherzolitic age constraints above, H- and L- type diamonds are restricted to temperatures predominantly greater than 1100 °C with a maximum of 1160 °C (Figure 16.6), distinctively higher than the eclogitic diamonds. There is a noticeable scatter displayed by diamonds with nitrogen concentrations less than 150 ppm (log 150 = 2.2). At these levels the IR spectra are close to detection limits and thus errors are accentuated due to the extremely small and fragmented nature of the diamonds resulting in greater scatter in the data. Consequently, the errors in determining the % B nitrogen aggregation state are larger, commonly on the order or 1-2 % (absolute). The relationship between % B aggregation and %N as B indicates that the greatest source for errors occur at low aggregation states, namely less than 20% B aggregation. For example, if a sample has a B aggregation level of 4 ± 1 %, converting this to % N as B gives a range of 10 % (for %B = 3) to 20 % (for %B = 5). Such a range of % N as B will explain the scatter at low nitrogen concentrations. Also, at low nitrogen aggregation states any error has a far greater effect in determining %N as B than at higher levels. However, it is still apparent that nitrogen aggregation does not exceed 20%, which, combined with weak spectra, may explain the large scatter observed in the data for H-type diamonds. If the low N concentration data is ignored due to its inaccuracy, then the maximum temperature becomes 1120 °C. Because of the low nitrogen concentration and aggregation state of H-type diamonds the precision of nitrogen aggregation (and thus time-temperature) is not as reliable due to the weak spectra which are susceptible to baseline adjustments automatically made during acquisition and processing.

16.4.6.2 Eclogitic diamonds: FTIR time averaged temperatures

Applying the eclogitic age constraints above, eclogitic diamonds are restricted to between a minimum temperature isotherm of 1060 °C and a clearly defined maximum of 1100 °C (Figure 16.7). If the age is changed to the isochron's error limits (2.96 or 4.16 Ga) then the minimum and maximum temperatures change by only 10 °C up or down respectively, insignificant for upper mantle geothermobarometry. The range of eclogitic temperatures is unusually limited compared to diamond suites from other locations that often yield a range of nitrogen aggregation characteristics and thus temperatures (Taylor et al., 1995a, 1995b, 1995c; Milledge et al., 1995). Independent of which Archæan age is used, the eclogitic diamond suites show a temperature range of 40 to 60 °C. Whilst in the broader picture of upper mantle geothermobarometry this represents a tight temperature constraint, the data display a noticeable scatter for FTIR calculations. Several possibilities exist to explain this observed scatter:

(i) the error of determining %N as B,

(ii) the transmission of the IR beam averaging different nitrogen aggregation states of at least two diamond growth zones, or

(iii) a depth profile (and thus different temperatures) for the various diamonds within the mantle.

The first possibility may explain some of the scatter, particularly since the diamonds are of such low aggregation and any error will be compounded. A small error in the determination of %B aggregation has a far greater change in %N as B for low aggregation levels than for high levels. For eclogitic samples, however, the nitrogen concentrations are such that the nitrogen aggregation state can be determined precisely and it is unlikely that this is the cause of all the scatter.

If only the spectra from whole diamonds are plotted then the scatter is partially removed and a majority plot between the 1080 and 1100 °C isotherm, with sample AHM K12 diamond C the only exception (Figure 16.7). In contrast, broken diamond specimens record temperatures down to 1060 °C. This can be explained if there are two (or more) diamond growth zones, with each infra-red transmission passing through differing percentages of each. Therefore, if spectra are taken through the

centre of diamonds, and assuming concentric growth and a constant or decreasing temperature after diamond formation, then whole diamonds would represent the maximum transmission percentage of the first diamond growth stage and thus record the maximum time-average mantle residence temperature. In contrast, the diamond fragments represent various ratios of the two growth zones recording lower temperatures. Detailed studies of zoned diamond plates often show a decrease in temperature from core to rim growth zones (Udachnaya and Mir plates: Bulanova, 1995). However, assuming at least two growth zones, the maximum temperature recorded will be lower than the actual core formation temperature due to the diluting affect of the IR transmission passing through an unknown percentage of the cooler outer growth zones. Such a process is possible at Newlands with CL images of eclogitic diamonds displaying complex patterns and indicating more than one period of diamond growth. However, it is not possible to determine the time difference between the growth zones, and thus FTIR results represent an average.

The third possibility is that the temperature differences represent real physical differences between the various diamonds and, by inference, the relative depths of their host xenoliths. However, the calculated temperatures observed in diamonds from a single xenolith, namely, AHM K8, AHM K12, and AHM K14, span the entire eclogitic temperature range. Therefore, whilst it is possible that the xenoliths were sampled at various depths from the upper mantle, a temperature depth profile cannot explain the observations in all cases. Furthermore, the data do not yield results that are precise and accurate enough to determine a depth profile.

16.4.6.3 Run-of-mine diamonds: FTIR time averaged temperatures

The run-of-mine diamonds show a distinct grouping (at a fixed age of 3.56 Ga) around the 1100 °C isotherm, but scatter to the higher temperatures. This supports the above hypothesis in that the diamonds are whole specimens (with good quality spectra) and do not range to the lower temperatures observed in the E-type fragments.

16.4.6.4 Harzburgitic diamonds: FTIR ages

If the harzburgitic xenoliths had experienced temperatures in the 900 to 1100 °C range throughout their history then to achieve the level of nitrogen aggregation observed the H-type diamonds must be older than the Earth. Two possibilities exist to explain this obvious paradox: either the xenoliths have experienced higher temperatures than those just prior to entrainment in the kimberlite, or, alternatively, the diamonds experienced some form of stress or strain, which is believed to lower nitrogen activation energies and thus increase the aggregation rate (Evans, 1992). In reality, it is likely that both possibilities have played a role.

Applying the various time-averaged temperature isochrons reveals that the diamonds must have resided in the upper mantle at temperatures greater 1150 °C over the billion year time period, or in excess of 1200 °C over hundreds of millions of years, or greater than 1250 °C for millions of years. Higher temperatures result in even younger required ages, with a temperature in excess of 1350 °C required for diamond ages to be tens of thousands of years, as argued for some Siberian peridotitic diamonds (Shimizu and Sobolev, 1995; Shimizu et al., 1997). If the Archæan xenolith ages are representative of the diamond formation event, then the calculated time-averaged residence temperatures are 50 to 100 °C greater than some of the current ambient temperatures. This temperature is a time integrated determination and thus the temperature of diamond formation was likely to be even higher.

16.4.6.5 Eclogitic Diamonds: FTIR ages

Ambient temperatures for the diamond-bearing eclogitic xenoliths also range from 900 to 1100 °C, depending on the geothermobarometer applied. Even so, such low temperatures correspond to Archæan age isochrons. The same scenario applies as for H-type diamonds described above. If the Archæan xenolith ages are representative of the diamond formation event, then the calculated time-averaged residence temperatures are 50 to 100 °C greater than some of the current ambient temperatures.

16.4.6.6 Run-of-mine Diamonds: FTIR ages

As is expected, run-of-mine diamonds overlap both H- and E- type diamond fields (Figure 16.7).

16.5 DISCUSSION

The diamonds from Newlands display a range of Nitrogen concentrations, with a distinctive separation between H- and E- type diamonds. The vast majority of H-type diamonds have nitrogen concentrations less than 100 at. ppm., many with no FTIR detectable nitrogen. Furthermore, they are only associated with the H-type diamonds at Newlands. This is very unusual, as Type II diamonds are rare in nature. Furthermore, at other localities an association between eclogitic diamond sources and Type II diamonds has been observed (Milledge et al., 1983; Gurney, 1989) and potentially large Type II diamonds from Premier and Letseng (J.J. Gurney, pers com., 1998), although most of the diamonds are commonly of unknown paragenesis. However, this is clearly not the case at Newlands. In contrast to the H-type diamonds, E-type diamonds contain significant concentrations of nitrogen.

It should be noted that the nitrogen concentration is an average; different growth areas of a single diamond crystal may exhibit spectral characteristics representing different aggregation states, even containing both Type I and II zones (Berman, 1965; Evans 1976; Hanley et al., 1977). Detailed studies of diamonds from Udachnaya (Bulanova, 1995), George Creek (Chinn et al., 1998), Yakutia (Trautman et al., 1997), and Australia (Trautman et al., 1997) have shown that nitrogen concentrations can vary by three orders of magnitude over the distance of ~10-20 μm. However, detailed FTIR studies on plates were not conducted, even though some Newlands eclogitic diamonds display multiple growth zones. Nevertheless, variations of nitrogen concentrations within individual diamonds at Newlands are consistent with these observations, albeit on at a lower order of magnitude.

Combining nitrogen concentration and platelet peak position allows classification of the vast majority of diamonds of unknown paragenesis into either E- or H- type.

Based on these two variables a statistical program was able to correctly classify the vast majority of unknown samples. Only a small percentage of diamonds cannot be classified in the narrow range where L-type diamonds overlaps both the E- and H-type parageneses. The sample set of L-type diamonds analysed is small (only 5 diamonds) and there appear to be no distinctive FTIR signatures to separate them from either E- or H- type diamonds.

The positive relationship between platelet peak position and nitrogen concentration appears to be uni-directional; that is, high platelet peak position implies a high nitrogen concentration, but the reverse need not apply. It is possible to have high nitrogen concentrations but no platelet development (Figure 16.5), as observed for up to 20 % of E-type or run-of-mine diamonds at Newlands. Consequently, an "ideal" relationship exists between nitrogen concentration and platelet absorbance, but other factors affect the development (or regression?) of platelets. One of these factors is likely to be temperature. A negative relationship, though not strong, exists between platelet peak position and temperature.

Eclogitic xenolith AHM K8 displays distinctive major and trace element geochemistry relative to all the other diamond-bearing xenoliths. However, the diamonds contained within eclogite AHM K8 do not display any characteristics different from the other diamond-bearing eclogites. This implies that the eclogitic diamonds in sample AHM K8 are from the same source and time-temperature constraints as the other eclogitic diamonds.

16.5.2 Plastic deformation

It is uncertain what effect deformation has on nitrogen aggregation and ultimately time-temperature calculations. Experimental work subjecting diamonds to radiation damage show that the aggregation process is enhanced whilst platelets are destroyed (Evans, 1992). Aggregation from Type Ib to IaA was enhanced by a factor of 50 after 6 MeV electron irradiation (H.J. Milledge, pers. com.). However, it is uncertain as to the effect natural geologic stress and strain on a diamond has on nitrogen kinetics, but it seems likely that the aggregation process is enhanced (H.J. Milledge, pers. com). Recent experiments have shown that plastic deformation of diamond commences at

~900 °C (H.J. Milledge, pers. com). Therefore, any diamonds showing evidence of being subjected to stress or strain (see chapter 5) may have higher aggregation states than otherwise anticipated, and thus yield *maximum* temperature and *minimum* time constraints. The activation energy used in time-temperature calculations is assumed to remain constant (i.e. no stress or strain) for the whole diamond throughout its history, which may be billions of years. Consequently, the longer the mantle residence time of the diamond the less likely this assumption is to hold.

Harris et al. (1983) noted a strong correlation between plastic deformation features and the brown colouration of southern African diamonds. In contrast, the brown colouration of diamonds from George Creek (Colorado) was associated with the presence of CO_2 -bearing diamond (Chinn, 1995). The Newlands diamonds show no evidence of CO_2 IR peaks at 2376 and 650 cm^{-1} (Schrauder and Navon, 1993; Chinn, 1995), but brown or yellow/brown diamonds are commonly present - van Heerden and Gurney (1994) determined that 53-56 % of diamonds are brown or grey. However, the brown diamonds are predominantly a very pale brown or amber colour and not the deep and darker brown observed by Harris et al. (1993). There appears to be no evidence in the FTIR spectra to suggest that the brown/pale brown diamonds of Newlands have suffered deformation resulting in increased nitrogen aggregation states or platelet development.

Diamond A of harzburgite AHM D2 ranges from 300 to 600 at. ppm, whilst many of the H-type diamonds are Type II or near-Type II. This diamond also displays evidence of strain patterns under birefringence, however, it is not possible to assess whether the variation is due to different growth zones or strain on the diamond, or both. Other diamonds also show some evidence from cathodoluminescence and birefringence of multiple growth zones and/or having experienced some form of deformation (Chapter 15). If this is the case, the effect on nitrogen aggregation appears to be minimal.

16.5.3 Diamond FTIR time-temperature constraints

In general, low N aggregation states (<20%), such as those displayed by Newlands diamonds, are indicative of either existence in the cool portion of the mantle keel or of an extremely young diamond. The low aggregation state of the diamonds can be achieved by two means:

(i) the diamonds are very young and thus aggregation did not proceed far before the process was quenched by eruption of the host kimberlite, or

(ii) the diamonds resided in a thermally stable portion of the mantle at low temperatures for an extended period of time.

A heating event such as transportation in a kimberlite magma over a period of hours or days (commonly regarded as the time frame of kimberlite eruption (Mitchell, 1986, 1995)) will have no effect on nitrogen aggregation (Taylor et al., 1990). However, in the mantle, a heating pulse is not a short-lived event and any thermal perturbation will increase the nitrogen aggregation rate in the diamond. Even if the diamonds had an age of 3.2 Ga, aggregation would be less than 20% for a nitrogen concentration of 1500 atomic ppm at temperatures of less than 1100 °C.

If the diamonds are young then it would be expected that the temperature of formation to be similar to the ambient temperature. Therefore, geothermometry on the xenoliths would yield temperatures similar to diamond formation. For both E- and H- type diamonds the xenoliths have temperatures ranging from 900 to 1100 °C. The minimum age, given by the maximum temperature (in this case 1100 °C) is on the order of billion of years. This is a contradiction of the initial assumption of the diamonds being young. In addition, if the diamond formation temperatures were higher, for example 1350 °C (required to achieve the level of nitrogen aggregation on a time-scale of 100,000 years) then the xenoliths would then have to cool ~300 °C to less than 1050 °C in approximately 100 000 years and totally re-equilibrate before transportation to the Earth's surface in the kimberlite. Furthermore, a temperature greater than 1350 °C corresponds to a depth well in excess of 250 km on a 37 - 38 mW/m^2 cratonic geotherm considered representative at Newlands (Chapter 6). This temperature or depth is considered unlikely at Newlands as it is greater than for any

observed xenolith where geothermobarometry limits the maximum depth to which the Newlands kimberlite sampled the mantle to ~200 km or ~1200 °C. This applies, in particular, to diamond-bearing xenoliths and is consistent with theories that Group II kimberlites, like Newlands, originate from shallower depths than Group I kimberlites (Mitchell, 1995). Consequently such a young age and high temperature of formation is considered to be unreasonable and therefore none of the peridotitic diamonds at Newlands are of the young age reported by Shimizu and co-workers (Shimizu and Sobolev, 1995; Shimizu et al., 1997).

If, on the other hand, the xenoliths resided in a stable portion of the mantle then the ambient temperatures would be representative of diamond formation temperatures, and thus the minimum age is on the billion of year time-scale.

An Archæan age for H- and E- type diamonds corresponds to a time-average temperature of greater than 1100 °C. As the ambient temperatures for diamond-bearing xenoliths are commonly less than 1050 °C, and down to 900 °C, the xenoliths their diamonds have experienced cooling on the order of at least 100 °C since diamond formation in the Archæan to kimberlite eruption (at 114 Ma: Smith et al., 1985). This magnitude of mantle cooling is in agreement with the results of studies on inclusions in diamonds from the Kaapvaal and Siberian cratons (Gurney, 1989; Griffin et al., 1992, 1993; Navon, 1999).

The possibility of being able to correctly classify diamonds based on their spectra could prove invaluable, particularly in the study of inclusions in diamonds. Individual sulphide inclusions (for example, Pearson et al., 1999) are studied for constraining diamonds ages and mantle events. However, there are problems in assigning the diamond to the correct paragenesis without independent information as sulphides occur in both peridotitic and eclogitic parageneses. At Newlands the non-destructive technique of FTIR spectroscopy will allow the study of a greater range of inclusions with defined diamond parageneses.

GENERAL DISCUSSION 17

17.1 INTRODUCTION

Diamond formation and the relationship with the upper mantle has been studied in depth over the last three decades (see Chapter 1 for a general discussion). Even so, much of the petrological, geochemical, and geochronological data for the upper mantle can not be adequately explained by current hypotheses. Accordingly many questions remain unanswered, some of which are very controversial, particularly as views change as more data becomes available. Amongst these questions is the fundamental broad topic: *what is (are) the origin(s) of diamonds?* The recent papers of Navon (1999) and Helmstaedt and Harrap (1999), presented at the 7th International Kimberlite Conference, summarised the current status of knowledge relating to diamond formation and their host rocks in the SCLM. The following discussion will attempt to supplement these broad discussions, and integrate the results of the diamond-bearing xenoliths from Newlands investigated in this study.

The assessment of any hypothesis linking the formation of diamonds and their host rock is critically dependent on constraining what the sample represents in both time and space. Given that the majority of known kimberlites in southern Africa erupted in the Tertiary or Cretaceous, including Newlands, there is a substantial geological period of the Earth's history in which the diamonds may have formed. A generalised model for the origin of diamonds and their associated host rocks at Newlands is complex due to the broad scale investigation of this study. Nevertheless, certain constraints point to preferred models and an attempt has been made to collate all the data in this thesis into a realistic geological history for the diamond-bearing xenoliths beneath Newlands. Therefore, the following sections summarise the key observations of the diamond-bearing samples from Newlands, incorporating mineralogy, major and trace element compositions of key mineral phases, P-T constraints, ages of formation, and

diamond characteristics. After which a generalised discussion of current hypotheses as to the origin of diamond-bearing peridotities and eclogites will ensue.

17.2 SUMMARY OF DIAMOND-BEARING GARNET MACROCRYSTS FROM NEWLANDS

To date, studies have revealed that the vast majority of diamonds are associated with peridotites and eclogites. Ignoring the apparently relatively small percentage of diamonds of unknown affinity, the primary mineralogy and geochemistry of the diamond source region has been well-documented (see Chapter 1 for a summary). Nevertheless, the diamond-bearing peridotitic garnet macrocrysts from Newlands, whilst consistent with the broad observations of past studies, yield some new results.

17.2.1 Peridotitic Compositions associated with diamonds

The Newlands diamond-bearing garnet macrocrysts display a wide range of mineral compositions. Garnet compositions indicate affinities to both harzburgitic and lherzolitic peridotites, although no clinopyroxene was observed in hand specimen or petrographically in any xenolith. The majority are harzburgitic in nature – that is, they have highly depleted (highly magnesian) compositions for all the major minerals present (garnet, chromite, olivine). Specifically, the garnets are high-Cr, extremely sub-calcic, strongly depleted (usually) in Ti, Zr, Y and Ga, but enriched with incompatible elements Sr and LREEs. In addition, they display an unusual sinusoidal LREE enriched pattern. The chromites are high-Cr and low-Ti, whilst the olivine is highly refractory. These garnet, chromite and olivine signatures are similar to those observed in the majority of peridotitic diamond inclusions and diamond-bearing peridotities, and a relatively small percentage of peridotitic xenoliths (for example, Shimuzu, 1975; Richardson et al., 1984; Shimizu and Richardson, 1987; Griffin et al., 1992; Stachel et al., 1998, 1999). The solitary "pristine" garnet diamond inclusion has the most sub-calcic composition observed at Newlands. Moreover, it is significantly lower in calcium than the garnet from the host xenolith (which is nevertheless still extremely sub-calcic). Similar differences were found at Finsch (Gurney et al., 1979; Shee et al., 1982; Viljoen et al., 1992) and Udachnaya kimberlites (Sobolev et al., 1984; Pokhilenko and Sobolev, 1986), where garnet

diamond inclusions extended to more sub-calcic compositions than either the diamond-bearing peridotites or concentrate garnets.

A small percentage of the diamond-bearing garnet macrocrysts at Newlands are, however, calcium saturated in nature. Specifically, three samples have high-Cr calcic garnet compositions, two of which are the highest Cr-Ca compositions observed at Newlands. Whilst calcium saturated garnets diamond inclusions or diamond-bearing peridotites are known from around the world (see discussion in chapter 1), the compositions of these three specimens from Newlands have not been observed previously in either inclusions in diamonds or diamond-bearing peridotites. The compositions of calcium saturated garnets are a function of pressure, temperature and the whole rock bulk chemistry (Sobolev, 1977; Gurney, 1984; Boyd et al., 1993; Gurney et al., 1993; Gurney and Zweistra, 1995). The boundary line (as derived by Gurney (1984)) commonly used to define "*harzburgitic (G10)*" and "*lherzolitic (G9)*" garnets[17] approximates 45 kbar only (Gurney et al., 1993). Thus, it is possible for the diamond-bearing calcic garnet macrocrysts at Newlands (which plot on the lherzolitic (G9) side of the boundary line) to actually be of the harzburgitic paragenesis and genetically related to other sub-calcic diamond-bearing garnet macrocrysts from Newlands. Indeed, at Newlands major element geochemical trends for the diamond-bearing garnet macrocrysts and diamond-free garnet macrocrysts as well as empirical observation of garnet compositions in association with clinopyroxene indicate that this hypothesis is plausible (see section 4.8.1.1). However, as there are very few garnets at Newlands that have similar Cr-Ca characteristics, and with such a small data set, it is not possible to conclusively determine whether the calcic diamond-bearing garnet macrocrysts are associated with the sub-calcic harzburgitic diamond-bearing garnet macrocrysts or are a separate paragenesis at Newlands.

17.2.2 Ambient Physical Conditions

Geothermometry on the diamond-bearing garnet macrocrysts from Newlands yields temperatures ranging from 900 to 1050 °C. Assuming these xenoliths lie on a lower than normal cratonic geotherm of between 37-38 mW/m^2 – as indicated by diamond-

[17] This terminology is used in this study.

free multiphase xenoliths at Newlands and common for Group II kimberlites in Southern Africa of similar ages to Newlands – then these temperatures are consistent with pressures of 40 to 55 kbar (approximately 125 to 160 km depth). Such P-T conditions fall within the diamond stability field. The maximum temperature for any diamond-bearing garnet macrocryst is ~ 1050 °C, within error of the maximum temperature recorded at Newlands for any xenolith. Thus it is not possible to determine if this temperature is a maximum for the diamond-bearing garnet macrocrysts at Newlands or this was the point at which the Newlands kimberlite was able to entrain wall rocks on route to the surface.

17.2.3 Re-Os Isotopic Systematics

The diamond-bearing garnet macrocrysts from Newlands yield Re-Os model ages that clearly indicate they formed between the early Proterozoic and mid-Archæan . Furthermore, they display no age correlation with P-T conditions. These results are similar to peridotite xenoliths analysed from a variety of kimberlites across the Kaapvaal craton (Carlson et al., 1999). Combined with the study of Daniels et al. (1995), the Newlands garnet macrocrysts define a ε_{Nd}-γ_{Os} field that overlaps other Kaapvaal peridotite xenoliths (Pearson et al., 1995a). Unradiogenic initial Nd and Os are indicative of both ancient Re depletion and ancient LREE enrichment. However, no single-stage event involving melt depletion or melt addition can be reconciled with these processes (Shimizu and Richardson, 1987; Pearson et al., 1995a) and consequently they must be independent of each other.

17.2.4 Peridotitic Diamonds from Newlands

Based on FTIR results a significant proportion of harzburgitic diamonds are Type II or near Type II and any diamond found to contain little or no nitrogen at Newlands can be confidently ascribed to the harzburgitic paragenesis. Those peridotitic diamonds that do contain N are predominantly at concentrations less than 200 at. ppm. (with a maximum of 600 at. ppm.). The diamonds are low aggregation type IaAB – ranging from almost pure Type IaA to levels of up to 20% B aggregates.

It is particularly noteworthy that the few (possibly) lherzolitic diamonds yield nitrogen concentrations that fall into the "boundary zone" that separates the harzburgitic and eclogitic diamonds. However the lherzolitic diamond data set is too small to draw any definitive conclusions, yet the diamonds all have nitrogen concentrations at the limits of that observed in the larger harzburgitic diamond data set, leaving open the question of whether they may be a separate paragenesis or not.

The relatively low ambient temperatures determined for the diamond-bearing garnet macrocrysts combined with the diamond nitrogen concentrations and aggregation states of the peridotitic diamonds are consistent with diamond formation in the Archæan. Indeed, the lowest temperatures of ~ 900 °C yield calculated ages older than the Earth. This can be explained by two equally plausible possibilities. Firstly, if the calculated time-averaged residence temperatures for the diamonds was 50 to 100 °C greater than some of the current ambient temperatures, thus implying mantle cooling over the geological æons, then the data would be compatible. Alternatively, the diamonds may have experienced some type of strain event that led to increased nitrogen aggregation and the illusion of long mantle residence times. However, physical observations of the diamonds do not support the latter hypothesis.

Due to a lack of suitable diamond specimens in this study, it is not possible to determine how many, if indeed more than one, growth period(s) occurred for peridotitic diamonds.

17.2.5 Origin of Diamond-bearing Garnet Macrocrysts at Newlands

17.2.5.1 Origins of depleted harzburgites.

The origin of the highly depleted harzburgites and the diamonds associated with such rocks is controversial. There are currently two widely held opposing view points that have been presented over the past two decades as to the origin of highly depleted harzburgites: firstly the "*insitu melt residuum*" theory and the "*subducted metasomatised*" theory. These two models have received the most scientific discussion, yet they are by no means the only models. Indeed, models have also been proposed variously emphasising large-scale plume melting (Herzberg, 1993; Pearson

et al., 1995), and subducted/obducted oceanic lithosphere (Schulze, 1986; Helmstaedt and Schulze, 1989; de Wit et al., 1992) or island arcs (Rudnick et al., 1994).

Garnets and chromites of major element compositions such as those observed for the diamond-bearing peridotitic garnet macrocrysts at Newlands are associated with highly depleted harzburgites or dunites. Whole rock geochemistry of such peridotites from around the world (for example Carswell and Dawson, 1970; Maaloe and Aoki, 1977; Boyd, 1989; Boyd et al., 1997) revealed that they are depleted in incompatible major elements (such as Ca, Al and Fe) and enriched in compatible major elements (such as Mg and Cr) relative to a hypothetical primitive mantle composition (Ringwood, 1966; McDonough and Sun, 1995). This implies that these samples represent residues after significant melt extraction (O'Hara and Yoder, 1967; Boyd and Gurney, 1982; O'Hara et al., 1987; Boyd and Mertzman, 1987; Boyd, 1989). Comparison of the modal and chemical data of cratonic and modern oceanic peridotites indicated that they are genetically independent (Boyd, 1989; Boyd et al., 1993). Specifically, oceanic peridotites defined a trend of increasing Mg-number with modal olivine enrichment (known as the "*oceanic trend*"), whereas, in contrast, cratonic peridotites plot to the olivine poor (high Mg-number) side (Boyd, 1989; Boyd et al., 1993). Furthermore, their low modal olivine and high Fo-contents are not consistent with derivation from MORB residues; instead it was suggested that the cratonic peridotites represent high-pressure residues of Archæan komatiite formation (Boyd and Gurney, 1982; Richardson et al., 1984; Shimizu and Richardson, 1987; Boyd, 1989; Boyd et al., 1993).

However, such a model has difficulty explaining the high modal enstatite and the high chromium garnets (> 4 wt %). The partition coefficients for Cr/Al[18] between various peridotitic mineral phases and the melt are too low at the pressures and temperatures of komatiite extraction to account for the high-Cr content of the garnets (Bulatov et al., 1991; Canil and Wei, 1992; Stachel et al., 1998). For example, at P-T's expected for komatiite melt extraction, a garnet exsolving from an orthopyroxene with a Cr_2O_3/Al_2O_3 ratio of about 0.15 would have a ratio of about 0.075, equivalent to less than 2 wt% Cr_2O_3 (Stachel et al., 1998). Even though repeated melting would raise

[18] $D_{Cr/Al} = (Cr_2O_3/Al_2O_3)^{Mineral\ X} / (Cr_2O_3/Al_2O_3)^{Mineral\ Y}$

the Cr_2O_3/Al_2O_3 ratio it could not account for the high-Cr garnets commonly observed from the upper mantle. It is estimated that even after three stages of melt extraction the Cr_2O_3 concentration of garnet would not exceed 4 wt% (Bulatov et al., 1991; Canil and Wei, 1992; Stachel et al., 1998).

Therefore, to account for the high-Cr garnets, an alternative model was proposed where the melting occurred at lower pressures (i.e. within the spinel stability field, 5-20 kbar) (for example, Stachel et al., 1998, 1999). At such low pressures the Cr/Al partition coefficients are significantly higher and would yield residua with higher Cr contents and elevated Cr/Al ratios (Bulatov et al., 1991). Subsequent subduction into the garnet and diamond stability fields would generate high-Cr garnets. Further, metasomatic enrichment of silica after subduction would then cause enrichment of modal orthopyroxene to levels observed in cratonic peridotites and explain the relationship between Ni concentration and modal olivine (Ringwood, 1975; Kesson and Ringwood, 1989; Kelemen et al., 1992, 1998; Rudnick et al., 1994, 1995; Boyd and Canil, 1997).

17.2.5.2 The diamond formation event

All the models described above attempt to account for the harzburgites highly depleted nature. However, none account for the enrichment of some incompatible trace elements, in particular, elevated Sr and LREE concentrations (relative to the less depleted lherzolite) as observed for the diamond-bearing garnet macrocrysts at Newlands and in garnet diamond inclusions from other locations around the world. These signatures are regarded as relatively young events, not a primary feature of the garnet harzburgite formation. This, combined with petrographic evidence (for example, Harte, 1977), shows that the harzburgite (and the SCLM in general?), has undergone trace element enrichment and/or modal metasomatism prior to, or coeval with, diamond formation; however, the nature and timing of this event is uncertain.

The origin of the unusual chondrite normalised sinusoidal REE patterns has been attributed to (partial) re-equilibration during mantle metasomatism (for example, Shimizu and Richardson, 1987; Hoal et al., 1994; Stachel et al., 1998). Harte et al. (1982) suggested that the sinusoidal REE pattern observed in garnets could be

17.3 SUMMARY OF DIAMOND-BEARING ECLOGITES FROM NEWLANDS

17.3.1 Eclogitic compositions associated with diamonds

The diamond-bearing eclogites from Newlands yield garnet and clinopyroxene compositions that are relatively restricted compared to the extremely diverse range displayed by eclogitic diamond inclusions and diamond-bearing eclogites from around the world. For example, a study of 16 diamond-bearing eclogites from the Mir kimberlite yielded three distinct eclogitic groups with garnet CaO concentrations ranging from 2.65 to 13.64 wt% (Sobolev, 1983; Beard et al., 1996). In contrast, the diamond-bearing eclogites from Newlands have a garnet CaO concentration range of only 4.5 to 8 wt%, with the vast majority around ~5 wt%, similar to the low-Ca diamond-bearing eclogites from Mir (as defined by Beard et al., 1996) and eclogitic garnet inclusions from Jwaneng (for example Gurney et al., 1995; Richardson et al., 1998). In general, the samples from Newlands plot at the Fe-rich, Mg-depleted extremes, with major and trace element mineral chemistry equivalent to *Group I eclogites*, i.e., enriched garnet Na_2O and clinopyroxene K_2O concentrations (MacGregor and Carter, 1970; McCandless and Gurney, 1989) or *Group B eclogites*, i.e., enriched Na and Mg in clinopyroxene (Coleman et al., 1965; Shervais et al., 1988; Taylor and Neal, 1989; and Neal et al., 1990). Bulk rock major element compositions (calculated assuming a 50:50 garnet-clinopyroxene ratio) are compositionally similar to ancient (Proterozoic or Archæan?) magnesian basalts.

Furthermore, the geochemistry of the diamond-bearing eclogites at Newlands is distinct from the vast majority of of diamond-free eclogitic groups defined at Newlands. One of the four diamond-free eclogitic groups has a geochemistry that overlaps the diamond-bearing eclogites and are classified as Group I or Group B eclogites even though no diamonds were observed; the other three diamond-free eclogitic groups are classified as Group II or Group A eclogites. The Group I diamond-free eclogites are probably genetically related to diamond-bearing eclogites and the absence of diamonds is associated with their small sample size.

generated from the metasomatism of garnet lherzolite by a carbonititic fluid. This metasomatic event at Newlands is associated with the introduction of Zr, Y, Ga, Ti, LREE and MREE but very little HREE. Similar observations were determined at Udachnaya (Richardson et al., 1997), Akwatia (Stachel and Harris, 1997), and Roberts Victor (Stachel et al., 1998). In contrast, Burgess (1987) and Burgess and Harte (1998) suggest that it may arise as a result of extensive garnet fractionation from basic-ultrabasic melt, because of the extreme variation in garnet/melt distribution coeffiecents across the REE.

The relationship between this metasomatic event(s) and diamond formation(s) is unclear. There is an irrefutable relationship between the majority of high-Cr sub-calcic garnets (with sinusoidal REE patterns) and diamonds. The fundamental reason why the diamond formation event would preferentially select these garnets over the volumetrically dominant lherzolitic garnets the world over is unknown. Stachel and co-workers (Stachel and Harris, 1997; Stachel et al., 1998, 1999) propose that disequilibrium between multiple inclusions from single host diamonds support their interpretation that diamond formation was associated with this re-enrichment event. However, such a supposition may not be correct - it is probable that some inclusions in diamonds pre-date diamond formation and, furthermore, diamonds are known to grow in more than one process or phase, with an uncertain time period elapsing in between. Therefore, it does not hold that multiple inclusions in diamonds should be in equilibrium, nor represent the equilibrium conditions of one diamond growth phase.

The harzburgitic garnets have a sinusoidal REE pattern due to preferentially accepting the LREEs and MREEs over the HREEs. In contrast, the lherzolitic garnets have no such signature. Here the LREE elements would be preferentially incorporated into clinopyroxene. Hence, the more calcic garnets, assumed to be in equilibrium with clinopyroxene, trend towards a fertile garnet pattern with a HREE enriched plateau. Similar observations for diamond inclusion garnets from Mwadui (Tanzania) (Stachel et al., 1999) and Akwatia (Ghana) (Stachel and Harris, 1997), and diamond-bearing peridotites from Roberts Victor (South Africa) (Stachel et al., 1998) lends support for such a model.

17.3.2 Ambient Physical Conditions

The P-T ranges displayed by the eclogites are within the diamond stability field. Assuming that the diamond-bearing eclogites are lying on a geotherm (determined for Newlands to be 37-38 mW/m^2) then the P-T conditions range from 920 to 1080 °C at calculated geotherm dependant pressures of 42 to 58 kbar (approximately 130 to 170 km depth). The maximum temperature for the diamond-bearing eclogites is within error of the maximum temperature recorded at Newlands for any xenolith. As for diamond-bearing garnet macrocrysts, it is not possible to determine whether this temperature is a maximum for the diamond-bearing eclogites at Newlands or this was the point at which the Newlands kimberlite was able to entrain wall rocks on route to the surface.

17.3.3 Re-Os Isotopic Systematics

The diamond-bearing eclogites from Newlands yield Re-Os model ages and systematics that clearly indicate formation between the early Proterozoic and mid-Archæan. The scatter observed in the isochron prevents a precise age determination, although it is apparent that the Re-Os systematics yield ages similar to diamond-bearing eclogites from Udachnaya (Pearson et al, 1995c) and Group I eclogites from Roberts Victor (Shirey et al., 1998).

17.3.4 Eclogitic Diamonds from Newlands

Based on FTIR results, all of the eclogitic diamonds contain nitrogen (ranging from 500 to 3000 at. ppm.) and are thus classified as Type I diamonds - in contrast to the majority of harzburgitic diamonds at Newlands. Any diamond that has N concentrations over 600 at. ppm. at Newlands can be confidently ascribed to the eclogitic paragenesis. The diamonds are low aggregation type IaAB – ranging from almost pure Type IaA to levels of up to 20% B aggregates.

Ambient temperatures for diamond-bearing eclogites range from a minimum of 920 to a maximum of 1080 °C, depending on the geothermobarometer applied. Such

temperatures combined with the eclogitic diamond nitrogen concentrations and aggregation states are consistent with diamond formation in the Archæan. Conversely, using assumed Archæan ages, the nitrogen concentration and aggregation states of the eclogitic diamonds fall along an isotherm and define a narrow range of time-averaged temperatures of 1060 to 1080 °C. This indicates a similar origin and mantle storage for the eclogitic diamonds, consistent with their derivation from a solitary diamondiferous eclogitic unit, and implies the spread in ambient geothermobarometic calculations may be an artifact of the methodology. Whilst it is not possible to accurately state this temperature range (as FTIR isotherms are time dependant), the nitrogen aggregation state of the Newlands eclogitic diamonds is consistent with storage in the lithospheric mantle at temperatures of between 1050 - 1100 °C on a billion year time scale (as expected from Re-Os isotopic dating of the eclogite xenoliths). If they were stored at time-averaged temperatures lower than 1050 °C, such as most of the current ambient temperatures recorded just prior to capture in the kimberlite, then the calculated diamond ages would be older than the Earth. Therefore, it appears that the eclogitic unit in which the diamonds resided has cooled on the order of at least 100 °C since formation in the Archæan.

Cathodoluminescence indicates that the eclogitic diamonds have at least three major distinctive growth phases, punctuated by periods of diamond resorption.

17.3.5 Preliminary Stable Isotopic Results

Preliminary unpublished work has started on oxygen isotopes on garnet and clinopyroxene from Newlands eclogites at the University of Cape Town using laser fluorination and carbon isotopes on Newlands eclogitic diamonds at Queens University, Kingston, Canada. The oxygen isotopic composition of garnet and clinopyroxene range from 5.5 to 8 ‰, overlapping but extending to higher than mantle values (5.5‰: Kyser, 1991; Mattey et al., 1994). Of the three Newlands eclogitic diamonds analysed for carbon isotopic composition, one yields approximately -10 ‰ whilst the other two are similar to mantle carbon values of approximately -4 to -5 ‰ (Kirkley et al., 1991). These oxygen and carbon isotope signatures are indicative of material that has interacted within surfical environments,

1996). In particular, they are similar in composition to the "*low-Ca*" diamond-bearing eclogites from Siberia, which were equated to the volcanic sequence at the top of oceanic crust (Beard et al., 1996) that later experienced partial melting on the order of 15-30 % (in equilibrium with silicic melts such as tonalites and trondhjemites that formed the volumetrically Archæan dominant TTG granite suite) (Ireland et al., 1994; Rollinson, 1997). However, the relationship between eclogite, which is believed to account for a minor percentage of the SCLM, and the volumetrically dominant ancient TTG suite granites is tenuous.

The Newlands diamond-bearing eclogites Re and Os concentrations are similar to those from Roberts Victor (Shirey et al., 1998) but are significantly different from Udachnaya (Pearson et al., 1995). This opens up the possibility of different origins (genetic precursors?) for the diamond-bearing eclogite protoliths beneath these portions of Kaapvaal and Siberian cratons, respectively. However such a conclusion cannot be substantiated based on only three locations from two cratons. The majority of the samples from Newlands overlap the komatiite field in Re-Os concentration space but also extend into the fields for primitive ocean island basalt (OIB) and continental flood basalt (CFB) picrites, but not present day mid-ocean ridge basalts (MORB). Consequently, if the Newlands eclogitic protolith was formed in an Archæan ocean floor environment and accreted to the SCLM then it is likely that it represents komatiitic ocean ridge products or primitive portions of oceanic plateaus or islands.

The eclogitic diamond carbon source appears to also come from the subducted protolith, as potentially indicated by the sparse carbon isotopic analyses at Newlands, but supported by the wealth of eclogitic diamonds analysed from around the world, (for example, Javoy et al., 1986; Kirkley et al., 1991; Deines et al., 1991). However, the specific nature and origin of this carbon source within the subducted protolith is still uncertain.

Whilst the "*subduction*" model is favoured for the diamond-bearing eclogites at Newlands (and for most eclogites elsewhere around the world), it is not definitive of all the other diamond-free eclogites present at Newlands. The range of eclogites at Newlands is clearly not limited to those analysed in this study and at least four groups

for example the hydrothermal vent MORB proto-environment (McCandless and Gurney, 1997), although current data sets are small.

17.3.6 The Origin of Diamond-bearing Eclogites at Newlands

Eclogites are now known to occur over a diverse range of pressures and temperatures (that extends from the upper mantle and into the lower crust) and accordingly display a variety of textures and compositions. The origin of eclogites is controversial and there are currently two widely held opposing viewpoints: the "*subduction*" model and "*mantle derived cumulates and residua*" model. The "*subduction*" model is arguably the most popular hypothesis, and has gained wide-spread support over recent years, particularly as more stable isotope studies become available (for example, Helmstaedt and Doig, 1975; Jagoutz et al., 1984; MacGregor and Manton, 1986; Shervais et al., 1988; Schulze and Helmstaedt, 1988; Helmstaedt and Schulze, 1989; Taylor and Neal, 1989; Neal et al., 1990; Jacob et al., 1994, McCandless and Gurney, 1997).

The Re-Os systematics, major and trace element mineral chemistry, and stable isotopes (albeit preliminary) of the diamond-bearing eclogites from Newlands are consistent with a protolith that has interacted within surfical environments. Therefore, the subduction hypothesis is the favoured model for the origin of the diamond-bearing eclogites at Newlands. Whilst a definitive age for the eclogites is not possible, Re-Os systematics indicate formation in the mid- to late- Archæan. Accepting the subduction hypothesis for the origin of the eclogites and the diamonds, such an age implies the operation of plate tectonics since the early part of the Earths history, potentially only hundreds of millions of years after the crust formed, in contrast to arguments that advocate plate tectonics only started in the Proterozoic (e.g. Hamilton, 1998). It is likely that Archæan plate tectonics involved young, hot, small lithospheric plates with thicker mafic crust relative to modern plate tectonics (see Helmstaedt and Harrap (1999) and references therein.)

More specifically, the diamond-bearing eclogites from Newlands have major and trace element compositions that fall within those displayed by numerous diamond-bearing eclogites and eclogitic diamond inclusions from around the world (for example, Jerde et al., 1993; Snyder et al., 1993, 1995; Jacob et al., 1994; Beard et al.,

have been visually and geochemically defined, whilst kyanite and corundum eclogites are known to exist and probably represent other eclogitic groups. In addition, many of the diamond-free eclogites at Newlands have mineral chemistry that is consistent with Group A eclogites. Such eclogites are proposed to be mantle derived cumulates and residues (Snyder et al., 1997 and references therein). A similar proposal of multiple origins for eclogites has been put forward for the wealth of diverse eclogites studied from Yakutia, and even at one location (for example Mir and Udachnaya) by Taylor, Snyder and co-workers (Jerde et al., 1993; Snyder et al., 1993; Ireland et al., 1994; Snyder et al., 1995; Taylor et al., 1996; Snyder et al., 1997; Snyder et al., 1998). Further work on the diamond-free eclogites at Newlands is required to elucidate such a model.

17.4 General Discussion

17.4.1 The Mantle "Stratigraphy" beneath Newlands

How the various rock units, and in particular, the diamond-bearing layers, represented in the Newlands kimberlite mantle-derived xenolith suites are spatially and temporally related is uncertain, but certain logical constraints can be made. Assuming that it is possible to relatively position the various rock units beneath Newlands using geothermobarometry (see discussion below), then the mantle stratigraphy would look as follows. The harzburgitic rocks are the deepest xenolith suite and located within the diamond stability field, including the harzburgitic diamond-bearing garnet macrocrysts. The lherzolitic rocks extend to much lower P-T's that transgress the diamond-graphite boundary, but display a significant amount of overlap with the harzburgitic rocks. The eclogitic rocks occur at various levels throughout the upper mantle, notably some of which are in the diamond stability field, including the diamond-bearing eclogites. The relative position of other minor xenolith suites from Newlands (as identified in Chapter 2, but not analysed) is unknown. The solitary websterite analysed occurs well into the graphite stability field, however no conclusions can be drawn based on one sample.

Based on the absence of asthenospheric xenoliths it has been proposed that Group II kimberlites (such as Newlands) originate within the cratonic root or slightly above the lithosphere-asthenosphere boundary (Smith et al., 1985; Haggerty, 1986, 1991; Mitchell, 1995). Such an origin for Newlands could explain the maximum temperature of ~ 1100 °C for any xenolith and the (apparent) absence of high-T sheared peridotites. Accordingly, the maximum temperature of ~ 1100 °C would not represent the true upper extent of either diamond-bearing peridotite or eclogite. Furthermore, whilst geothermobarometry on Newlands xenoliths is consistent with a shallow kimberlite origin, it does not disprove the possibility of a deeper origin.

17.4.1.1 Problems with geothermobarometry

It seems prudent here to mention the views of Helmstaedt and Harrap (1999) that caution against the use of geothermobarometry to determine a mantle stratigraphy. It is often assumed that two xenoliths of different paragenesis cannot occur in the same P-T space. This premise is based on the assumption that mineral equilibra were not frozen prior to kimberlite emplacement, and rocks with different P-T histories could have been structurally juxtaposed without re-equilibrating. In criticising this, Helmstaedt and Harrap (1999) the reasoning of the "*chaotic stratigraphy of a surface mountain belt*". They further point out that upper mantle xenolith geothermobarometry is hampered, amongst other aspects, by the errors associated with the calibration of the various geothermobarometers, and in many cases, the uncertainties with determining Fe^{2+}/Fe^{3+} ratios. In general, no mantle geothermometer will yield results with precision better than ~ 50 °C and ~ 3 kbar (for example Brey and Kolher, 1990; Sobolev et al., 1999), whilst accuracy is undetermined. Spatially, the precision of current mineral equilibrium geothermobarometry is clearly too diffuse to show any clear-cut separation of the various rock suites, particularly when applied to a volumetrically minor but economically significant mantle paragenesis such as diamond-bearing xenoliths. Furthermore, the absolute P-T's are dependant on the geothermobarometer pairing chosen. Because a variety of geothermobarometer combinations must be used on the various rock types, neither the precision nor accuracy can be assessed when combined. The apparent continuum of P-T's at Newlands indicates an intimate and

spatially complex integrated upper mantle or is it a function of the inadequacies of the methodology?

17.4.2 Implications for cratonic formation

The early Proterozoic to mid-Archæan Re-Os ages obtained for both the diamond-bearing garnet macrocryst and diamond-bearing eclogites at Newlands are consistent with previous studies. Whole rock Re-Os studies of cratonic SCLM peridotite xenoliths derived from the Kaapvaal (Walker et al., 1989; Pearson et al, 1995a; Carlson et al, 1999), Siberian (Pearson et al, 1995b) and Wyoming (Carlson and Irving, 1994) cratons indicate that the majority of the peridotite xenoliths were formed in the early Proterozoic and late Archæan. Both spinel- and garnet- facies peridotites derived from Kaapvaal and Siberian cratons have a dominant Re-Os model age mode between 2.5 and 3.0 Ga, but range from 1.2 to 3.6 Ga. Similarly, eclogites from the Kaapvaal (Shirey et al., 1998) and Siberia (Pearson et al., 1995) cluster around mid Archæan isochron arrays.

Studies using incompatible element isotopic systems such as Rb-Sr, Sm-Nd and U-Th-Pb are consistent with the ancient origins of upper mantle xenoliths and inclusions in diamonds (for example, Kramers, 1979; Richardson et al., 1984; Smith et al., 1989; Jacob et al., 1994). With the solitary exception of the Proterozoic kimberlite Premier, the model ages of upper mantle xenoliths and inclusions in diamonds are also significantly older than the kimberlite from which the samples were obtained[19]. Peridotitic inclusions are consistent with at least two periods of incompatible trace element enrichment at around 1.9-2.0 Ga (Richardson et al., 1993; Richardson and Harris, 1997) and 3.2-3.3 Ga (Richardson et al., 1984), respectively. However, incompatible element systems (such as Rb-Sr or Sm-Nd) can be, and usually are, reset by mantle events, such as metasomatism, and thus represent minimum ages for diamond and/or SCLM formation. In contrast, Re-Os isotope systematics can potentially "see through" metasomatic events and record the original depletion event.

[19] Other lines of evidence, such as diamond FTIR studies, indicate that the diamonds from Premier are not contemporaneous with the kimberlite.

All these ancient isotopic ages (possibly representing both formation and "re-setting" events) overlap the major crustal building periods of the Kaapvaal craton (de Wit et al., 1992). This implies that cratonic root stabilisation beneath the Kaapvaal and craton is potentially coeval with crustal formation (Kramers, 1979; Richardson et al., 1984; Richardson et al., 1990; Richardson and Harris, 1997). The presence of diamond in some of the specimens from both the Kaapvaal and Siberian xenoliths (this study; Pearson et al., 1995a) imply that the SCLM extended to depths of approximately 200 km by the end of the Archæan. In addition, the apparent lack of any systematic age variation with calculated equilibrium conditions implies that the SCLM and overlying continental crust nuclei have been coupled since formation (Pearson et al., 1995a,b; Carlson et al., 1999).

The association of continental crust formation, basalt-depletion of mantle peridotite and the presence of subducted oceanic crust, all of overlapping age, suggests that cratonic lithospheres were created in settings similar to modern convergent margins. Once formed, these assemblages remain coupled and, under favourable circumstances, can survive the destructive forces of plate tectonics over geological æons.

SUMMARY AND CONCLUSIONS 18

18.1 COMPOSITION AND TERMAL STATE OF THE MANTLE BENEATH NEWLANDS

The lithosphere sampled by the Newlands kimberlite comprises of a wide variety of upper mantle rock types: harzburgite, lherzolite, websterite, wehrlite, dunite, eclogite, megacrysts. Furthermore, diamond-bearing xenoliths of harzburgite, lherzolite and eclogite were observed.

Eighteen peridotitic garnet macrocrysts (1 to 3 cm in size) were observed to contain diamond and one with graphite. Their mineralogy consists predominantly of lilac garnet with diamond (or graphite) ± chromite and altered silicates. No primary clinopyroxene was observed in any of the specimens. The diamonds were generally very small and occur in two primary forms, namely (< 1 mm) single octahedra or octahedra aggregates. The garnet compositions are predominantly of harzburgitic affinity - high-Cr (> 8 wt%), Ti-depleted, and extremely sub-calcic (< 3 wt%). However, three specimens have lherzolitic affinities - high-Cr calcic compositions. The chromites are Cr-rich, Ti-depleted, whilst the solitary olivine is extremely refractory. The harzburgitic G10 garnets display a narrow range of trace element signatures. Compared to the lherzolitic G9 garnets they are relatively depleted in Zr, Y, Ga, and Ti, whilst, in contrast, Sr and LREEs are enriched. The $[REE]_n$ patterns are all very similar and display the unusual LREE sinusoidal pattern. The most calcic garnet analysed at Newlands yields a $[REE]_n$ pattern similar to "fertile" lherzolitic mantle garnets. The major and trace element geochemistry of the harzburgitic G10 garnets is similar to the multitude of diamond inclusion studies and the few diamond-bearing peridotites, whilst that of the lherzolitic garnets is distinctly different. Geothermometry yields temperatures ranging from 900 to 1050 °C, equivalent to pressures of 40 to 55 kbar (based on a 37-38 mW/m^2 geotherm determined from Newlands coarse peridotites). This P-T range is within the diamond stability field.

Four diamond-bearing peridotitic garnet macrocrysts were analysed for whole rock Re-Os systematics. All are Re depleted and yield a range of ages spanning from the Proterozoic (minimum T_{RD} 1.8 Ga) to the mid-Archæan (maximum T_{MA} 3.5 Ga).

Seventeen eclogites (2 to 6 cm in size) were observed to contain diamond. They modally dominated by coarse-grained garnet and clinopyroxene, with primary trace phases including sulphides and rutile. Alteration is pervasive and ranges from minor grain boundary intrusions to massive mineral (primarily clinopyroxene) replacement. The diamonds display a considerably wider range of characteristics than those from the peridotitic garnet macrocrysts. The diamonds range in size from approximately 100 μm within diamond aggregates to large single crystals up to 2 mm. The dominant morphology is octahedral but there are also significant numbers of cubes and dodecahedrons, and some cubo-octahedrons. Cathodoluminescence indicates that the diamonds grew in at least three distinct periods. The garnets have Na_2O concentrations greater than 0.07 wt%, whilst the clinopyroxenes have K_2O concentrations greater than 0.08 wt%. Both phases are Fe-rich and Ca- and Mg- poor relative to diamond-free eclogites from Newlands. The garnets display a very restricted range of trace element compositions and are relatively enriched in Ga, Zn, Mn and Ti, and depleted in Cr and Ni relative to diamond-free eclogites from Newlands. The garnets also display an extremely consistent REE trace element geochemistry that is $[HREE]_n$ enriched. The clinopyroxenes, as with the garnets, display a very restricted range of trace element compositions (with one exception). They are relatively enriched in Ga, Zn, Zr, Mn and Ti, and depleted in Ni relative to diamond-free eclogites from Newlands. The clinopyroxenes also display a very restricted REE trace element geochemistry that is $[LREE]_n$ enriched. Bulk rock major element compositions (calculated assuming a 50:50 garnet-clinopyroxene ratio) are compositionally similar to Archæan magnesian basalts. A statistical analysis of eclogites at Newlands indicates that those associated with diamonds have a discernible geochemistry. The diamond-bearing eclogites, with one exception, have textures and mineral geochemistry equivalent to Group I or Group B eclogites (depending on the classification scheme used). Geothermometry yields temperatures between 920 to 1080 °C, equivalent to pressures between 42 and 58 kbar (based on a 37-38 mW/m^2 geotherm), which lies within the diamond stability field. Re-Os

systematics for the diamond-bearing eclogites are indicative of formation ages in the Archæan. In addition, it is apparent that the eclogites had $^{187}Os/^{188}Os$ substantially higher than that of a chondritic mantle at circa 3 Ga. The Re-Os systematics, major and trace element mineral chemistry, and stable isotopes (albeit preliminary) of the diamond-bearing eclogites from Newlands are consistent with a protolith that has interacted within surfical environments. Therefore, the subduction hypothesis is the favoured model for the origin of the diamond-bearing eclogites at Newlands. Assuming that the Newlands diamond-bearing eclogitic protolith was formed in an Archæan ocean floor environment and accreted to the SCLM then it is likely that it represents komatiitic ocean ridge products or primitive portions of oceanic plateaus or islands.

18.2 CHARACTERISITCS OF NEWLANDS DIAMONDS

FTIR spectra indicate that the peridotitic and eclogitic diamonds display different nitrogen concentrations and platelet peak positions. Specifically, the vast majority of harzburgitic diamonds are Type II (or near Type II) whilst eclogitic diamonds are Type I. Therefore nitrogen concentrations can be confidently used to ascribe the diamonds paragenesis at Newlands. This difference implies that the peridotitic and eclogitic diamonds at Newlands are derived from separate sources. Both sets of diamonds have type IaAB aggregation states ranging from 0 to 20 %. Such nitrogen concentrations and aggregation states are consistent with diamond formation in the Archæan for both parageneses, based on proxy times (Re-Os isotopes) or temperatures (geothermometry). Time-average temperatures imply that the diamonds formed at higher temperatures than their ambient levels at the time of kimberlite eruption. An Archæan age for harzburgitic and eclogitic diamonds corresponds to a time-average temperature of greater than 1050 °C. As the ambient temperatures for diamond-bearing xenoliths are commonly less than 1050 °C, and down to 900 °C, the xenoliths and their diamonds have experienced cooling on the order of at least 100 °C since diamond formation in the Archæan to kimberlite eruption (at 114 Ma: Smith et al., 1985).

The possibility of being able to correctly classify diamonds based on their spectra could prove invaluable, particularly in the study of inclusions in diamonds. Individual sulphide inclusions (for example, Pearson et al., 1999) are studied for constraining diamonds ages and mantle events. However, there are problems in assigning the diamond to the correct paragenesis without independent information as sulphides occur in both peridotitic and eclogitic parageneses. At Newlands the non-destructive technique of FTIR spectroscopy will allow the study of a greater range of inclusions with defined diamond parageneses.

18.3 AGE OF FORMATION : LITHOSPHERIC AND CRATONIC IMPLICATIONS

The early Proterozoic to mid-Archæan Re-Os ages obtained for both the diamond-bearing garnet macrocryst and diamond-bearing eclogites at Newlands overlap the major crustal building periods of the Kaapvaal craton (de Wit et al., 1992). This implies that cratonic root stabilisation beneath the Kaapvaal craton is potentially coeval with crustal formation (Kramers, 1979; Richardson et al., 1984; Richardson et al., 1990; Richardson and Harris, 1997). The presence of diamond implies that the SCLM may have extended to depths of approximately 200 km by the end of the Archæan. In addition, the apparent lack of any systematic age variation with calculated equilibrium conditions implies that the SCLM and overlying continental crust nuclei have been coupled since formation (Pearson et al., 1995a,b; Carlson et al., 1999). Once formed, these assemblages remain coupled and, under favourable circumstances, can survive the destructive forces of plate tectonics over geological æons.

Accepting the subduction hypothesis for the origin of the eclogites and the diamonds, combined with their geologically old ages, implies the operation of plate tectonics since the early part of the Earths history, potentially only hundreds of millions of years after the crust formed. It is likely that Archæan plate tectonics involved young, hot, small lithospheric plates with thicker mafic crust relative to modern plate tectonics.

REFERENCES

AI, Y., 1994, A revision of the garnet-clinopyroxene Fe^{+2}-Mg exchange geothermometer: *Contrib. Mineral. Petrol.*, 115, p. 467-473.

BALLHAUS, C., BERRY, R.F., & GREEN, D.H., 1991, High-pressure experimental calibration of the olivine-orthopyroxene-spinel oxygen barometer: implications for the oxidation state of the upper mantle: *Contrib. Mineral. Petrol.*, 107, p. 27-40.

BARTOSHINSKY, Z.V., 1960, Diamonds from eclogites from the Mir pipe (in Russian): *Geol. Geofiz.*, p. 130-131.

BARTOSHINSKY, Z.V., KHARKIV., A.D., BOTKUNOV., A.L., & SOBOLEV, N.V., 1973, New data on the diamonds from the Mir Pipe (in Russian): *Geol. Geofiz.*, 14(5), p. 108-112.

BEARD, B.L., FRARACCI, K.N., TAYLOR, L.A., SNYDER, G.A., CLAYTON, R.N., MAYEDA, T.K., & SSOBOLEV, N.V., 1996, Petrography and geochemistry of eclogites from the Mir kimberlite, Yakutia, Russia: *Contributions to Mineralogy and Petrology,* 125, p. 293-310.

BECK, R., 1898, Die diamantenlagerstatte von Newland in Griqua Land West: *Zeit. Prakt. Geol*, p. 163-164.

BECK, R., 1899, Neues von den Afrikanischen Diamantlagerstatten: *Zeit. Prakt. Geol.*, p. 417-419.

BELL, D.R., 1981, Ultramafic xenoliths from the Koffiefontein kimberlite pipe, R.S.A.: B.Sc. Thesis, Univ. of Cape Town.

BENCE, A.E. & ALBEE, A.L., 1968, Empirical correction factors for the electron microanalysis of silicates and oxides: *J. Geol.*, 76, p. 382-403.

BERMAN, R.G, 1965, *Physical Properties of diamond*, Clarendon press, Oxford.

BERMAN, R.G., ARANOVICH, L.Y., & PATTISON, D.R.M. 1995, Reassessment of the garnet-clinopyroxene Fe-Mg exchange thermometer II. Thermodynamic analysis: *Contrib. Mineral. Petrol.,* 119, p. 30-42.

BERMAN, R.G., & SIMON, F., 1955, The graphite-diamond equilibrium: *Z. Elektrochem.*, 59, p. 333-338.

BIBBY, D.M., 1982, Impurities in natural diamond: *Chem. Phys. Carbon*, 18, p. 3-91.

BONNEY, T.G., 1899, The parent-rock of the diamond in South Africa: *Geology Magazine,* 6, p. 309-321.

BONNEY, T.G., 1899, The original rock of the South African diamond: *Natural Science*, 15, p.173-182.

BONNEY, T.G., 1900, Additional notes on boulders and other rock specimens from the Newlands Diamond Mines, Griqualand West: *Proc.Roy. Soc. London*, 67, p. 475-484.

BOULLIER, A.M., & NICOLAS, A., 1973, Texture and fabric of peridotite nodules from kimberlite at Mothae, Thaba Putsoa and Kimberley. In: NIXON, P.H., (ed.), Lesotho Kimberlites: *Maseru, Lesotho National Development Corp.* p. 57-66.

BOULLIER, A.M., & NICOLAS, A., 1975, Classification of textures and fabrics of peridotite xenoliths from South African kimberlites. In: AHRENS, L.H., DAWSON, J.B., DUNCAN, A.R. & ERLANK, A.J., (eds.), Physics and Chemistry of the Earth: *Pergamon Press,* 9, p. 467-475.

BOYD, F.R., 1973, A pyroxene geotherm: *Geochim. et Cosmochim. Acta,* 37, p. 2533-2546.

BOYD, F.R., 1974, Ultramafic nodules from the Frank Smith kimberlite pipe, South Africa: *Carnegie Inst. Year Book 1973-1974,* p. 285-293.

BOYD, F.R., 1975, Stress-heating and compositional variations in enstatites from sheared lherzolites: *Carnegie Inst. Year Book 1974-1975,* p. 525-528.

BOYD, F.R., 1989, Kaapvaal spinel peridotites: Evidence of Cratonic origin: *Carnegie Inst. Year Book 1988-1989*, p. 3-6.

BOYD, F.R., & CANIL, D., 1997, Peridotite xenoliths from the Slave craton, Northwest Territories: *Abs 7th Annual V.M. Goldschmidt Conf., Houston*, p. 34-35.

BOYD, F.R., & ENGLAND, J.L., 1960, Apparatus for phase equilibrium measurements at pressures up to 50 kb and temperatures up to 1750 °C: *J. Geophys. Res.*, 65, p. 741-748.

BOYD, F.R., FUJI, T. & DANCHIN, R.V., 1976, A noninflected geotherm for the Udachnaya kimberlite pipe, U.S.S.R.: *Carnegie Institution Washington, Year Book*, 1975, p. 523-531.

BOYD, F.R., & GURNEY, J.J., 1982, Low-calcium garnets: key to craton structure and diamond crystallisation: *Carnegie Inst., Washington Yearbook*, 81, p. 261-267.

BOYD, F.R., & MERTZMAN, S.A., 1987, Composition and structure of the Kaapvaal lithosphere, Southern Africa, in MYSEN, B.O. (ed.), Magmatic Processes: Physiochemical Principles. *The Geochemical Society*, p. 3-12.

BOYD, F.R., & NIXON, P.H., 1972, Ultramafic nodules from the Thaba Putsoa kimberlite pipe: *Carnegie Inst. Year Book,* 81, p. 362-373.

BOYD, F.R., & NIXON, P.H., 1973, Origin of the ilmenite-silicate nodules in kimberlites from Lesotho and South Africa. In: NIXON, P.H. (ED.), Lesotho National Development Corporations: *Maseru,* p. 254-268.

BOYD, F.R., & NIXON, P.H., 1975, Origins of the ultramafic nodules from some kimberlites of northern Lesotho and the Monastery Mine, South Africa: *Physics and Chemistry of the Earth*, 9, p. 431-454

BOYD, F.R., & NIXON, P.H., 1978, Ultramafic nodules from the Kimberley pipes, South Africa: *Geochim. Cosmochim. Acta.*, 42, p. 1367-1382.

BOYD, F.R., PEARSON, D.G., NIXON, P.H., & MERTZMAN, S.A., 1993, Low-calcium garnet harzburgites from southern Africa: their relations to craton structure and diamond crystallisation: *Contrib. Mineral. Petrol.*, 113, p. 352-366.

BOYD, F.R., POKHILENKO, N.P., PEARSON, D.G., MERTZMAN, S.A., SOBOLEV, N.V., & FINGER, L.W., 1997, Composition of the Siberian cratonic mantle: evidence from Udachnaya peridotite xenoliths: *Contrib. Mineral. & Petrol.*, 128, p. 228-246.

BOYD, S.R., PINEAU, F., & JAVOY, M., 1994, Modelling the growth of natural diamonds: *Chem. Geol.*, 116, p. 29-42.

BREY, G.P., DOROSHEV, A., & KOGARKO, L., 1991, The join pyrope-knorringite: experimental constraints for a new geothermobarometer for co-existing garnet and spinel: *Ext. Abs. 5th Int. Kimberlite Conf.*, p. 26-28.

BREY, G.P. & KÖHLER, T., 1990, Geothermobarometry in four-phase lherzolites: II New thermometers and practical assessment of existing thermobarometers: *J. Petrol.*, 31, p. 1353-1378.

BREY, G.P., KÖHLER, T., & NICKEL, K.G., 1990, Geothermobarometry in four-phase lherzolites: I Experimental results from 10 to 60 kbar: *J. Petrol.*, 31, p. 1313-1352.

BULANOVA, G.P., 1995, The formation of diamond: *J. Geochem. Explor.*, 53, p. 1-23.

BULANOVA, G.P., GRIFFIN, W.L., & RYAN, C.G., 1998b, Nucleation environment of diamonds from Yakutian kimberlites: *Mineral. Mag.*, 62, p. 209-312.

BULANOVA, G.P., GRIFFIN, W.L., RYAN, C.G., SHESTAKOVA, O.Y., & BARNES, S.J., 1996, Trace elements in sulfide inclusions from Yakutia diamonds: *Contrib. Mineral. Petrol.*, 124, p. 111-125.

BULANOVA, G.P., GRIFFIN, W.L., KAMINSKY, F.V., DAVIES, R.M., RYAN, C.G., ANDREW, A., SPETSIUS, Z.V., & ZAHKARCHENKO, O.D., 1998, Diamonds from Zarnitsa and Dalnaya kimberlites (Yakutia): *Ext. Abs. 7th Internat. Kimb. Conf., Cape Town, South Africa*, p. 113-116.

BULANOVA, G.P., & PAVLOVA, L.A., 1991, The evolution of natural diamond growth conditions: *Ext. Abs. 5th Int. Kimb. Conf.*, p. 488-489.

BULANOVA, G.P., SPETSIUS, Z.V., & LESKOVA, N.V., 1990, Sulfides in diamonds and mantle xenoliths from kimberlite pipes of Yakutia (in Russian): *Nauka, Novosibirsk*, 118 pp.

BULATOV V., BREY, G.P., & FOLEY, S.F., 1991, Origin of low-Ca, high-Cr garnets by recrystallization of low-pressure harzburgites: *Ext. Abs. 5th Int. Kimb. Conf., CPRM Spec Publ.*, 2, p. 29-31.

BUNDY, F.R., 1980, The P, T phase and reaction diagram for elemental carbon, 1979: *J. Geophys. Res.*, 85, p. 6930-6936.

BURGESS, S.R., 1997, The evolution of the sub-cratonic mantle seen in mantle xenoliths: *Unpubl. PhD Thesis, University of Edinburgh.*

BURGESS, S.R., & HARTE, B., 1999, Tracing lithosphere evolution through the analysis of heterogeneous G9/G10 garnets in peridotite xenoliths, 1: Major element chemistry: *Proc. 7th Int. Kimb. Conf., Vol 1*, p. 66-80.

CANIL, D., 1994, An experimental calibration of the "Ni-in-garnet" geothermometer with applications: *Contrib. Mineral. Petrol.*, 117, p. 410-420.

CANIL, D., 1996, An experimental calibration of the nickel in garnet geothermometer with applications: reply: *Contrib. Mineral. Petrol.*, 124, p. 219-223.

CANIL, D., & WEI, K., 1992, Constraints on the origin of mantle-derived low Ca garnets: *Contrib. Mineral. Petrol.*, 109, p. 421-430.

CANIL, D., & O'NEILL, 1996, Distribution of ferric iron in some upper-mantle assemblages: *J. Petrol.*, 37, p. 609-635.

CARLSON, R.W., & IRVING, A.J., 1994, Depletion and enrichment history of subcontinental lithospheric mantle: an Os, Sr, Nd and Pb isotopic study of ultramafic xenoliths from the north western Wyoming Craton: *Earth Planet. Sci. Lett.*, 126, p. 457-472.

CARLSON, R.W., PEARSON, D.G., BOYD, F.R., SHIREY, S.B., IRVINE, G., MENZIES, A.H., & GURNEY, J.J., 1999, Re-Os systematics of lithospheric peridotites: implications for lithosphere formation and preservation: *Proc. 7th Int Kimberlite Conf, Cape Town, Vol. 1*, p. 99-108.

CARSWELL, D.A., & DAWSON, J.B., 1970, Garnet peridotite xenoliths in South African kimberlite pipes and their petrogenesis: *Contrib. Mineral. Petrol.*, 25, p. 163-184.

CARSWELL, D.A., & GIBB, F.G.F., 1980, Geothermometry of garnet lherzolite nodules with special reference to those from the kimberlites of Northern Lesotho: *Contrib. Mineral. Petrol.*, 74, p. 403-416.

CARSWELL, D.A., & GIBB, F.G.F., 1987, Garnet lherzolite xenoliths in the kimberlites of northern Lesotho: revised P-T equilibration conditions and upper mantle paleogeotherm: *Contrib. Mineral. Petrol.*, 97, p. 473-487.

CARTIGNY, P., HARRIS, J.W., & JAVOY, M., 1999, Eclogitic, peridotitic, and metamorphic diamonds and the problems of carbon recycling – the case of Orapa (Botswana): *Proc. 7th Int Kimberlite Conf, Cape Town, Vol. 1*, p. 117-124.

CHESLEY, J.T., RUDNICK, R.L. & LEE, C.-T., 1999, Re-Os systematics of mantle xenoliths from the East African Rift: Age, structure, and history of the Tanzanian craton : *Geochim. Cosmochim. Acta.*, 63, p. 1203-1217.

CHINN, I.L., 1995, A study of unusual diamonds from the George Creek K1 kimberlite dyke, Colorado: *Ph.D. Thesis, University of Cape Town*, pp. 94.

CHINN, I.L., GURNEY, J.J., HARTE, B., FITZSIMONS, I.C.W., & MILLEGE, H.J., 1998, Nitrogen contents of diamond plates: a comparison of FTIR and SIMS analyses: *Ext. Abs. 7th Int. Kimb. Conf., Cape Town*, p. 152-155.

CHINN, I.L., GURNEY, J.J., MILLEDGE, H.J., TAYLOR, W.R., & MCCALLUM, M.E., 1995, CO_2-bearing diamonds from the George Creek K1 kimberlite dike of the Colorado-Wyoming State-line district: *Ext. Abstr. 6th Int. Kimberlite Conf. Russia*, p. 113-115.

CLACKSON, S.G., MOORE, M., WALMSLEY, J.C., & WOODS, G.S., 1990, The relationship between platelet size and the frequency of the B' infrared absorption peak in type Ia diamond: *Phil. Mag.*, B62, p. 115-128.

CLARK, C.D., & DAVEY, S.T., 1984, One-phonon infrared absorption in diamond: *J. Phys. C: Solid St. Phys.*, 17, p. 1127-1140.

CLARK, C.D., COLLINS, A.T., & WOODS, G.S., 1992, Absorption and luminescence spectroscopy. In FIELD, J.E., (ED.), *The Properties of natural and synthetic diamond*, p. 35-79, Academic Press.

CLEMENT, C.R., & REID, A.M., 1989, The origin of kimberlite pipes: An interpretation based on a synthesis of geological features displayed by southern African occurrences. In: *Kimberlites and Related Rock, ROSS, J. (ed.): Geological Society of Australia, Special Publ.*, 14, p. 632-646.

CLEMENT, C.R., & SKINNER, E.M.W., 1979, A textural-genetic classification of kimberlites: *Trans. Geol. Soc. Sth. Afr.*, 88, p. 403-409.

COLLINS, R.J., & FAN, H.Y., 1954, *Phys. Rev.*, 93, p.674.

COLLINS, A.T., & LIGHTOWLERS, E.C., 1979, Electrical properties: In FIELD, J.E., (ED.), *The properties of diamond, Academic Press*, p. 79-105.

COLEMAN, R.G., LEE, D.E., BEATTY, L.B., & BRANNOCK, W.W., 1965, Eclogites and eclogites: their similarities and differences: *Geol. Soc. Am. Bul.*, 76, p. 483-508.

COOPER, G.I., 1990, Microspectroscopy of diamond in relation to mantle processes: *Unpub. PhD thesis*, University College London.

CREASER, R., PAPANASTASSIOU, D., & WASSENBERG, G., 1991, Negative thermal ion mass spectrometry of osmium, rhenium and iridium: *Geochim. Cosmochim. Acta*, 55, 397-401.

DANCHIN, R.V., FERGUSON, J., MCIVER, J.R., & NIXON, P.H., 1975, The composition of late stage kimberlitic liquids as revealed by nucleated autoliths: *Phys. Chem. Earth*, 9, pp. 605-617.

DANIELS, L., 1980, Some aspects of the xenolith suite from the Newlands kimberlites, South Africa: *Unpub. Hons. thesis*, Univ. of Cape Town, pp. 59.

DANIELS, L.R.M., & GURNEY, J.J., 1991, Oxygen fugacity constraints on the Southern African lithosphere: *Contrib. Mineral. Petrol.*, 108, p. 154-161.

DANIELS, L.R.M., RICHARDSON, S.H., MENZIES, A.H., DE BRUIN, D., & GURNEY, J.J., 1995, Diamondiferous garnet macrocrysts in the Newland kimberlite, South Africa – Rosetta stone from the Kaapvaal craton keel: *Ext. Abstr. 6th Int. Kimberlite Conf. Russia*, p. 121-123.

DAVIES, G., 1976, The A nitrogen aggregate in diamond – its symmetry and possible structure: *J. Phys C: Solid St. Phys*, 9, p. L537-L542.

DAVIES, G., 1979, Cathodoluminescence: In FIELD, J.E., (ED.), *The properties of diamond, Academic Press*, p. 165-181.

DAVIES, G., & BOYD, F.R., 1966, The join $Mg_2Si_2O_6$-$CaMgSi_2O_6$ at 30 kb pressure and its application to pyroxenes from kimberlite: *J. Geophys. Res.*, 71, p. 3567-3576.

DAVIES, G., & SUMMERSGILL, I., 1973, Nitrogen dependant optical properties of diamond: *Diamond Research 1973*, p. 6-15, Industrial Diamond Information Bureau, London.

DAVIES R.M., GRIFFIN, W.L, PEARSON, N.J., ANDREW, A.S., DOYLE, B.J., O'REILLY, S.Y., 1999, Diamonds from the deep: Pipe DO-27, Slave Craton, Canada: *Proc. 7th Int Kimberlite Conf, Cape Town, Vol. 1*, p. 148-155.

DAWSON, J.B., 1980, Kimberlites and their xenoliths: *Springer-Verlag, Berlin*, pp. 272.

DAWSON, J.B., 1984, Contrasting types of upper mantle metasomatism: In KORNPROBST, J., (ED.), *Kimberlites II: the Mantle and Crust-Mantle Relationships: Eelsevier, Amsterdam*, p. 289-294.

DAWSON, J.B., & SMITH, J.V., 1975, Occurrence of diamond in a mica-garnet lherzolite xenolith from kimberlite: *Nature*, 254, p. 580-581.

DAWSON, J.B., & STEPHENS, W.E., 1975, Statistical classification of garnets from kimberlites and associated xenoliths: *J. Geol.*, 83, p. 589-607.

DE WIT, M.J., ROERING, C., HART, R.J., ARMSTRONG, R.A., RONDE, C.E.J.D., GREEN, R.W.E., TREDOUX, M., PEBERDY, E., & HART, R.A., 1992, Formation of an Archaean continent: *Nature*, 357, p. 553-562.

DEER, W.A, HOWIE, R.A, & ZUSSMAN, J., 1992, An introduction to the rock forming minerals: *Longman scientific and technical, Essex, England*, pp. 696.

DEINES, P., 1980, The carbon isotope composition of diamonds: relationship to diamond shape, colour, occurrence and vapour composition: *Geochim. Cosmochim. Act.*, 44, p. 943-961.

DEINES, P., & HARRIS, J.W., 1995, Sulphide inclusion chemistry and carbon isotopes of African diamonds: *Geochim. Cosmochim. Acta*, 59, p. 3173-3188.

DEINES, P., HARRIS, J.W., & GURNEY, J.J., 1987, Carbon isotopic composition, nitrogen content and inclusion composition of diamonds from the Roberts Victor kimberlite, South Africa: Evidence for 13C depletion in the mantle: *Geochim. Cosmochim. Acta*, 51, p. 1227-1243.

DEINES, P., HARRIS, J.W., & GURNEY, J.J., 1991, The carbon isotopic composition and nitrogen content of lithospheric and asthenospheric diamonds from the Jagersfontein and Koffiefontein Kimberlite, South Africa: *Geochim. Cosmochim. Acta*, 55, p. 2615-2625.

DELANY, J.S., SMITH, J.V., & NIXON, P.H., 1979, Manganese thermometer for mantle peridotites: *Contrib. Mineral. Petrol.*, 71, p. 157-169.

DOROSHEV, A.M., BREY, G.P., GIRNIS, A.V., TURKIN, A.I., & KOGARKO, L.N., 1997, Pyrope-knorringite garnets in the Earth's mantle: experiments in the MgO-Al2O3-SiO2-Cr2O3 system: *Russ. Geol. Geophys.*, 38, p. 559-586.

EGGLER, D.H., & BAKER, D.R., 1982, Reduced volatiles in the system C-O-H, implications to mantle melting, fluid formation, and diamond genesis. In: AKIMOTO, S., & MANGHNANI, M.H., (EDS.), *High Pressure Research in Geophysics, Centre Acad. Publ. Tokyo*, p. 237-250.

ELDRIDGE, C.S., COMPSTON, W., WILLIAMS, I.S., HARRIS, J.W., & BRISTOW, J.W., 1991, Isotope evidence for the involvement of recycled sediments in diamond formation: *Nature*, 353, p. 649-653.

ELDRIDGE, C.S., COMPSTON, W., WILLIAMS, I.S., HARRIS, J.W., BRISTOW, J.W., & KINNY, P.D., 1995, Applications of the SHRIMP I ion microprobe to the understanding of processes and timing of diamond formation: *Economic Geology*, 90, p. 271-280.

ELLAM, R. M., CARLSON, R. W., & SHIREY, S. B., 1992, Evidence from Re-Os isotopes for plume-lithosphere mixing in Karoo flood basalt genesis: *Nature*, 359, p. 718-721.

ELLIS, D.G., & GREEN, D.H., 1979, An experimental study of the effect of Ca upon garnet-clinopyroxene Fe-Mg exchange equilibria: *Contrib. Mineral. Petrol.*, 71, p. 13-22.

ERLANK, A.J. & KUSHIRO, I., 1970, Potassium contents of synthetic pyroxenes at high temperatures and pressures: *Carneg. Inst. Wash. Yearbook*, 68, p. 439-442.

ERLANK, A.J., WATERS, F.G, HAWKESWORTH, C.J., HAGGERTY, S.E, ALLSOPP, H.L., RICKARD, A.S., & MENZIES, M.A., 1987, Evidence for mantle metasomatism in peridotitic nodules from the Kimberley pipes, South Africa: In MENZIES, M.A., & HAWKESWORTH, C.J. (EDS.), *Mantle Metasomatism, Academic Press, London*, p. 221-311.

EVANS, T., 1976, Diamonds: *Contemp. Phys.*, 17, p. 45-70.

EVANS, T., 1992, Aggregation of nitrogen in diamond. In: FIELD, J.E., (ED.), *The Properties of Natural and Synthetic diamonds, Academic Press, London*, p. 259-290.

EVANS, T., & HARRIS, J.W., 1989, Nitrogen aggregation, inclusion temperatures and the age of diamonds: In ROSS, J., JAQUES, A.L., FERGUSON, J., GREEN, D.H., O'REILLY, S.Y., DANCHIN, R.V., & JANSE, A.J.A., (EDS.), *Kimberlites and Related Rocks, Geol. Soc. Austrl. Spec. Publ.*, 14, p. 1001-1006.

EVANS, T., & KIFLAW, I., LUYTEN, W., VAN TENDELOO, G., & WOODS, G.S., 1995, Conversion of platelets into dislocation loops and voidite formation in type IaB diamonds: *Proc.R.Soc.Lond.*, A449, p. 295-305.

EVANS, T., & QI, Z., 1982, The kinetics of aggregation of nitrogen atoms in diamond: *Proc. Roy. Soc. Lond.*, A381, p. 159-178.

FERGUSON, J., MARTIN, H, NICHOLAYSON, L.O., & DANCHIN, R.V., 1975, Gross Brukkaros: a kimberlite-carbonate volcano: *Phys. Chem. Earth*, 9, p. 219-234.

FIELD, J.E., (ed), 1992, The properties of natural and synthetic diamond: *Academic Press, London.*

FINNERTY, A.A., 1989, Xenolith-derived mantle geotherms: whither the inflection?: *Contrib. Mineral. Petrol.*, 102, p. 367-375.

FINNERTY, A.A., & BOYD, F.R., 1984, Evaluation of thermobarometers for garnet peridotites: *Geochim. Cosmochim. Acta.*, 48, p. 15-27.

FINNERTY, A.A., & BOYD, F.R., 1987, Thermobarometry for garnet peridotite xenoliths: a basis for mantle stratigraphy: In NIXON, P.H. (ED.), *Mantle Xenoliths, Wiley, New York*, p. 381-412.

FUNG, A.T., & HAGGERTY, S.E., 1995, Petrography and mineral compositions of eclogites from the Koidu kimberlite complex, Sierra Leone: *J. Geophys. Res.*, 100, p. 20451-20473.

GALIMOV, E.M., 1991, Isotope fractionation related to kimberlite magmatism and diamond formation: *Geochim. Cosmochim. Acta.*, 55, p. 1697-1708.

GANGULY, J., CHENG., W., & TIRONE., M., 1996, Thermodynamics of aluminosilicate garnet solid solution: new experimental data, an optimized model, and thermometric applications: *Contrib. Mineral. Petrol.*, 126, p. 137-151.

GIARAMITA, M.J., & DAY, H., 1990, Error propagation in calculations of structual formulas: *Amer. Mineral.*, 75, p. 170-182.

GOLDSCHIMDT, V. M., 1937, The principles of distribution of chemical elements in minerals and rocks: *J. Chem. Soc. London*, p. 655-673.

GRÄICHEN, W., 1903, Die Newlands-diamantminen, Sudadrika: Zeitschrift fur praktische Geologie: *Dezember.*, p. 448-452.

GRIFFIN, W.L., COUSENS, D.R., RYAN, C.G., SIE, S.H., & SUTER, G.F., 1989, Ni in chrome pyrope garnets: a new thermometer: *Contrib. Mineral. Petrol.*, 103, p. 199-203.

GRIFFIN, W.L., GURNEY, J.J., & RYAN, C.G., 1992, Variations in trapping temperatures and trace elements in peridotite-suite inclusions from African diamonds: evidence for two inclusion suites, and implications for lithosphere stratigraphy: *Contrib. Mineral. Petrol.*, 110, p. 1-15.

GRIFFIN, W.L., & RYAN, C.G., 1995, Trace elements in indicator minerals, area selection and target evaluation in diamond exploration: *J. Geochem. Explor.*, 53, p. 311-337.

GRIFFIN, W.L., SHEE, S.H., RYAN, C.G., WIN, T.T., & WYATT, B.A., 1999, Harzburgite to lherzolite and back again: Metasomatic processes in ultramafic xenoliths from the Wesselton kimberlite, Kimberley, South Africa: *Contrib. Mineral. Petrol.*, 134, p. 232-250.

GRIFFIN, W.L., SOBOLEV, N.V., RYAN, C.G., POKHILENKO, N.P., WIN, T.T., & YEFIMOVA, E.S., 1993, Trace elements in garnets and chromites, diamond formation in the Siberian lithosphere: *Lithos*, 29, p. 235-256.

GRÜTTER, H.S., APTER, D.B., & KONG, J., 1999, Crust-Mantle coupling: Evidence from mantle-derived xenocrystic garnets: *Proc. 7th Int. Kimb. Conf., Vol 1, Cape Town*, p. 307-313.

GRÜTTER, H.S., & QUADLING, K.E, 1999, Can sodium in garnet be used to monitor eclogitic diamond potential: *Proc. 7th Int. Kimb. Conf., Vol 1, Cape Town*, p. 314-320.

GURNEY, J.J., 1984, A correlation between garnets and diamonds in kimberlites. In: Kimberlite Occurrence and Origin: A basis for conceptual models in exploration: In GLOVER, J.E., & HARRIS, P.G., (EDS.), *Geology Department and University Extension, University of Western Australia*, 8, p. 143-166.

GURNEY, J.J., 1989, Diamonds. In: ROSS, J., JAQUES, A.L., FERGUSON, J., GREEN, D.H., O'REILLY, S.Y., DANCHIN, R.V., & JANSE, A.J.A., (EDS.) *Kimberlites and Related Rocks, Geol. Soc. Austrl. Spec. Publ. 14*, Vol. II, p. 935-965.

GURNEY, J.J., BRISTOW, J.W., & MOORE, A.E., 1978, Orientation study on the use of indicator minerals compositions in prospecting for diamondiferous kimberlites: *Unpub. report by Minerale dienste, Cape Town to Falconbridge Explorations, Johannesberg.*

GURNEY, J.J., HARRIS, J.W., OTTER, M.L., AND RICKARD, R.S., 1995, Jwaneng diamond inclusions: *Ext. Abs. 6th Inter. Kim. Conf., Novosibirsk*, p. 208-210.

GURNEY, J.J., HARRIS, J.W., & RICKARD, R.S., 1979, Silicate and oxide inclusions in diamonds from Finsch kimberlite pipe: In BOYD, F.R., & MEYER, H.O.A., (EDS.): *Kimberlites, Diatremes and Diamonds, AGU*, p. 1-15.

GURNEY, J.J., HARRIS, J.W., & RICKARD, R.S., 1984a, Minerals associated with diamonds from the Roberts Victor Mine: *Proc. 3rd Int. Kimb. Conf.*, IIB, p. 25-32.

GURNEY, J.J., HARRIS, J.W., & RICKARD, R.S., 1984b, Silicate and oxide inclusions in diamonds from the Orapa Mine, Botswana: In KORNPROBST, J., (ED.), *Kimberlite II: The Mantle and Crust-Mantle Relationships, Elsevier, Amsterdam,* p. 3-10.

GURNEY, J.J., HARTE, B., & COX, K.G., 1975, Mantle xenoliths in the Matsoku kimberlite pipe: *Phys. Chem. Earth,* 9, p. 507-529.

GURNEY, J.J., & HATTON, C.J., 1989, Diamondiferous minerals from the Star Mine, South Africa: *Spec. Publ. Geol. Soc. Aust 14,* p. 1022-1028.

GURNEY, J.J., HELMSTAEDT, H.H., & MOORE, R.O., 1993, A review of the use and application of mantle mineral geochemistry in diamond exploration. *Pure and Applied Chemistry,* 65, p. 2423-2442.

GURNEY, J.J., & MENZIES, A.H., 1998, Small Mines Field Guide, 7IKC Cape Town, 1997.

GURNEY, J.J., MOORE, R.O., OTTER, M.L., KIRKLEY, M.B., HOPS, J.J., & MCCANDLESS, T.E., 1991, Southern African kimberlites and their xenoliths: In KAMPUNZU, A.B., & LUBALA, R.T., (EDS.), *Magmatism in Extensional Structural Settings: the Phanerozoic African Plate, Springer-Verlag, Berlin,* p. 495-536.

GURNEY, J.J., & SWITZER, G.S., 1973, The discovery of garnets closely related to diamonds in the Finsch Pipe, South Africa: *Contrib. Minerals. Petrol.,* 39, p. 103-116.

GURNEY, J.J., & ZWEISTRA, P., 1995, The interpretation of the major element compositions of mantle minerals in diamond exploration: *J. Geochem. Explor.,* 53, p. 293-309.

HAGGERTY, S.E., 1979, Spinels in high pressure regimes: In BOYD AND MEYER (Eds.), p. 183-196.

HAGGERTY, S.E., 1986, Diamond genesis in a multiply-constrained model: *Nature,* 320, p. 34-38.

HAGGERTY, S.E., 1991, Emplacement and implications of ultra-deep xenoliths and diamonds from the transition zone: *Proc. 5th Inter. Kimb. Conf., Brazil, Comphania de Pequisa de Recursos Minerais, Special Publication,* 2/91, p. 157-159.

HAGGERTY, S.E., 1994, Superkimberlites: a geodynamic window into the Earths's core: *Earth Planet. Sci. Lett.,* 122, p. 57-69.

HALL, A.E., & SMITH, C.B., 1984, Lamproite diamonds – are they different?: IN GLOVER & HARRIS (EDS.) *Kimberlite occurrence and origin: a basis for conceptual models in exploration, Geol. Dept. Uni. Western Aust., Pub. 8,* p. 167-212.

HAMILTON, W.B., 1998, Archean Tectonics and magmatism: *Int. Geol. Rev.,* 40, P. 1-39.

HANLEY, P.L., KIFLAWI, I., & LANG, A.R., 1977, On topographically identifiable sources of cathodoluminescence in natural diamonds: *Phil. Trans. R.. Soc. Lond.,* A284, p. 329-368.

HARLEY, S.L., 1984, An experimental study of the partitioning of Fe and Mg between garnet and orthopyroxene: *Contrib. Mineral. Petrol.,* 86, p. 359-373.

HARMAN, H.H., 1967, Modern Factor Analysis, Chicago: Univeristy Press of Chicago.

HARRIS, J.W., 1987, Recent physical, chemical and isotopic research of diamonds. In: Mantle Xenoliths, NIXON, P.H. (ed.): *John Wiley and Sons, Chichester, England,* p. 447-500.

HARRIS, J.W., 1992, Diamond geology. In: FIELD, J.E., (ed) The properties of natural and synthetic diamond: *Academic Press, London,* p. 345-393.

HARRIS, J.W., & GURNEY, J.J., 1979, Inclusions in diamond. In: FIELD, J.E., (Editor), The Properties of Diamond: *Academic Press, London,* p. 555-591.

HARRIS, J.W., HAWTHORNE, J.B., & OOSTERVELD, M.M., 1983, A comparison of diamond characteristics from the De Beers pool mines, Kimberley, South Africa: In KORNPROBST, J. (ED.), *Annales Scientifiques de l'Universiti de Clermont Ferrand II, Elsevier, Amstedam,* 74, p. 1-13.

HARRIS, J.W., HUTCHISON, M.T., HURSTHOUSE, M., LIGHT, M., & HARTE, B., 1997, A new tetragonal silicate mineral occurring as inclusions in lower-mantle diamonds: *Nature,* 387, p. 486-488.

HARRIS, J.W., MILLEDGE, H.J., BARRON, T.H.K., & MUNN, R.W., 1970, Thermal expansion of garnets included in diamond: *J. Geophys. Res.*, 75, p. 5775-5792.

HART, S.R., & RAVIZZA, G.E., 1995, Os partitioning between phases in lherzolite and basalt, in BASU A., & HART, S.R., (eds): American Geophysical Union Monograph, 95, Washington: *American Geophysical Union,* p. 123-144.

HARTE, B., 1977, Rock nomenclature with particular relation to deformation and recrystallisation textures in olivine bearing xenoliths: *Journal of Geology,* 85, p. 279-288.

HARTE, B., 1983, Mantle peridotites and processes – the kimberlite sample. In: Hawkesworth, C.J., & Norry, M.J., (eds.) Continental basalts and mantle xenoliths: *Shivaa Nantwick,* p. 46-91.

HARTE, B., 1987, Metasomatic events recorded in mantle nodules. In: Nixon, P.H., (Ed.): Mantle Xenoliths, p. 46-91 *Shiva Publishing.*

HARTE, B., COX., K.G., & GURNEY, J.J., 1975, Petrography and geological history of upper mantle xenoliths from the Matsoku kimberlite pipe: *Phys. Chem. Earth,* 9, p. 477-506.

HARTE, B., & GURNEY, J.J., 1975, Ore mineral and phlogopite mineralisation within ultramafic nodules from the Matsoku kimberlite pipe, Lesotho: *Carnegie Inst. Washington Yearb.,* 74, p. 528-536.

HARTE, B., & GURNEY, J.J., 1981, The mode of formation of chromium-poor megacryst suites from kimberlites: *Journal of Geology,* 89, p. 749-753.

HARTE, B., GURNEY, J.J., & HARRIS, J.W., 1980, The formation of peridotitic suite inclusions in diamonds: *Contrib. Mineral. Petrol.,* 72, p. 181-190.

HARTE, B., & HARRIS, J.W., 1994, Lower mantle mineral associations preserved in diamonds: *Mineral. Mag.*, 58A, p. 384-385.

HARTE, B., & HAWKESWORTH, C.J., 1989, Mantle domains and mantle xenoliths, 4th International Kimberlite Conference: *Kimberlites and Related Rocks,* Vol. 2, *Geol.Soc. Aust. Spec. Publ.* 14, p. 649-686.

HARTE, B., HUNTER, R.H., & KINNY, P.D., 1993, Melt geometry, movement and crystallization, in relation to mantle dykes, veins and metasomatism: *Philosophical Transactions of the Royal Society of London,* Aa342, p. 1-21.

HARTE, B., & KIRKLEY, M.B., 1996, Partitioning of trace elements between clinopyroxene and garnet: Data from mantle eclogites: *Chem. Geol.,* 136, p. 1-24.

HARTE, B., WINTERBURN, P.A., & GURNEY, J.J., 1987, Metasomatic phenomena in garnet peridotire facies mantle xenoliths from the Matsoku kimberlite pipe, Lesotho. In: Mantle Metasomatism (eds. Menzies, M.A., & Hawkesworth, C.J.) *Academic Press, London,* p. 145-220.

HATTON, C.J., 1978, The Geochemistry and origin of xenoliths from the Roberts Victor Mine: *Unpub. PhD. Dissertation, University of Cape Town.*

HATTON, C.J., & GURNEY, J.J., 1979, A diamond-graphite eclogite from the Roberts Victor mine: IN BOYD, F.R. AND MEYER, H.O.A. (EDS.), *Kimberlites, Diatremes and Diamonds,* p. 29-36, A.G.U., Washington.

HATTON, C.J., & GURNEY, J.J., 1987, Roberts Victor eclogites and their relation to the mantle. In: NIXON, P.H., (ed.) Mantle Xenoliths, p. 453-463, *Wiley, Chichester.*

HAURI, E.H., & HART, S.R., 1996, Rhenium abundances and systematics in oceanic basalts: *Chem. Geol.*, 139, p. 185-205.

HAURI, E.H., LASSITER, J.C., & DEPAOLO, D.J., 1996, Osmium isotope systematics of drilled lavas from Mauna Loa, Hawaii: *J. Geophys. Res.*, 101, p. 11793-11806.

HAURI, E.H., PEARSON, D.G., BULANOVA, G.P., & MILLEDGE, H.J., 1999, Microscale variations in C and N isotopes within mantle diamonds revealed by SIMS: *Proc. 7th Int Kimberlite Conf, Cape Town, Vol. 1*, p. 341-347.

HELMSTAEDT, H.H., & DOIG, R., 1975, Eclogite nodules from kimberlite pipes of the Colorado Plateau – samples of subducted Franciscantype oceanic lithosphere: *Physics and Chemistry of the Earth*, 9, p. 95-111.

HELMSTAEDT, H.H., & HARRAP, R.M., 1999, Tectonic aspects of the diamond – kimberlite connection: testing for explanatory coherence in upper mantle models: *Proc. 7th Int Kimberlite Conf, Cape Town, Vol. 1*, p. 361-371.

HELMSTAEDT, H.H., & SCHULZE, D.J., 1989, Southern African kimberlites and their mantle sample: implications for Archean tectonics and lithosphere evolution. In: Kimberlites and Related Rocks, ROSS, J., (ed.): *Geological Society of Australia, Special Publication*, 14, p. 358-368.

HENDERSON, P., 1982, *Inorganic Geochemistry*: Pergamon Press.

HERZBERG, C.T., 1993, Lithosphere peridoties of the Kaapvall craton: *Earth and Planetary Science Letters*, 120, p. 13-29.

HILLS, D.V., & HAGGERTY, S.E., 1989, Petrochemistry of eclogites from the Koidu kimberlite complex, Sierra Leone: *Contrib. Mineral. Petrol.*, 103, p. 397-422.

HINTON, R.W., 1996, Ion microprobe analysis in geology: in *Potts, P.J., Bowles, J.F.W., Reed, S.J.B., & Cave, M.R. (eds.), Microanalytical Techniques in Geosciences, Chapman and Hall, London*, p. 234-289.

HOAL, K.E.O., HOAL, B.G., ERLANK, A.J., & SHIMIZU, N., 1994, Metasomatism of the mantle lithosphere recorded by rare earth elements in garnets, *Earth Planet. Sci. Letters.*, 126, p. 303-313.

HUTCHINSON, M.T., 1997, Composition of the deep transition zone and lower mantle shown by diamonds and their inclusions: *Unpub. PhD Thesis, University of Edinburgh*, U.K., pp. 646.

IRELAND, T.R., RUDNICK, R.L. & SPETSIUS, Z., 1994, Trace elements in diamond inclusions from eclogites reveal link to Archean granites: *Earth and Planetary Science Letters*, 128, p. 199-213.

JACOB, D.E., JAGOUTZ, E., LOWRY, D., MATTEY, D., & KUDRJAVTSEVA, G., 1994, Diamondiferous eclogites from Siberia: Remnants of Archean oceanic crust: *Geochimica et Cosmochimica Acta*, 58, p. 5191-5207.

JACQUES, A.L., O'NEILL, H.ST.C., SMITH, C.B., MOORE, J., CHAPPELL, B.W., 1990, Diamondiferous peridotite xenoliths from the Argyle (AK1) lamproite pipe, Western Australia: *Contrib. Mineral. Petrol.*, 104, p. 255-276.

JAGOUTZ, E., DAWSON, J.B., HOERNES, S., SPETTEL, B., & WANKE, H., 1984, Anorthositic oceanic crust in the Archean Earth: *15th Lunar Planet. Sci. Conf.*, 395-396 (abstr.).

JAVOY, M., PINEAU, F., & DELORME, H., 1986, Carbon and nitrogen isotopes in the mantle: *Chem. Geol.*, 57, p. 41-62.

JAVOY, M., PINEAU, F., & DEMAIFFE, D., 1984, Nitrogen and carbon isotopic composition in the diamonds of Mbuji Mayi (Zaire): *Earth Planet. Sci. Lett.*, 68, p. 399-412.

JERDE, E.A., TAYLOR, L.A., CROZAZ, G., SOBOLEV, N.V. & SOBOLEV, V.N., 1993, Diamondiferous eclogites from Yakutia, Siberia: Evidence for a diversity of protoliths: *Contrib. Mineral. Petrol.*, 114, p. 189-202.

JOHNSON, J.P., 1908, Note on the lherzolite and eclogite boulders from the Roberts Victor Mines: *Trans. Geol. Soc. S. Afr.*, 10, p.112-114.

KAISER, W., & BOND, W.L., 1959, Nitrogen, a major impurity in common type I diamond: *Phys.Rev.*, 115, p. 857-863.

KANDA, H., OHSAWA, T., & YAMAOKA, S., 1990, Formation of nitrogen pairs in synthetic diamond durning growth: In SAITO, S. (ed.) *Science and Tecnology of New Diamond*, p. 339-344.

KELEMEN, P.B., DICK, H.J.B., & QUICK, J.E, 1992, Formation of harzburgite by passive melt/rock reaction in the upper mantle: Nature, 358, p. 635-641.

KELEMEN, P.B., 1998, One view on the genesis of cratonic periodoties: *Ext. Abs. 7th Int. Kimb. Conf., Cape Town*, p. 398-401.

KELLER, R.A, TAYLOR, L.A., SNYDER, G.A, SOBOLEV, N.V., CARLSON, W.D., BEZBORODOV, S.M., & SOBOLEV, N.V., 1999, Detailed pull-apart of a diamondiferous eclogite xenolith: Implications for mantle processes during diamond genesis: *Proc. 7th Int. Kimb. Conf., 1*, p. 397-402.

KENNEDY, C.S., & KENNEDY, G.C., 1976, The equilibrium boundary between graphite and diamond: *J. Geophys. Res.*, 81, p. 2467-2470.

KESSON, S.E., & RINGWOOD, A.E., 1989, Slab-mantle interactions, 2. The formation of diamonds: *Chem. Geol.*, 78, p. 97-118.

KIRKLEY, M.B., GURNEY, J.J., & LEVINSON, A.A., 1991, Age, origin and emplacement of diamonds: Scientific advances in the last decade: *Gems and Geology*, 27, p. 465-479.

KIRKLEY, M.B., GURNEY, J.J., OTTER, M.L., HILL, S.J., & DANIELS, L.R.M., 1991, The application of C isotope measurements to the identification of the sources of C in diamonds, a review: *Appl. Geochem.*, 6, p. 477-494.

KLUMP, J., 1995, An in depth study of the garnets from Swartruggens dykes: *Unpub. Hons thesis, Uni. Of Cape Town*, pp. 45.

KLYUEV, Y.A., DUDENKOV, Y.A., & NEPSHA, V.I., 1973, *Geochem. Int.*, 10, p. 781.

KÖHLER, T., & BREY, G.P., 1990, Calcium exchange between olivine and clinopyroxene calibrated as a geothermobarometer for natural peridotites from 2 to 60kb with applications: -*Geochim. Cosmo. Acta*, 54, p. 2375-2388.

KOPYLOVA, M.G., GURNEY, J.J., & DANIELS, L.R.M., 1997, Mineral inclusions in diamonds from the River Ranch kimberlite, Zimbabwe: *Contrib. Mineral. Petrol.*, 129, p. 366-384.

KRAMERS, J.D., 1979, Lead, uranium, strontium, potassium and rubidium in inclusion-bearing diamonds and mantle-derived xenoliths from southern Africa: *Earth Planet. Sci. Lett.*, 42, p. 58-70.

KROGH, E.J., 1988, The garnet-clinopyroxene Fe-Mg geothermometer – a reinterpretation of existing experimental data: *Contrib. Mineral. Petrol.*, 99, p. 8-44.

KYSER, T.K., 1991, Stable isotopes in the Continental Lithospheric Mantle: In Continental Mantle (ed. MENZIES, M.A.), *Clarendon Press*, p. 127-156.

LAWLESS, P.J., 1977, Some aspects of the mineral chemistry of the peridotite xenolith suite from the Bultfontein diamond mine, Kimberley, South Africa: *Unpub. PhD. Thesis, Univ. of Cape Town.*

LAWLEY, D.N., AND MAXWELL, A.E, 1971, Factor analysis as a statistical mthod, New York: *American Elseiver.*

LAX, M. & BURSTEIN, E., 1955, Infrared lattice absorption in ionic and homopolar crystals: *Phys. Rev.*, 97 p. 39-52.

LEE, H.Y., & GANGULY, J., 1988, Equilibrium compositions of coexisting garnet and orthopyroxene: experimental determinations in the system FeO-MgO-Al_2O_3-SiO_2 and applications: *J.Petrol.*, 29, p. 93-113.

LOUBSER, J.H.N., & VAN WYK, J.A., 1981, *Diamond Conference Abstracts, Reading,* p. 35-40, (unpublished).

LOUBSER, J.H.N., & WRIGHT, A.C.J., 1973, Discussion on the Endor and ESR spectra of diamonds with the N3 optical system: *Diamond Research, Industrial Diamond Information Bureau,* p. 16-20.

LOWRY, D., MATTEY, D.P., MACPHERSON, C.G., & HARRIS, J.W., 1993, Oxygen isotope variations among peridotitic and eclogitic syngenetic inclusions in diamond: *Terra Abstr.*, 5, p. 373-374.

LUTH, R.W., 1993, Diamonds, eclogites and the oxidation state of the Earth's mantle: *Science,* 261, p. 66-68.

LUTH, R.W., & CANIL, D., 1993, Ferric iron in mantle-derived pyroxenes and a new oxybarometer for the mantle: *Contrib. Mineral. Petrol.*, 113, p. 236-248.

LUTH, R.W., VIRGO, D., BOYD, F.R., & WOOD, B.J., 1990, Feric iron in mantle-derived garnets: Implications for thermobarometry and for the oxidation state of the mantle: *Contrib. Mineral. Petrol.,* 104, p. 56-72.

MAALOE, S., & AOKI, K., 1977, The major element composition of the upper mantle estimated from the composition of lherzolites: *Contributions to Mineralogy & Petrology,* 63, p. 161-173.

MACGREGOR, I.D., 1974, The system MgO-Al2O3-SiO2: solubility of Al2O3 in enstatite for spinel and garnet peridotite compositions: *Am. Min.*, 59, p. 110-119.

MACGREGOR, I.D., & CARTER, J.L., 1970, The chemistry of clinopyroxenes and garnets of eclogite and peridotite xenoliths from the Roberts Victor mine, South Africa: *Phys. Earth Planet. Int.*, 3, p. 391-397.

MACGREGOR, I.D., & MANTON, W.I., 1986, Roberts Victor eclogites: Ancient oceanic crust: *Journal of Geophysical Research,* 91, B14, p. 14063-14079.

MATTHEWS, M. HARTE, B., & PRIOR, D., 1992, Mantle garnets: A cracking yarn: *Geochimica et Cosmochimica Acta,* 56, p. 2633-2642.

MATTER, V., 1972, George Patton 1830-1914. Historical Society of Kimberley and Northern Cape: *Kimberley Series,* 1, p. 47-51.

MATTEY, D., LOWRY, D., & MACPHERSON, C., 1994, Oxygen isotope composition of mantle peridotite: *Earth Planet. Sci. Lett.*, 128, p. 231-241.

MCCALLUM, M.E., & EGGLER, D.H., 1976, Diamonds in an upper mantle peridotite nodule from kimberlite in southern Wyoming: *Science,* 192, #4236, p. 253-256.

MCCAMMON, C. A., 1999, Methods for determination of Fe3+/ΣFe in microscopic samples: *Proc. 7th Int Kimberlite Conf, Cape Town, Vol. 2,* p. 540-545.

MCCANDLESS, T.E. & COLLINS, D.S., 1989, A diamond-graphite eclogite from the Sloan 2 kimberlite, Colorado, USA: *Proc. 4th Int. Kimb. Conf., Perth. Geol. Soc. Aust.Spec. Pub. 14*, p. 1063-1069.

MCCANDLESS, T.E., & GURNEY, J.J., 1989, Sodium in garnet and potassium in clinopyroxene: criteria for classifying mantle eclogites: *Proc. 4th Int. Kimb. Conf., Perth. Geol. Soc. Aust.Spec. Pub. 14*, p. 827-833.

MCCANDLESS, T.E., & GURNEY, J.J., 1997, Diamond eclogites, comparison with carbonaceaous chondrites, carbonaceaous shales, and microbial carbon-enriched MORB: *Russian Geology and Geophysics*, 38, p. 394-404.

MCDONOUGH, W.F., & SUN, S-S, 1995, The composition of the Earth: *Chemical Geology,* 120, p. 223-253.

MCDADE, P., & HARRIS, J.W., 1999, Syngenetic inclusion bearing diamonds from Letsang-la-Terai, Lesotho: *Proc. 7th Int Kimberlite Conf, Cape Town, Vol. 2,* p. 557-565.

MARTIN, C.E., 1991, Os isotopic characteristics of mantle derived rocks: *Geochim. Cosmochim. Acta.*, 55, p. 1421-1434.

MEISEL, T., WALKER, R.J., & MORGAN, J.W., 1986, The Osmium isotopic composition of the Earth's primitive upper mantle: *Nature*, 383, p. 517-520.

MENDELSSOHN, M.J., & MILLEDGE, H.J., 1995, Geologically significant information from routine analysis of the mid-infrared spectra of diamonds, *Internat. Geol. Rev.*, 37, p. 95-110

MENDELSSOHN, M.J., & MILLEDGE, H.J., 1995, Morphological characteristics of diamond populations in relation to temperature-dependant growth and dissolution rates: *Int. Geol. Rev.*, 37, p. 285-312.

MENZIES, A.H., & BAUMGARTNER, M.C., 1998, Application of garnet geothermobarometry to southern African kimberlites: *Ext. Abs. 7th Int. Kimb. Conf., Cape Town*, p. 570-572.

MENZIES, M.A., 1990, (ed.) *Continental Mantle: Clarendon Press, Oxford*, pp. 184.

MENZIES, M.A, & HAWKESWORTH, C.J. (EDS.), 1987, Mantle Metasomatism, *Academic Press, London.*

MEYER, H.O.A, 1987, Inclusions in diamond: In: Nixon, P.H. ed., Mantle Xenoliths: *Chichester, J. Wiley and Sons*, p. 501-522.

MEYER, H.O.A., & BOYD, F.R., 1969, Inclusions in diamonds: *Carnegie Inst. Washington Yearb., 68*, p. 315-320.

MEYER, H.O.A., MILLEDGE, H.J., SUTHERLAND, F.J., & KENNEWELL, P., 1997, Unusual diamonds and unique inclusions from New South Wales, Australia: *Proc. 6th Int. Kimb. Conf., Vol 2: Diamonds: Characterisation, genesis and exploration, Russian Geology and Geophysics*, 38, p. 305-331.

MEYER, H.O.A, ZHANG, A., MILLEDGE, H.J., & MENDELSSOHN, M.J., 1994, Diamonds and inclusions in diamonds from Chinese kimberlites: In Meyer H.O.A. and Leonardos, O.H. (Eds.), Diamonds: Characterisation, Genesis and Exploration, *CPRM Spec. Publ. 1B/93*, p. 98-105.

MILLEDGE, H.J., BULANOVA, G.P., TAYLOR, W.R., WOODS, P.A., & TURNER, P.H., 1995, Internal morphology of Yakutian diamonds – a cathodoluminescence and infrared mapping study: *Ext. Abs. 6th Int. Kimb. Conf. Novosibirsk, Russia*, p. 384-386.

MILLEDGE, H.J., & MENDELSSOHN, M.G., 1988, Infrared microspectroscopy with special reference to computer-controlled mapping of inhomogeneous specimens, in *Creaser, C.S., & Davies, A.M.C. (eds.): Analytical Applications of Spectroscopy, Roy. Soc. Chem.*, London, p. 217-226.

MILLEDGE, H.J., MENDELSSOHN, M.G., SEAL, M., ROUS, J.E., SWART, P.K., & PILLINGER, C.T., 1983, Carbon isotopic variation in special type II diamonds: *Nature*, 303, p. 791-795.

MITCHELL, R. H., 1986, Kimberlites: Mineralogy, Geochemistry, and Petrology: *Plenum Press*, New York, pp. 442.

MITCHELL, R. H., 1995, Kimberlites, Orangeites, and Related Rocks: *Plenum Press*, New York, pp. 410.

MOFOKENG, S.W., 1996, Some aspects of the geochemistry of the Frank Smith Kimberlite pipe mantle nodules: *Hons. thesis*, Univ. Cape Town, unpublished, pp. 31

MOFOKENG, S.W., 1998, A comparison of the nickel and the conventional geothermometers with respect to th eJagersfontein and the Matsoku kimberlite peridotite xenoliths: *Unpub. Msc Thesis, University of Cape Town.*

MOORE, R.O., & GURNEY, J.J., 1985, Pyroxene solid solution in garnets included in diamond: *Nature*, 318, p. 553-555.

MOORE, R.O., & GURNEY, J.J., 1989, Mineral inclusions in diamond from the Monastry kimberlite, South Africa. In: ROSS, J., JAQUES, A.L., FERGUSON, J., GREEN, D.H., O'REILLY, S.Y., DANCHIN, R.V., & JANSE, A.J.A., (eds.), Kimberlites and Related Rocks: *Geol. Soc. Austrl. Spec. Publ. 14, vol II*, p. 1029-1041.

MOORE, R.O., GURNEY, J.J., & FIPKE, C., 1989, The development of advance technology to distinguish between diamondiferous and barren diatremes: *Geological Survey of Canada Open file report 2124.*

MORIMOTO, N., 1998, Nomenclature of pyroxenes: *Min. Mag.*, 52, P. 535-550.

MORGAN, J.W., 1986, Ultramafic xenoliths: clues to the Earth's late accreationary history: *J. Geophs. Res.*, 91, p. 12375-12387.

MORGAN, J.W., GOLIGHTLY, D.W., & DORRZAPF, A.F., 1991, Methods for the separation of rhenium, osmium and molybdenum applicable to isotope geochemistry: *Talanta*, 38, p. 259-265.

NAVON, O., 1991, Infrared determination of high internal pressures in diamond fluid inclusions: *Nature*, 353, p. 746-748.

NAVON, O., 1999, Diamond formation in the Earth's mantle: *Proc. 7th Int Kimberlite Conf, Cape Town, Vol. 2*, p. 618-621.

NEAL, C.R., TAYLOR, L.A., DAVIDSON, J.P., HOLDEN, P., HALLIDAY, A.N., NIXON, P.H., PACES, J.B., CLAYTON, R.N., & MAYEDA, T.K., 1990, Eclogites with oceanic crustal and mantle signatures from the Bellsbank kimberlite: South Africa. Part 2: Sr, Nd, and O isotope geochemistry: *Earth and Planetary Science Letters*, 99, 362-379.

NICKEL, K.G. & GREEN, D.H., 1985, Empirical geothermobarometry for garnet peridotites and implications for the nature of the lithosphere, kimberlites and diamonds: *Earth and Planetary Science Letters*, 73, p.158-168.

NIXON, P.H., 1987, Kimberlite xenoliths and their cratonic setting. In: Nixon, P.H. (ed.), Mantle xenoliths: *Wileey, Chichester*, p. 215-239.

NIXON, P.H., & BOYD, F.R., 1973, Petrogenesis of the granular and sheared ultrabasic nodule suite in kimberlites. In: *NIXON, P.H., 1973*, p. 48-56.

NIXON, P.H., VAN CALSTERAN PWC., BOYD, F.R., & HAWKESWORTH, C.J., 1987, Harzburgites with garnets of diamond facies from southern African kimberlites. In: Nixon, P.H. (ed.) Mantle xenoliths: *Wiley, Chichester*, p. 523-533.

NOVAK, G.A. & GIBBS, G.V., 1971, The crystal chemistry of the silicate garnets: *American Mineralogist*, 56, p. 791-825.

O'HARA, M.J., SAUNDERS, M.J., & MERCY, E.L.P., 1987, Garnet-peridotite, primary ultrabasic magma and eclogite; interpretation of upper mantle processes in kimberlite: *Physics and Chemistry of the Earth*, 9, p. 571-604.

O'HARA, M.J., & YODER, H.S., 1967, Formation and fractionation of basic magmas at high pressures: SCOTT, J., *Geol.*, 3, p. 67-117.

O'NEILL, H.C., JACQUES, A.L., SMITH, C.B., & MOON, J., 1986, Diamond bearing peridotite xenoliths from Argyle AKI pipe. In: 4th Int. Kimb. Conf. Perth. Ext. Abstr.: *Geol, Soc. Aust.*, 16, p. 300-302.

O'NEILL, H.C, & WOOD, B.J., 1979, An experimental study of Fe-Mg partitioning between garnet and olivine and its calibration as a geothermometer: *Contrib. Mineral. Petrol.*, 70, p. 59-70.

O'NIONS, R.K., 1987, Relationship between chemical and convective layering in the Earth: *Journal of the Geological Society London*, 144, 259-274.

O'REILLY, S.Y. & GRIFFIN, W.L., 1995, Trace element partitioning between garnet and orthopyroxene in mantle derived pyroxenites and eclogites: P-T-X controls: *Chem. Geol.*, 121, p. 105-130.

OTTER, M.L., 1990, Diamonds and their mineral inclusions from the Sloan diatremes, Colorado-Wyoming state line kimberlite district, North America: *Unpub. PhD Thesis, University of Cape Town, RSA*.

OTTER, M.L., GERNEKE, D.A., HARTE, B., GURNEY, J.J., HARRIS, J.W., & WILDING, M.C., 1991, Diamond growth histories revealed by cathodoluminescene and carbon isotope studies: *Ext. Abstr. 5th Int. Kimberlite Conf. Brazil*, p. 318-319.

OZIMA, M, 1989, Gases in diamond: *Ann. Rev. Earth Planet. Sci.*, 17, p. 361-384.

OZIMA, M., & ZASHU, S., 1983, Primitive helium in diamonds: *Science*, 219, p. 1067-1068.

PEARSON, D.G., BOYD, F.R., HAGGERTY, S.E., PASTERIS, J.D., FIELD, S.W., NIXON, P.H., & POKHILENKO, N.P., 1994, The characterisation and origin of graphite in cratonic lithospheric mantle: a petrological carbon isotope and Raman spectroscopic study: *Contrib. Mineral. Petrol.*, 115, p. 449-466.

PEARSON, D.G., CARLSON, R.W., SHIREY, S.B., BOYD, F.R., & NIXON, P.H., 1995a, Stabilization of Archaean lithosphere mantle: a Re-Os isotope study of peridotite xenoliths from the Kaapvaal craton: *Earth and Planetary Science Letters*, 134, p. 341-357.

PEARSON, D.G., SHIREY, S.B., BULANOVA, G.P., CARLSON, R.W., & MILLEDGE, H.J., 1998, Single crystal Re-Os isotope study of sulphide inclusions from a Siberian diamond: *Geochim. Cosmochim. Acta*. p., 63, p. 703-712.

PEARSON, D.G., SHIREY, S.B., BULANOVA, G.P., CARLSON, R.W., & MILLEDGE, H.J., 1999, Dating and paragenetic distinction of diamonds using the Re-Os isotope system: Applications to some Siberian diamonds: *Proc. 7th Int. Kimberlite Conf. S. Africa*, p. 626-636.

PEARSON, D.G., SHIREY, S.B., CARLSON, R.W., BOYD, F.R., POKHILENKO, N.P., & SHIMIZU, N., 1995b, Re-Os, Sm-Nd, and Rb-Sr isotope evidence for thick Archaean lithospheric mantle beneath the Siberian craton modified by multistage metasomatism: *Geochimica et Cosmochimica Aca.*, 59, p. 959-977.

PEARSON, D.G., SHIREY, S.B., HARRIS, J.W., & CARLSON, R.W., 1998b, Sulphide inclusions in diamonds from the Koffiefontein kimberlite, South Africa: constraints on diamond ages and mantle Re-Os systematics: *Earth. Planet. Sci. Lett.*, 160, p. 311-326.

PEARSON, D.G., SNYDER, G.A., SHIREY, S.B, TAYLOR, L.A., CARLSON, R.W., & SOBOLEV, N.V., 1995c, Archæan Re-Os age for Siberian eclogites and constraints on Archæan tectonics: *Nature*, 374, p. 711-713.

POKHILENKO, N.P. & SOBOLEV, N.V., 1986, Xenoliths of diamondferous peridotites from Udachnaaya kimberlite pipe: *Fourth Internat Kimberlite Conf., Extend Abstr. Geol. Soc. Aust. Abstr.* 16, p. 309-311.

POKHILENKO, N.P., SOBOLEV, N.V., & LAVRENT'EV, Y.G., 1977, Xenoliths of diamondiferous ultramafic rocks form Yakutian kimberlites: *Ext. Abstr. 2nd Int. Kimberlite Conf. USA.*

POLLACK, H.N. & CHAPMAN, D.S., 1977, On the regional variation of heat flow, geotherms and lithospheric thickness: *Tectonophysics*, 38, p. 279-296.

PROZESKY, V.M., PRYBYLOWICZ., W.J., VAN ACHTERBERGH, E., CHURMS, C.L., PINEDA, C.A., SPRINGHORN, K.A, PILCHER, J.V., RYAN, C.G., KRITZINGER, J., SCHMITT, H., & SWART, T., 1995, The NAC nuclear microprobe facility: *Nucl. Instr. Meth. Phys. Res.*, B104, p. 36-42.

PYLE, J.M., & HAGGERTY, S.E., 1997, Eclogites and the metasomatism of eclogites from the Jagersfontein Kimberlite: Punctuated transport and implications for alkali magmatism, *Geochim. Cosmochim. Acta*, 67, p. 1207-1231.

RAMSAY, R.R., 1992, Geochemistry of diamond indicator minerals, *Unpub. PhD thesis, Uni. Western Australia.*

REID, A.M., BROWN, R.W., DAWSON, J.B., WHITFIELD, G.G., & SIEBERT, J.C., 1976, Garnet and clinopyroxene compositions in some diamondiferous eclogites: *Contrib Mineral. Petrol.*, 58, p.203-220.

REISBERG, L.C., & LORAND, J.P., 1995, Longevity of sub-continental mantle lithosphere from osmium isotope systematics in orogenic peridotite massifs: *Nature*, 376, p. 159-162.

REISBERG, L., ZINDLER, A., MARCANTONIO, F., WHITE, W., WYMAN, B., & WEAVER, B., 1993, Os isotope systematics in ocean island basalts: *Earth Planet. Sci. Lett.*, 120, p. 149-167.

RICHARDSON, S.H., 1986, Latter-day origin of diamonds and eclogitic paragenesis: *Nature*, 322, p. 623-626.

RICHARDSON, S.H., CHINN, I.L., & HARRIS, J.W., 1998, Age and origin of eclogitic diamonds from the Jwaneng kimberlite, Botswana: *Extended Abstracts, 7IKC, Cape Town*, p. 734-736.

RICHARDSON, S.H., ERLANK, A.J., HARRIS, J.W., & HART, S.R., 1990, Eclogitic diamonds of Proterozoic age from Cretaceous kimberlites: *Nature*, 346, p. 54-56.

RICHARDSON, S.H., GURNEY, J.J., ERLANK, A.J., & HARRIS, J.W., 1984, Origin of diamonds in old enriched mantle: *Nature*, 310, p. 198-202.

RICHARDSON, S.H., HARRIS, J.W., & GURNEY, J.J., 1993, Three generations of diamonds from old continental mantle: *Nature*, 366, p. 256-258.

RICHARDSON, S.H., & HARRIS, J.W., 1997, Antiquity of peridotitic diamonds from the Siberian craton: *Earth. Planet. Sci. Lett.*, 151, p. 271-277.

RICKARD, R.S., HARRIS, J.W., GURNEY, J.J., & CARDOSO, P., 1989, Mineral inclusions in diamonds from Koffiefontein Mine: *Kimberlites and Related Rocks*, 14, p. 1054-1062.

RICKWOOD, P.C., GURNEY, J.J., & WHITE-COOPER, D.R., 1969, The nature and occurrences of eclogite xenoliths in the kimberlites of Southern Africa. Upper mantle symposium: *Trans. Geol. Soc. S.Afr., Spec. Publ.*, 2, p. 371-393.

RICKWOOD, P.C., & MATHIAS, M., 1970, Diamondiferous eclogite xenoliths in kimberlite: *Lithos*, 3, p. 223-235.

RINGWOOD, A.E., 1966, Chemical evolution of the terrestrial planets: *Geochimica et Cosmochimica Acta*, 30, p. 41-104.

RINGWOOD, A.E., 1975, Composition and Petrology of the Earth's Mantle: *McGraw-Hill, New York,* p. 618.

ROBERTSON, R., FOX, J.J., & MARTIN, A.E., 1934, Two types of diamond: *Phil.Trans.R.Soc.Lond.*, A232, p. 463.

ROBINSON, D.N., 1979, Diamond and graphite in eclogite xenoliths from kimberlite. In: BODY, F.R., & MEYER, H.O.A., (Editors), The Mantle Sample: Inclusions in Kimberlites and Other Volcanics: *American Geophysical Union, Washington, DC.*

ROBINSON, D.N., 1979, Surface textures and other features of diamonds: *Ph.D. thesis (unpubl.), University of Cape Town, South Africa,* pp. 221.

ROBINSON, D.N., GURNEY, J.J., & SHEE, S.R., 1984, Diamond eclogite and graphite eclogite xenoliths from Orapa, Botswana. In: KORNPROBST, J., (Editor), Kimberlites II: The Mantle and Crust-Mantle Relationships: *Elsevier, Amsterdam,* p. 11-24.

ROBINSON, D.N., SCOTT, J.A., VAN NIEKER, K.A., & ANDERSON, V.G., 1989, The sequence of events reflected in the diamonds of some southern African kimberlites. In: ROSS, J.R., et al., (Eds.). Kimberlites and Related Rocks, Vol2: Their Crustal/Mantle Setting, Diamond and Diamond Exploration: *Geol. Soc. Aust. Spec. Publ.* 14, p. 980-990.

ROLLINSON, H., 1997, Eclogite xenoliths in west African kimberlites as residues from Archaean granitoid crust formation: *Nature*, 389, p. 173-176.

ROY-BARMAN, M., & ALLEGRE, C.J., 1994, $^{187}Os/^{188}Os$ ratios of mid-ocean ridge basalts and abyssal peridotites: *Geochim. Cosmochim. Acta.*, 58, p.5043-5054.

ROY-BARMAN, M., & ALLEGRE, C.J., 1995, $^{187}Os/^{186}Os$ in oceanic island arc basalts: tracing oceanic crust recycling in the mantle: *Earth Planet. Sci. Lett.*, 133, p. 411-421.

RUDNICK, R.L., ELDRIDGE, C.S., & BULANOVA, G.P., 1993, Diamond growth history from in situ measurement of Pb and S isotopic compositions of sulfide inclusions: *Geology*, 21, p. 13-16.

RUDNICK, R.L., MCDONOUGH, W.F, ORPIN, A., 1994, Northern Tanzanian peridotite xenoliths: a comparison with Kaapvaal peridotites and inferences on metasomatic interactions: In Meyer H.O.A. and Leonardos, O.H. (Eds.), Kimberlites, related rocks and mantle xenoliths, *CPRM Spec. Publ. 1A/93*, p. 336-353..

RUIZ, J., MCCANDLESS, T.E., & HELMSTAEDT, H.H., 1999, Re-Os model ages for eclogitc xenoliths from the Colorado Plateau, USA: *Proc. 7th Int Kimberlite Conf, Cape Town, Vol. 2* , p. 736-740.

RYAN, C.G., COUSENS, D.R., SIE, S.H., GRIFFIN, W.L., & SUTER, G.F., 1990, Quantitative PIXE microanalysis of geological material using the CSIRO proton microprobe: *Nucl. Instr. Meth. Phys. Res.*, B47, p. 55-71.

RYAN, C.G., GRIFFIN, W.L, & PEARSON, N.J., 1996, Garnet geotherms: Pressure-temperature data from Cr-pyrope garnet xenocrysts in volcanic rocks: *J. Geophys. Res.*, B3, p. 5611-5625.

RYAN, C.G., & JAMIESON, D.N., 1993, Dynamic analysis: On-line quantitative PIXE micro-analysis and its use in overlap-resolved elemental mapping: *Nucl. Instr. Meth. Phys. Res.*, B77, p. 203-214.

SCHRAUDER, M., & NAVON, O., 1993, Solid carbon dioxide in a natural diamond: *Nature*, 365, p. 42-44.

SCHRAUDER, M., & NAVON, O., 1994, Hydrous and carbonatitic fluids in fibrous diamonds from Jwaneng, Botswana: *Geochim. Cosmochim. Acta.*, 58, p. 761-771.

SCHULZE, D.J., 1986, Calcium anomalies in the mantle and a subducted metaserpentinite origin for diamonds: *Nature,* 319, p. 483-485.

SCHULZE, D.J., & HELMSTAEDT, H.H., 1988, Coesite-Sanidine eclogites from kimberlite: products of mantle fractionation or subduction: *J. Geol.*, 96, p. 435-444.

SCHULZE, D.J., WIESE, D. & STEUDE, J., 1996, Abundance and distribution of diamonds in eclogite revealed by volume visualization of CT X-Ray scans: *J. Geology*, 104, p. 109-113.

SELLSCHOP, J.P.F., 1975, Evidence on the environment of diamond genesis from trace element studies of natural diamonds, *Diamond Research*, p. 35-41.

SELLSCHOP, J.P.F., 1992, In: FIELD, J.E. (ed.) *The properties of natural and synthetic diamond*, London, Academic press, p. 91.

SHARP, W.E., 1966, Pyrrhotite: a common inclusion in South African diamonds: *Nature*, 211, p. 402-403.

SHATSKY, V.S., & SOBOLEV, N.V., 1993, Some aspects of origin of diamonds in metamorphic rocks: *Dokl. Akad. Nauk*, 331, p. 1217-1219.

SHATSKY, V.S., SOBOLEV, N.V., & VAVILOV, M.A., 1995, Diamond-bearing metamorphic rocks of the Kokchetav Massif (northern Kazakhstan). In: Coleman, R.G., Wang, X., (eds.) *Ultrahigh-pressure metamorsphism*, p. 427-455.

SHEE, S.R., 1978, The mineral chemistry of xenoliths from the Orapa kimberlite pipe, Botswana: *MSc Thesis, U of CapeTown, Rondebosch.*

SHEE, S.R., & GURNEY, J.J, 1979, The mineralogy of xenoliths from Orapa, Botswana: In BOYD AND MEYER, p. 37-49.

SHEE, S.R., GURNEY, J.J., ROBINSON, D.N., 1982, Two diamond-bearing peridotite xenoliths from the Finsch Kimberlite, South Africa: *Contrib. Mineral. Petrol.*, 81, p. 79-87.

SHERVAIS, J.W., TAYLOR, L.A., LUGMAIR, G.W., CLAYTON, R.N., MAYEDA, T.K., & KOROTEV, R.L., 1988, Early Proterozoic oceanic crust and the evolution of subcontinental mantle: eclogites and related rocks from southern Africa: *Geological Society of America Bulletin*, 100, 411-423.

SHIMIZU, N, 1975, Rare earth elements in garnets and clinopyroxenes from garnet lherzolite nodules in kimberlites: *Earth and Planetary Science Letters*, 25, p. 26-32.

SHIMUZU, N., & ALLEGRE, C.J., 1978, Geochemistry of transition elements in garnet lherzolite nodules in kimberlites: *Contributions to Mineralogy and Petrology*, 67, p. 41.50.

SHIMIZU, N., & RICHARDSON, S.H., 1987, Trace element abundance patterns of garnet inclusions in peridotitic suite diamonds: *Geochim Cosmochim. Acta*, 51, p. 755-758.

SHIMIZU, N., & SOBOLEV, N.V., 1995, Young peridotitic diamonds from the Mir kimberlite pipe: *Nature*, 375, p. 394-397.

SHIMIZU, N., GURNEY, J.J., & MOORE, R., 1989, Trace element geochemistry of garnet inclusions in diamonds from the Finsch and Koffiefontein kimberlite pipes: *28th IGC, Workshop on diamonds*, p. 100-101.

SHIMIZU, N., SOBOLEV, N.V., & YEFIMOVA, E.S., 1997, Chemical heterogeneities of inclusion garnets and juvenile character of peridotitic diamonds from Siberia: *Russ. Geol. Geophys.*, 38, p. 356-372.

SHIREY, S.B., 1997, Re-Os isotopic compositions of mid-continent rift system picrites: implications for plume-lithosphere interaction and enriched mantle sources: *Canadian Journal of Earth Science*, 34, p. 89-503.

SHIREY, S.B., CARLSON, R.W., GURNEY, J.J., & HEERDEN, L.V., 1998, Re-Os systematics of eclogites from Roberts Victor: Implications for diamond growth and Archean tectonic processes: *Extended Abstracts 7IKC, Cape Town.*

SHIREY, S.B., & WALKER, R.J., 1995, Carius tube digestions for low-blank rhenium-osmium analysis: *Analytical Chemistry*, 67, P. 2136-2141.

SKINNER, C.P., 1989, The petrology of peridotite xenoliths from the Finsch kimberlite, South Africa: *Sth. African J. Geol.*, 92, p. 197-206.

SKINNER, E.M.W., & CLEMENT, C.R., 1979, Mineralogical classification of southern African kimberlites, In: BOYD, F.R. AND MEYER, H.O.A. (eds) 1: Kimberlites, diatremes and diamonds: Their geology and geochemistry: *Proceedings of the Second International Kimberlite Conference*, AGU, p. 129-139.

SMITH, C.B., 1983, Rubidium – strontium, uranium – lead and samarium – neodymium isotopic studies of kimberlite and selected mantle derived xenoliths: *Unpub. PhD Thesis, Univ. of the Witwatersrand.*

SMITH, C.B., ALLSOPP, H.L., KRAMERS, J.D., HUTCHINSON G., & RODDICK, J.C., 1985b, Emplacement ages of Jurassic-Cretaceous South African kimberlites by the Rb-Sr method on phlogopite and whole-rock samples: *Trans. Geol. Soc. S. Africa*, 88, 249-266.

SMITH, C.B., GURNEY, J.J., HARRIS, J.W., ROBINSON, D.N., SHEE, S.R., & JAGOUTZ, E., 1989, Sr & Nd isotopic systematics of diamond-bearing eclogite xenoliths and eclogitic inclusions in diamond from southern Africa. In: *Proc. 4th Int. Kimb. Conf., Perth. Geol. Soc. Aust. Spec. Pub. 14*, p. 332-333.

SMITH, C.B., GURNEY, J.J, SKINNER, E.M.W., CLEMENT, C.R., & EBRAHIM, N., 1985a, Geochemical character of southern African kimberlites: a new approach based on isotopic constraints: *Trans. Geol. Soc. Sth. Africa*, 88, p. 267-280.

SMITH, C.B., LUCAS, H., HALL, A.E., & RAMSAY, R.R., 1991, Diamond prospectivity and indicator mineral chemistry: a Western Australian perspective. In: Ext. Abstr., 5th Int. Kimb. Conf.: *CPRM, Spec. Publ. 2/91, Brasilia.*

SMITH, C.B., SCHULZE, D.J., BELL, D.R., & VILJOEN, K.S., 1995, Bearing of the subcalcic, Cr-poor megacryst suite on kimberlite petrogenesis and lithospheric structure: *6th Int. Kimberlite Conf., Novosibirsk, (extended abstracts)*, p. 546-548.

SNYDER, G.A., JERDE, E.A., TAYLOR, L.A., HALLIDAY, A.N., SOBOLEV, V.N., & SOBOLEV, N.V., 1993, Nd and Sr isotopes from diamondiferous eclogites, Udachnaya kimberlite pipe, Yakutia, Siberia: evidence of differentiation in the early Earth?: *Earth and Planetary Science Letters*, 118, p. 91-100.

SNYDER, G.A., TAYLOR, L.A., BEARD, B.L., CROZAZ, G., HALLIDAY, A.N., SOBOLEV, V.N., & SOBOLEV, N.V., 1998a, Reply to a comment by Jacob, D., et al, on "The origins of Yakutian eclogite xenoliths": *Journal of Petrology*, 39, in press.

SNYDER, G.A., TAYLOR, L.A., CROZAC, C., HALLIDAY, A.N., BEARD, B.L., SOBOLEV, V.N., & SOBOLEV, N.V., 1997, The origin of Yakutian eclogite xenoliths: *Journal of Petrology*, 38, 1, p. 85-113.

SNYDER, G.A., TAYLOR, L.A., JERDE, E.A., CLAYTON, R.N., MAYEDA, T.K., DEINES, P., ROSSMAN, G.R., & SOBOLEV, N.V., 1995, Archaean mantle heterogeneity and the origin of diamondiferous eclogites, Siberia: evidence from stable isotopes and hydroxyl in garnets: *American Mineralogist*, 80, p. 799-809.

SOBOLEV, N.V., 1977, Deep seated inclusions in kimberlites and the problem of the composition of the upper mantle, *Amer. Geophys. Union, Washington*, Washington, pp. 279 (English Trans. of Russian edition *Izzdatel'stvo Nauka, SSSR.*, 1974, by BROWN, D.A.).

SOBOLEV, N.V., 1983, Parageneses of the diamonds and the problems of mineral formation in deep seated conditions: *Zap.Vses.Mineral.Obsh.*, 112, p. 389-397.

SOBOLEV, N.V., BAKUMENKO, I.T., YEFIMOVA, E.S., & POKHILENKO, N.P, 1991, Morphological features of macrodiamonds, contents of sodium in garnet and potassium in clinopyroxene from two eclogite xenoliths from the Udachnaya kimberlite pipe, Yakutia (in Russian): *Dokl. Akad. Nauk. SSSR*, 321, p. 585-591.

SOBOLEV, N.V., KAMINSKY, F.V., GRIFFIN, W.L., YEFIMOVA, E.S., WIN, T.T., RYAN, C.G., & BOTKUNOV, A.I., 1997, Mineral inclusions in diamonds from the Sputnik kimberlite pipe, Yakutia: *Lithos*, 39, p. 135-157.

SOBOLEV, N.V., & KUZNETSOVA I.K., 1966, Mineralogy of diamond-bearing eclogites (in Russian): *Doklady Acad. Sci. U.S.S.R.*, 167, p. 1365-8.

SOBOLEV, N.V., LAVRENT'YEV, YU. G., POSPELOVA, L.N. & SOBOLEV, YE V., 1969, Chrome pyropes from Yakutian diamonds (in Russian): *Doklady Aakademii Nauk SSSR*, 189, p. 162-165.

SOBOLEV, N.V., LAVRENT'YEV, YU., G., POSPELOVA, L.N., & USOVA, L.V., 1973, Chrome-rich garnets from kimberlites of Yakutia and their parageneses: *Contrib. Mineral. Petrol.*, 40, p. 39-52.

SOBOLEV, N.V., POKHILENKO, N.P., & YEFIMOVA, E.S., 1984, Diamond-bearing peridotite xenoliths in kimberlites and the problem of the origin of diamonds: *Sov. Geol. Geophys*, 25, p. 62-76.

SOBOLEV, N.V., & SHATSKY, V.S., 1990, Diamond inclusions in garnet from metamorphic rocks: a new environment for diamond formation: *Nature*, 343, p. 742-746.

SOBOLEV, N.V., YEFIMOVA, E.S., TAYLOR, L.A., SNYDER G.A. & SOBOLEV, V.N., 1996, Major and trace element variations in multiple eclogitic inclusions in individual diamonds from Yakutia, Russia: *Trans. Amer. Geophys. Union (EDS)*, 77, p .287.

SOBOLEV, V.N., MCCAMMON, C.A., TAYLOR, L.A., SNYDER, G.A., & SOBOLEV, N.V., 1999, Precise Mössbauer milliprobe determination of ferric iron in rock-forming minerals and limitations of electron microprobe analysis: *Amer. Mineral.*, 84, p. 78-85.

SPETSIUS, Z.V., 1995, Occurrence of diamond in the mantle: a case study from the Siberian Platform. In: GRIFFIN, W.L., (Editor), Diamond Exploration: Into the 21st Century: *J. Geochem. Explor.*, 53, p. 25-39.

SPETSIUS, Z.V., & GRIFFIN, W.L., 1997, Trace elements in minerals from eclogites from Udachnaya pipe, Yakutia: *Proc. 6th Int. Kimb. Conf., Russian Geol. And Geophysics*, 38, p. 240-246.

SPETSIUS, Z.V., & GRIFFIN, W.L., 1998, Secondary phases associated with diamonds in eclogites from from the Udachnaya kimberlite pipe: implications for diamond genesis: *Ext. Abs. 7th Int. Kimb. Conf., Cape Town*, p. 850-851.

STACHEL, T., & HARRIS, J.W., 1997a, Syngenetic inclusions in diamond from the Birim Field (Ghana) - a deep peridotitic profile with a history of depletion and re-enrichment: *Contrib Mineral Petrol*, 127, p. 336-352.

STACHEL, T., & HARRIS, J.W., 1997b, Diamond precipitation and mantle metasomatism - evidence from the trace element chemistry of silicate inclusions in diamonds from Akwatia, Ghana: *Contrib. Mineral. Petrol.*, 129, p. 143-154.

STACHEL, T., HARRIS, J.W., & BREY, G.P., 1998a, Rare and unusual mineral inclusions in diamonds from Mwadui, Tanzania: *Contrib. Mineral. Petrol.*, 132, p. 34-47.

STACHEL, T., HARRIS, J.W., & BREY, G.P., 1999, REE Patterns of Peridotitic and Eclogitic inclusions in diamonds from Mwadui (Tanzania): *Proc. 7th Int. Kimb. Conf.*, 2, p. 829-835.

STACHEL, T., VILJOEN, K.S., BREY, G., & HARRIS, J.W., 1998b, Metasomatic processes in lherzolitic and harzburgitic domains of diamondiferous lithospheric mantle: REE in garnets from xenoliths and inclusions in diamonds: *Earth Planet. Sci. Lett.*, 159, p. 1-12.

STEVENS, J, 1986, *Applied multivariate statistics for the social sciences*, Hillsdale, NJ., Erlbaum.

SUNAGAWA, I., 1984, Morphology of natural and synthetic diamond crystals. In: Sunagawa, I., (ed.), Materials science of the Earth's interior: *Terra Sci. Publ., Tokyo, Japan*, p. 303-330.

SUNAGAWA, I., 1989, Diamond growth at low and high pressure. In: Ext. Abstr., Workshop on Diamonds: *28th Int. Geol. Conf.*, p. 109-112.

SUTHERLAND, G.B.B.M., BLACKWELL, D.E., & SIMMERAL, W.G., 1954, The problem of the two types of diamond: *Nature*, 174, p. 901.

SWEENEY, R.J., PROZESKY, V., & PRZYBYLOWICZ, W., 1995, Selected trace and minor element partitioning between peridotite minerals and carbonatite melts at 18-46 kb pressure: *Geochim. Cosmochim. Acta*, 59(18), p. 3671-3684.

TAPPER, U.A.S., MCMURRAY, W.R., ACKERMANN, G.F., CHURMS, C.L., DE VILLIERS, G., FOURIE, D., GROENEWALD, P.J., KRITZINGER, J., PINEDA, C.A., PILCHER, J.V., SCHMIDT, H., SPRINGHORN, K., & SWART, T., 1993, High-brightness proton beams at the NAC nuclear microprobe: *Nucl. Instr. Meth.*, B77, p. 17-24.

TAYLOR, L.A., & NEAL, C.R., 1989, Ecglogites with oceanic crustal and mantle signatures from the Bellsbank kimberlite, South Africa, Part I: Mineralogy, petrography, and whole rock chemistry: *Journal of Geology*, 97, 551-567.

TAYLOR, L.A., SNYDER, G.A., CROZAZ, G., SOBOLEV, V.N., YEFIMOVA, E.S., & SOBOLEV, N.V., 1996, Eclogitic inclusions in diamonds: Evidence of complex mantle process over time: *Earth and Planet. Sci. Lett.* 142, p. 535-551.

TAYLOR, W.R., BULANOVA, G., & MILLEDGE, H.J., 1995, Quantitative nitrogen aggregation studies of some Yakutian diamonds: constraints on the growth, thermal and deformation history of peridotitic and eclogitic diamonds: *Ext. Abstr. 6th Int. Kimberlite Conf. Russia*, p. 608-610.

TAYLOR, W.R., CANIL, D., & MILLEDGE, H.J., 1996, Kinetics of Ib to IaA nitrogen aggregation in diamond: *Geochim. Cosmochim. Acta.*, 60, p. 4725-4733.

TAYLOR, W.R., GURNEY, J.J., & MILLEDGE, H.J., 1995, Nitrogen aggregation and cathodoluminesence characteristics of diamonds from the Point Lake kimberlite, Slave Province, NWT, Canada: *Ext. Abs. 6th Int.Kimberlite Conf., Novosibirsk*, p. 614-616.

TAYLOR, W.R., JAQUES, A.L., & RIDD, M., 1990, Nitrogen-defect aggregation characteristics of some Australasian diamonds, time-temperature constraints on the source regions of pipe and alluvial diamonds: *American Mineralogist*, 75, p. 1290-1310.

TAYLOR, W.R., & MILLEDGE, H.J., 1995, Nitrogen aggregation character, thermal history, and stable isotope composition of some xenolith-derived diamonds from Roberts Victor and Finch: *Ext. Abs. 6th Int.Kimberlite Conf., Novosibirsk*, p. 620-622.

TOFT, P.B., HILLS, D.V., & HAGGERTY, S.E., 1989, Crustal evolution of the granulite to eclogite transition in xenoliths from kimerlites in the west African craton, *Tectonphys.*, 161, p. 213-231.

TRAUTMAN, R.L., GRIFFIN, B.J., TAYLOR, W.R., SPETSIUS, Z.V., SMITH, C.B., & LEE, D.C., 1997, A comparison of microdiamonds from kimberlite and lamproite of Yakutia and Australia: *Russian Geology and Geophysics*, 38, p. 341-355.

TSAI, H.M., MEYER, H.O.A., MOREAU, J., MILLEDGE, J., 1979, Mineral inclusions in diamond: Premier, Jagersfontein and Finsch kimberlites, South Africa, and Williamson mine, Tanzania. In: BOYD, F.R.,

MEYER, H.O.A., (eds), Kimberlites, diatremes, and dimonds: their geology, petrology, and geochemistry: *Am. Geophys Union, Washington, DC*, p. 16-26.

URUSOVSKAYA, A.A., & ORLOV, YU.L., 1964, Nature of plastic deformation of diamond crystals: *Dokl.Akad.Nauk,S.S.S.R.*, 154, p. 112-115.

VAN ACHTERBERGH, 1994, The development of the National Accelerator Centre Proton Microprobe as an analytical tool in geochemistry: *Unpub. MSc. Thesis*, University of Cape Town.

VAN COLLER, B.R., 1995, An in depth study of the Newlands Kimberlite cluster: *Hons thesis*, Uni. Of Cape Town (unpublished), pp.39.

VAN HEERDEN, L.A, & GURNEY, J.J, 1994, Diamond grades at Newlands Kimberlite, Part 1: Blow 2: *Unpubl. Report for Gem Mining.*

VILJOEN, K.S, 1995, Graphite- and diamond-bearing eclogite xenoliths from the Bellsbank kimberlites, Northern Cape, South Africa: *Contrib. Mineral. Petrol.*, 121, P. 414-423.

VILJOEN, K.S., ROBINSON, D.N., SWASH, P.M., GRIFFIN, W.L., OTTER, M.L., RYAN, C.G., & WIN, T.T., 1994, Diamond and graphite-bearing peridotite xenoliths from the Roberts Victor kimberlite, South Africa. In: MEYER, H.O.A., & LEONARDOS, O.H., (eds.), Proc. 5th Int. Kimberlite Conf. Kimberlites I: Kimberlites, Related Rocks and Mantle Xenoliths: *Companhia de Pesquisa de Recursos minerais, Rio de Janeiro*, p. 285-303.

VILJOEN, K.S., SMITH, C.B., & SHARP, Z.D., 1996, Stable and radiogenic isotope study of eclogite xenoliths from the Orapa kimberlite, Botswana: *Chemical Geology*, 131, p. 235-255.

VILJOEN, K.S., SWASH, P.M., OTTER, M.L., SCHULZE, D.J., & LAWLESS, P.J., 1992, Diamondiferous garnet harzburgites from the Finsch kimberlite, Northern Cape, South Africa: *Contrib. Mineral. Petrol.*, 110, p.133-138.

WAGNER, P.A., 1911, Petrographic notes on the kimberlite occurances in the Pretoria District: *Trans. Gol. Soc. S. Afr.*, 14, p.43-63.

WAGNER, P.A., 1914, The diamond fields of southern Africa: Johannesburg: *The Transvaal Leader*, pp. 346.

WALKER, D.A., 1979, Textural and compositional studies of eclogites from the Roberts Victor kimberlite, South Africa: *Unpub. MSc thesis*, Oxford University, Oxford, England.

WALKER, R.J., CARLSON, R.W, SHIREY, S.B., & BOYD, F.R., 1989, Os, Sr, Nd, and Pb isotope systematics of southern African peridotite xenoliths: implications for the chemical evolution of subcontinental mantle: *Geochim. Cosmochim. Acta*, 53, p. 1583-1595.

WALKER, R.J., SHIREY, S.B., & STECHER, O., 1988, Comparative Re-Os, Sm-Nd and Rb-Sr isotope and trace element systematics for Archean komatiite flows from Munro Township, Abitibi Belt, Ontario: *Earth and Planetary Science Letters*, 87, p. 1-12.

WATERS, F.G., 1986, A suggested origin of MARID nodules in kimberlites by high pressure crystallisation of lamproitic magma. In: Fourth Int. Kimberlite Conf., Perth, Extended Abstracts: *Abstr. Ggeol. Soc. Aust. Ser.*, 16, p. 352-354.

WEBB, S.A.C., & WOOD, B.J., 1986, Spinel-pyroxene-garnet relationships and their dependence on Cr/Al ratio: *Contrib. Mineral. Petrol.*, 92, p. 471-480.

WELLS, P.R.A., 1977, Pyroxene thermometry in simple and complex systems: *Contrib. Mineral. Petrol.*, 62, p. 129-139.

WESTERLUND, K., 2000, A geochemical study of diamonds, diamond inclusion minerals and other mantle minerals from the Klipspringer kimberlites, South Africa: *Unpub MSc Thesis, University of Cape Town*, pp. 171

WINTERBURN, P.A., 1987, Geochemical studies of peridotite xenoliths from South African kimberlites: *Unpubl. PhD Thesis, University of Edinburgh.*

WINTERBURN, P.A., & HARTE, B., 1987, Metasomatism in coarse peridotite nodules from the Jagersfontein kimberlite pipe: *Terra Cognita,* 7, p. 395-396.

WINTERBURN, P.A., HARTE, B., & GURNEY, J.J., 1990, Peridotite xenoliths from the Jagersfontein kimberlite pipe: 1. Primary and primary-metasomatic mineralogy: *Geochimica et Cosmochimica Acta,* 54, p. 329-341.

WOOD, B.J., & FRASER, D.G., 1977, *Elemental thermodynamics for geologists*: Oxford University Press, Great Britain, pp. 303.

WOODLAND, A.B. & O'NEILL, H. ST C., 1993, Synthesis and stability of $Fe_3^{2+}Fe_2^{3+}Si_3O_{12}$ garnet and phase relations with $Fe_3Al_2SiO_{12} - Fe_3^{2+}Fe_2^{3+}Si_3O_{12}$ solutions: *Am. Mineral.*, 78, p. 1002-1015.

WOODS, G.S., 1986, Platelets and the infrared absorptionof type Ia diamonds: *Proc.R.Soc.Lond.,* 407, p. 219-238.

WOODS, G.S., & COLLINS, A.T., 1983, Infrared absorption spectra of hydrogen complexes in type I diamonds: *J.Phys.C: Solid St. Phys.*, 44, p. 471-475.

WOODS, G.S., PURSER, G.C., MTIMKULU, A.S.S., & COLLINS, A.T., 1990, The Nitrogen Content of Type Ia Natural Diamonds: *J.Phys. C:Solid St. Phys.*, 51, p. 1191-1197.

WOODS, G.S., VAN WYK, J.A., & COLLINS, A.T., 1990b, *Phil. Mag.*, B62, p. 589-594.

YEFIMOVA, E.S., SOBOLEV, N.V., & POSPELOVA, L.N., 1983, Sulfide inclusions in diamonds and specific features of their paragenesis: *Zap. Vsesoy. Mienral. Obsh. (in Russ.)*, 112, p. 300-310.

ZEZIN, R.B., SAPARIN, G.V., SMIRNOVA, E.P., OBYDEN, S.K., & CHUKICHEV, M.V., 1990, Cathodoluminescence of natural diamonds from Jakutian deposits: *Scanning,* 12, p. 326-333.